INFORMATION TO USERS

This manuscript has been reproduced from the microfilm master. UMI films the text directly from the original or copy submitted. Thus, some thesis and dissertation copies are in typewriter face, while others may be from any type of computer printer.

The quality of this reproduction is dependent upon the quality of the copy submitted. Broken or indistinct print, colored or poor quality illustrations and photographs, print bleedthrough, substandard margins, and improper alignment can adversely affect reproduction.

In the unlikely event that the author did not send UMI a complete manuscript and there are missing pages, these will be noted. Also, if unauthorized copyright material had to be removed, a note will indicate the deletion.

Oversize materials (e.g., maps, drawings, charts) are reproduced by sectioning the original, beginning at the upper left-hand corner and continuing from left to right in equal sections with small overlaps.

Photographs included in the original manuscript have been reproduced xerographically in this copy. Higher quality 6" x 9" black and white photographic prints are available for any photographs or illustrations appearing in this copy for an additional charge. Contact UMI directly to order.

The Role of Exogenous Fatty Acids and Endogenous Lipid
in the Synthesis and Secretion of
Apolipoprotein B_{100}-Containing Lipoproteins
in the Hep G2 Cell Line

by

Paul Andrew Grandmaison

Submitted in partial fulfilment of the requirements
for the degree of Doctor of Philosophy

at

Department of Biochemistry and Molecular Biology
Dalhousie University
Halifax, Nova Scotia
June 1999

DALHOUSIE UNIVERSITY

FACULTY OF GRADUATE STUDIES

The undersigned hereby certify that they have read and recommend to the Faculty of

Graduate Studies for acceptance a thesis entitled "The Role of Exogenous Fatty Acids

and Endogenous Lipid in the Synthesis and Secretion of Apolipoprotein B_{100}-

Containing Lipoproteins in the Hep G2 Cell Line"

by   Paul Andrew Grandmaison

in partial fulfillment of the requirements for the degree of Doctor of Philosophy.

Dated: June 25, 1999

External Examiner

Research Supervisor

Examining Committee

ii
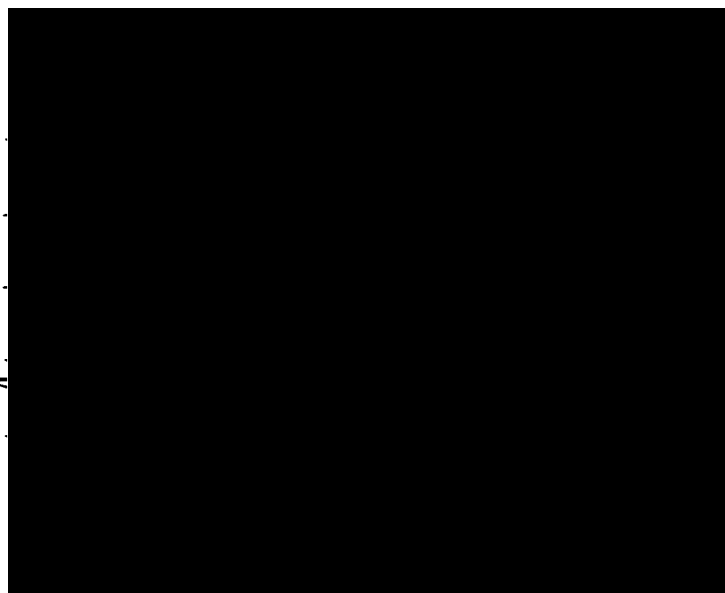
Dalhousie University

Date: June 25. 1999

Author: Paul Andrew Grandmaison

Title: The Role of Exogenous Fatty Acids and Endogenous Lipid in the Synthesis and Secretion of Apolipoprotein B_{100}–Containing Lipoproteins in the Hep G2 Cell Line

Department: Biochemistry and Molecular Biology

Degree: Ph.D.   Convocation: Fall   Year: 1999

To Angela,

My dream come true.

Table of Contents

vii

List of Figures

List of Tables

Abstract

Hep G2 cells were used to investigate the relative contribution of exogenous fatty acids and mobilization of stored triacylglycerol (TAG) for apo B-containing lipoprotein 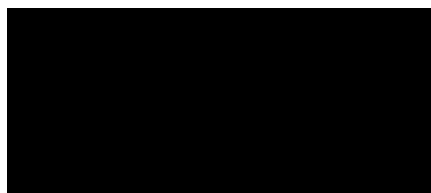(LpB) assembly, which may influence plasma concentrations of atherogenic lipoproteins. TAG-rich LpB of LDL size were isolated from culture media by heparin chromatography following incubations with oleate or myristate. Percent composition of lipid classes was similar after oleate or myristate incubations; however, lipid molecular species were skewed towards species containing the exogenous fatty acid. The isolation of LpB was important for metabolic studies since 22–28% of total TAG in the media and 31–55% of total cholesteryl esters in the media were not associated with apo B.

The relative use of exogenous fatty acid versus stored TAG in LpB assembly was studied by analysis of cellular and LpB lipid molecular species. Cells were incubated with oleate for 18 hours to define the molecular species of cellular lipid and chased with myristate for increasing periods of time or with cerulenin for two sequential chases. Myristate-containing lipid species were rapidly secreted in LpB and were secreted at a constant rate for up to 12 hours. Stored oleate-containing TAG species continued to be secreted throughout myristate chases, although at a decreasing rate. Cells secreted more TAG mass after oleate incubation followed by myristate chases than when chased with oleate whereas cells chased with oleate accumulated more cellular TAG mass compared to cells chased with myristate. Thus, stimulation of TAG secretion and TAG storage may be independent events. Cerulenin inhibited the secretion of LpB lipid mass when cells were chased without fatty acid; however, cerulenin increased secreted LpB lipid mass when cells were incubated with fatty acid and only had minor effects on TAG molecular species. The minimum percentage of LpB TAG that was consistent with mobilizing cellular lipid without modification or via a total or partial hydrolysis/re-esterification cycle was <23%. Esterification of exogenous fatty acid for LpB assembly was consistent with a minimum of 41% of the LpB TAG. Therefore, esterification of exogenous fatty acid was the primary source of TAG for the assembly of LpB in Hep G2 cells.

Abbreviations

ACAT	acyl-coenzyme A:cholesterol acyltransferase
AGP	1-acyl-sn-glycerol-3-phosphate
AILN	N-acetyl-leucyl-leucyl-norleucinal
apo	apolipoprotein(s)
apo(a)	apolipoprotein(a)
APOBEC	apolipoprotein B editing complex
ARF	adenosine diphosphate-ribosylation factor
BFA	brefeldin A
bp	base pair(s)
BSA	bovine serum albumin
BSTFA	N,O-bis[trimethylsilyl]trifluoroacetamide
C18 CE	cholesterol esterified by C18 fatty acid
cDNA	complementary deoxyribonucleic acid
CE	cholesteryl ester(s)
CETP	cholesteryl ester transfer protein
CoA	coenzyme A
DAG	diacylglycerol(s)
DGAT	diacylglycerol acyltransferase
DHAP	dihydroxyacetone-phosphate
EDTA	ethylenediamine tetraacetic acid
EM	electron microscopy
ER	endoplasmic reticulum
FBS	fetal bovine serum
G3P	sn-glycerol-3-phosphate
GDP	guanosine diphosphate
GLC	gas-liquid chromatography
GlcNAc	N-acetylglucosamine
GTP	guanosine triphosphate
h	hour(s)
HDL	high-density lipoprotein(s)
HMG-CoA	3-hydroxy-3-methylglutaryl coenzyme A
HTGL	hepatic triglyceride lipase
HTP	hydroxylapatite
IDL	intermediate-density lipoprotein(s)

LCAT	lecithin:cholesterol acyltransferase
LDH	lactate dehydrogenase
LDL	low-density lipoprotein(s)
LDL-R	low-density lipoprotein receptor
Lp(a)	lipoprotein(a)
LpB	apolipoprotein B-containing lipoprotein(s)
LpB:E	apolipoproteins B and E-containing lipoprotein(s)
LPL	lipoprotein lipase
LRP	low-density lipoprotein receptor related protein
MAG	monoacylglycerol(s)
Man	mannose
MEM	minimum essential media
MGAT	monoacylglycerol acyltransferase
min	minute(s)
MME	monomethylethanolamine
mRNA	messenger ribonucleic acid
MTP	microsomal triglyceride transfer protein
NANA	N-acetylneuraminic acid (or sialic acid)
PAPH	phosphatidic acid phosphohydrolase
PBS	phosphate buffered saline
PDI	protein disulphide isomerase
PEG	N-polyethyleneglycol 6000
PL	phospholipid(s)
PLC	phospholipase C
PLTP	phospholipid transfer protein
PMSF	phenylmethylsulphonyl fluoride
SDS	sodium dodecyl sulphate
TAG	triacylglycerol(s)
TLC	thin-layer chromatography
Tricine	tris(hydroxymethyl)methylglycine
Tris	tris(hydroxymethyl)aminomethane
tRNA	transfer ribonucleic acid(s)
WHHL	Watanabe-heritable hyperlipidemic
VLDL	very-low-density lipoprotein(s)

Acknowledgements

I would like to pay a special tribute to my parents, Ken and Donna, for teaching me to pay attention to details and to be stubborn. Mark and Jeannine, my brother and sister, have been a constant source of support.

Throughout all the gruesome carnage and clashing of steel, my adventures in high fantasy with Dan Brown, James Boyd, Michael Crawley, and Marc Gaudet have helped me to stay grounded in reality. Well, somewhat grounded.

Finally, I would like to thank Sifu Tong Yau-Sun and the senior Taiji students of the Nova Scotia School of Kung Fu and Taiji—Chris Young, Richard Robertson, Kevin Kane, Ron Pizzo, Steve Cameron, Nick Woolsey, Bret Wentzel, Calvin Creighton, John MacDonald, Danuta Snyder, John Smith, Darryl Hemlow, John Fitzgerald, and Corrie Watt—for all of their help and friendship during my pursuit of the ultimate potential.

Computer work was done on a Macintosh whenever possible.

A point to ponder...

"I know that most men, including those at ease with problems of the greatest complexity, can seldom accept even the simplest and most obvious truth if it be such as would oblige them to admit the falsity of conclusions which they have delighted in explaining to colleagues, which they have proudly taught to others, and which they have woven, thread by thread, into the fabric of their lives."

Count Leo Tolstoy

I. Introduction

A. Preamble

The catabolic products of very-low-density lipoprotein (VLDL), intermediate-density lipoproteins (IDL) and low-density lipoproteins (LDL), are known risk factors in cardiovascular disease (Havel & Kane, 1995a, 1995b). Current evidence suggests that the size of secreted VLDL plays a role in determining the size and nature of IDL and LDL, which will impact upon their clearance from the plasma (Packard & Shepherd, 1997). Large, triacylglycerol (TAG)-rich VLDL subfractions appear to be metabolized to small, dense LDL subfractions, which are strongly linked to atherogenesis. Thus, the potential atherogenicity of IDL and LDL may be, in part, predetermined during the synthesis of VLDL. The assembly of lipid with apolipoprotein B is a poorly understood metabolic event. Analysis of the contribution of lipid from exogenous, stored, and *de novo* synthetic pools in VLDL synthesis: the mechanism(s) of lipid transport to the site of VLDL assembly; and the process of lipid packaging during VLDL synthesis will help to define the role of IDL and LDL in atherosclerosis.

B. Overview of Lipoproteins

i. Lipoprotein Structure and Classification

Lipoproteins are complexes of both protein and lipid. The protein components of lipoproteins are apolipoproteins (apo) or apoproteins. To address the problem of transporting hydrophobic lipid through aqueous environments, a strategy of encapsulating a neutral lipid core with a monolayer of polar lipids evolved. Thus, phospholipids (PL) and cholesterol solubilize TAG and cholesteryl esters (CE). Apoproteins can act as ligands for receptors, as co-factors for enzymes, and in directing the secretion of lipid from cells. Apoproteins can be divided into two groups: non-exchangeable (apo B) and exchangeable (apo A-I, A-II, A-IV, C-I, C-II, C-III, and E). The exchangeability of most apoproteins allows the metabolic processes of lipoproteins to dynamically adapt. Lipoproteins can become targets of enzymes or receptors by acquiring apoproteins. After processing, the exchange of apoproteins can trigger a new metabolic phase.

Lipoproteins can be classified by density from ultracentrifugation or by mobility in non-denaturing electrophoretic gels (Table 1). The separation by density shows an inverse correlation between lipoprotein size and density, which reflects the catabolic loss of buoyant neutral lipid from the core while maintaining some dense apoprotein. The categories based upon density have corresponding electrophoresis bands. The separation of lipoproteins by ultracentrifugation is the basis of the typical nomenclature.

1

Lipoprotein Class	Density (g/ml)	Electrophoretic Mobility	Apoprotein Content	Diameter (nm)	Molecular Mass (kDa)
Chylomicrons	<0.93	remains at origin	A-I, A-II, B_{48}	75–1200	50 000–1 000 000
VLDL	0.930–1.006	pre-β	A-IV, B_{100}, C-I, C-II, C-III, E	30–80	10 000–80 000
IDL	1.006–1.019	slow pre-β	B_{100}, C-I, C-II, C-III, E	25–35	5 000–10 000
LDL	1.019–1.063	β	B_{100}	18–25	2 300
Lp(a)	1.040–1.090	slow pre-β	(a), B_{100}	25–30	~2 800
HDL_2	1.063–1.125	α	A-I, A-II, A-IV, C-I, C-II, C-III, E	9–12	360
HDL_3	1.125–1.210	α	A-I, A-II	5–9	175

Lipoprotein Class	Percent Composition by Dry Weight				
	apoprotein	cholesterol	PL	CE	TAG
Chylomicrons	2	2	7	3	86
VLDL	8	7	18	12	55
IDL	19	9	19	29	23
LDL	22	8	22	42	6
HDL_2	40	5	33	17	5
HDL_3	55	4	35	13	3

Table 1: **Physical properties of human lipoproteins.** Data was obtained from Havel and Kane (1995a).

ii. Lipoprotein Metabolism

Lipoprotein metabolism was recently reviewed (Beisiegel, 1998: Chapman *et al.*, 1998: Havel & Kane, 1995a, 1995b; Tall, 1998, 1995). Intestinal villi cells package dietary lipids along with apo As and B into TAG-rich chylomicrons (Figure 1, panel A) and secrete chylomicrons into the lymph. Chylomicrons enter the circulation via the subclavical vein. In the circulation, chylomicrons interact with high-density lipoproteins (HDL) to acquire apo Cs and E. Lipoprotein lipase (LPL), which requires apo C-II as a co-factor, hydrolyses dietary TAG and some PL in the chylomicrons. Thus, addition of apo C-II primes chylomicrons for LPL hydrolysis. Loss of core lipid necessitates proportional losses of surface material. Hence, shrinking chylomicrons transfer apoproteins and polar lipids to HDL. Phospholipid transfer protein (PLTP) facilitates the loss of PL from the chylomicrons. The low-density lipoprotein receptor (LDL-R), the low-density lipoprotein receptor-related protein (LRP), and the VLDL receptor clear TAG-depleted chylomicron remnants from the circulation via receptor-mediated endocytosis (Beisiegel, 1995: Cooper, 1997). LPL was shown to increase binding of chylomicron remnants to the LRP (Beisiegel *et al.*, 1991). It is thought that the LRP is the major receptor for chylomicron remnant clearance, which occurs predominantly in the liver.

The liver of animals produces VLDL to mobilize endogenous TAG to extra-hepatic tissues (Figure 1, panel B). The nascent VLDL contains apo B when secreted from the liver. In the plasma, the VLDL acquires apo Cs and E from HDL. When VLDL acquires apo C-II, it becomes a substrate for lipolysis by LPL which hydrolyses TAG and some PL. With the lipolysis of TAG from the VLDL, there is a concurrent loss of cholesterol, PL, and apo Cs: all of which can be incorporated into HDL. PLTP assists the transfer of PL from VLDL to HDL. The reduction of lipid content increases the density of the VLDL to the IDL class. Hepatic triglyceride lipase (HTGL), which does not require apo C-II for activity, can complete the catabolism of VLDL to LDL by hydrolysing TAG and some PL. With further loss of core material, the IDL transfers PL, cholesterol, and apo E to HDL. Again, PLTP facilitates the transfer of PL from apo B-containing lipoproteins (LpB) to HDL. The LDL-R clears both IDL and LDL from the circulation by receptor-mediated endocytosis. It was shown that other receptors, *i.e.* the VLDL receptor and the LRP, play a role in the clearance VLDL and its metabolites from the circulation (Beisiegel, 1995).

HDL returns cholesterol to the liver for catabolism via reverse cholesterol transport (Figure 1, panel C). The dominant apoprotein in HDL is apo A-I. The liver and intestine secrete HDL as a discoidal complex of apo A-I and PL, known as pre-β HDL, which can absorb cholesterol and PL from the plasma membranes of cells and from the surface of VLDL, chylomicrons, and their metabolic products. Two other proteins associate with HDL—lecithin:
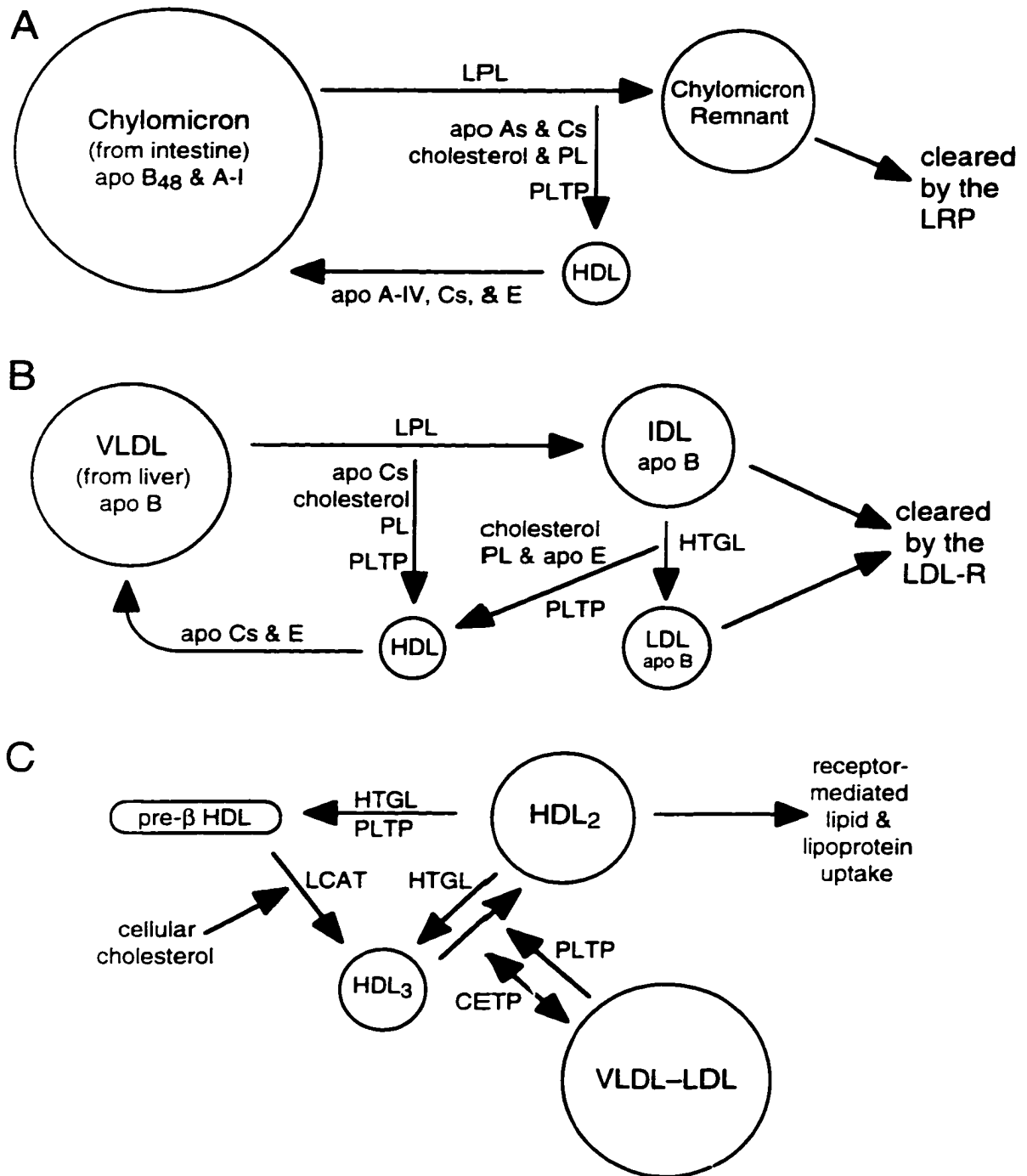
Figure 1: **A schematic overview of lipoprotein metabolism.** A: Exogenous lipid transport. B: Endogenous lipid transport. C: Reverse cholesterol transport.

cholesterol acyltransferase (LCAT) and cholesteryl ester transfer protein (CETP). LCAT, which is activated by apo A-I, catalyses the transfer of an acyl group from the sn-2 position of phosphatidylcholine to the hydroxyl group of cholesterol. Serum albumin binds released lysolecithin. The CE synthesised by LCAT collects between the bilayer of PL, transforming the discoidal HDL into a dense, spherical HDL_3 particle. CETP catalyses the exchange of neutral lipid between HDL and LpB. CETP transfers CE from HDL to VLDL and its catabolic products while shuttling TAG back to HDL from LpB at a nearly equal molar ratio. Thus, CETP can modify dense HDL_3, which has a primarily CE core, to less dense HDL_2, which is enriched in TAG (Table 1). Concurrent with the activity of CETP, PLTP transfers PL from LpB to HDL. The exchange of CE into VLDL-LDL results in LDL being the primary transporter of cholesterol in humans. Thus, HDL takes excess cholesterol from the body, esterifies cholesterol to CE with LCAT, transfers CE to LDL by CETP, and clears CE from the plasma as LDL is removed via receptor-mediated endocytosis by the liver. Reverse cholesterol transport concludes with the liver metabolizing excess cholesterol to bile acids which are excreted.

HDL is also capable of interacting directly with hepatocytes to return lipids to the liver. HTGL hydrolyses TAG and PL from the large HDL_2 particles, reducing the HDL_2 to the more dense HDL_3. Also, HTGL and PLTP were shown to reduce HDL_2 to pre-β HDL (Marques-Vidal et al., 1997). HDL_2 may be cleared from the plasma by receptors that recognize apo E. Finally, HDL delivers CE to hepatocytes via a poorly understood HDL receptor. It was suggested that this receptor may be the scavenger receptor SB-BI (Acton et al., 1996) which acts only to bind the HDL; it does not internalize the HDL by receptor-mediated endocytosis (Tall, 1998).

iii. The Assembly of LpB

In essence, the assembly of lipoproteins is a packaging problem. How has metabolism dealt with the issue of coordinating the synthesis of protein and lipid? Since PL, cholesterol, CE, TAG, and apo B are the basic elements of chylomicrons and VLDL, it may be assumed that they are all required to some degree in the assembly of LpB.

C. Apo B

i. Nomenclature

Apo B is the major structural protein found in chylomicrons, chylomicron remnants, VLDL, IDL, and LDL. The nomenclature of apo B is based on the centile system (Kane et al., 1980). Of the two naturally synthesised apo Bs, apo B_{48} is slightly smaller than half the size of the full length apo B_{100}. Other subscripts refer typically to carboxyl-terminal

truncation constructs or mutants which use the centile system to indicate the portion of apo B_{100} emulated.

ii. Apo B Gene

The elucidation of the sequence of the apo B gene was a significant breakthrough in understanding lipoprotein metabolism. The initial reports were from complementary deoxyribonucleic acid (cDNA) sequences (Chen et al., 1986; Knott et al., 1986a, 1986b; Law et al., 1986; Yang et al., 1986) and were confirmed by genomic sequencing (Blackhart et al., 1986; Carlsson et al., 1986; Cladaras et al., 1986; Wagener et al., 1987). The apo B messenger ribonucleic acid (mRNA) is 14.1 k base pairs (bp) long and produces a 4563-amino-acid protein with a 27-amino-acid-residue signal sequence in an in vitro translation system. The calculated molecular mass of the mature 4536-amino-acid-residue apo B_{100} is 513 kDa. Since apo B constitutes the protein mass of LDL, the sequence data indicates that there is one molecule of apo B per LDL particle (Knott et al., 1986a).

The apo B gene contains 43 kbp, only three fold larger than the mRNA (Blackhart et al., 1986; Cladaras et al., 1986) and has 29 exons and 28 introns. The introns agree well with the GT–AG rule (Blackhart et al., 1986; Wagener et al., 1987), which marks the beginning and end of introns, and range from 107–2950 bp in size. The introns are disproportionately clustered in the 5′ region of the gene, with 24 of the introns residing in the amino-terminal region of apo B. The exons range in size from 39–7572 bp, with two exons being very large: exon 26 is 7572 bp and exon 29 is 1906 bp. The human apo B gene is on the short arm of chromosome 2, between 2p23–2p24 (Deeb et al., 1986; Knott et al., 1985; Law et al., 1985).

iii. Apo B mRNA Editing

Apo B_{100} and apo B_{48} were believed to be related proteins as apo B_{100} and apo B_{48} produced similar peptide maps (Elovson et al., 1981) and the amino terminus of apo B_{100} shared monoclonal (Curtis & Edgington, 1982; Elovson et al., 1981; Marcel et al., 1982; Milne & Marcel, 1985) and polyclonal antibodies epitopes (Protter et al., 1986) with apo B_{48}. Thus, apo B_{48} appeared to be a proteolytic product of apo B_{100}. Apo B_{48} and apo B_{100} were shown to lack a precursor-product relationship in human fetal intestinal tissue since both were produced in equal proportions throughout a short pulse-chase study (Glickman et al., 1986). Apo B was recognized to be a single gene when apo B_{48} and apo B_{100} cDNA hybridized in Southern blot analysis (Higuchi et al., 1987) and antibody mapping of an apo B polymorphism demonstrated parallel expression of the polymorphism for both apo B_{48} and apo B_{100} (Young et al., 1986).

The mRNA of apo B can be edited. Gln_{2153} of apo B is changed to an in-frame stop codon UAA in the cDNA of human intestine (Chen et al., 1987; Powell et al., 1987). The added stop codon was only seen in the mRNA of tissue expressing apo B_{48}, not in the genomic deoxyribonucleic acid or in tissues in which apo B_{100} was transfected. The editing complex or editosome, which could edit in vitro when combined with apo B mRNA constructs, was isolated from rat hepatocyte extract (Smith et al., 1991). The editosome could be inhibited by proteases but not by RNases, which suggested guide nucleotides were not involved (Greeve et al., 1991; Harris et al., 1993). The editing mechanism was shown to involve cytidine deamination when cytidine, with radioactive ribose or pyrimidine ring moieties, labelled the U_{6666} product (Hodges et al., 1991; Johnson et al., 1993).

The catalytic subunit of the apo B mRNA editing complex, APOBEC-1, was cloned (Lau et al., 1994; Teng et al., 1993; Yamanaka et al., 1994) and the human gene was sequenced (Fujino et al., 1998). The protein was 27 kDa, dimeric (Lau et al., 1994; Oka et al., 1997), and expressed in liver, kidney, spleen, intestine, and lung (Teng et al., 1993). When APOBEC-1 was expressed in the human hepatocyte cell line, Hep G2, the cells became editing competent. Editing was enhanced when APOBEC-1 was transfected into the rat hepatocyte cell line, McA-RH7777 (Driscoll & Zhang, 1994; Navaratnam et al., 1993a; Teng et al., 1993).

The editing process is specific as only C_{6666} is edited with high efficiency despite the presence of 375 CAA sequences in apo B mRNA (Smith et al., 1991). The construction of deletion and point mutations demonstrated three domains were important for efficient editing: a 6-base enhancer sequence immediately 5' to C_{6666}, a 5-base spacer region immediately 3' to C_{6666}, and an 11-base mooring region 3' of the spacer sequence (Figure 2, Backus & Smith, 1992, 1991; Driscoll et al., 1993; Shah et al., 1991). It was proposed that the mooring region was the binding site of the editosome, the spacer region placed APOBEC-1 by C_{6666}, and the enhancer region helped to stabilize the protein: mRNA complex (Backus & Smith, 1992).

A variety of auxiliary proteins were identified in the editosome. UV irradiation of the editosome linked two proteins, p44 and p66, to the flanking regions of the apo B mRNA (Harris et al., 1993). p66 was shown to be UV cross-linked to the mooring sequence (Navaratnam et al., 1993b; Yang et al., 1997). Lau et al. (1997) were able to clone a 37 kDa protein which bound apo B mRNA and APOBEC-1. Both the immunodepletion of this APOBEC-1-binding protein and expression of its anti-sense ribonucleic acid inhibited editing of apo B. Interestingly, the APOBEC-1-binding protein was expressed in many tissues: spleen, thymus, prostate, testes, ovary, intestine, pancreas, heart, brain, lung, and liver (Lau et al., 1997). The editosome appears to have functions in tissues other than those that edit apo B.

Auxiliary Proteins

APOBEC-1

5′ —|GACAUAUA UGAUA C AAUUUGAUCAGUAUA UUA|— 3′

Enhancer
Sequence

Spacer
Region

Mooring Region
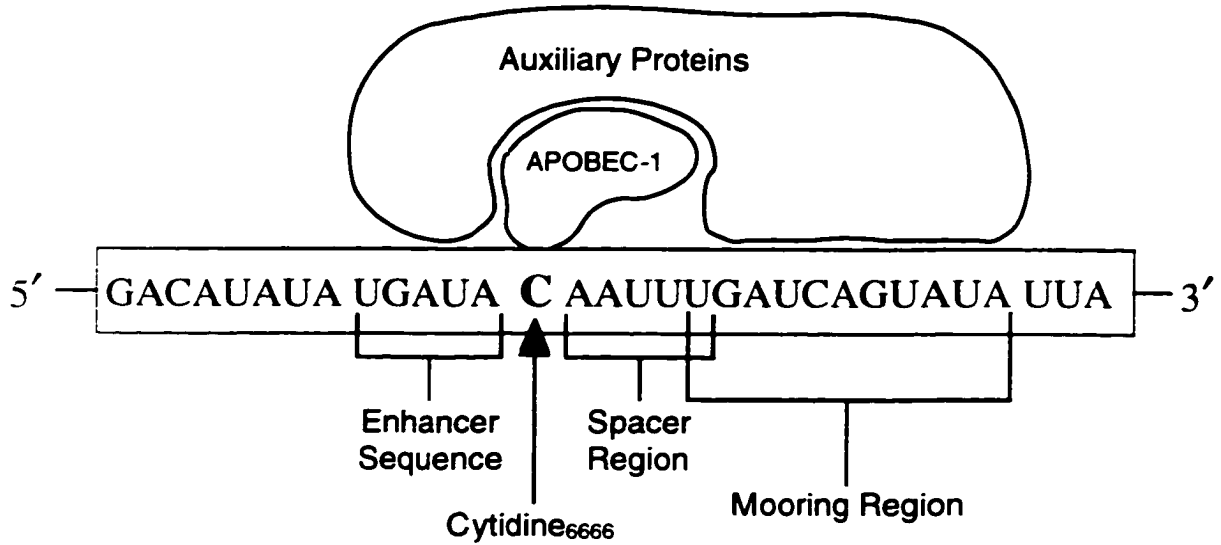
Cytidine$_{6666}$

Figure 2: **Editosome target site in apo B mRNA.** The sequence information surrounding cytidine$_{6666}$ defines the point of editing in apo B. The mooring region, uridine$_{6671}$ to adenosine$_{6681}$, is the site of editosome binding. The spacer region, adenosine$_{6667}$ to uridine$_{6671}$, properly aligns the editosome such that APOBEC-1 subunit is juxtaposed to cytidine$_{6666}$. The editosome may interact with the mRNA, 5′ of the edited cytidine at the enhancer sequence, uridine$_{6661}$ to adenosine$_{6665}$.

iv. Apo B Structure

The primary sequence of apo B_{100} is hydrophobic, more so than the other apoproteins but less than that of an integral membrane protein (Chen *et al.*, 1986). The carboxyl terminus is more hydrophobic than the full-length protein, with hydrophobicity on par with integral membrane proteins. Five distinct regions within apo B were observed by trypsin mapping. The amino-terminal domain was trypsin accessible, the second domain contained both trypsin accessible and inaccessible subdomains, the third domain was trypsin inaccessible, the fourth domain contained both trypsin accessible and inaccessible domains, and the carboxyl-terminal domain was trypsin inaccessible (Yang *et al.*, 1994, 1990, 1989, 1986).

Based on the primary sequence of apo B, several groups predicted secondary structures (Chen *et al.*, 1986; Knott *et al.*, 1986a; Law *et al.*, 1986; Olofsson *et al.*, 1987). Knott *et al.* (1986a) noted apo B was hydrophobic throughout the protein and the hydrophobicity was marked by amphipathic structures. They found one amphipathic α-helix at residues 2000–2600 and four proline-rich clusters of the motif acidic-aromatic-polar-aliphatic-proline. Such a motif allows for the formation of amphipathic β-sheets (De Loof *et al.*, 1987; Knott *et al.*, 1986a; Law *et al.*, 1986). De Loof *et al.* (1987) also identified structural homology between amphipathic α-helices of apo B and other apoproteins. Segrest *et al.* (1994) developed a set of rules based on exchangeable apoproteins and globular proteins to define amphipathic α-helices. The non-polar face of the lipid-associating helix tends to be more hydrophobic than in globular proteins. Segrest *et al.* (1994) also tested for amphipathic β-sheet content. They found apo B had a pentapartite structure with an overall motif of NH_2-α_1-β_1-α_2-β_2-α_3-COOH. These five domains, which alternate between high α-helical content and high β-sheet structure, corresponded well with trypsin mapping results. The α-helical region of the amino-terminus is accessible to trypsin, both β-sheet regions contain alternating trypsin accessible and inaccessible subdomains, and the second and third α-helices are inaccessible to trypsin. Segrest *et al.* (1994) proposed that the first α-helix in the amino-terminal region was globular in nature, the two β-sheet regions bound lipid irreversibly, and the second and third α-helical clusters reversibly bound lipid.

v. Covalent Modifications of Apo B

a. Disulphides

The apo B sequence contains 25 cysteines, of which 12 were clustered in the first 500 amino acids (Chen *et al.*, 1986; Knott *et al.*, 1986a; Law *et al.*, 1986). Cardin *et al.* (1982) reported (when apo B was thought to be a dimer) that 12 out of 14 cysteines in apo B form disulphide bridges; thus, Knot *et al.* (1986a) concluded that apo B should have no

more than 3 free cysteine residues. After characterizing 23 of the 25 cysteines, Yang *et al.* (1990) reported that only 16 of the cysteine residues form disulphide bridges and all 12 of the cysteines in the amino-terminal region form disulphides. Proper disulphide bridge formation was demonstrated to be essential in the secretion of apo B. Shelness and Thornburg (1996) incubated the human hepatoblastoma cell line Hep G2 with dilute concentrations of dithiothreitol to interfere with disulphide formation. If the cells were incubated with dithiothreitol during the synthesis of the amino-terminal 20–25% of apo B, secretion was inhibited. The amino-terminal 25% of apo B contains seven of the eight disulphide bonds in apo B. However, if the cells were incubated with dithiothreitol after the synthesis of the amino-terminal region, apo B secretion was normal and the amino-terminal disulphides resisted reduction. Huang and Shelness (1997) reported the second and fourth disulphide were essential for the secretion of apo B; however, Tran *et al.* (1998) found only the fourth disulphide to be critical for the synthesis of VLDL. Both groups found that their disulphide mutants impaired secretion of apo B but had little effect on apo B translation. These data suggested disulphide bonds were essential for the amino-terminal domain of apo B to achieve proper conformation for VLDL assembly.

b. Apolipoprotein(a)

Berg (1963) initially reported apolipoprotein(a) (apo(a)) was a novel antigenic factor associated with LDL. This modified LDL was termed lipoprotein(a) (Lp(a)). Apo(a) was cloned by McLean *et al.* (1987) and the structure of apo(a) was remarkably similar to plasminogen. Apo(a) was comprised of the signal sequence, multiple copies of the kringle 4 domain, the kringle 5 domain, and an inactive protease domain of plasminogen. The homology between the domains of the two proteins ranged from 75–100%. Apo(a) was found to be highly polymorphic, with 34 different isoforms reported, resulting in a size range of 300–800 kDa (Marcovina *et al.*, 1993). The variability was imparted by different copy numbers of the iterated kringle 4 domain, ranging from 12–51 copies. Apo(a) was found to be linked to apo B_{100} by a disulphide bridge, connecting Cys_{4326} of apo B_{100} (Callow & Rubin, 1995) to the only unpaired cysteine in the penultimate kringle 4 domain of apo(a) (Koschinsky *et al.*, 1993). This disulphide was suggested to be formed in the plasma as only Lp(a) was found in plasma and only apo(a) could be isolated intracellularly (Koschinsky *et al.*, 1993; White & Lanford, 1995). Apo(a) has been implicated as an independent risk factor in cardiovascular disease (reviewed in Huby *et al.*, 1997; Scanu & Edelstein, 1995).

c. Acylation

Apo B was reported to be acylated based on observations that Hep G2 cells incorporated [^{14}C]stearate and [^{14}C]palmitate into apo B in equal molar quantities. The fatty acids were acylated via thiol-linkages to cysteine residues and 10 thiol-esters were estimated to be present in apo B (Hoeg et al., 1988; Huang et al., 1988). Evidence was also found for the existence of intramolecular thiol linkages between cysteine residues and neighbouring amino-acid residues with acidic side chains (Huang et al., 1988; Lee, 1991). However, the reported thiol-esters, disulphides, and free cysteine side chains exceed the 25 cysteine residues in apo B$_{100}$. These data either question the ability to differentiate between the covalent bonds formed by cysteine residues or suggests some heterogeneity in the thiol modifications of apo B. Acylation of cysteines would increase the affinity of apo B for lipid (Lee, 1991) and may play a role in preventing the formation of improper disulphides.

d. Glycosylation

The primary sequence of apo B$_{100}$ contains 19 potential asparagine-linked glycosylation sites of the motif Asn-x-Thr/Ser, with a cluster of 5 potential sites between residues 3197–3438 (Chen et al., 1986; Cladaras et al., 1986; Knott et al., 1986a; Law et al., 1986; Yang et al., 1986). Sixteen of the potential glycosylation sites were found to be glycosylated (Yang et al., 1989) with the carbohydrate moiety comprising 4–9% of the mass of apo B (Lee & Breckenridge, 1976; Swaminathan & Aladjem, 1976; Vauhkonen et al., 1985). The determination of oligosaccharide structure in human apo B produced two fractions: a neutral high-mannose fraction and an acidic complex-oligosaccharide fraction. These two oligosaccharide fractions comprised more than half of the carbohydrate mass in apo B$_{100}$ (Lee & Breckenridge, 1976; Swaminathan & Aladjem, 1976). The high-mannose oligosaccharide fraction was comprised of mannose (Man) and N-acetylglucosamine (GlcNAc) residues. Apo B contained 37% high-Man which compared to only 5% high-Man structures found in total serum proteins (Vauhkonen et al., 1985). The most prominent form of the high-Man oligosaccharide was Man$_5$GlcNAc$_2$ (Taniguchi et al., 1989; Vauhkonen et al., 1985). The complex-oligosaccharide fraction contained 2 mol of N-acetylneuraminic acid (NANA or sialic acid), 5 mol of Man, 2 mol of galactose, and 3 mol of GlcNAc (Lee & Breckenridge, 1976; Swaminathan & Aladjem, 1976). Variations of this structure included removal of some of the GlcNAc and mannose residues (Swaminathan & Aladjem, 1976; Taniguchi et al., 1989).

The importance of glycosylation in apo B is controversial. Glycosylation was reported not to play an essential role in apo B synthesis as treatment with tunicamycin eliminated the addition of oligosaccharides to apo B without impairing synthesis (Janero et al.,

1984; Siuta-Mangano *et al.*, 1982; Struck *et al.*, 1978). However, the secretion of apo B was reduced up to 40% after the treatment with tunicamycin. Glycosylation of apo B may assist proper folding; thus, the elimination of glycosylation may increase the misfolding of apo B.

The role of glycosylation in the binding of apo B to the LDL-R was studied. Shireman and Fisher (1979) enzymatically removed all carbohydrate from LDL and found uptake by fibroblasts was similar to control LDL. Attie *et al.* (1979) desialylated LDL with neuraminidase and found the rate of clearance from the plasma of pigs and rats was the same as control LDL. However, desialylated LDL was found to clear more rapidly from human plasma (Malmendier *et al.*, 1980). This increased rate of clearance was supported by studies which correlated high levels of apo B_{100} sialylation with low plasma cholesterol concentrations in rabbits (Fujioka *et al.*, 1994; Tsunemitsu *et al.*, 1992). Thus, the negative charge imparted by the NANA may play a role in the binding of apo B to the LDL-R.

e. Phosphorylation

Apo B was reported to be phosphorylated in rat hepatocytes (Davis *et al.*, 1984; Sparks *et al.*, 1988). Davis *et al.* (1984) were able to detect only phosphorylation of serine residues in apo B_{48} whereas Sparks *et al.* (1988) were able to detect phosphoserine in both apo B_{48} and B_{100}. Diabetic rats, which were insulin-independent, phosphorylated apo B up to 31 fold higher than control rats and tyrosine replaced serine as the dominantly phosphorylated amino-acid residue (Sparks *et al.*, 1988). Insulin was found to decrease the secretion apo B without changing apo B translation. The reduced secretion of apo B was suggested to be due to intracellular degradation, with apo B_{100} being more sensitive to insulin than apo B_{48} (Jackson *et al.*, 1990). Jackson suggested the increase in phosphorylation reduced the lipid affinity of apo B which lead to its increased degradation. Mathur *et al.* (1993) reported the human intestinal cell line CaCo-2 phosphorylated apo B_{48} and okadaic acid treatment increased the levels of phosphorylation. Okadaic acid did not affect translation of apo B but halved the secretion of apo B_{48} and reduced the secretion of B_{100} to 75% of controls. Swift (1996) examined the intracellular site of phosphorylation and reported that the Golgi apparatus was the major site of phosphorylation. Swift detected no phosphorylation in the rough endoplasmic reticulum (ER) and found apo B_{48} was phosphorylated more readily than apo B_{100}. This would indicate important post-translational modifications were made in the Golgi. Taken in total, these data would suggest phosphorylation of apo B plays a regulatory role in determining whether apo B is degraded or secreted.

vi. Apo B Conformation on the Surface of a Lipoprotein

Apo B was proposed to be in an elongated conformation upon the surface of lipo-proteins. The near absence of disulphide bonds outside of the amino-terminal domain would not impose a restricted conformation upon apo B. Electron microscopy of LDL, both of LDL affixed to grid then delipidated (Chatterton et al., 1991; Phillips & Schumaker, 1989) and of LDL frozen in vitreous ice (Spin & Atkinson, 1995), suggested apo B forms a belt which circumscribes the lipoprotein. Antibodies of defined apo B-binding epitopes were used with electron microscopy to determine the three-dimensional orientation and position upon the surface of LDL (Chatterton et al., 1995, 1991). Chatterton and colleagues proposed a ribbon and bow model for the orientation of apo B on lipoproteins: apo B circumscribed the lipoprotein once, looped into a hemisphere, and extended into the opposite hemisphere, crossing over itself near the LDL-R binding site (Figure 3). The ribbon made up the amino-terminal 89% of apo B and the bow was in the carboxyl-terminal region.

vii. Binding Sites on Apo B

a. LDL Receptor Binding Sites

The LDL receptor (LDL-R) clears LDL from the plasma, specifically binding apo B_{100} and apo E (reviewed in Brown & Goldstein, 1986). It does not bind apo B_{48} (Hui et al., 1984). Antibodies, which recognized the apo B_{100} LDL-R binding domain, were best able to bind apo B_{100} associated with small LDL and were not effective in binding apo B_{100} associated with VLDL (Teng et al., 1985). McNamara et al. (1996) performed detailed calculations regarding volume and surface area of lipid in LDL and showed the percentage of surface area occupied by lipid decreased with lipolysis. They concluded that apo B_{100} was required to decrease its thickness on the surface of LDL to cover more of the surface of LDL. These results suggest apo B_{100} undergoes conformational changes with the decreasing volume of the lipoprotein and these changes are necessary for apo B_{100} to bind to the LDL-R.

The sequence data demonstrated residues 3352−3369 of apo B_{100}, a region rich in basic residues, are 67% similar with the apo E LDL-R binding domain (Chen et al., 1986; Cladaras et al., 1986; Knott et al., 1985). Yang et al. (1986) demonstrated a synthetic peptide containing residues 3345−3381 of apo B_{100} could bind to the LDL-R. However more than the presence of positive charge was important in the binding of apo B_{100} to the LDL-R since methylation of lysine, which preserves its positive charge, and chemical modifications of lysine to remove its positive charge both eliminated binding (Tikkanen et al., 1982; Weisgraber et al., 1978). Thus, unaltered lysine residues in apo B_{100} appeared to be important in binding to the LDL-R. Several reports mapped apo B_{100} with antibodies and some monoclonal antibodies inhibited LDL-R binding (Knott et al., 1985; Milne et al., 1989,

A: Normal Binding

B: Impaired Binding

C: Enhanced Binding
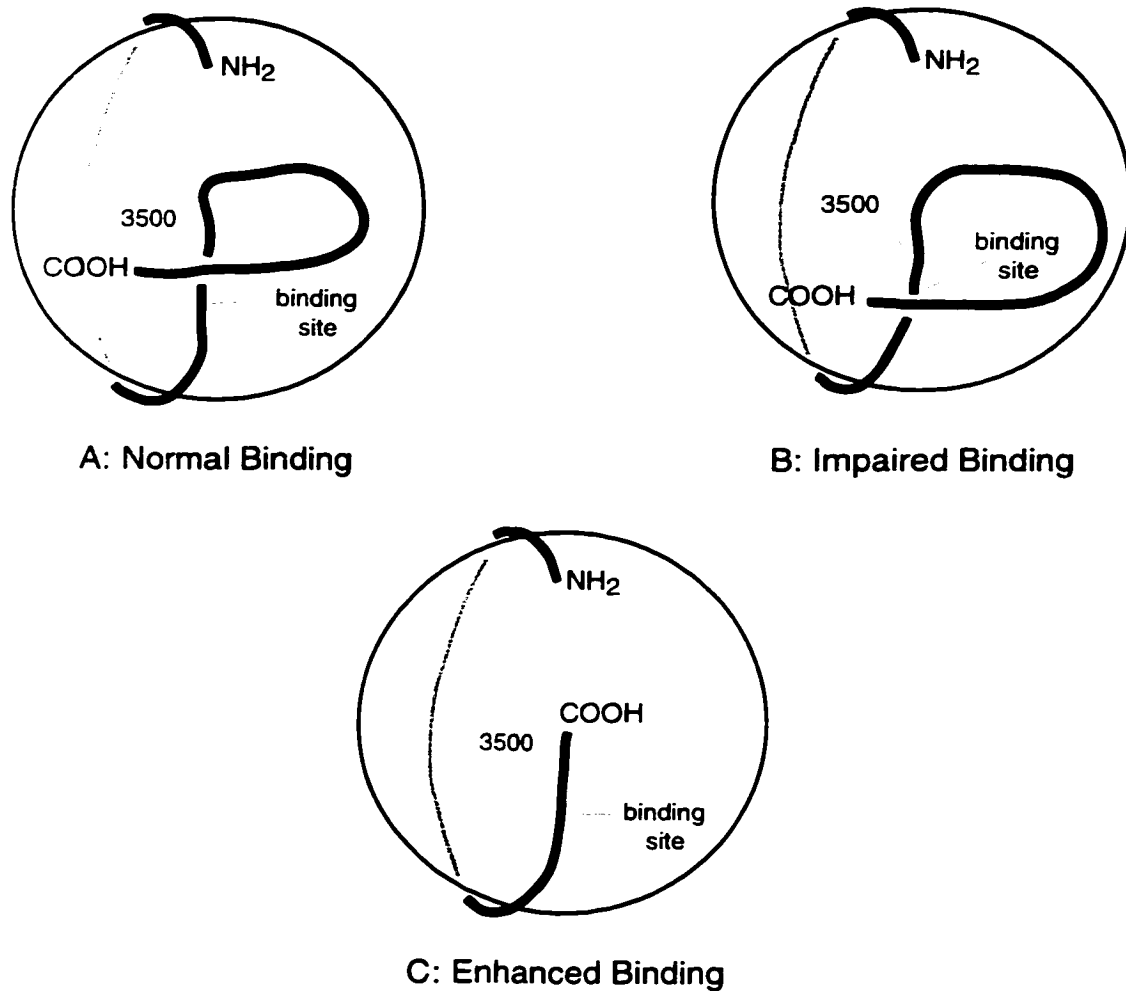
Figure 3: **The ribbon and bow model of apo B on the surface of a lipoprotein.** The ribbon domain of apo B, the amino-terminal 89% of the protein. encircles the lipoprotein once. The carboxyl-terminal bow domain loops into one hemisphere on the lipoprotein and extends into the opposite hemisphere, crossing over itself (adapted from Borén *et al.*. 1998a). A: With the bow correctly positioned over arginine$_{3500}$, the binding site is exposed and the apo B is binding competent. B: Mutations at residue 3500 result in the binding site being obstructed and apo B is not able to bind the LDL-R. C: Truncated apo B. *i.e.* apo B$_{80}$, is binding competent as residues 3359–3369 are accessible.

1983; Pease et al., 1990; Tikkanen et al., 1982). Milne and co-workers (1989) were able to localize the epitopes of some antibodies to show several sites in the area of residues 3000–4000 competed with LDL binding. Specifically, three antibodies proximal to Arg_{3500} abolished binding. This agreed well with reports that mutations at residue 3500 have been associated with hyperlipidaemia (Gaffney et al., 1995; Soria et al., 1989; Tai et al., 1998). Borén et al. (1998a) generated a series of mutants and proved residue 3500 had an absolute requirement for arginine to allow LDL-R binding. They also demonstrated truncated apo B mutants had a higher binding capacity for the LDL-R than apo B_{100}. Borén and colleges used the bow and ribbon model of apo B_{100} (Chatterton et al., 1995) to explain their results (Figure 3). They proposed the bow was in a conformation such that carboxyl-terminal residues of apo B_{100} covered the LDL binding site in VLDL. With delipidation, the bow of apo B_{100} slid down to interact with Arg_{3500}, exposing the LDL-R-binding domain. Mutations at residue 3500 prevented the proper exposure of the LDL-R-binding domain which inhibited binding. Carboxyl-terminal truncations of apo B, i.e. apo B_{80}, were not able to occlude the binding site and thus were always binding competent. Truncations of apo B more avidly bound the LDL-R than apo B_{100}, suggesting the carboxyl terminus of apo B_{100} provided some steric hindrance at the binding site.

b. Heparin Binding Sites

Glycosaminoglycans were shown to bind apo B under physiological conditions (Bernfeld et al., 1957; Iverius, 1972). Cardin et al. (1987) concluded there were two high-affinity and five low-affinity, heparin-binding sites on apo B from Scatchard analysis. These heparin-binding sites were mapped onto apo B by proteolytic cleavage and sequencing of peptides which were bound by heparin chromatography. The high- and low-affinity binding sites were found to be enriched in basic amino-acid residues and the sites were spread throughout apo B, with some close to the LDL-R binding site (Hirose et al., 1987; Weisgraber & Rall, 1987). The similar clustering of positive charge in the heparin-binding sites and the LDL-R-binding site suggested that one site may play both roles (Cladaras et al., 1986). Mahley et al. (1979) demonstrated reduction of positive charges on apo B prevented heparin-manganese precipitation and heparin-Sepharose isolation of VLDL and LDL whereas methylation of lysine residues had no effect upon heparin binding to apo B. Since methylation of lysine residues prevented the binding of the LDL-R to apo B (Tikkanen et al., 1982; Weisgraber et al., 1978), the heparin- and LDL-R-binding sites were probably distinct.

viii. Apo B Expression

In animals, the liver can produce both apo B_{48} and B_{100} for the mobilization of endogenous lipid whereas the intestine produces apo B_{48} to package exogenous lipid (Chapman. 1980). In humans. the liver produces only apo B_{100} for VLDL synthesis (Glickman *et al..* 1986; Kane *et al.,* 1980). In rats, adult liver expresses both apo B_{48} and B_{100} (Demmer *et al..* 1986; Elovson *et al.,* 1981). Apo B mRNA was observed in the adrenals (Demmer *et al..* 1986). Human and mouse heart were recently reported to express apo B_{100} and secreted LDL-sized LpB (Borén *et al.,* 1998b; Nielsen *et al.,* 1998).

Apo B was shown to be constitutively expressed in liver models. For example. butyrate stimulated apo B synthesis (Kaptein *et al.,* 1992, 1991) and insulin inhibited the secretion of apo B (Pullinger *et al.,* 1989; Sparks & Sparks, 1990) without affecting the apo B mRNA concentration. Post-transcriptional and post-translational mechanisms seem to play regulatory roles in the expression of apo B.

D. Role of Lipids in LpB Assembly

i. Phospholipids

Active synthesis of PL was demonstrated to be important in the secretion of VLDL. Yao and Vance (1988) used a choline deficient rat model to show restoration of choline or methionine to the animal restored normal VLDL secretion. Choline-deficient rats had similar numbers of LpB in their ER as normal rats; however, there was a decline in the number of particles in Golgi of choline-deficient rats. Choline-deficient rats were suggested to be degrading apo B between the ER and the Golgi (Verkade *et al.,* 1993). The secretion of carboxyl-terminal truncated apo B constructs. which form VLDL with a neutral lipid core (White *et al..* 1992). was shown to be stimulated by choline supplementation in choline-deficient rats (Vermeulen *et al..* 1997) and with PL precursors added before or during translation of the apo B construct (Rusiñol *et al..* 1996). Stimulation of VLDL secretion was neither seen when supplements were supplied after translation of the apo B construct nor from apo B constructs which did not acquire a neutral lipid core. Newly synthesised PL was preferentially added to VLDL (Rusiñol *et al..* 1997; Vance, 1989; Zhou *et al.,* 1998). The normal synthesis of PL appears to be important in synthesis and secretion of LpB. It is interesting to note active synthesis of sphingolipids does not appear to be critical in the synthesis of VLDL since the inhibition of ceramide synthesis with Fumonisin B1 did not inhibit the secretion of VLDL (Merrill *et al.,* 1995).

PL was implicated as playing an important role during the translocation of apo B. The apo B_{17} carboxyl-terminal truncation was shown to spontaneously bind PL despite its inability to acquire a neutral lipid core (Herscovitz *et al.,* 1991). Incubations with mono-

methylethanolamine (MME), a structural analogue of both choline and ethanolamine, inhibited secretion of VLDL (Vance, 1991). Further experiments with MME demonstrated the effect of MME was early in the assembly of VLDL. MME did not impair translation of apo B (Rusiñol *et al.*, 1993a); it inhibited truncated apo B constructs that were large enough to form a neutral lipid core from entering the lumen of the ER. These apo B constructs were degraded in the ER. Small apo B truncations, which did not associate with neutral lipid, were not affected by MME (Rusiñol & Vance, 1995). When MME was fed to rats, the VLDL TAG concentration was halved and the plasma concentration of apo A-I increased (Rusiñol *et al.*, 1996). Overall, these data suggest PL participates in crucial early steps in the assembly of VLDL; during translocation of apo B into the lumen of ER and during initial lipidation of apo B.

PL was shown to be a source of TAG in the assembly of VLDL. In rat hepatocytes, the loss of cellular PL label was observed to be greater than the labelled PL secreted. Incubations with PL labelled in its fatty acid moieties resulted in some of the label being recovered in the VLDL TAG (Bar-On *et al.*, 1971; Wiggins & Gibbons, 1996). The phospholipase A_2 inhibitor *p*-bromophenacyl bromide reduced secretion of TAG by 40% in rat hepatocytes (Gibbons & Wiggins, 1995a, 1995b; Wiggins & Gibbons, 1996). Apo B was reported to possess a phospholipase A activity (Parthasarathy & Barnett, 1990; Reisfeld *et al.*, 1993). This suggested apo B actively participated in its own lipidation by hydrolysing PL and incorporating fatty acids into VLDL as TAG. The elucidation of the pathway by which PL contributes to VLDL TAG may help to clarify the initial lipidation of apo B.

ii. Cholesterol and Cholesteryl Esters

A variety of approaches were employed to assess the role of cholesterol and cholesteryl esters in the assembly of VLDL. Dashti (1992) concluded incubations with cholesterol had no effect upon the secretion of apo B but 25-hydroxycholesterol was shown to stimulate the secretion of apo B by stimulating the accumulation of hepatic CE mass (Carlson & Kottke, 1989; Dashti, 1992). The secretion of apo B was shown to be inhibited by the 3-hydroxy-3-methylglutaryl coenzyme A (HMG-CoA) reductase inhibitors such as lovastatin (Cianflone *et al.*, 1990) and mevinolin (Carlson & Kottke, 1989) in the human hepatoma cell line Hep G2 and pravastatin in rabbit hepatocytes (Tanaka *et al.*, 1993). Depleting cellular CE mass, not cholesterol, was shown to be responsible for the inhibition of apo B secretion. Acyl-coenzyme A:cholesterol acyltransferase (ACAT) inhibitors were demonstrated to reduce the secretion of apo B in miniature pigs (Burnett *et al.*, 1998), African green monkeys (Carr *et al.*, 1995), and Hep G2 cells (Cianflone *et al.*, 1990; Kohen Avramoglu *et al.*, 1995). Secreted apo B mass was found to correlate best with intracellular CE mass

(Carr *et al.*, 1995; Dashti, 1992; Kohen Avramoglu *et al.*, 1995; Tanaka *et al.*, 1993). These data suggest that CE plays a critical role in the secretion of apo B.

These conclusions were contested, sometimes using the identical inhibitors in the same model system. Wu *et al.* (1994) used the same ACAT inhibitor as Cianflone *et al.* (1990) and Kohen Avramoglu *et al.* (1995) and observed no effect upon the secretion of apo B by Hep G2 cells. Wu and colleagues (1994) found only the inhibition of TAG synthesis reduced the mass of secreted apo B. Graham *et al.* (1996) were able to deplete up to 85% of the CE mass using either of two ACAT inhibitors and reduction of CE mass did not affect the secretion of apo B. The effect of cholesterol was also disputed when Furukawa and Hirano (1993) were only able to stimulate the secretion of apo B with oleate. The secretion of apo B was not affected by 25-hydroxycholesterol nor the HMG-CoA inhibitor fluvastatin despite its influence on CE mass. They concluded that only TAG synthesis protected apo B from degradation. Wu and co-workers (1994) also transfected Hep G2 cells with HMG-CoA reductase which doubled the intracellular mass of CE but did not enhance the secretion of apo B. These data seem to dispute CE as having a critical role in altering the secretion of apo B and attribute the observations of increased secretion of apo B to TAG synthesis.

There is some published evidence which suggests modest levels of CE are required to associate with apo B during VLDL assembly. The CE to apo B molar ratio was reported to be 783–1875 in the African green monkey liver perfusion model (Carr *et al.*, 1995; Rudel *et al.*, 1997) and 307–330 in the VLDL of a human patient deficient in CETP (Teh *et al.*, 1998). These observations may indicate the amount of CE present in nascent VLDL *in vivo* and suggests a role for CE in the initial lipidation of apo B.

There appears to be reasonable evidence that CE is important in the lipidation of apo B and its role may be at the initial lipidation of apo B. However, the different ACAT and HMG-CoA reductase inhibitors have displayed variable results within and between different model systems which obfuscates the exact metabolic effect of each inhibitor and the roles of cholesterol and CE in VLDL assembly.

iii. Triacylglycerol

The importance of TAG in VLDL synthesis is self-evident as the probable purpose of VLDL is the delivery endogenous TAG to extra-hepatic tissues. The metabolic origin of TAG and the mode of apo B lipidation is disputed. The *de novo* synthesis of fatty acids was demonstrated to make only a minor contribution to VLDL TAG (Kalopissis *et al.*, 1981; Gibbons & Burnham, 1991), with a calculated maximum contribution to nascent VLDL of 30% (Yang *et al.*, 1996). Other sources of TAG must be accessed in the synthesis of VLDL. Chao *et al.*

(1986) reported similar initial rates of exogenous fatty acid incorporation into the cytoplas-mic and microsomal pools of TAG. However, Gibbons *et al.* (1992) noted that there was a lag phase of 12 hours (h) before maximal secretion of TAG, which lead them to suggest ex-ogenous fatty acids first entered the storage pool of TAG before being utilized in the assem-bly of VLDL.

There are at least two distinct pools of TAG in hepatocytes: a large cytosolic pool with a slow turnover rate and a small microsomal pool with a rapid turnover rate (Bar-On *et al.*, 1971; Mayes, 1976). Labelling experiments demonstrated the secreted mass of VLDL exceeds the capacity of the microsomal TAG pool; yet, the microsomal TAG mass was main-tained (Bar-On *et al.*, 1971). Cytosolic TAG was suggested to replenish the microsomal pool. Bar-On and colleagues also reported the specific activity of glycerol label was lower in the microsomal and secreted fractions than in the cytosolic floating fat. They concluded that there was turnover of TAG when it was moved from the cytosol to the microsomes and this metabolic event removed glycerol. These observations were confirmed (Francone *et al.*, 1989; Mooney & Lane, 1981; Wiggins & Gibbons, 1992) and the TAG used in the syn-thesis of VLDL was proposed to be mobilized by complete hydrolysis to fatty acids which were re-esterified to TAG at the site of LpB assembly in the ER.

Based on the ratio of specific radioactivity of the glycerol and oleate moieties, rat hepatocytes were estimated to mobilize 70% of their VLDL TAG from a hydrolysis/re-esteri-fication cycle of cytosolic TAG (Wiggins & Gibbons, 1992). They also found Hep G2 cells were deficient in the hydrolysis/re-esterification cycle, estimating that only 20% of the VLDL TAG of Hep G2 cells was mobilized via complete hydrolysis. Since Hep G2 cells are human hepatoblastoma cells producing apo B_{100}, the cycle of hydrolysis and re-esterification was suggested to be important in the assembly of apo B_{48} but not in apo B_{100}. However, Salter *et al.* (1998) recently reported a hydrolysis/re-esterification cycle in hamster hepatocytes that was comparable to the rat. Since the liver of hamsters produces only apo B_{100}, they con-cluded that there was no significant difference in the manner in which TAG was recruited for apo B_{100} or for apo B_{48}.

In these experiments, Gibbons and co-workers only pre-incubated the hepatocytes with oleate label and did not chase with fatty acids. Their calculations of relative specific mass ratios required the hepatocytes to be chased without fatty acid to prevent dilution of labelled TAG. The system used was non-physiological since the liver is always exposed to fatty acid, either from lipoproteins in the fed state or albumin in the starved state. Elimin-ating exogenous fatty acids as a source for VLDL TAG would over-emphasize the role of stored lipid in the lipidation of apo B.

The hydrolysis of TAG for mobilization to the site of VLDL synthesis was refined by studies examining the exact stereochemistry of the cytosolic and VLDL TAG molecular species. Using chiral chromatography coupled to mass spectrometry, Yang et al. (1996, 1995) observed that the sn-1,2-diacylglycerol (DAG) moiety of TAG from VLDL and liver cytosol were similar whereas the sn-2,3-DAG moieties were different. This would require only partial hydrolysis of the cytosolic TAG to DAG for mobilization to the site of VLDL assembly. The differences at the sn-1-position suggested that some hydrolysis went beyond DAG to mono-acylglycerol (MAG). They calculated a minimum of 60% of the VLDL TAG from rats could be attributed to partial hydrolysis of stored TAG followed by re-acylation.

The partial hydrolysis of cytosolic TAG may not fully address the observed loss of glycerol label. Gibbons et al. focused upon the ratio of specific activities between the labelled fatty acid and glycerol moieties of TAG. His group reported that there was futile hydrolysis of TAG: after the cytosol TAG has been hydrolysed, it was re-esterified and the TAG remained in the cytosol (Duerden & Gibbons, 1990; Wiggins & Gibbons, 1992). Depending on the rate of this turnover, which has been suggested to be low, reports of glycerol loss during mobilization to the ER will be over-estimated and may become significant. Recognizing that complete hydrolysis was reported in a non-physiological model, partial hydrolysis of cytosolic lipid may adequately describe in vivo TAG mobilization.

The mechanism of hydrolysis of the cytoplasmic TAG has been pursued. The hydrolytic activity was reported to be inhibited by the generic lipase inhibitor tolbutamide but the activity was not sensitive to either chloroquine or 3,5-dimethylpyrazol over a 24 h period (Wiggins & Gibbons, 1992). However, Francone et al. (1989) observed inhibition of VLDL secretion by chloroquine in a 2 h incubation. The lipase was concluded neither to be lysosomal lipase nor hormone-sensitive lipase. The lipase was shown to be insulin insensitive, improving the argument against hormone-sensitive lipase as a candidate for the lipolytic activity (Gibbons & Wiggins, 1995a, 1995b; Salter et al., 1998). The hydrolysis/re-esterification cycle may be the mechanism for reduced VLDL secretion in models fed fish oils as Hebbachi et al. (1997) observed that both the cycle of hydrolysis/re-esterification and VLDL secretion were reduced in rats fed fish oils. Thus, the lipase may prefer saturated fatty acid moieties in cytosolic TAG. A TAG hydrolase activity associated with a 60 kDa protein, purified from an ER fraction and cytosolic lipid droplets in porcine liver, was proposed to be a candidate for the lipase involved in the hydrolysis/re-esterification cycle (Lehner et al., 1999; Lehner & Verger, 1997).

The mechanism of re-esterification will depend upon the degree of hydrolysis. If the cytosolic TAG were completely hydrolysed, fatty acids would be expected to form fatty acyl-coenzyme A (CoA) esters and enter the phosphatidic acid pathway to be restored to

TAG. Figure 4 depicts an overview of the *de novo* synthesis of TAG (reviewed in Lehner & Kuksis, 1996; Vance, 1996). The acylation of *sn*-glycerol-3-phosphate (G3P) by G3P acyltransferase yields 1-acyl-*sn*-glycerol-3-phosphate (AGP). An alternate source of AGP can be obtained by the acylation of dihydroxyacetone-phosphate (DHAP) by DHAP acyltransferase to 1-acyl-DHAP and subsequent reduction by the nicotinamide adenine dinucleotide phosphate (reduced form)-dependent 1-acyl-DHAP reductase. The second acylation step, catalyzed by AGP acyltransferase, produces phosphatidate from AGP. The dephosphorylation of phosphatidate by phosphatidic acid phosphohydrolase (PAPH) produces *sn*-1,2-DAG. The final step, and only committed step in the synthesis of TAG, occurs with the last acylation event when *sn*-1,2-DAG is acylated by diacylglycerol acyltransferase (DGAT). G3P and AGP acyltransferases are compartmentalized in the outer mitochondrial membrane and in the cytosolic surface of the ER. The products of phosphatidic acid, *i.e.* phospholipids, typically contain saturated acyl chains in the *sn*-1 position and unsaturated acyl chains in the *sn*-2 position, which reflects the preference of G3P acyltransferase towards saturated fatty acyl-CoA esters and AGP acyltransferase towards unsaturated acyl-CoA esters. DHAP acyltransferase is located in peroxisomes and 1-acyl-DHAP reductase activity is found both in peroxisomes and in the ER. Isoforms of PAPH can be isolated from several intracellular locations: the plasma membrane, peroxisomes, mitochondria, ER, and cytoplasm. PAPH appears to be an example of enzymatic regulation through translocation since the ER isoform can exchange between the ER membrane, where it is active, and the cytosol, where it is inactive. DGAT is localized to the cytosolic leaflet of the ER.

If the hydrolysis of cytosolic TAG were incomplete, then released DAG and/or MAG may be expected to enter the MAG pathway (see Figure 5, reviewed in Lehner & Kuksis, 1996). It should be noted that the MAG pathway is primarily found in the intestinal villi cells to process MAG and fatty acids absorbed from the gut. The direct acylation of MAG to TAG is achieved via two acylation steps in the ER. Monoacylglycerol acyltransferase (MGAT) acylates 2-MAG to DAG, producing either *sn*-1,2-DAG or *sn*-2,3-DAG. MGAT tends to acylate at the *sn*-1 position. DGAT completes the synthesis of TAG by acylating DAG. It is necessary for the DGAT associated with the MAG pathway to be active at both the *sn*-1 and *sn*-2 positions. It is possible that the DGAT activity of the phosphatidic acid and MAG pathways are different isoforms.

The *de novo* synthesis of TAG via the phosphatidic acid pathway is believed to occur on the cytoplasmic surface of the smooth ER. The assembly of lipoproteins would require the lipid synthesised to be accessible to the lumen of the ER. TAG synthesis was noted in the rough ER (Glaumann *et al.*, 1975), placing synthetic activity proximal to the translation of apo B. Carnitine acyltransferase activity in the hepatic microsomal fractions of rats was

Figure 4: **The biosynthesis of TAG from phosphatidate.** The *de novo* synthesis of TAG occurs with the sequential acylation of *sn*-glycerol-3-phosphate at the *sn*-1 position followed by the *sn*-2 position to generate phosphatidate. Dihydroxyacetone-phosphate can be acylated and then reduced to yield an alternate source of 1-acyl-*sn*-glycerol-3-phosphate. Phosphatidate is then dephosphorylated to *sn*-1,2-diacylglycerol and triacylglycerol results from the final acylation step. The enzymes in this pathway are: ① *sn*-glycerol-3-phosphate acyltransferase, ② dihydroxyacetone-phosphate acyltransferase, ③ acyldihydroxyacetone-phosphate reductase, ④ 1-acyl-*sn*-glycerol-3-phosphate acyltransferase, ⑤ phosphatidic acid phosphohydrolase, and ⑥ diacylglycerol acyltransferase.
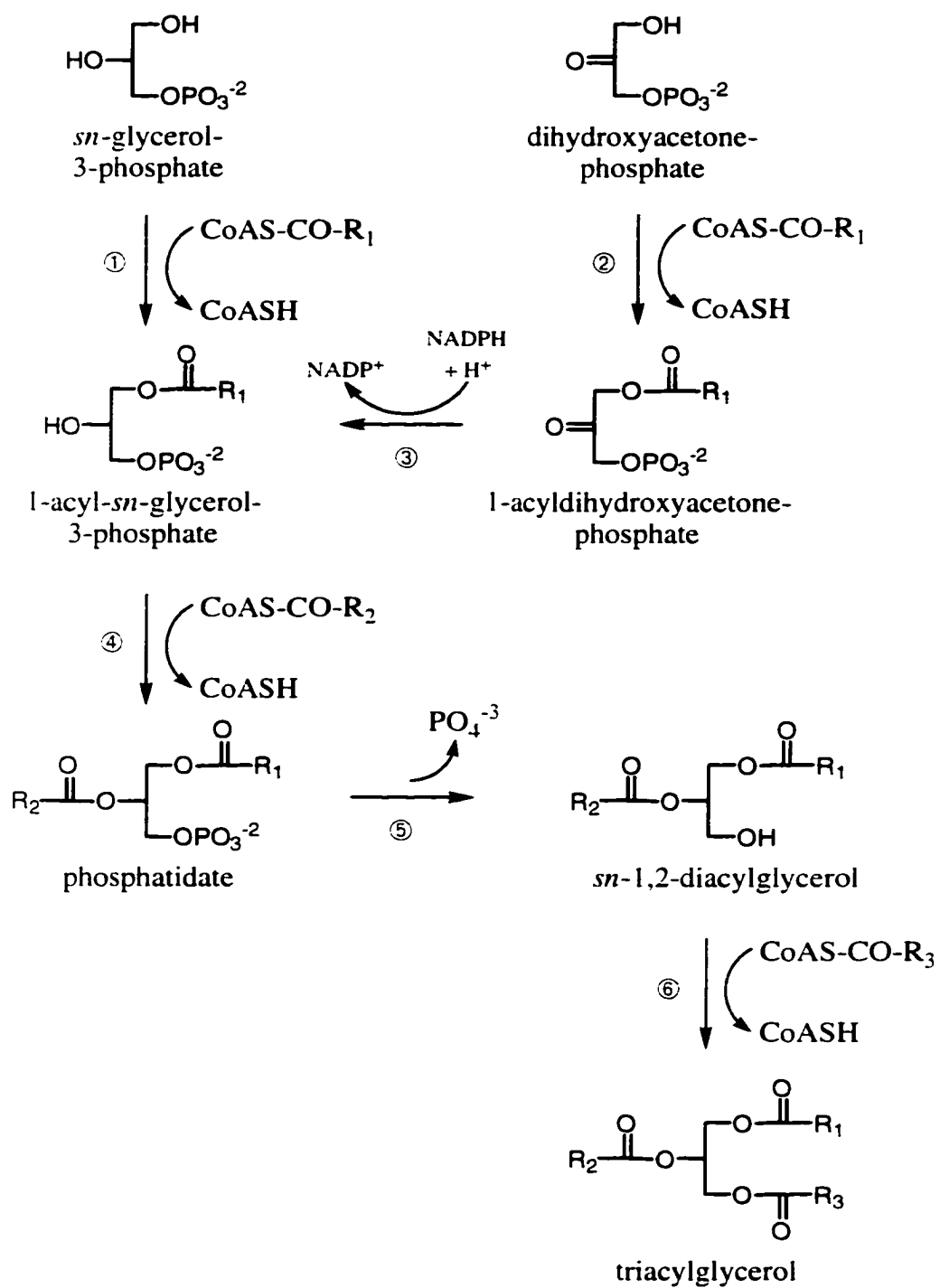
Figure 4: **The biosynthesis of TAG from phosphatidate.**
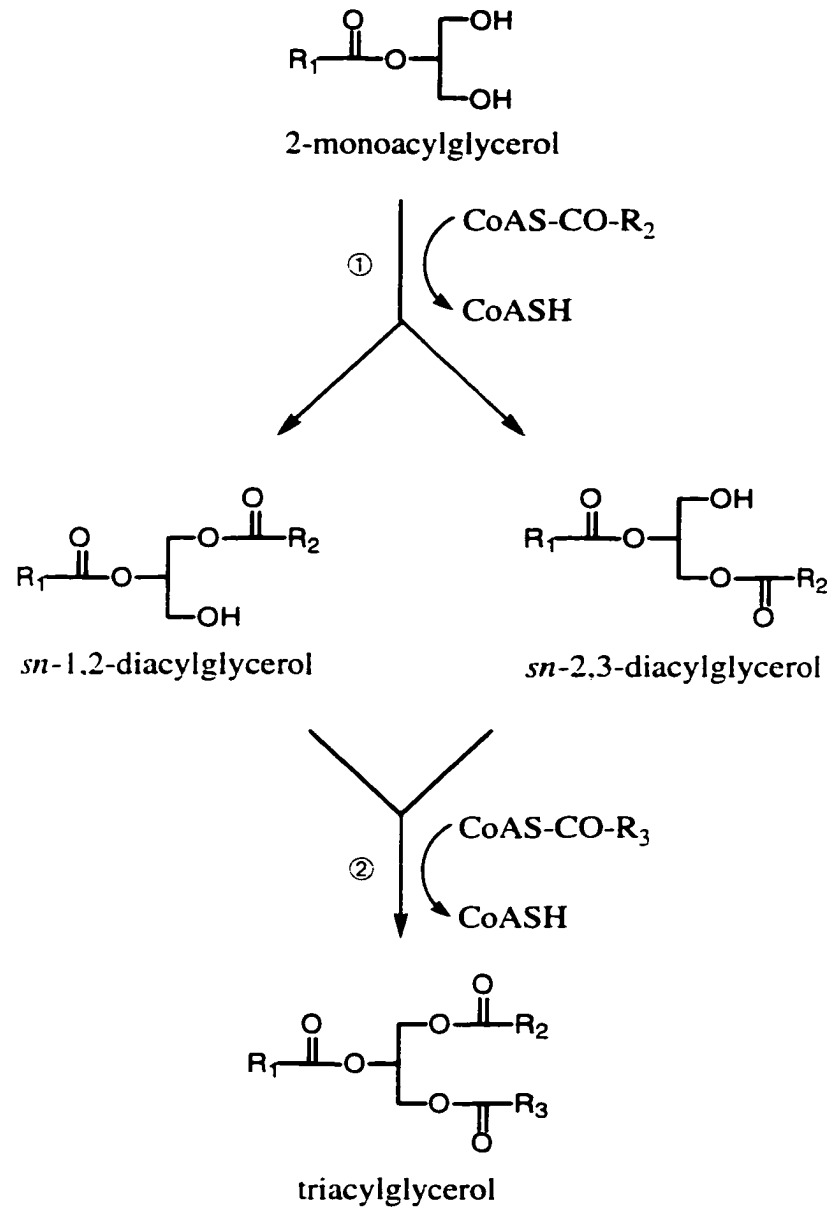
Figure 5: **The biosynthesis of TAG from MAG.** The synthesis of triacylglycerol from 2-monoacylglycerol is a result of two acyltransferase reactions catalyzed by the following enzymes: ① monoacylglycerol acyltransferase and ② diacylglycerol acyltransferase.

reported (Broadway & Saggerson, 1995a, 1995b; Lilly *et al.*, 1990; Markwell *et al.*, 1973; Murthy & Pande, 1994, 1993). This would allow for the movement of fatty acyl-CoA esters into the lumen for lipid synthesis. There were recent reports of DGAT activity in both the cytosolic and lumenal monolayers of rat hepatic microsomes (Owen *et al.*, 1997; Zammit, 1996). Thus, it was postulated that enzymes on the cytosolic leaflet of the ER synthesize *sn*-1.2-DAG and the DAG transversely diffuses across the ER membrane to the lumenal leaflet, where the proposed lumenal DGAT produces TAG from lumenal DAG and fatty acyl-CoA. The TAG produced by this lumenal DGAT may be more accessible to lipoproteins. If the lumenal and cytosolic activities of the ER DGAT were different isoforms, this could allow for independent regulation of DGAT, with the cytosolic activity being tuned to general TAG synthesis and the lumenal activity being responsive to lipoprotein-assembly feedback. Also, Coleman and Haynes (1984) observed MGAT activity in the suckling rat. Thus, it is possible that cytosolic TAG partially hydrolysed to MAG or DAG could be exported to the ER where it could be acylated to TAG via the MAG pathway. However, it should be noted that the MGAT activity reported by Coleman and Haynes declined as the rats aged, with adult rats expressing little MGAT activity in the hepatic ER. This may limit the rate at which MAG can be re-esterified to TAG, reducing its contribution to the assembly of lipoproteins. Overall, the enzymatic machinery appears to be in place to restore the lipolytic products of cytosolic TAG back to TAG in the ER lumen.

iv. Microsomal Triglyceride Transfer Protein

Wetterau and colleagues made a significant contribution to the understanding of VLDL assembly with the discovery of microsomal triglyceride transfer protein (MTP; reviewed by Wetterau *et al.*, 1997). The MTP complex was first isolated from bovine liver microsomes and was found to transfer TAG, CE, and PL between small unilamellar vesicles (Wetterau & Zilversmit, 1986, 1985, 1984). The mechanism of transport was shown to be shuttling, as a stable MTP:lipid intermediate could be isolated (Atzel & Wetterau, 1993). MTP displayed a distinct preference for the transport of neutral lipid, selectively moving TAG. CE. and PL in a molar ratio of 1:0.56:0.018, respectively. MTP poorly transported polar lipids (Jamil *et al.*, 1995; Wetterau & Zilversmit, 1985). The MTP complex was shown to be an obligate heterodimer consisting of protein disulphide isomerase (PDI), an ubiquitous microsomal protein which assists other proteins in folding by rearranging disulphide bonds (Bulleid & Freedman, 1988), and a 97 kDa MTP subunit, which contained the lipid-binding site (Wetterau *et al.*, 1991a, 1991b). MTP was only found to be expressed in liver and intestine microsomes (Wetterau & Zilversmit, 1985).

The importance of MTP was first shown when it was linked to abetalipoproteinæm-ia. Patients studied had impaired transport activity of TAG between small unilamellar vesi-cles *in vitro* (Wetterau *et al.*, 1992) and MTP mutations were observed (Sharp *et al.*, 1993). Metabolic links between apo B and MTP were displayed when the secretion of LpB from cells which do not synthesis apo B was possible only when MTP and apo B constructs con-taining the amino terminus plus lipid-binding domains were co-expressed (Gretch *et al.*, 1996; Leiper *et al.*, 1994). Physical interactions between apo B and MTP were first shown with their co-precipitation by antibodies directed against either protein (Patel & Grundy, 1996; Wu *et al.*, 1996). Hussain *et al.* (1997) demonstrated apo B bound to immobilized MTP with high affinity and MTP bound best to apo B carboxyl-terminal truncation constructs or to delipidated apo B. Lysine and arginine residues in the amino terminus of apo B. crit-ical for MTP binding, were demonstrated to be distinct from the LDL-R and heparin binding sites (Bakillah *et al.*, 1998). The amino-acid sequence of residues 430–570 of apo B was demonstrated to be crucial for binding to MTP (Hussain *et al.*, 1998) and suggested to con-tain a MTP-binding site. Thus, initial folding of the globular amino-terminal domain of apo B may present an MTP-binding site, which may start the assembly of LpB.

Wetterau and co-workers have developed inhibitors to MTP. When compound BMS-200150 was incubated with Hep G2 cells, the secretion of apo B was inhibited in a dose-dependent manner (Jamil *et al.*, 1996). When compound 9 was fed to rats. hamsters. and Watanabe-heritable hyperlipidemic (WHHL) rabbits, dose-dependent decreases were ob-served in the plasma TAG concentrations. with the WHHL rabbits reaching normal levels (Wet-terau *et al.*, 1998). Compound 9 did not appear to cause any untoward effects in the liver. Overall. these data indicate that MTP plays a crucial role in the lipidation of apo B, the heter-odimer interacts with the amino-terminal globular region of apo B, and the importance of MTP in lipidation of apo B may diminish in the later stages of VLDL assembly.

E. Assembly of LpB

i. Translation and Translocation of Apo B

The assembly of VLDL ultimately starts with the translation and translocation of apo B. It has been shown that the translocation of apo B took 10 minutes (min) in chick hepato-cytes (Janero *et al.*, 1984) and 14 min in Hep G2 cells (Olofsson *et al.*, 1987). Both were followed by a 30 min lag phase before secretion. In rat hepatocytes, most of the lag be-tween translocation and secretion of apo B occurred in the ER (Borchardt & Davis, 1987); however. it was reported that in chick hepatocytes the half-time through the Golgi was twice that of the ER (Bamberger & Lane, 1988). These differences may reflect variation between birds and mammals.

The rate of both translation and translocation was suggested to be variable and both processes were reported to temporarily suspend and then resume (Chuck *et al.*, 1990; Pease *et al.*, 1995). These events were termed translational pausing and translocational pausing. Translocational pausing was demonstrated to be independent of translational arrest when apo B constructs were translated without microsomes. When microsomes were added to the system, translocational pausing was observed as the translated apo B construct inserted into the ER lumen (Chuck & Lingappa, 1993). A controversial proposal has been put forth suggesting that translocational pausing of apo B can occur while translation is active, resulting in domains of apo B which are cytosolically exposed. The cytosolic presentation of apo B domains was demonstrated by proteolytic degradation of apo B domains that were not protected by microsomes, immunodetection of exposed apo B epitopes that were not shielded by microsomes, and UV cross-linking of apo B to peripheral membrane proteins associated with ribophorins on the cytoplasmic leaflet of the ER (Chuck *et al.*, 1992; Chuck & Lingappa, 1993, 1992; Davis *et al.*, 1990; Du *et al.*, 1998; Du *et al.*, 1994; Hegde & Lingappa, 1996). After the resumption of translocation, protease protection was restored and immunodetection was eliminated which suggested that apo B had exited from its paused state and became fully translocated into the lumen of the microsomes. These exposed domains of apo B were atypical transmembrane structures as apo B was extractable from microsomal membranes by alkaline carbonate, similar to peripheral membrane proteins. The protease inhibitor *N*-acetyl-leucyl-leucyl-norleucinal (ALLN) increased the proportion of apo B in the paused state which suggested that paused apo B tended to be degraded (Du *et al.*, 1998). Translocational pausing was enhanced in hepatocytes from rats fed MME, suggesting that microsomes enriched in MME-containing PL were more prone to pausing (Rusiñol *et al.*, 1998). A 33-amino-acid sequence in apo B was reported to mediate translocational pausing (Chuck & Lingappa, 1992) and hydrophilic residues were found to be critical to translocational pausing (Chuck & Lingappa, 1993). Assessment of the apo B sequence revealed three regions containing clusters of pause sequences: the amino-terminal 20%, the 44–47% region from the amino terminus, and the 65–95% region from the amino terminus of apo B. However, a consensus sequence for translocational pausing was not found (Kivlen *et al.*, 1997). These experiments were done with rabbit reticulocyte, dog pancreas, wheat germ, and rat hepatocyte lysates which would suggest that translocational pausing is a generalized phenomenon for apo B, not a hepatocyte-specific event.

These data have been contested by other groups who reported the efficient translocation of apo B. They observed apo B to be resistant to proteolytic degradation throughout translation and translocation (Ingram & Shelness, 1996; Leiper *et al.*, 1996; Pease *et al.*, 1995, 1991; Shelness *et al.*, 1994; Tran *et al.*, 1998). Apo B was also glycosylated (Leiper

et al., 1996; Pease *et al.*, 1991; Shelness *et al.*, 1994; Wong & Torbati, 1994), which suggested apo B had entered the ER. Some of the experimental protocols used by Lingappa and co-workers (Hegde & Lingappa, 1996) to demonstrate translocational pausing employed a translation "trap"—the mRNA lacked a stop codon so apo B would remain bound to the ribosome as a peptidyl-transfer ribonucleic acid (tRNA). Pease and co-workers (1995) have challenged this method, showing that the persistence of the tRNA was responsible for the formation of transmembrane structures since apo B expressed from constructs including stop codons was protected from proteolysis.

ii. Regulation of Apo B by Degradation

Based upon observations that radiolabelled apo B was lost from cellular samples and the label was not fully recovered in the media, apo B appears to be degraded intracellularly (Adeli, 1994; Bonnardel & Davis, 1995; Borchardt & Davis, 1987; Borén *et al.*, 1990; Boström *et al.*, 1988; Davis *et al.*, 1990, 1989; Furukawa *et al.*, 1992; Rusiñol & Vance, 1995; Sakata *et al.*, 1993; Sato *et al.*, 1990; White *et al.*, 1992; Yao *et al.*, 1997). The amount of degradation was high, with up to 64% of apo B lost in rat hepatocytes (Borchardt & Davis, 1987). Thus, the answer for coordinating protein and lipid synthesis in the assembly of lipoproteins appears to lie in constitutive synthesis of apo B, which allows the availability of lipid components to regulate assembly. When conditions permit sufficient quantities of lipid to be available, a nascent LpB appears to be assembled and secreted. When conditions are not suitable for the delivery of lipid to apo B, poorly lipidated apo B appears to be destined for proteolysis.

The site of degradation is controversial. Insulin was shown to stimulate the degradation of apo B by increasing its level of phosphorylation in the Golgi (Sparks & Sparks, 1990). This suggested the Golgi apparatus is the site of degradation. Monensin, an inhibitor of vesicle transport from the *trans*-Golgi to the plasma membrane (Mollenhauer *et al.*, 1990), was used to show that there was no lag phase between the restoration of protein secretion and the resumption of apo B secretion (Furukawa *et al.*,1992). This suggested a pool of secretion-competent LpB in the Golgi was resistant to degradation. Wang *et al.* (1995) showed apo B degradation was inhibited by monensin, suggesting a post-Golgi compartment contributed to apo B degradation. However, Davis *et al.* (1990) suggested degradation of apo B was completed in the ER when they were not able to detect degradation peptides from apo B in the Golgi. The use of brefeldin A (BFA), an inhibitor of vesicle transport from the ER to Golgi but not the retrograde transport from *cis*-Golgi to ER (Fujiwara *et al.*, 1988), yielded variable results. BFA was shown 1) to reduce the degradation of apo B in rat hepatocytes (Wang *et al.*, 1995), 2) to have no effect on the rate of degradation

of apo B in choline-deficient rat hepatocytes (Fast & Vance, 1995), and 3) to stimulate degradation of apo B in Hep G2 cells (Furukawa et al., 1992: Sato et al., 1990). Conflicting conclusions have been drawn about the site of apo B degradation, which may reflect the mixing of ER and Golgi by BFA in the different models and conditions used.

There are separate pools of apo B within the secretory apparatus: membrane-associated and lumenal (Bamberger & Lane, 1988; Borén et al., 1990; Boström et al., 1986; Cartwright & Higgins, 1995). A comprehensive study by Cartwright and Higgins (1996) demonstrated different protease activities throughout the secretory pathway were involved in the degradation of apo B. The use of o-phenanthroline, a zinc metalloprotease inhibitor, or leupeptin, a serine/cysteine protease inhibitor, increased the mass of apo B secreted into the media, found in the lumenal Golgi, and associated with microsomal membranes (also Wang et al., 1995). ALLN, calpain inhibitor I, or aprotinin, a serine protease inhibitor, prevented the loss of apo B from the membrane fraction of the trans-Golgi but there was no change in the mass of apo B found in the Golgi lumen or secreted into the media (also Bonnardel & Davis, 1995; Rusiñol & Vance, 1995; Sakata et al., 1993). Also, Adeli et al. (1997a) have identified an ALLN-sensitive protease from the ER of Hep G2 cells which associates with apo B. Thus, it appears that there are two pools of apo B in the microsomes: a proteolytic-susceptible membrane-associated pool and a secretion-competent lumenal pool. It should also be noted that lumenal degradation of apo B has been observed in the ER (Adeli et al., 1997b; Cartwright & Higgins, 1995). Apo B appears to have the opportunity to shift from the membrane pool to the lumenal pool and become secretory competent: however, Apo B which was associated with the membrane upon reaching the trans-Golgi appears to be doomed to destruction by protease activities that are sensitive to either ALLN or aprotinin.

The shift from the membrane-associated, degradation-susceptible fraction to the lumenal secretory-competent fraction was best affected by incubations with exogenous fatty acid, especially oleate (Boström et al., 1988; Cartwright & Higgins, 1996; Dixon et al., 1991; Moberly et al., 1990). By stimulating the synthesis of lipid, with TAG in particular, more apo B mass was found to shift from the membrane fraction to the lumen of the ER. The increased secretion of apo B from hepatocytes incubated with oleate was not due to increased synthesis of apo B (Boström et al., 1988; Dixon et al., 1991). The synthesis and/or mobilization of lipid appears to be limiting in the assembly of LpB.

A new development in the degradation of apo B is the proposed involvement of the proteasome (reviewed in Coux et al., 1996). Proteins bound to the ER membrane and ER lumenal proteins were previously demonstrated to be transferred from the ER to the cytosol for degradation by the proteasome (Werner et al., 1996; Wiertz et al., 1996). Cellular apo

B was shown to be ubiquitinated in Hep G2 cells and proteasomal inhibitors reduced apo B degradation in Hep G2 cells (Benoist & Grand-Perret, 1997; Fisher *et al.*, 1997; Yeung *et al.*, 1996; Zhou *et al.*, 1998). However, the proteasome inhibitor MG132 was shown not to affect the degradation of apo B_{100} in the rat hepatoma line McA-RH7777 (Tran *et al.*, 1998). Inhibitors of the proteasome, which were observed to decrease the amount of apo B degraded. did not stimulate secretion of apo B. This suggested proteasomes were digesting apo B which was not in the secretory-competent pool. Translocational arrest was proposed to be linked to degradation since inhibiting proteasomes antagonized the increased degradation of apo B caused by inhibiting MTP (Benoist & Grand-Perret, 1997). Also, ubiquitination of apo B was observed to occur before apo B was fully translocated (Zhou *et al.*, 1998). Full-length apo B. which had been glycosylated, was also observed to be ubiquitinated (Liao *et al.*, 1998). This suggested apo B, which was in the ER for glycosylation. was returned to the cytosol for ubiquitination. Cytosolic chaperone proteins have been shown to mediate the interaction of apo B with the proteasome (Fisher *et al.*, 1997; Zhou *et al.*, 1995). Thus, if apo B was improperly translocated, cytosolic chaperones may interact with domains of apo B exposed to the cytosol. The binding of chaperones may direct the ubiquitination of apo B. targeting it for proteasomal termination. Translocated apo B may also be returned to the cytosol for a similar fate.

Overall, a variety of conditions, which may restrict the assembly of LpB, appears to leave poorly lipidated and improperly folded apo B associated with the microsomal membranes. It appears that the membrane-associated, secretion-incompetent apo B can be eliminated by proteolytic digestion by a number of enzyme activities throughout the secretory pathway.

iii. Lipidation of Apo B

The mechanism of lipidation of apo B is a topic that continues to be highly controversial and the exact site of lipidation in the secretory pathway is contested. Transit through the ER was observed to determine the rate of apo B secretion (Borchardt & Davis, 1987). The immunoprecipitable apo B particles from the ER and Golgi were found to be similar (Rusiñol *et al.*, 1993b), suggesting that LpB are completely assembled before exiting the ER. Other groups concluded the Golgi was the site of lipidation since the half-life of apo B in the secretion pathway was reported to be longer in the Golgi than in the ER (Bamberger & Lane. 1988) and the majority of lipid was co-precipitated with apo B from the *trans*-Golgi (Higgins, 1988). Also, apo B was predominantly associated with the membrane fraction until it reached the Golgi where more was able to move into the lumenal fraction (Cartwright & Higgins, 1992). However, some workers concluded apo B acquires some

lipid in the ER and the remainder in the Golgi (Borén *et al.*, 1992; Boström *et al.*, 1988, 1986: Cartwright & Higgins, 1995; Janero & Lane, 1983; Swift, 1995).

Lipidation of apo B was postulated to commence as apo B was translated and translocated into the ER. Apo B was shown to interact with ER chaperones independently of its lipidation state (Linnik & Herscovitz, 1998). These interactions with ER chaperones may mediate the initial folding of apo B. Since apo B is very hydrophobic and the amino terminus can associate with PL, the initial folding of the amino terminus of apo B to a globular structure was suggested to promote the association of apo B with the lumenal leaflet of the ER (Boström *et al.*, 1986; Knott *et al.*, 1986a; Olofsson *et al.*, 1987). This would allow apo B to acquire PL and cholesterol. The presence of apo B may stabilize the membrane and could allow significant quantities of neutral lipid to build up between the leaflets of the ER membrane. The nascent VLDL would join the secretion-competent pool by budding off from the membrane. Some TAG (Glaumann *et al.*, 1975) and CE (Hashimoto & Fogelman, 1980) synthesis was reported in the rough ER, which would be required for this proposal.

The discovery of MTP complicated this story. MTP was recognized to interact with the amino terminus of apo B after initial folding and disulphide formation (Ingram & Shelness, 1997). This interaction occurred both co- and post-translocationally. The presence of MTP may permit apo B to behave more like a typical secretory protein, with apo B directly entering the lumen of the ER and folding into its native conformation while receiving lipid from MTP (Gordon, 1997). However, this would contradict the observations that apo B is associated with the membrane. Perhaps availability of lipid and the rate at which MTP can deliver lipid while apo B is being translated/translocated will determine whether apo B will go directly into the lumen or if it will first associate with the lumenal leaflet of the ER to acquire lipid. Since MTP preferentially transfers neutral lipid over PL, all apo B may spend a portion of its time interacting with ER membrane to acquire PL and cholesterol. In conditions where lipid availability to apo B is good, the association between apo B and the ER membrane may be brief. Apo B was shown to associate with membrane fractions in the smooth ER, suggesting that apo B can move into the ER lumen at a later time (Cartwright & Higgins, 1995). Apo B appears to be lipidated both co-translationally and post-translationally. In conditions where lipid is not as readily available, the shift of apo B to the lumen could be assisted by MTP (Hamilton *et al.*, 1998). Rustæus *et al.* (1998) used BFA to increase the size of the apo B pool associated with the ER membrane in the McA-RH7777 model. Inhibiting MTP impaired the movement of apo B_{100} from the membrane pool into the lumen of the ER. Thus, MTP may be required to properly lipidate the amphipathic β-sheets of apo B which irreversibly bind lipid.

The exact mechanism of lipidation of apo B is disputed. The argument centres around the mode of lipidation: is the lipidation of apo B, or the assembly of LpB, a continuous process or does it occur in discrete phases? The literature refers to the one- and two-step models. The one-step model asserts that apo B is continuously lipidated whereas the two-step model asserts that apo B is initially lipidated by MTP but the bulk of lipid is added later by interacting and merging with lipid droplets in the ER.

The secretory pathway was shown to contain apo B particles at different densities. The particles were found in the HDL and in the LDL-VLDL density ranges (Borén et al., 1992; Boström et al., 1988). The HDL-like apo B particles may represent apo B in its initial stages of lipidation, having acquired some neutral lipid, and the VLDL-sized particles would probably be a secretion-competent particle, having completed its assembly.

The two-step model suggests there are distinct rates at which lipid is added to apo B. Assembly of LpB was reported to occur in the chick hepatocyte with biphasic kinetics (Janero & Lane, 1983), suggesting a multi-step mode of assembly. The McA-RH7777 rat hepatocyte cell line was used to demonstrate the two steps can be dissociated. When cells were incubated in normal media, only particles of HDL density were produced, which represented the product of the first step. When oleate was added, LpB of VLDL density were secreted. Thus, the addition of exogenous fatty acid was concluded to rescue the second step in McA-RH7777 cells. (Borén et al., 1994) Borén and co-workers also noted in pulse-chase studies that cycloheximide had no effect on the secretion of labelled apo B_{100} 15 min after the chase, which corresponds to the time it takes for apo B_{100} to be translated. Adeli and co-workers (1997b) also observed in Hep G2 cells that the shift of apo B_{100} from the ER membrane fraction to the lumenal fraction was not inhibited by cycloheximide. Only active translation of apo B_{100} appeared to be required for the assembly of LpB_{100}. However, secretion of apo B_{48} by McA-RH7777 cells was impaired by cycloheximide throughout the incubation. Thus, another gene product may be required for the lipidation of apo B_{48} but was not required for apo B_{100}.

During vesicle trafficking in the secretory pathway, adenosine diphosphate-ribosylation factor (ARF) binds to a membrane to initiate formation of coatomers. ARF is a guanine nucleotide-binding protein. When ARF binds guanosine triphosphate (GTP), ARF can associate with membranes. With the hydrolysis of GTP to guanosine diphosphate (GDP) plus phosphate ion, ARF dissociates from the membrane. Once ARF releases GDP, it can bind GTP to re-associate with membranes. BFA is believed to inhibit a nucleotide exchange enzyme, trapping ARF in its soluble, GDP-bound form (Donaldson et al., 1992; Helms et al., 1993; Randazzo et al., 1993).

Incubating McA-RH7777 cells with low concentrations of BFA, which still allowed for some protein secretion, inhibited apo B_{48} particles of HDL density from maturing to VLDL size (Rustæus *et al.*, 1995). The second step of apo B lipidation appeared to be inhibited. This effect was reversible since removing BFA from the incubation medium restored VLDL secretion in approximately one hour. These observations lead Rustæus and colleagues to postulate that the second step required a GTP/GDP-dependent cycle.

In a seminal study by Gordon *et al.* (1996), transfection of apo B_{53} and MTP into HeLa cells, a cervical cell line that abundantly synthesis lipid, did not result in the secretion of VLDL or chylomicrons. Only a LpB of HDL density was secreted by the transfected HeLa cells. These observations suggested the initial lipidation of apo B could be achieved only by the co-expression of MTP and other factors were required for the complete assembly of LpB. These investigators also used BMS-192951, a MTP inhibitor that becomes active when irradiated with UV light at 365 nm, in McA-RH7777 cells to study the assembly of LpB. When the rat hepatoma cells were pulsed to label apo B, irradiated to activate BMS-192951, and then chased, VLDL secretion was inhibited. If the irradiation occurred after the completion of the first step, normal VLDL was secreted. This also suggested that MTP was required only for the initial lipidation of apo B. However, these findings were contradicted by Wang *et al.* (1997), who also used the MTP inhibitor BMS-192951 in the McA-RH7777 cell model. Wang and colleagues found that inhibiting MTP abolished the secretion of VLDL but did not eliminate the formation of HDL-sized LpB_{48}. These observations suggested that MTP was required for the addition of bulk lipid during the second step of VLDL assembly.

The proposal that the second step occurs by the fusing of HDL-sized LpB with apoprotein-free particles was based upon observations of lipid droplets in the smooth ER of rat hepatocytes (Alexander *et al.*, 1976). Immunoelectron microscopy methods suggested these lipid droplets did not contain apo B. Recently, similar observations have been made in the enterocytes of mice that only express apo B in the liver and yolk sac. These cells formed chylomicron-sized lipid particles in the smooth ER despite the inability of intestinal cells to produce apo B (Hamilton *et al.*, 1998). These chylomicron-like particles were not secreted for the most part. Perhaps an intestinal and hepatic-specific ARF directs lipid into the lumen of the ER to form lumenal lipid droplets.

The most compelling data to support the single-step model was provided by a comparison of immunoprecipitated apo B from the ER and Golgi of rat hepatocytes. The molar ratio of apo B to lipid was similar between those two subcellular fractions although the mass of apo B was 7–10 fold higher in the Golgi (Rusiñol *et al.*, 1993b). LpB particles of HDL density, which are postulated to be the particles formed after the first step of the two-step model, should have reduced the TAG to apo B ratio in the ER. This would suggest either

they were absent or that they were rapidly converted to VLDL. These data suggested the bulk of lipid had associated with apo B before entering the Golgi but would not preclude lipid exchange in the Golgi.

Overall, it would seem that the bulk of lipid is added to apo B while it is in the ER and once the apo B particles move to the Golgi, the lipid content of the LpB could exchange with the lipid pool in the Golgi. Variations between experimental models may reflect differences in the rate at which LpB proceeds through the secretory pathway and in the availability of lipid, especially TAG.

iv. Model of VLDL Assembly

A favoured model of VLDL assembly which is emerging is depicted in Figure 6. This model may be extended to include chylomicron assembly. Apo B is translated and translocated into the ER. Apo B may interact with the lumenal leaflet of the ER, where it can acquire PL and cholesterol. After the initial folding of the amino terminus of apo B, MTP can recognize and begin its essential transfer of neutral lipids to apo B. With this initial acquisition of lipid, apo B is transformed into an HDL-sized lipoprotein. Depending upon factors such as the availability of lipid, this initial stage of lipidation may occur co-translationally or post-translationally. The portion of apo B which remains associated with the membrane tends to be degraded. There appears to be numerous proteolytic activities throughout the secretory pathway to eliminate apo B that becomes misfolded or poorly lipidated. The second phase of apo B lipidation adds the bulk of the core lipids found in VLDL. This step may draw upon lipid stored in the cytosol which is mobilized by a lipolytic event. Lipolysis of cytosolic TAG may be complete (Wiggins & Gibbons, 1992) or partial (Yang et al., 1996, 1995). Mobilized fatty acyl-CoA, MAG, and DAG are synthesized back to TAG for assembly. The final enzymatic step is catalyzed by DGAT, which is normally associated with the cytosolic surface of the ER membrane. There may also be a lumenal DGAT activity (Owen et al., 1997). The mobilized lipid may form apoprotein-free liposomes (Alexander et al., 1976; Hamilton et al., 1998) which seems to involve a GDP-GTP cycle (Rustaeus et al., 1995). The transfer of lipid from the synthetic site to the liposomes may be assisted by MTP (Hamilton et al., 1998). A fusion event between an HDL-like LpB and a lipid droplet results in the formation of a nascent VLDL in the ER. The nascent VLDL continues on through the secretory pathway and is secreted.

F. The Hep G2 Cell Line

The Hep G2 cell line was derived from a hepatic biopsy from a 15-year-old male Caucasian (Aden et al., 1979). The Hep G2 cell line is believed not to be infected with the
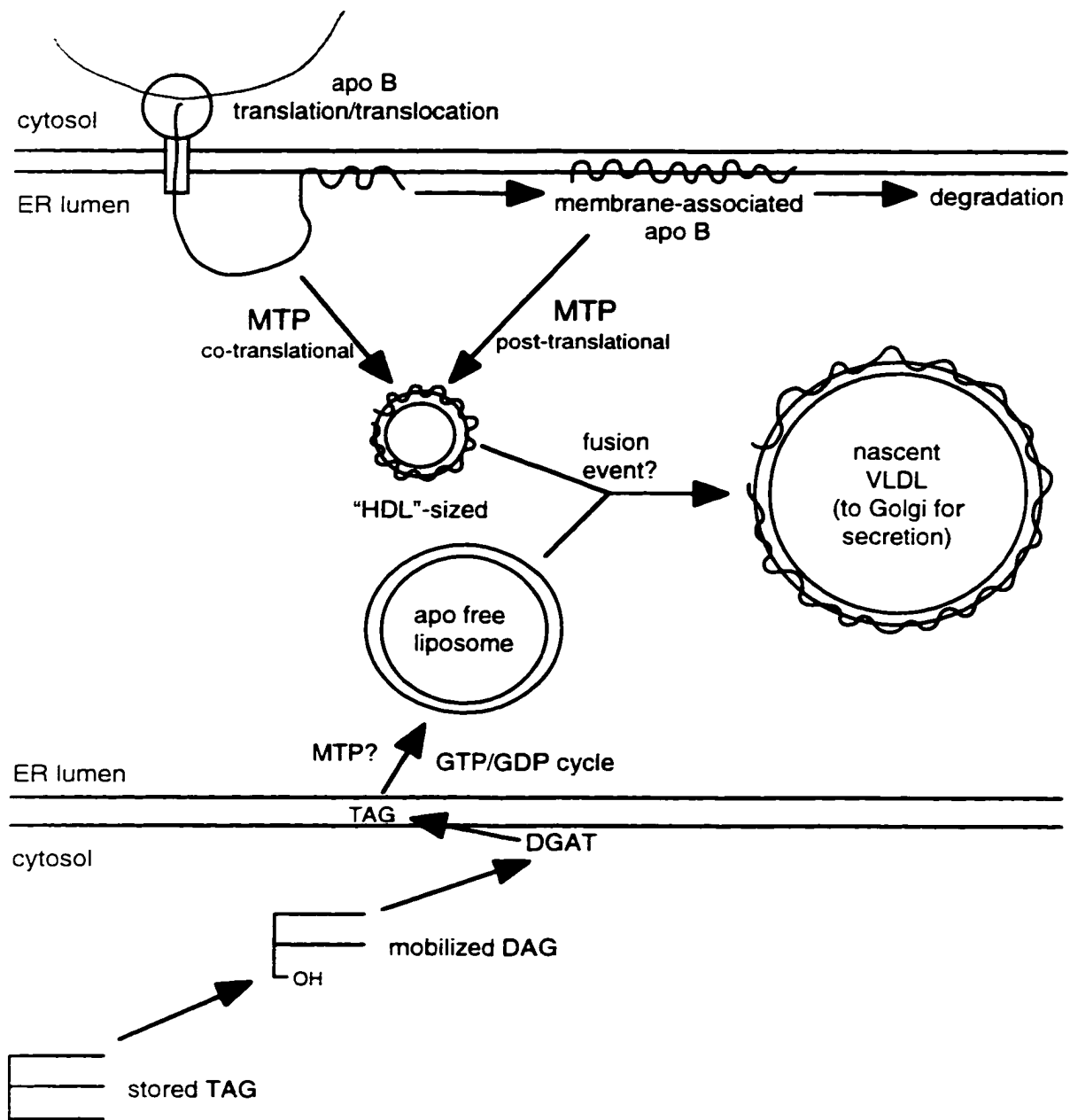
Figure 6: **The assembly of nascent VLDL.**

hepatitis B virus since the hepatitis virus has not been observed to be integrated into its genome nor does Hep G2 appear to express the hepatitis B surface antigen (Knowles et al., 1980). Hep G2 cells were found to synthesize a range of major proteins (e.g. albumin. fibrinogen. plasminogen, and transferrin) and receptors (e.g. LDL, œstrogen. and insulin receptors) which would be expected to be produced by hepatocytes (Knowles et al.. 1980). Its ease of maintenance along with its perceived absence of hepatitis B made Hep G2 cells popular in a wide variety of cellular and metabolic studies. including the metabolism of cocaine (Falk et al., 1995) and the uptake of plutonium (Planas-Bohne & Duffield, 1988). Hep G2 first showed promise as a model system for lipoprotein metabolism when it was shown to produce the major apoproteins: apo A-I, A-II, B_{100}, C-I, C-II, and E (Zannis et al.. 1981). Hep G2 cells robustly produce lipids (reviewed in Dixon & Ginsberg, 1993: Javitt. 1990). The secretion of lipoproteins (Rash et al.. 1981), the receptor-mediated endocytosis of LDL (Havekes et al., 1983), and the down-regulation of the LDL-R and HMG-CoA reductase by LDL cholesterol (Dashti et al.. 1984) were reported. These initial observations spawned numerous lipoprotein studies which have made the Hep G2 cell line a well defined system.

There are issues which detract from Hep G2 being a good model of lipoprotein metabolism. It has a modal chromosome number of 55 which stems from trisomies of chromosomes 1, 6, 9, 15, and 17 and a tetrasomy of chromosome 2 (Simon et al.. 1982). This is a concern since apo B is on chromosome 2. Also. it is unknown if regulatory systems are compromised by these chromosomal abnormalities. Hep G2 cells fail to synthesis LpB of VLDL size. Although it does secrete TAG-rich particles. the LpB are the size of LDL (Dashti et al.. 1987: Dashti & Wolfbauer, 1987: Dixon & Ginsberg, 1993: Ellsworth et al.. 1986: Gibbons et al., 1994: Homan et al., 1991: Thrift et al.. 1986: Wang et al.. 1988). This was interpreted as a failure of Hep G2 to preform the second step of apo B lipidation (Gibbons et al.. 1994). Nevertheless, Hep G2 should be viewed as a mutant model system which may contain important evidence of the mechanism of apo B lipidation. Restoration of normal VLDL secretion in the Hep G2 cells line would mark a significant advancement of the understanding of lipoprotein metabolism.

The cell culture medium used to incubate Hep G2 cells was phenol red free. Phenol red was demonstrated to be a weak œstrogen (Berthois et al., 1986). Physiological concentrations of 17β-œstradiol in Hep G2 were shown to increase apo C-II concentrations 2.5 fold and apo A-I concentrations 2 fold compared to controls (Tam et al.. 1985). The increased apoprotein mass was due to elevated levels of apo A-I (Archer et al., 1986) and apo C-II mRNA (Archer et al., 1985) and the augmented levels of apo A-I and apo C-II secreted into the medium could be antagonized by testosterone (Tam et al.. 1986). Apo B

and apo E were not affected by 17β-œstradiol at physiological concentrations but were induced at a pharmacological dose of 500 nM (Tam *et al.*, 1986). Also in Hep G2 cells, 17β-œstradiol induced a 141% increase in LDL-R-specific surface binding (Semenkovich & Ostlund, 1987). Thus, the inclusion of phenol red in the culture medium at a typical concentration of 28.2 μM in MEM may be sufficient to stimulate the induction of apo A-I, B, C-II, and E as well as the LDL-R. Alterations in apoprotein and LDL-R expression may impact upon apoprotein distribution amongst the lipoproteins, may increase the total CE content of the lipoproteins via increased concentrations of apo A-I interacting with LCAT, and may increase the removal of lipoproteins from the medium by enhanced receptor-mediated endocytosis.

G. Rationale

Work done previously in the Breckenridge laboratory examined the lipoproteins secreted by the Hep G2 cell line. Concerns were raised about the analysis of the whole media to determine the lipid composition of the LpB. Since the Hep G2 cell line only secretes a minute portion of its total cellular lipid, cell lysis may add similar amounts of lipid to the media. Hep G2 also secretes apo As; thus, a portion of the total lipid in the media should be assigned to HDL, not LpB.

The first goal of this project was to refine the analysis of lipoproteins secreted by Hep G2 cells by isolating and concentrating the lipoproteins by affinity chromatography. By employing serial chromatography, LpB may be isolated from the media followed by the isolation of the apo A-containing lipoproteins. In concert with the chromatographic fractionation of media, the influence of exogenous fatty acids upon lipid composition of secreted lipoproteins may be studied.

The second goal of this project was to study the role of exogenous fatty acids and endogenous stored lipid on the assembly of LpB. This was done with two major studies involving novel pulse-chase experiments. Pulse-chase studies could be done using lipid mass—not radiolabels—by determining total lipid profiles by gas-liquid chromatography. Hep G2 cells were incubated with oleate to load the endogenous lipid pool with oleate-containing species. This would be most evident in the TAG pools. The cells would be chased with myristic acid, a fatty acid at minor concentrations under normal physiological conditions. By observing the lipid species for oleoyl and myristoyl moieties and the time it takes for them to appear in the media, conclusions may be drawn regarding the utilization of stored lipid and newly acquired fatty acids in the assembly of LpB. How rapidly can exogenous fatty acids be incorporated into secreted LpB? Is the stored TAG partially hydrolysed to DAG or MAG? Is it completely hydrolysed to glycerol? Or is the stored TAG added to apo B without modification?

The first study used a simple time course in which the Hep G2 cells were chased with myristate for up to 12 h. This would define the transition from employing oleate-containing lipids stored during the loading incubation to using the myristate from the chase incubation for the synthesis of lipoproteins. The second study sought to improve on confounding results. The presence of palmitate impaired the interpretation of the lipid species. By adding an inhibitor of fatty acid synthase during the incubations of the second study, it was hoped that the data would be improved. Also during the second study, the cells were chased with myristate for two sequential incubations. This should help to define whether the LpB assembly process has access to the stored oleate-containing lipid pools throughout the chase period. After Hep G2 cells start incorporating the myristate into the secreted lipoproteins. does the lipoprotein synthesis still have access to the stored oleate? Or is the synthesis of lipoproteins in Hep G2 cells driven by the supplied exogenous fatty acids?

II. Materials and Methods

A. Materials

Hep G2 cells were obtained from the American Tissue Culture Collection (Rockville. Maryland). Minimum essential media (MEM) Eagle modified and phenol red free. sodium bicarbonate, D-(+)-glucose, sodium oleate, sodium myristate, cholesterol, tricaprin, cholesteryl palmitate, cholesteryl oleate, trimyristin, tripalmitin, triolein. sodium dodecyl sulphate (SDS), phenylmethylsulphonyl fluoride (PMSF), Folin & Ciocalteu's phenol reagent. phospholipase C (PLC) type 1 from *Clostridium perfringens (C. welchii)* EC 3.1.4.3, tris(hydroxymethyl)aminomethane (Tris), tris(hydroxymethyl)methylglycine (Tricine), *N*-polyethyleneglycol 6000 (PEG), cerulenin, [1-^{14}C]-acetic acid (aqueous), and [1-^{14}C]-myristic acid (ethanol solution), were purchased from Sigma-Aldrich Canada (Oakville. Ontario). Dulbecco's phosphate buffered saline (PBS), fetal bovine serum (FBS). L-glutamine (100x solution). MEM non-essential amino acids (100x solution), MEM sodium pyruvate (100x solution). penicillin G sodium salt (10,000 units/ml)–streptomycin sulphate (10,000 μg/ml solution), trypsin–ethylenediamine tetraacetic acid (EDTA; 10x solution), and porcine intestinal mucosa heparin were purchased from Life Technologies Gibco BRL (Burlington, Ontario). Fatty-acid-free or enzyme-linked-immunosorbent-assay grade bovine serum albumin (BSA) was purchased either from Sigma or from Randox Laboratories (Mississauga. Ontario). Costar 96-well microtitre plates and Corning T-75 and T-150 cell culture flasks were obtained from Corning Costar (Cambridge, Massachusetts). FALCON 6-well culture plates were obtained from Becton Dickinson (Mississauga, Ontario). Nalgene cellulose nitrate sterilization filter units (0.2 μm, 115 ml capacity) and surfactant-free cellulose acetate bottle-top filters (0.2 μm. 500 ml capacity) were obtained from Nalge (Rochester. New York). Heparin-Sepharose CL-6B was purchased from Pharmacia Biotech Canada (Baie d'Urfé. Québec). Bio-Gel hydroxylapatite (HTP) and Econo-Pac HTP cartridges were purchased from Bio-Rad (Mississauga, Ontario). Spectra/Por dialysis tubing (54 mm x 50 feet. 3.5 kDa molecular mass cut-off) was obtained from Spectrum Medical Industries (Houston. Texas). SeaKem LE agarose and GelBond plastic gel supports were obtained from FMC BioProducts (Rockland, Maine). Ovine anti-human apo A-I antibody and ovine anti-human apo B antibody were purchased from Bœhringer Mannheim Canada (Laval, Québec). Anti-human apo E antibody from rabbit was prepared previously (Tam *et al.*, 1981). Anti-human albumin antibody from rabbit was obtained from Behring Diagnostics (Somerville, New Jersey). *N,O*-bis[trimethylsilyl]trifluoroacetamide (BSTFA) was purchased from Supelco (Oakville, Ontario). A capillary Vu-Union connector was purchased from

Chromatographic Specialties (Brockville, Ontario). L-α-Distearoyl phosphatidylcholine was purchased from Serdary Research Laboratories (London, Ontario). EcoLite liquid scintillation cocktail was obtained from ICN (Montréal, Québec). [1-^{14}C]-oleate (ethanol solution) was purchased from New England Nuclear/Du Pont Canada (Mississauga, Ontario). Cyto-Tox 96 non-radioactive cytotoxicity assay kit was obtained from Promega (Madison, Wisconsin). Fisherbrand silica G Redi/Plates for thin layer chromatography (TLC) (20 x 20 cm, 250 μm layer thickness, 60 Å silica) were purchased from Fisher Scientific (Dartmouth, Nova Scotia). 2',7'-Dichlorofluorescein was obtained from Eastman Kodak (Rochester, New York). Whatman LKC$_{18}$F reverse phase TLC plates (20 x 20 cm, 200 μm layer thickness, 60 Å silica) were obtained from Whatman (Clifton, New Jersey). Absolute ethyl alcohol (minimum 99.8%) was obtained from RDL Alcohols (Grimsby, Ontario). All reagents were of analytical grade, all compounds used for cell culture were tissue culture tested, and all water used was deionized and sterile filtered by a Millipore Milli-Q Reagent Water System at 15 MΩ/cm (Milli-Q water).

B. Cell Culture

i. Preparation of Cell Culture Medium

The basic cell culture media were prepared from powered MEM in Milli-Q water. Sodium bicarbonate was added to the MEM at 26.2 mM and the D-(+)-glucose concentration was elevated from the basal MEM value of 5.5 mM to 27.7 mM. The pH of the media were adjusted to 7.15 with 0.1 M HCl at room temperature. The media were sterilized by filtration, using a 0.22 μm bottle-top filter under negative pressure in a laminar flow hood. The media were supplemented with 10% FBS, 1.0 mM sodium pyruvate, 0.1 mM non-essential amino acids, 4.0 mM L-glutamine, 100 units/ml penicillin G, and 100 μg/ml streptomycin sulphate. Serum-free media were identical to the basic culture medium save the absence of FBS. The media were stored in the dark at 4 °C and were used within a fortnight. Before use, the culture media were warmed to 37 °C.

The D-(+)-glucose concentration was elevated to emulate the glucose concentration in portal blood. The increased glucose concentration would maintain high concentrations of glycolytic intermediates and reduce the energy requirement from β-oxidation of fatty acids. Later experiments sought to reduce the influence of de novo fatty acid synthesis upon the molecular species profiles of cellular and LpB-associated lipid. Experiments with fatty acid synthase inhibitor cerulenin eliminated the addition of extra glucose to the MEM to reduce the stimulation of lipogenesis, as 25 mM glucose was shown to increase the mass of TAG in Hep G2 compared to control cells incubated with 5.5 mM glucose (Cianflone et al., 1992;

Wang *et al.*, 1988). However, these findings were recently contested by Jiang *et al.* (1998) when they reported 30 mM glucose had no effect upon *de novo* synthesis of TAG.

ii. Conditions for Cell Maintenance and Growth

Hep G2 cells were incubated at 37 °C in a humid atmosphere of 5% CO_2:95% air. Experiments were started by thawing fresh aliquots of Hep G2 cells. Into Corning T-75 flasks. 10 ml of warm culture media were dispensed and 0.75 ml of thawed cells in cryogenic solution were added to the medium. The cells were incubated for 2 h to allow the cells to attach to the flask. The medium was removed to eliminate cell debris and residual cryogenic solution which contained 10% dimethyl sulphoxide. The cells were fed with 15 ml of fresh culture medium and the culture medium was changed every 2 days.

Subculturing was done every 10−14 days, as the cells approached 100% confluency. The cells were split at a maximum ratio of 1:6 and were not used above 25 passages. Seeding Hep G2 cells densely appeared to reduce the formation of foci. Hep G2 cells were detached with mild proteolysis by exposing the cells to 5 ml of 0.25% trypsin−5.3 mM EDTA in PBS for 5 min. The trypsin−EDTA solution was aspirated off and 10 ml of culture media were added to the flask. The cells were suspended into the medium by repeatedly drawing the medium through a Pasteur pipette. The suspended cells from all flasks were pooled together and the volume was brought up to the volume required to seed the new flasks. (T-75 flasks required 10 ml of cell suspension; T-150, 15 ml; and 6-well plates, 1.5 ml.) T-75 flasks were seeded with 10 ml of cell suspension and the cells were incubated for 2 h to allow the cells to attach. The medium was removed to eliminate residual trypsin and unattached cells. The cells were re-fed with 15 ml of fresh medium and the culture medium was changed every 2 days.

For production of lipid mass and determination of heparin-Sepharose column recovery, cells were seeded into Corning T-150 flasks with 15 ml of cell suspension, were re-fed with 20 ml medium after 2 h to remove residual trypsin, and were grown to confluency with 20 ml of medium, changing the medium every 2 days. For radioactive labelling experiments used in testing cerulenin conditions, cells were seeded into FALCON 6-well plates with 1.5 ml of cell suspension, were re-fed with 2 ml medium after 2 h to remove residual trypsin, and were grown to confluency with 2 ml medium, changing the medium every 2 days. Experimental incubations started when the average flask reached 100% confluency, which took 7−10 days for both the T-150 flasks and the 6-well plates. The maximum length of experimental incubation was 30 h. Although each flask had some foci by the time the average flask reached confluency, the experimental incubation time did not appear to increase the average number of foci.

iii. Preparation of Fatty Acid–BSA Solutions

Fatty acid solutions for experimental cell incubations were prepared by a variation on the method of Van Harken *et al.* (1969). Sodium salts of the fatty acids were used directly at a concentration of 0.6 mM and were complexed to BSA in a 7:1 molar ratio. Based on a molecular mass of 66.3 kDa (Brown, 1975), 86 µM BSA was defined as 0.568%. BSA was added to the required volume of serum-free culture medium (typically >100 ml) minus 5 ml. The BSA solution was stirred at room temperature for a minimum of 1 h to solubilize the BSA. The fatty acid sodium salt was dissolved in 5 ml of PBS heated to approximately 90 °C, was allowed to cool for approximately 30 seconds, and was added to the stirring solution of BSA. By adding fatty acid dissolved in 5 ml of heated PBS, the final volume was restored. Fatty acid–BSA solutions were left to stir over night at 4 °C and were sterilized by filtration using 0.22 µm low-protein-binding filters under negative pressure in a laminar flow hood. Fatty acid–BSA solutions were stored in the dark at 4 °C and were used within 48 h. Before use, fatty acid–BSA solutions were warmed to 37 °C.

iv. Heparin Treatment of Cells

Hep G2 cells were reported to secrete a lipase which was identical to HTGL, as identified by Western blotting (Busch *et al.*, 1989a). HTGL was suggested to be most active with lipoproteins of IDL size (Thuren *et al.*, 1991). The small size of VLDL which Hep G2 secretes may be a good substrate for HTGL. For this reason, the Hep G2 cells were treated with heparin to remove HTGL to prevent lipolysis of nascent VLDL. Porcine intestinal mucosa heparin with an activity of 140 units/mg was prepared at a concentration of 1 mg/ml heparin in PBS and was sterilized by filtering through a 0.22 µm filter under negative pressure in a laminar flow hood. Before use, the heparin solution was warmed to 37 °C. Five millilitres of heparin solution were added to each flask and the cells were incubated for 15 min with periodic mixing. The heparin solution was removed and the cells were washed twice with 5 ml of warm PBS. Heparin solutions and PBS washes were discarded. Heparin treatments were done before the addition of fatty acid–BSA solutions at the beginning of all experimental incubations. Hep G2 cells which were re-fed with fresh fatty acid–BSA solutions received an addition heparin treatment before the second incubation. In later experiments, Hep G2 cells were incubated for a third time with fresh fatty acid–BSA solution. Cells that were incubated for a third time with fatty acid were not treated with heparin prior to the third incubation with fresh fatty acid–BSA solution.

v. **Harvesting of Samples**

After the incubation period, conditioned media were decanted from culture flasks into 50 ml round-bottom, polyallomer centrifuge tubes. Cells were rinsed twice with ice-cold PBS (5 ml were used to wash the cells in T-150 flasks and 0.5 ml were used to wash the 6-well plates). PBS washes were combined with their respective conditioned media. Aliquots of stock solutions of NaN_3 (10%), EDTA (0.5 M), and PMSF (250 mM in anhydrous ethanol) were added to all samples to achieve final concentrations of 0.02%, 1.0 mM, and 0.5 mM, respectively. The conditioned media were centrifuged in a Beckman J2-21 centrifuge using a JA-17 rotor at 14,000 rpm (20,000 g) for 30 min to remove cellular debris. After centrifugation, the conditioned media were decanted into 50 ml polypropylene screw-capped tubes and were stored at 4 °C.

Cells were harvested with a rubber policeman and were suspended into ice-cold PBS by repeatedly drawing the media through a Pasteur pipette. Cells from T-150 flasks were suspended into 5 ml of ice-cold PBS and cells from 6-well plates were suspended into 2 ml of ice-cold PBS. Cell suspensions were transferred to 15 ml polypropylene screw-capped tubes. Flasks and plates were washed with ice-cold PBS, using the same volume as the initial cell harvest. The flask and plate washes were combined with the initial cell suspensions, yielding final volumes of 10 ml from the T-150 flasks and 4 ml from the 6-well plates. Aliquots of NaN_3, EDTA, and PMSF stock solutions were added to all samples to achieve final concentrations of 0.02%, 1.0 mM, and 0.5 mM, respectively. Cellular samples were stored temporarily at -20 °C (during analysis of samples) while long-term storage of cellular samples was at -80 °C (after analysis of samples).

C. Experimental Incubations

i. Single Fatty Acid Incubations

To establish how Hep G2 cells react to fatty acid challenges, cells were incubated with a single fatty acid, either oleate or myristate. Later experiments would use a combination of both oleate and myristate incubations. Thus, cellular and LpB-associated lipid molecular species needed to be defined after incubations with individual fatty acids. Oleate—BSA and myristate—BSA solutions containing 0.6 mM fatty acid and 27.7 mM glucose were prepared. Hep G2 cells were grown to confluency in Corning T-150 flasks with media containing 27.7 mM glucose. To achieve sufficient lipoprotein mass to permit analysis, the media of three T-150 flasks were pooled together. Thus, a group of three flasks constituted a single incubation. To prepare for experimental incubations, maintenance media were removed and the cells were incubated with serum-free media for 6 h. The serum-free media were

removed and the cells were treated with heparin. Experimental incubations were started with the addition of fatty acid–BSA solution. After an 18 h incubation period, media and cells were harvested (Figure 7). Two groups of flasks were incubated with oleate and were paired with two control groups of flasks that were incubated with an equal concentration of BSA without fatty acid. On a separate day, two groups of flasks were incubated with myristate and were also paired with two control groups of flasks that were incubated with an equal concentration of BSA without fatty acid.

Media from a group of three flasks were pooled together and were first fractionated on heparin-Sepharose columns, as described below. The heparin-Sepharose unretained fraction was further fractionated by HTP chromatography as described below. The HTP-unretained fractions or dual-unretained (unretained by both heparin-Sepharose and HTP) were lyophilized and solubilized in PBS (Figure 8). Two aliquots were taken from each chromatographic fraction (each approximately 45% of the fraction) for total lipid profile determination by gas-liquid chromatography (GLC). Apoproteins were determined by electroimmunoassay. The presence of BSA in the fractions was tested by Ouchterlony double diffusion. Cellular protein concentrations were determined by the Markwell modification of the Lowry assay (Lowry et al., 1951; Markwell et al., 1978).

ii. Oleate-Load and Single Myristate-Chase Experiments

Incubations were undertaken to elucidate possible mechanisms involved in the mobilization of stored TAG in the assembly of LpB. Hep G2 cells were loaded with oleate-containing lipid species by incubating the cells with oleate. The media were then switched to myristate. By monitoring lipid species which contain myristate, a trace fatty acid under normal physiological conditions, use of exogenous and endogenous lipids in the synthesis of nascent VLDL was investigated.

Cells were grown to confluency in T-150 flasks with media containing 27.7 mM glucose. Hep G2 cells were treated with heparin to start the incubation. Groups of three flasks were incubated for 18 h with 0.6 mM oleate–BSA solution and 27.7 mM glucose levels. After oleate-loading incubations, the media were harvested. The cells were treated again with heparin and were incubated with 0.6 mM myristate–BSA solution for 3, 6, 9, or 12 h. After the myristate-chase incubation, the media and cells were harvested (Figure 9). Media from a group of three flasks were pooled together for analysis. Controls were re-incubated with oleate during the chase period. Experiments were done in triplicate. To simplify the oleate-load and myristate-chase experiment, different harvests were incubated on different days (Table 2). The oleate-load, 6 h, and 12 h harvests were done on the same

heparin
treatment

| 6 h -serum | 18 h +oleate or myristate |

A   B   C
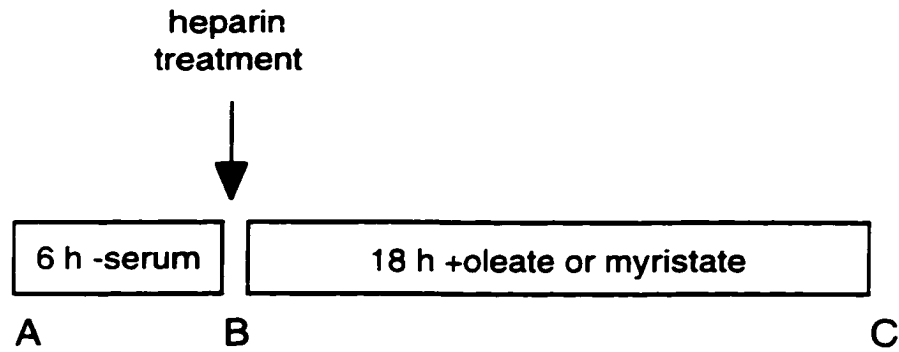
Figure 7: **Schedule for the single fatty acid incubations.** After the Hep G2 cells grew to confluency, the cells were switched to serum-free culture medium (A). After a 6 h pre-incubation. serum-free media were removed, cells were treated with heparin (arrow), and cells were incubated for 18 h with 0.6 mM oleate or myristate complexed to BSA. Controls did not receive exogenous fatty acid (B). After the incubation, media and cells were harvested (C).
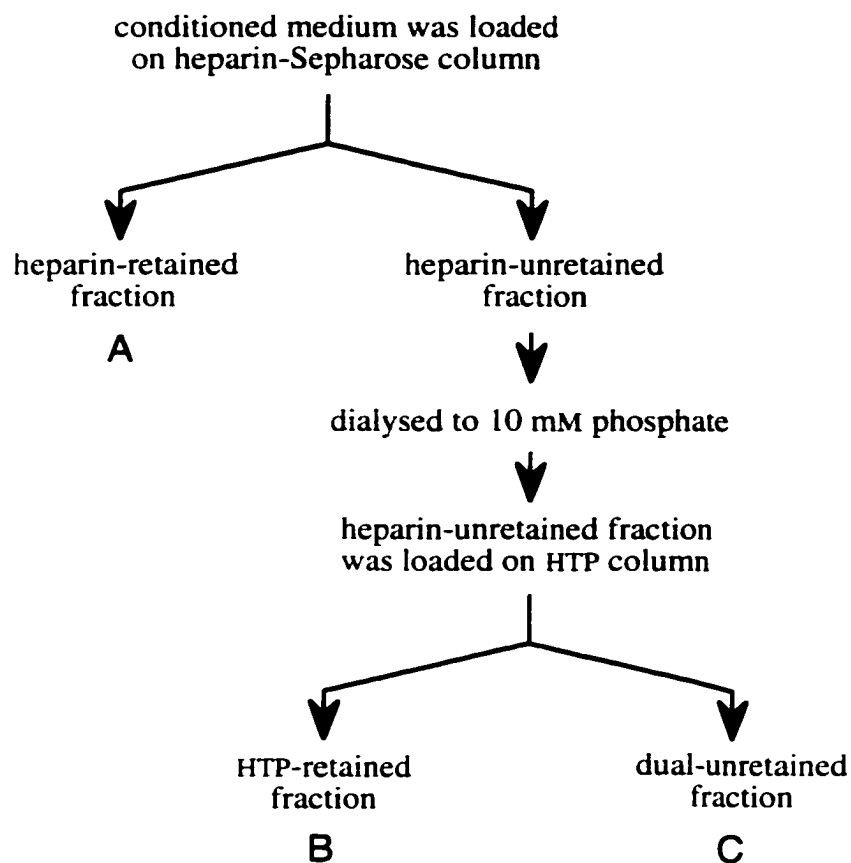
Figure 8: **The chromatographic fractionation of single fatty acid incubations.** Media from 18 h incubations with either oleate, myristate, or BSA alone were fractionated serially on heparin-Sepharose and then HTP yielding heparin-retained (A), HTP-retained (B), and dual-unretained fractions (C).
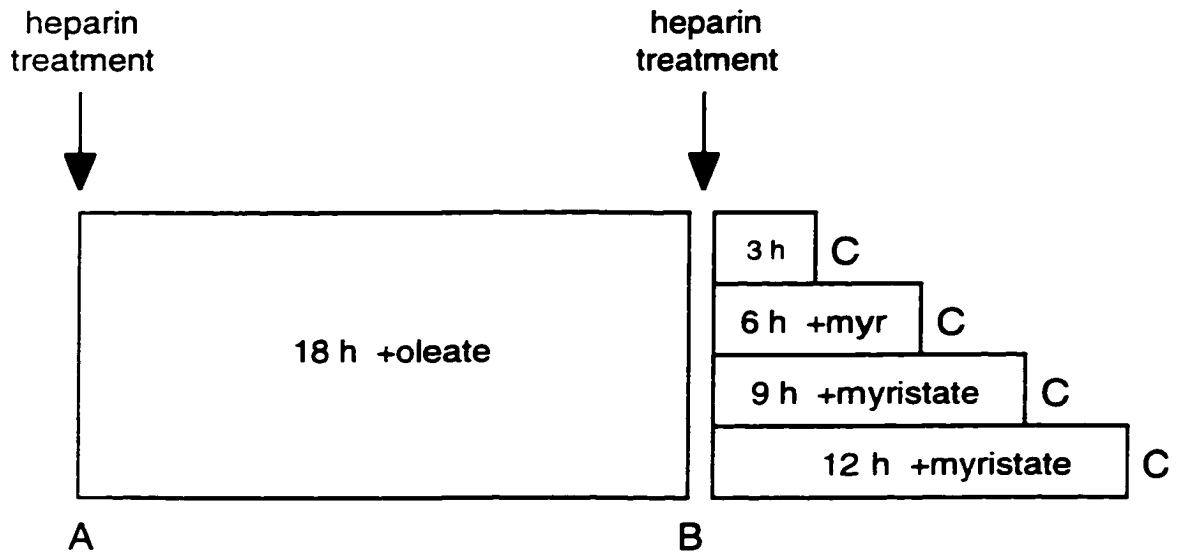
Figure 9: **Schedule for the oleate-load and single myristate-chase incubations.** After Hep G2 cells grew to confluency, cells were treated with heparin (arrow) and were pre-incubated with 0.6 mM oleate for 18 h (A). After the oleate-loading incubation, the conditioned medium was harvested, the cells were treated with heparin (arrow), and the cells were incubated for 3, 6, 9, or 12 h with 0.6 mM myristate complexed to BSA (B). As a control, cells were chased with oleate. After the second incubation, the media and cells were harvested (C). myr=myristate.

Day	Oleate Load (18 h)	Chase Incubation							
		3 h		6 h		9 h		12 h	
		myr	ole	myr	ole	myr	ole	myr	ole
1	x			x	x			x	x
2	x			x	x			x	x
3	x			x	x			x	x
4		x	x			x	x		
5		x	x			x	x		
6		x	x			x	x		

Table 2: **Timetable for the oleate-load and single myristate-chase incubations.** The incubation times were grouped as shown above. All cells were pre-incubated for 18 h with oleate to load cellular lipid pools with oleate; however, cells were only harvested immediately after the oleate-load incubation on days 1–3. myr=myristate; ole= oleate.

days and the 3 h and 9 h harvests were done on the same days. Myristate chases and paired oleate controls were always incubated on the same day.

Media were fractionated on heparin-Sepharose. Total lipid profiles of LpB fractions and cellular samples were determined. Cellular protein was determined by the method of Markwell.

iii. Cerulenin Dose Curve
a. Incubation Conditions

Cerulenin or 2R,3S-epoxy-4-oxo-trans-7,10-dodecadienamide is an irreversible inhibitor of fatty acid synthase (Christie et al., 1981; Omura, 1981). A dose curve was done to determine a concentration of cerulenin which maximized inhibition of fatty acid synthesis and minimized cytotoxicity. Inhibition of de novo fatty acid synthesis was monitored by the incorporation of acetate label into lipids, especially TAG. Inhibition of elongation of fatty acids was monitored by labelling with myristate and determining the label which entered palmitate and oleate pools. The cerulenin dose-curve incubations were similar to the oleate-load and single myristate-chase incubations; however, the Hep G2 cells were chased with two sequential myristate incubations. Hep G2 cells were grown to confluency in 6-well plates. The cellular lipid pool was loaded with oleate-containing lipid species by an 18 h incubation with oleate–BSA solution plus 0, 2.5, 5, 10, or 25 µg/ml of cerulenin. The cerulenin was added from a stock solution in ethanol. Controls were incubated with equal volume of ethanol. After the 18 h incubation, the media were harvested and the cells were incubated with label which was delivered in 0.6 mM myristate–BSA solution. Some flasks received 0.417 µCi/ml of [1-^{14}C]-myristate for the determination of fatty acid elongation while different lots of cells were incubated with 1 µCi/ml of [1-^{14}C]-acetate for the determination of de novo fatty acid synthesis. The cells were incubated with the 0.6 mM myristate–BSA solution, label, and cerulenin for 6 h. After the 6 h incubation, the media were harvested and the cells were re-incubated with fresh 0.6 mM myristate–BSA solution, label, and cerulenin. After the second sequential myristate incubation, the media and cells were harvested. Experiments were done in triplicate and all incubations were done on the same day.

b. Determination of Toxicity

Aliquots of media were used to determine toxicity of the cerulenin dose by monitoring release of lactate dehydrogenase (LDH) activity in the medium. A Promega kit, which couples the oxidation of lactate to pyruvate with the reduction of a tetrazolium salt to a formazan red dye that strongly absorbs at 490 nm, was used. The assay was done in 96-well plates and was read with a Bio-Rad model 3550 Microplate Reader.

c. Determination of Acetate Incorporation

In the determination of acetate incorporation, cellular samples were extracted into chloroform:methanol (Bligh & Dyer, 1959). The upper phase was discarded and the organic phase was back-washed with ideal upper phase (methanol:0.74% KCl (aqueous): chloroform, 48:47:3, v/v/v; Folch et al., 1957) twice. The organic phase was transferred to a drying vial, evaporated to dryness under N_2, and the lipids were solubilized in chloroform. Samples were run on silica G TLC plates, resolved with a solvent system of heptane: isopropyl ether:acetic acid, 15:10:1 (v/v/v; Breckenridge & Kuksis, 1968). Cold standards for cholesterol, CE, and TAG were also run on the plates. Plates were scanned with a Bio-Rad Molecular Imager System to determine radiolabel migrations and cold standards were visualized by spraying with 2',7'-dichlorofluorescein.

d. Determination of Myristate Elongation

Determination of the elongation of myristate was done by extracting aliquots of cellular samples with chloroform:methanol (Bligh & Dyer, 1959). The upper phase was discarded and the organic phase was back-washed with ideal upper phase (methanol:0.74% KCl (aqueous):chloroform, 48:47:3, v/v/v; Folch et al., 1957) twice. The organic phase was dried down and the lipids were saponified in 0.5 M KOH by heating to 60 °C for 1 h. After the incubation, the samples were cooled to room temperature and neutralized with 6 M HCl. The fatty acids were extracted twice into petroleum ether. The petroleum ether was combined and dried down. The fatty acids were methylated by incubating with 6% sulphuric acid in methanol at 75 °C for 12 h. Fatty acid methyl esters were extracted twice into petroleum ether. Unlabelled fatty acid methyl esters standards were prepared from myristate, palmitate, stearate, and oleate. Samples and standards were spotted on Whatman LKC₁₈F reverse phase TLC plates and were resolved with a solvent system of acetonitrile: methanol (1:1, v/v). The plates were counted by scintillation using a Bioscan System 200 Imaging Scanner with a Bioscan Auto Changer 4000. Cold standards were visualized by spraying with 0.17 M $NaCr_2O_7$ in 40% sulphuric acid and charring the plate in a 150 °C oven (Bertetti, 1954, as cited in Krebs et al., 1969).

iv. Oleate-Load and Double Myristate-Chase with Cerulenin Experiments

In order to better determine the influence of exogenous fatty acid and endogenous lipid, steps were taken to reduce the level of lipogenesis. Glucose concentration was lowered to the basal MEM value of 5.5 mM to reduce the energy surplus. Cells were incubated with cerulenin to reduce the level of palmitate contributed by de novo synthesis of fatty acids.

Hep G2 cells were grown to confluency in T-150 flasks in culture medium with 5.5 mM glucose. A group of three flasks constituted a single incubation. To start the incubation, cells were treated with heparin. The cells were loaded with oleate-containing lipid species by incubating the cells for 18 h with 0.6 mM oleate–BSA solution, at basal glucose concentration, and 10 µg/ml cerulenin. After the oleate-loading incubation, media were harvested. The cells were treated again with heparin and were incubated with 0.6 mM myristate–BSA solution containing 10 µg/ml cerulenin for 6 h. After the first myristate-chase incubation, the medium was harvested. The cells were re-fed with fresh 0.6 mM myristate–BSA solution containing 10 µg/ml cerulenin without a heparin treatment and were incubated for another 6 h chase. After the second sequential myristate incubation, the media and cells were harvested (Figure 10). The media from each group of flasks were pooled together for analysis. Fatty acid controls were incubated with serum-free media or with oleate–BSA solution during the two chase incubations. Cerulenin controls were incubated with equal volumes of the carrier solvent ethanol. Experiments were done in triplicate on separate days (Table 3). A myristate chase with a paired oleate control chase, both incubated with and without cerulenin, were incubated on the same day. Incubations that chased the cells with serum-free media were done on separate days.

D. Chromatography

i. Heparin-Sepharose Affinity Chromatography

Heparin-Sepharose affinity chromatography was based upon the method of Huff and Telford (1984). All heparin-Sepharose chromatography was performed at 4 °C, all solutions were degassed under a vacuum, and the pH of all solutions was adjusted to 7.4 at 4 °C. Heparin equilibrium buffer was 50 mM NaCl, 1.23 mM Na_2HPO_4, 0.77 mM KH_2PO_4, and 0.02% NaN_3; heparin elution buffer was 0.8 M NaCl, 1.23 mM Na_2HPO_4, 0.77 mM KH_2PO_4, and 0.02% NaN_3; and heparin sanitization buffer was 8.0 M urea, 50 mM NaCl, 1.23 mM Na_2HPO_4, 0.77 mM KH_2PO_4, and 0.02% NaN_3.

One and a quarter grams of powered heparin-Sepharose CL-6B were swollen in 250 ml distilled water and packed into 8 mm x 15 cm columns. Heparin-Sepharose columns were washed with 250 ml of distilled water, equilibrated with 250 ml of heparin equilibrium buffer, and the flow rate was adjusted to 10–12 ml/h. Incubation media from a pool of three T-150 culture flasks was loaded directly onto heparin-Sepharose columns, at the NaCl concentration of the medium (0.12 M). After samples were loaded, columns were washed with 10 ml of heparin equilibrium buffer. The unretained volume of the incubation media and the column wash were pooled together. The bound fraction was eluted with heparin elution buffer in a discontinuous gradient and 1–2 ml fractions were collected. Protein
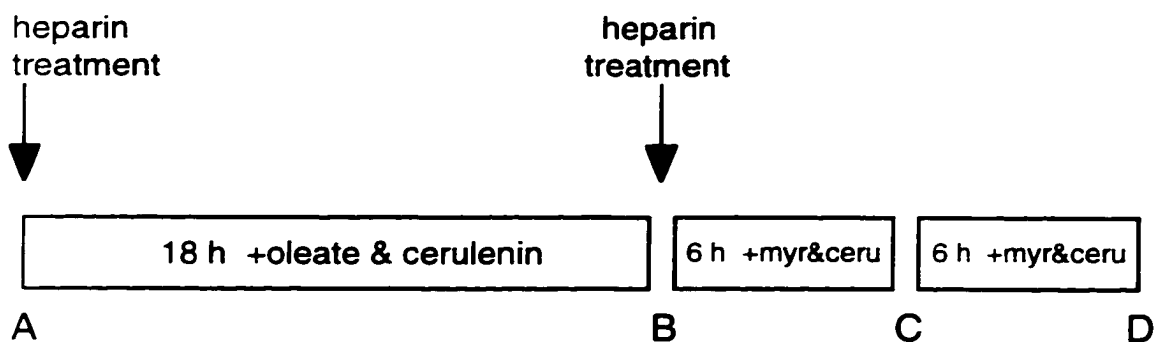
Figure 10: **Schedule for the oleate-load and double myristate-chase incubations.** After Hep G2 cells grew to confluency, cells were treated with heparin (arrow) and were pre-incubated with 0.6 mM oleate plus 10 µg/ml cerulenin for 18 h (A). After the oleate-loading incubation, conditioned media were harvested, cells were treated with heparin (arrow), and cells were incubated for 6 h with 0.6 mM myristate plus 10 µg/ml cerulenin (B). After the first myristate incubation, the conditioned media were harvested and the cells were re-fed with fresh 0.6 mM myristate plus 10 µg/ml cerulenin for a second 6 h incubation (C). After the second sequential myristate incubation, the media and cells were harvested (D). For fatty acid controls, cells were incubated with oleate or with serum-free medium during the two 6 h chase incubations. For cerulenin controls, cells were incubated in an equal volume of carrier (ethanol). myr=myristate, ceru=cerulenin.

Day	Chase Incubation					
	Myristate		Oleate		Serum-Free	
	+	−	+	−	+	−
1	x	x	x	x		
2	x	x	x	x		
3	x	x	x	x		
4					$x^\dagger$	$x^\dagger$
5					x	x

Table 3: **Timetable for the oleate-load and double myristate-chase incubation with cerulenin.** The incubation times were grouped as shown above. "+"=incubated with cerulenin; "−"=incubated without cerulenin; "†"=two groups of cells were incubate on day 4.

content was used to determine which fractions contained material bound by the heparin column. Protein-containing fractions were pooled for further analysis.

Between application of samples, heparin columns were regenerated with 15 ml of heparin equilibrium buffer. After the single fatty acid experiments were completed, concerns were raised about material incompletely eluted from the heparin-Sepharose column contaminating later samples. Thus, to insure that all material was eluted after a run, heparin columns were sanitized with 10 ml of heparin sanitization buffer and were regenerated exhaustively with heparin equilibrium buffer (minimum of 100 ml). The urea sanitization was done between application of samples from the oleate load–myristate chase time course experiments and all experiments with cerulenin.

ii. Evaluation of Heparin Column Recovery

To assess the recovery of lipoproteins from the heparin-Sepharose column, radio-labelled lipoproteins were prepared by incubating Hep G2 cells with [1-^{14}C]-oleic acid. Conditioned media were fractionated on heparin-Sepharose and the bound fraction was isolated a second time by heparin. Thus, the difference in the amount of label between the first and second fractionations was taken to be the percent recovery from the column.

Three T-150 flasks were grown to confluency for the recovery from heparin-Sepharose experiments. The experiment was run in a similar fashion as the single fatty acid experiments. The cells were incubated with 0.6 mM oleate–BSA solution with 27.7 mM glucose containing 0.6 µCi/ml [1-^{14}C]-oleic acid for 18 h. After the incubation, media and cells were harvested. Aliquots of media, before and after incubation, were taken for scintillation counting. The media from three flasks were pooled together and the conditioned media were fractionated by heparin-Sepharose chromatography, giving the first-bound and first-unretained fractions. Aliquots of the first-bound and first-unretained fraction were taken for scintillation counting. The heparin-Sepharose column was regenerated with 10 ml of heparin sanitization buffer and was equilibrated with 50 ml of heparin equilibrium buffer. The first-bound fraction was then dialysed against heparin equilibrium buffer using 4 L of buffer and the buffer was changed after 8 h. The first-bound fraction was removed from dialysis and the dialysis membrane was washed twice with 5 ml of Milli-Q filtered water. The membrane washes were combined with the first-bound fraction. The first-bound fraction was re-applied to the heparin-Sepharose column, generating a second-bound fraction and a second-unretained fraction. Aliquots of the second-bound and second-unretained fractions were taken for scintillation counting.

Aliquots for scintillation counting were mixed with 10 ml of EcoLite scintillation cocktail. Samples were counted in a Beckman LS 3801 Liquid Scintillation system.

iii. Hydroxylapatite Chromatography

The heparin-unretained fractions from single fatty acid incubations were further fractionated by HTP chromatography (Kostner et al., 1974; Kostner & Holasek, 1977; Tam & Breckenridge, 1987). Two types of HTP columns were used. Initially, Bio-Gel HTP was tried. Bio-Gel HTP was a powered HTP which had a range of particle sizes. Finer particles typically packed tightly around the larger ones. Over time, the back pressure was sufficient to decrease the flow rate. Because of the inability of these columns to sustain an even flow rate over the course of several fractionations, later experiments used an Econo-Pac HTP cartridge from Bio-Rad. Oleate incubations were fractionated with the Bio-Gel HTP and myristate incubations were fractionated by the Econo-Pac HTP cartridge.

All HTP chromatography was performed at 4 °C, all solutions were degassed under a vacuum, and all solutions were adjusted to pH 6.8 at 4 °C. HTP equilibrium buffer was 10 mM KH_2PO_4 and 0.02% NaN_3. HTP elution buffer was 0.65 M KH_2PO_4 and 0.02% NaN_3.

Bio-Gel HTP was hydrated in 250 ml of HTP equilibrium buffer. Five millilitres of swollen Bio-Gel HTP were packed into 13 mm x 15 cm columns. The flow rate was set to 30 ml/h and the columns were equilibrated with 250 ml of HTP equilibrium buffer. The Econo-Pac HTP cartridge was prepared for use by flushing 250 ml of HTP elution buffer through the cartridge. The flow rate was set to 0.5 ml/min and the cartridge was equilibrated with 500 ml of HTP equilibrium buffer. Unlike the heparin-Sepharose and Bio-Gel HTP columns, the HTP cartridge was placed, in series, after the peristaltic pump.

Unretained fractions from heparin-Sepharose chromatography were dialysed to HTP equilibrium buffer at a ratio of 100 ml of sample to 2 L of buffer. Dialysis was done at 4 °C and the buffer was changed twice over a 24 h period. Heparin-Sepharose unretained fractions were applied to HTP columns or a HTP cartridge at the specified flow rates. The HTP cartridge and columns were then washed with 10 ml of HTP equilibrium buffer and the HTP-unretained fractions were combined with the washes. HTP-bound fractions were eluted with HTP elution buffer in a discontinuous gradient and 1-2 ml fractions were collected. Protein-containing fractions were pooled for further analysis. Between the application of samples, HTP columns were repacked to improve the consistency of the flow rate and were regenerated with 15 ml of HTP equilibrium buffer. The HTP cartridge was regenerated in between samples with a minimum of 15 ml of HTP elution buffer followed by 15 ml of HTP equilibrium buffer.

HTP-unretained fractions or dual-unretained fractions (unretained by both heparin-Sepharose and HTP; see Figure 8) were dialysed against Milli-Q water at a ratio of 100 ml sample to 2 L water and the Milli-Q water was changed twice in a 24 h period. The dual-unretained fractions were shell frozen, lyophilized, and taken up in PBS.

E. Protein Determination

Protein content was determined by the Markwell *et al.* method (1978), scaled down to 96-well microtitre plates. Briefly, the Lowry *et al.* method (1951) was modified where 1.0% SDS was added to the alkaline copper reagent to solubilize protein in the presence of lipid. Potassium ion was eliminated by using disodium tartrate.

BSA was used as a standard, in a range of 20–200 µg/ml of protein. Data outside of this range was rejected during quantitation. The alkaline copper reagent was prepared daily by combining reagents A (2.0% Na_2CO_3, 0.4% NaOH, 0.16% sodium tartrate, and 1.0% SDS) and B (4.0% $CuSO_4 \cdot 5H_2O$) in the proportion of 100:1, respectively. The Folin phenol reagent was prepared daily by diluting equal volumes of 2.0 N Folin & Ciocalteu's phenol reagent and Milli-Q water.

Cellular samples were diluted in the following manner to ensure complete cell and organelle lysis. To 0.5 ml of cell suspension, 1.0 ml of 0.2 M NaOH was added and vortexed. Cellular samples were neutralized with 1.0 ml of 0.2 M HCl and were further diluted with 5 ml of 1% SDS. The total dilution was 15 fold with a final concentration of 27 mM NaCl. Protein-containing fractions isolated by chromatography were identified by diluting samples 5 fold in 96-well dishes. To the wells of 96-well plates, 50 µl of sample or standard were incubated with 150 µl of alkaline copper solution for 60 min. After the incubation period, 20 µl of Folin phenol reagent were added and incubated for 45 min. Samples were read in a Bio-Rad model 3550 Microplate Reader at 655 nm.

F. Gas-Liquid Chromatography

i. Preparation of Samples

The gas-liquid chromatography (GLC) method was based on the method of Kuksis *et al.* (1978b). All glassware used in total lipid profile determinations was exhaustively cleansed by sequential rinsing with methanol, chloroform:methanol (2:1, v/v), and then chloroform. GLC sample vials for auto-injection were sanitized by immersion in concentrated nitric acid for a minimum of 7 days to remove residues from previous samples. The nitric acid was changed twice during the week. The vials were washed exhaustively with Milli-Q water and were baked at 100 °C until dry. PLC solution was made by dissolving 20–25 mg of PLC from *C. welchii* in 35 mM Tris, pH 7.3, which gave approximately 1 unit/ml PLC solution. PLC solution was stored at -20 °C and aliquots were thawed on the day of use. Tricaprin was used as an internal standard, dissolved in chloroform at a concentration of 100 µg/ml.

Aliquots for GLC analysis were transferred to Teflon-lined, screw-capped digestion vials. A maximum of 3 ml of sample was digested. To the aliquots, 1 ml of PLC solution, 1

ml of 1% CaCl$_2$, and 0.5 ml of diethyl ether were added to the digestion tube. The samples were digested for 2 h with constant agitation at 37 °C. At the end of the digest period, the lipids were extracted. Five drops of 0.1 M HCl and 2.5 ml methanol were added to each vial. The internal standard, dissolved in chloroform, was added to all samples in relation to the lipid content: 20 μg of tricaprin to cellular samples and 1.25 −2 μg tricaprin to media samples. Chloroform was added to raise the total volume of chloroform to 2.5 ml. The mixture was vortexed thoroughly and was centrifuged at 2000 rpm to separate the two phases. To remove aqueous contamination from the lower phase, the organic phase was back-washed with ideal upper phase (methanol:0.74% KCl (aqueous):chloroform, 48:47:3, v/v/v: Folch et al., 1957). The top aqueous layer was aspirated off and approximately 1 ml of ideal upper phase was added. The sample was vortexed and centrifuged at 2000 rpm for 10 min to separate the two phases. Back-washing was repeated twice. The lower organic phase was removed from under the final ideal upper phase. The organic phase was dried by passing through an anhydrous Na$_2$SO$_4$ drying column. Drying columns were prepared by packing a plug of glass wool and approximately 2.5 g of anhydrous Na$_2$SO$_4$ into short Pasteur pipettes. After the application of samples, drying columns were flushed with approximately 2 ml of chloroform to ensure all of the sample had eluted. The organic layer was collected in flat-bottomed drying vials and was evaporated to dryness with gentle heating under a stream of N$_2$.

To silate DAG and ceramides (created by the PLC digest) and cholesterol, 100 μl of BSTFA were added to the drying vial and samples were derivatized for 1 h at room temperature (Kuksis et al., 1986). Excess BSTFA was evaporated with gentle heating under a stream of N$_2$. Samples were taken up in dichloromethane and transferred to GLC vials for auto-injection. Cellular samples were dissolved in 1.0 ml of dichloromethane and medium samples were dissolved in 150 μl of dichloromethane.

ii. Analysis of Samples

Samples were injected into a Hewlett-Packard model 5890 series II gas chromatograph with a Hewlett-Packard model 7673 automatic sampler. To allow for on-column injections, a 1 m x 0.53 mm internal diameter guard column was used. The guard column was connected to the analytical column with a Capillary Vu-Union connector which used graphite ferrules to hold the columns securely in a silica connector. The analytical column was 15 m x 0.32 mm internal diameter with a 0.25 μm film thickness of 5% diphenyl :95% dimethylsiloxane co-polymer. The injector port was set to 250 °C, the flame-ionization detector port was set to 350 °C, and the initial carrier gas flow rate was 4.5 ml He/min. The oven temperature was programmed in the following manner (Figure 11): 170 °C was held
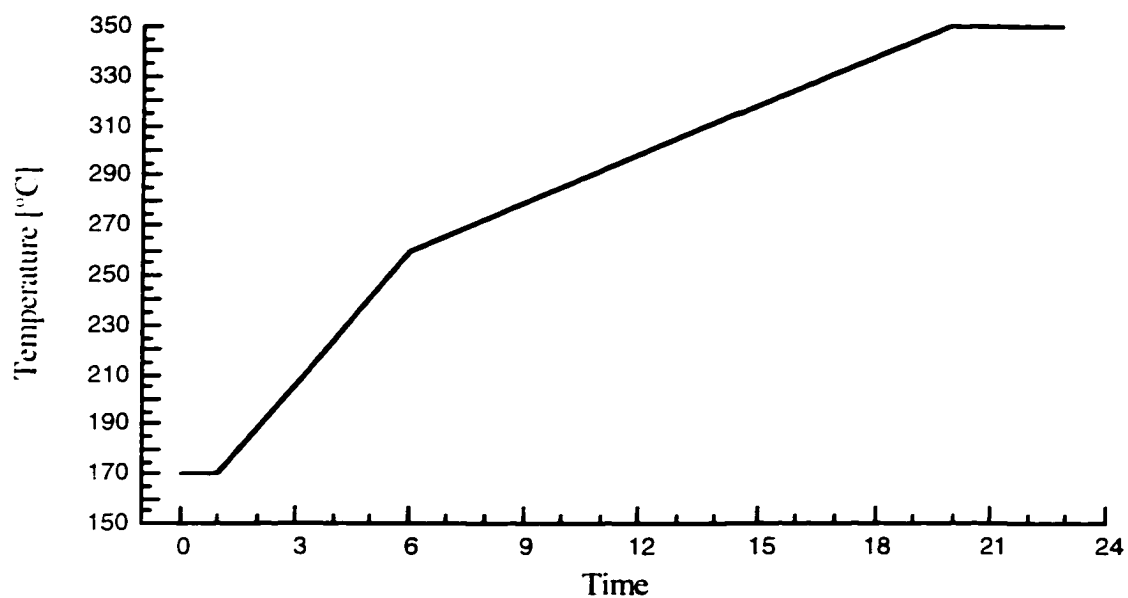
Figure 11: **Temperature program for gas-liquid chromatography.** The initial temperature of 170 °C was held for 1 min. The temperature was increased at 18 °C/min until 260 °C and then the rate was slowed to 6.5 °C/min until 350 °C. The final temperature was held for 3 min.

for 1 min. the temperature was increased to 260 °C at 18.0 °C/min, the rate was reduced to 6.5 °C/min until the oven reached 350 °C, and the final temperature was held for 3 min. The total time for a run was 22 min, 50.8 seconds.

Sample profiles appear in appendix A. Sample peaks were identified by retention time. An external standard of cholesterol, tricaprin, cholesteryl palmitate, cholesteryl oleate, tripalmitin, and triolein was regularly used to confirm the retention times from the sample injections. L-α-Distearoyl phosphatidylcholine and trimyristin standards were injected to confirm their retention times. The mass of sample peaks was calculated by comparing the area of the sample peak to the area of the internal standard tricaprin. Response factors were obtained from the external standard and were used to correct the areas reported for cholesterol. CE. and TAG in the sample runs. DAG peak masses were corrected to PL by a factor for choline (Kuksis et al., 1978b). DAG peaks, which also contained some ceramide, were assumed to be adequately described as only phosphatidylcholine. Particle diameters were estimated by the method of Shen et al. (1977; Kuksis et al., 1978a). The formula assumed the particles were spherical. Volumes occupied by CE and TAG in the neutral core and by cholesterol and PL in the surface monolayer were estimated. The diameter of the particles were calculated from the lipid volumes.

G. Electron Microscopy

Electron microscopy (EM) was used to confirm the lipoprotein diameter estimations based on lipid composition. Lipoproteins samples were stained negatively, employing 2% sodium phosphotungstate, pH 7.4 (Forte & Nordhausen, 1986). An aliquot of the heparin-bound fraction from an 18 h incubation with oleate—BSA was dialysed exhaustively to 50 mM NH_4HCO_3 in a microdialysis apparatus. Five microlitres of sample was applied to a carbon-Formvar coated 300 mesh copper grid and was allowed to evaporate. A drop of phosphotungstate stain was applied to the sample for 20 seconds and excess stain was removed by blotting with lint-free tissue. Samples were viewed with a Philips 300 electron microscope at 41,200—87,300 fold magnification. EM images were photographed and particle diameters were measured from the photographs. Sample EM photographs appear in appendix B.

H. Immunodetection Assays

i. Electroimmunoassay

Electroimmunoassay or "rockets" are electrophoretic gels that have antibodies penetrated throughout the gel (Laurell, 1972). The gel is adjusted to the isoelectric point of the

antibody: thus, the antibodies remain stationary in the gel. With the application of an electric field. the sample migrates from the cathode to the anode. While moving through the gel. the sample can interact with the antibodies. As antibody-antigen complexes form. the migration is retarded due to the increase in size. Since the wells are circular. the band that forms as the sample loads into the gel will be most concentrated in the centre, corresponding to the diameter of the well. Thus, it will take longer for the centre of the band to complex with sufficient antibodies to retard migration than the ends of the band. The result is a triangular or rocket-shaped band. The area of the rockets is proportional to the concentration. so quantification can be achieved by relating samples to a standard series.

The basic rocket buffer used for all apolipoproteins was 80 mM Tris. 24 mM Tricine. and 2.5 mM calcium lactate. pH 8.6. The rocket buffer for apo B included 0.025% Triton X-100. Gels were made by boiling agarose and PEG in the rocket buffer: 2% agarose plus 1% PEG was used for apo B and 1.3% agarose plus 1% PEG was used for apo A-I and apo E. Once the gel had cooled to 50 °C. 25 ml of gel was measured in a warmed graduated cylinder. Anti-apolipoprotein antibodies were added to the gel as follows: 4.8 µl anti-apo A-I/ml gel, 0.8 µl anti-apo B/ml gel, or 16 µl anti-apo E/ml gel. The gel was quickly mixed and was poured into a warmed, 10 cm x 18 cm x 2 mm gel plate, using GelBond as a solid support. Wells were drilled 4 mm in diameter, 7 ¼ mm centre to centre. which allowed 25 wells along the 18 cm side of the gel, 1.5 cm in from the edge.

Samples were diluted 2 and 4 fold and were adjusted to 0.1% Triton X-100. The standard for apo A-I was a HDL fraction which had been standardized for apo A-I content (Fesmire *et al.*, 1984) and was diluted to contain 4–9 µg/ml. The standard for apo B. a plasma enriched in LDL and standardized for apo B content (Rosseneu *et al.*. 1983). was diluted to contain 2–18 µg/ml. The standard for apo E was a VLDL fraction standardized for apo E content and diluted to contain 10–80 µg/ml (Tam *et al.*, 1981; Tam & Breckenridge, 1983). The apo A-I and B standards were donated by the laboratory of Dr. M. Tan.

The electrophoretic unit was refrigerated to 10 °C. Gels were run for 18 h at 2.0 V/cm for apo B and at 2.4 V/cm for apo A-I and apo E. After 18 h, gels were removed and rinsed with distilled water. Gels were wrapped in filter paper, pressed to dry for 1 h. and dried in an oven at 50 °C for 15 min. Gels were fixed and stained with 0.2% Coomassie Brilliant Blue R-250 in methanol:water:acetic acid (9:9:2, v/v/v) for 30 min with constant swirling. Gels were destained by visual inspection in the same solvent system.

ii. Ouchterlony Double Diffusion

Ouchterlony double diffusion assays were done as described by Dolphin *et al.* (1978). The gel was 2% agarose with 0.02% NaN_3 of a depth of 2 mm. Holes were drilled

in a star pattern: a central well (4 mm diameter) surrounded evenly by five wells with a 7.5 mm distance between centres. Serial dilutions of 0.0625 X–1 X of heparin- and HTP-retained aliquots were reacted with anti-human serum albumin antibodies, at room temperature, overnight. BSA was used as an antigen standard, in a concentration range of 0.003–0.05%.

I. Statistical Analysis

Student t-tests were performed to test for statistical significance. Tests were paired whenever possible. Differences were considered to be significant when $p < 0.05$.

III. Results

A. Single Fatty Acid Incubations

i. Rationale

The assembly and secretion of nascent VLDL particles by Hep G2 cells was studied. Work done previously in the Breckenridge laboratory demonstrated molecular species of cellular and total media lipids were altered when Hep G2 cells were incubated with fatty acids. Both cellular and total media lipids were skewed towards lipid molecular species that contained exogenous fatty acid (Froom, 1992). To improve lipid analysis of secreted lipoproteins, conditioned media was chromatographically fractionated to isolate LpB from other lipoproteins. Incubating Hep G2 cells with an exogenous fatty acid will skew the lipid molecular species towards lipids containing the exogenous fatty acid. By switching the incubation media to a different exogenous fatty acid, the molecular species of lipid in the secreted LpB will provide evidence for the use of stored lipid versus exogenous fatty acid in assembly of LpB in Hep G2 cells. If LpB total lipid profiles were skewed towards lipid molecular species containing the first fatty acid, LpB assembly drew more lipid from stored pools than exogenous fatty acid. If LpB total lipid profiles were skewed towards lipid molecular species containing the second fatty acid, LpB assembly was more strongly influenced by the current exogenous fatty acid than the lipid in stored pools. To pursue this goal, two fatty acids were selected: oleate and myristate. Oleate is a common fatty acid and stimulates lipid secretion in Hep G2 cells (Dashti & Wolfbauer, 1987; Dixon *et al.*, 1991; Ellsworth *et al.*, 1986; Homan *et al.*, 1991). Myristic acid is physiologically found in small but variable quantities in dietary lipids. Myristate could be used as a marker lipid since substantial quantities of myristate-containing lipids would only be possible by experimental manipulation. The initial goal of this project was to isolate LpB from apo A-I by heparin-Sepharose chromatography and then to isolate apo A-I from the remaining media by HTP chromatography in order to characterize the lipoproteins secreted after a single fatty acid incubation.

ii. Chromatographic Isolation

Lipoprotein fractions from single fatty acid incubations were isolated by sequential affinity chromatography (Figure 8). Combining three T-150 flasks gave a pool of conditioned medium (60 ml), which was loaded onto heparin-Sepharose columns. Heparin-retained fractions were recovered in 2.3–6.3 ml of eluate (9.5–26 fold concentration). HTP-retained fractions were recovered in 2.6–5.4 ml of eluate (11.1–23.1 fold concentration). Column chromatography effectively concentrated the lipoprotein fractions.

iii. Apolipoprotein Distribution

Electroimmunoassay was used to determine the apoprotein content in chromato-graphic fractions. Heparin-retained fractions contained apo B but not apo A-I (Figure 12, panel A). Trace amounts of apo E were detected by electroimmunoassay in heparin-retained fractions. The mass of apo B in heparin-retained fractions was usually high in relation to lipid (Figure 12, panel A), which gave an apo B to lipid mass ratio of 1.3. Typical values for the apo B to lipid ratio in human VLDL and LDL are 0.04 and 0.33, respectively (Shore & Shore, 1972). The high apo B to lipid ratio observed may have reflected differences in the immunoreactivity of the anti-apo B antibody towards poorly lipidated apo B associated with the LDL-like particles secreted by Hep G2 cells. The high values for apo B were not investigated further. When heparin-unretained pools from oleate incubations were further fraction-ated with BioGel HTP, approximately 77% of apo A-I were isolated in the HTP-retained fraction and the remainder was found in the dual-unretained fraction. When an Econo-Pac HTP cartridge was used to fractionate heparin-unretained pools from myristate incubations, all of the apo A-I were isolated in the HTP-retained fraction. The cartridge appeared to have a high-er apo A-I binding capacity than the powdered HTP had. Trace amounts of apo B (less than 1% of the total apo B mass) were detected by electroimmunoassay in HTP-retained fractions. Apo B was not observed in dual-unretained fractions. In the determination of apo E by elec-troimmunoassay, the sample rockets had a very different shape compared to the standard rockets. Migration of samples appeared normal; however, standard rockets tended to be blunt and stained more densely compared to sample rockets. Differences between standards and samples prevented reliable quantitation of apo E. The different immunoreactivity may have been due to changes in the conformation of apo E since standards were in glycerol sol-utions whereas samples were in aqueous buffer. On the basis of rocket area, 30% of apo E mass were estimated to be in HTP-retained fractions, with the remaining 70% of apo E mass present in dual-unretained fractions. Unlike apo A-I, fractionation with a HTP cartridge did not appear to shift more apo E mass from dual-unretained fractions to HTP-retained frac-tions, which suggested a substantial portion of apo A-I and apo E was not on the same par-ticle. Overall, heparin-Sepharose chromatography isolated LpB and HTP chromatography isolated lipoproteins containing apo A-I and/or apo E.

Ouchterlony double diffusion assays revealed significant amounts of albumin were present in HTP-retained and dual-unretained fractions (data not shown). Albumin was not detected in heparin-retained fractions. Under the chromatographic conditions used, albumin readily bound to HTP. Incomplete binding of apo A-I and apo E to HTP in some preparations may have resulted from competition by albumin. Because of the contamination of albumin

Figure 12: **Lipid and apolipoprotein mass of lipoprotein fractions isolated by sequential chromatography from Hep G2 medium.** Hep G2 cells were incubated for 18 h with oleate–BSA or myristate–BSA solutions. Controls for both incubations were incubated with BSA only on the same day. Media were fractionated by heparin-Sepharose (A) and then HTP (B) chromatography, leaving a dual-unretained fraction (C). Total lipid profiles were determined by GLC and were broken down into lipid classes. Apoproteins were determined by electroimmunoassay. Note that the figure has two Y axes, with the data separating at the break in the X axis. The left Y axis defines the lipid class data (cholesterol. PL. CE, and TAG columns) and the right Y axis marks the apoprotein data (apo A-I and apo B columns). Results are means with standard deviations from two incubations for each condition with duplicate analysis for each fraction. Incubation conditions: ▓ =oleate; ☐ =BSA control; ▒ =myristate; and ◩ =BSA control. chol=cholesterol.
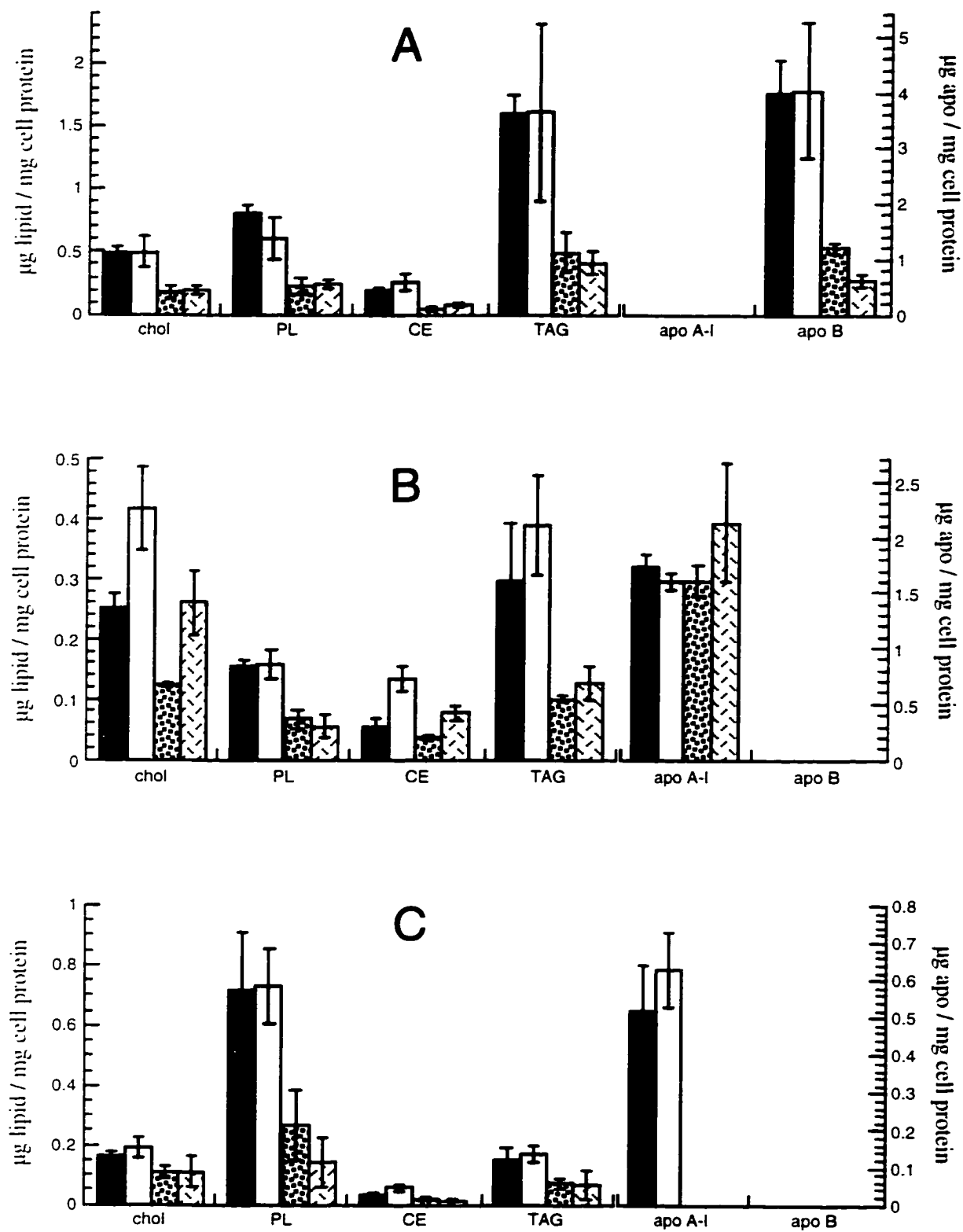
Figure 12

in the HTP-retained fractions and because heparin-Sepharose isolated all the LpB, further studies focused on LpB.

iv. Lipid Distribution

Total lipid profiles of the isolated fractions were determined by GLC and the distribution of secreted lipids, grouped as lipid classes, also appears in Figure 12. Substantial quantities of cholesterol, PL, CE, and TAG were found in all three chromatographic fractions. Heparin-retained fractions were most enriched with lipid, containing 53−62% of the total lipid found in the media. The heparin-retained fractions possessed 43−54% of total cholesterol found in the media: 41−48%, PL; 45−69%, CE; and 62−78%, TAG. HTP-retained fractions contained the majority of the remaining neutral lipid and had approximately a third of the total unesterified cholesterol found in the media. Dual-unretained fractions contained 43−49% of the total PL found in the media and also contained neutral lipid: 12−19% of the total CE and 7−11% of the total TAG found in the media. Although LpB possessed the majority of the total neutral lipid found in the media, it is important to note that 22−38% of the TAG and 31−55% of the CE were not associated with apo B. The presence of neutral lipid in fractions other than those which contain apo B illustrates the necessity to isolate apo B from the media in studies that focus on the production of nascent VLDL in cell culture.

The albumin present in HTP-bound and dual-unretained fractions questions the protein with which the lipid was associated. Human serum albumin was reported to bind cholesterol weakly at a molar ratio of 20:1 (Zhao & Marcel, 1996). From the perspective of cholesterol binding capacity of BSA, the mass of BSA used to complex the exogenous fatty acid was in a several hundred fold excess of the mass of cholesterol in both HTP-bound and dual-unretained fractions. Assuming BSA has cholesterol binding properties similar to human serum albumin, even a slight portion of the BSA used to bind the exogenous fatty acid could have bound all the cholesterol in either of the HTP-bound or dual-unretained fractions. The synthesis of albumin by Hep G2 cells will further increase the excess of albumin in the media. Thus, the cholesterol observed in HTP-bound and dual-unretained fractions may not be entirely associated with lipoproteins. For lipoprotein isolations to be effective, albumin must be separated from lipoproteins.

High levels of variability in the secreted mass of lipids and apolipoproteins were observed when comparing single fatty acid incubations to its BSA control and especially when comparing oleate treatments to myristate treatments (Figure 12). Control incubations were performed on the same day as the fatty acid treatments with the same lot of cells whereas different fatty acid treatments were preformed on different days. Lot-to-lot variation may have been significant. Some of the variability could be attributed to development of foci.

Cells within foci may be partially isolated from the media due to the limitations of diffu-
sion. In the context of lipoprotein metabolism, Hep G2 cells within foci may poorly absorb
exogenous fatty acids and thus may poorly secrete lipoproteins, while increasing the total
mass of cellular protein. Diminished synthesis from more cells will lower reported values
compared to a true monolayer of cells. However, when expressed in terms of percent
composition. the lipid content was remarkably consistent for the heparin-retained fraction.
Also. by expressing the lipid content of the fractions in terms of percent composition, the
comparison of the fractions to serum lipoproteins will be facilitated. Considering the varia-
bility observed in the lipid mass, the consistency of the lipid percent composition suggested
foci affected secretion of lipoprotein mass but did not alter the character of the lipoproteins.
The percent composition of lipid in isolated fractions (Figure 13) showed heparin-retained
fractions were 16—20% cholesterol, 21—26% PL, 5—9% CE, and 45—53% TAG. The percent-
age of total lipid for cholesterol and TAG in heparin-retained fractions were not significantly
different between oleate and myristate incubations. PL in the heparin-bound fraction was
23.7±1.1% of the total lipid after treatment with oleate and was significantly greater than PL
in the heparin-bound fraction after treatment with myristate (21.0±1.5% of total lipid; Fig-
ure 13. panel A). CE in the heparin-bound fraction was 6.1±0.4% of the total lipid after
treatment with oleate and was significantly higher than CE in the heparin-bound fraction
after treatment with myristate (4.9±0.1% of the total lipid; Figure 13, panel A). The slight
differences in percent of total lipid, some of which proved to be statistically significant,
between the various treatments suggested Hep G2 cells produced a regular LpB and the per-
cent composition of LpB was insensitive to incubation conditions. Heparin-retained had a
high content of unesterified cholesterol, which resulted in high cholesterol:PL molar ratios.
Cholesterol:PL molar ratios were highest in BSA only (1.55) and myristate (1.48) incuba-
tions. as compared to oleate (1.19). Typical values for cholesterol:PL ratios are 0.8 in VLDL
and 1.0 in LDL (Shore & Shore, 1972). The high proportion of cholesterol and PL in the
heparin-retained fractions suggested nascent VLDL secreted by Hep G2 cells were atypical.

Percent compositions of lipid in HTP-retained and dual-unretained fractions were
more variable. HTP-retained fractions had high levels of surface lipid, containing 34—50%
cholesterol and 10—21% PL. Neutral lipids were also present in substantial proportions for
nascent apo A-I and/or apo E-containing particles, which possessed 7—15% CE and 24—
39% TAG. HTP-retained fractions did not represent typical HDL since the fraction contained
more TAG than CE (Table 1). In view of substantial neutral lipid content, HTP-retained frac-
tions may have been a mixed population representing both spherical and discoidal particles.
Dual-unretained fractions contained predominantly surface lipids as cholesterol and PL
accounted for 79—82% of total lipid in the dual-unretained fraction. Regardless of the

Figure 13: **Lipid percent composition of lipoprotein fractions isolated by sequential chromatography from Hep G2 medium.** Hep G2 cells were incubated for 18 h with oleate–BSA or myristate–BSA solutions. Controls for both incubations were incubated with BSA only on the same day. Media were fractionated by heparin-Sepharose (A) and then HTP (B) chromatography, leaving a dual-unretained fraction (C). Total lipid profiles were determined by GLC. Lipid classes are shown as a percent of the total lipid in the fraction. Results are means with standard deviations from two incubations for each condition with duplicate analysis for each fraction. Incubation conditions: ■ =oleate; □ =BSA control; ▨ =myristate; and ▧ =BSA control. chol=cholesterol. Student t-tests showed statistical significance when comparing: a) PL as a percent of total lipid between oleate and myristate treatments in heparin-bound fractions, p=0.034, and b) CE as a percent of total lipid between oleate and myristate treatments in heparin-bound fractions, p=0.017.
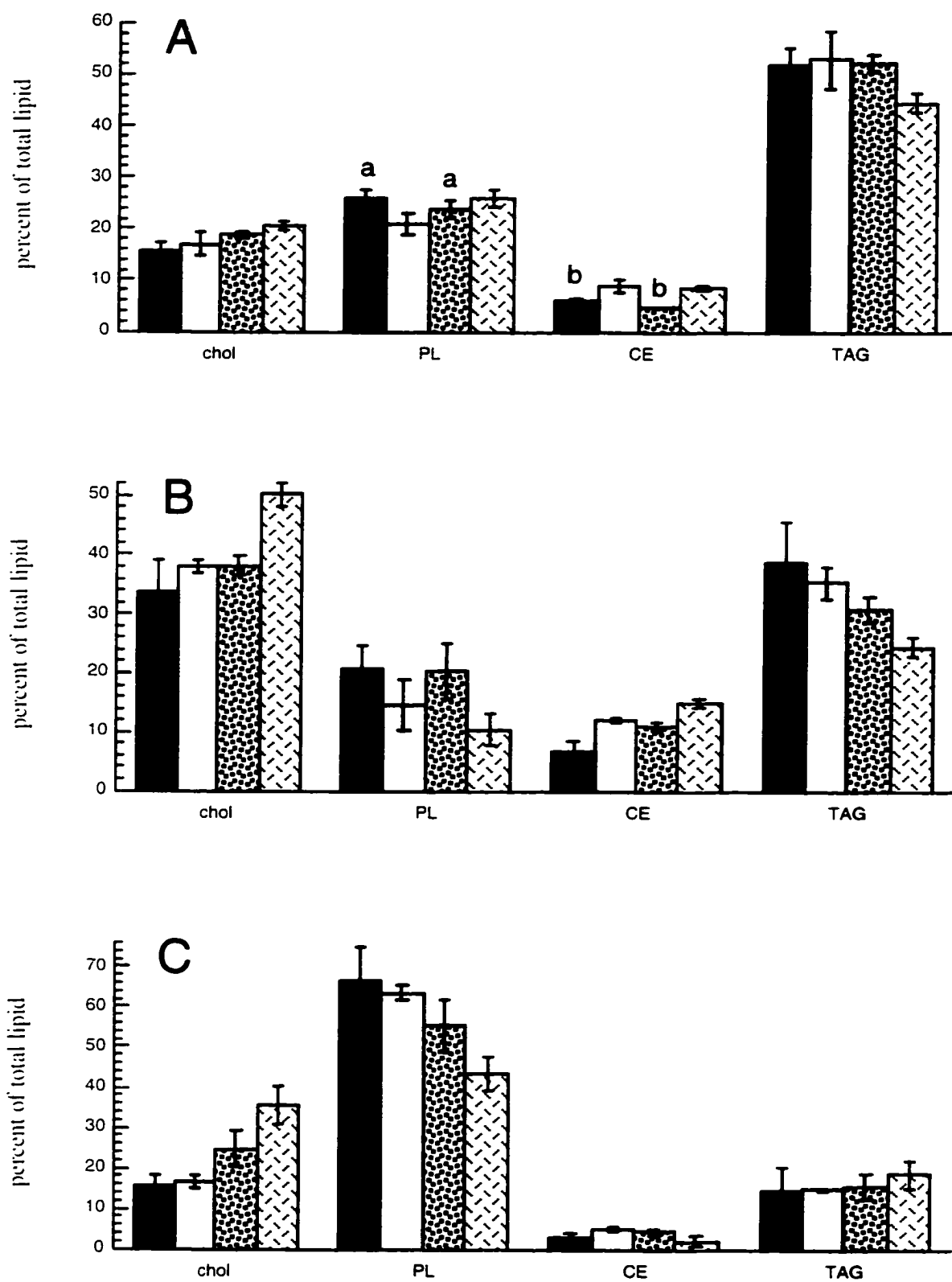
Figure 13

incubation conditions, the dual-unretained fractions contained 2–5% CE and 15–19% TAG and lacked both apo B and the majority of apo A-I.

v. Particle Diameters

Diameters of the lipoprotein particles in the various fractions were calculated (Shen et al.. 1977: Kuksis et al., 1978a) based on percent lipid composition (Figure 14, panel A). Particle estimates were consistent within each fraction, reflecting the consistency of the lipid composition. Particles in heparin-retained fractions were estimated to be 205±20 Å when incubated with oleate and 198±11 Å when incubated with myristate. Particles from a heparin-retained fraction of oleate treated cells measured by electron microscopy had a mean diameter of 215±114 Å (Figure 14, panel B). The majority of particles were in a range of 100–250 Å in diameter and were skewed to larger sizes. Standard deviations of the calculated diameter estimates were small compared to the electron microscopy measurements. which reflected the consistency of the lipid composition. The distribution of sizes observed in electron microscopy suggested Hep G2 cells secreted a diverse population of LpB. primarily of LDL size. Thus, the high proportion of surface lipid in the LpB may be attributed to substantial amounts of small diameter lipoproteins (<150 Å).

Calculated particle diameters of HTP-retained and dual-unretained fractions were also very consistent, which reflected a reciprocal relationship between cholesterol and PL and also between CE and TAG. Elevations in cholesterol were compensated by reduced PL levels, as were variations in CE content relieved opposite changes in TAG content.

vi. Relative Molar Lipid Distribution

Determination of total lipid profiles by GLC separates components based on polarity and vapour pressure. CE and TAG components of lipid samples were non-polar while PL and cholesterol were made to be non-polar by PLC digestion and silylation. Because of the large size of the lipid components. separation was effectively based on molecular mass. Thus, larger lipids eluted later in the profiles. PLC digestion also hydrolyses sphingolipids to ceramides. The GLC and running conditions used can not differentiate between DAG and ceramides. Therefore, each reported PL molecular species is a combination of DAG and some ceramides. In the case of PL and TAG, lipid species are reported as the total carbon numbers of the fatty acid moieties only, which ignores the glycerol moiety. Distribution of the individual lipid molecular species for PL, CE, and TAG are shown in Figures 15–17.

Molecular species of PL were influenced by exogenous fatty acids (Figure 15). PL species ranged from C30–C40. In heparin-retained fractions from control incubations. the major PL species was C34 PL (C16:C18), which was 36–39 mol % of the PL in the frac-
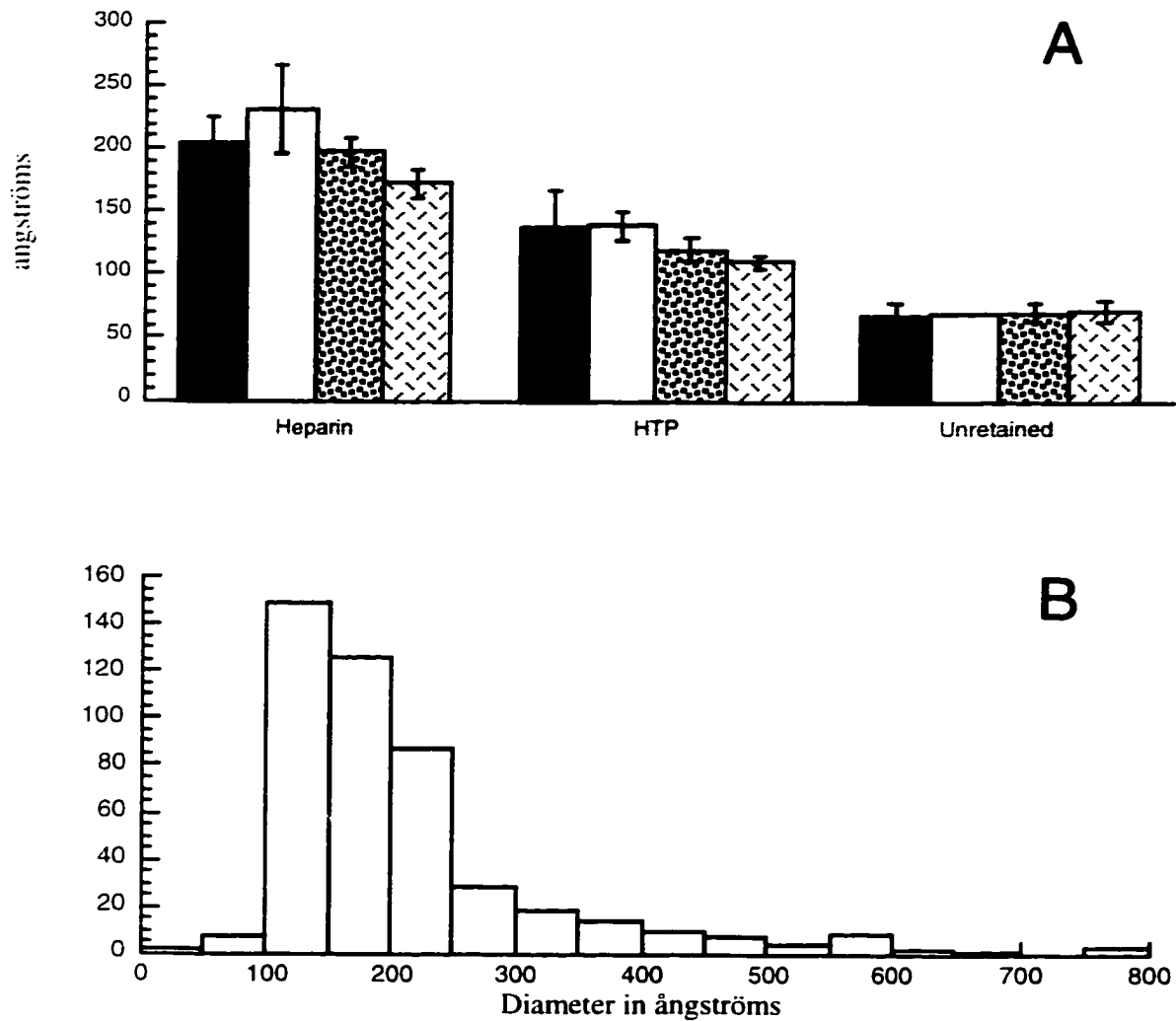
Figure 14: **Particle diameters of lipoprotein fractions isolated by sequential chromatography.** A: Particle diameters were calculated from lipid composition. Results are means with standard deviations from two incubations for each condition with duplicate analysis on each fraction. Incubation conditions: ■ = oleate; □ = BSA control; ▨ = myristate; and ▧ = BSA control. B: Hep G2 cells were incubated for 18 h with oleate. LpB were isolated from conditioned medium by heparin-Sepharose chromatography and particle diameters were measured by electron microscopy.

Figure 15: **Influence of a single exogenous fatty acid on the molecular distribution of PL secreted as distinct lipoproteins by Hep G2.** Hep G2 cells were incubated for 18 h with oleate– or myristate–BSA solutions. Controls for both incubations were incubated with BSA only on the same day. Conditioned medium was fractionated by heparin-Sepharose (A) and then HTP (B) chromatography, leaving a dual-unretained fraction (C). Total lipid profiles were determined by GLC. Carbon numbers refer to the total number of carbon atoms in the fatty acid moieties of the PL. Results are percent of total moles of PL in the fraction, expressed as means with standard deviations from two incubations with duplicate analysis for each fraction. Incubation conditions: ■ =oleate; □ =BSA control; ▦ =myristate; and ☑ =BSA control.
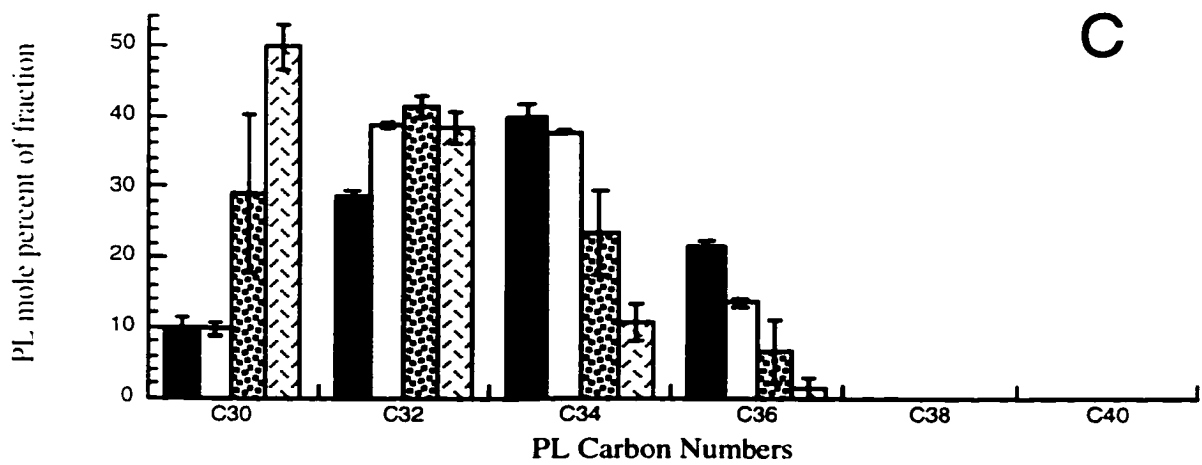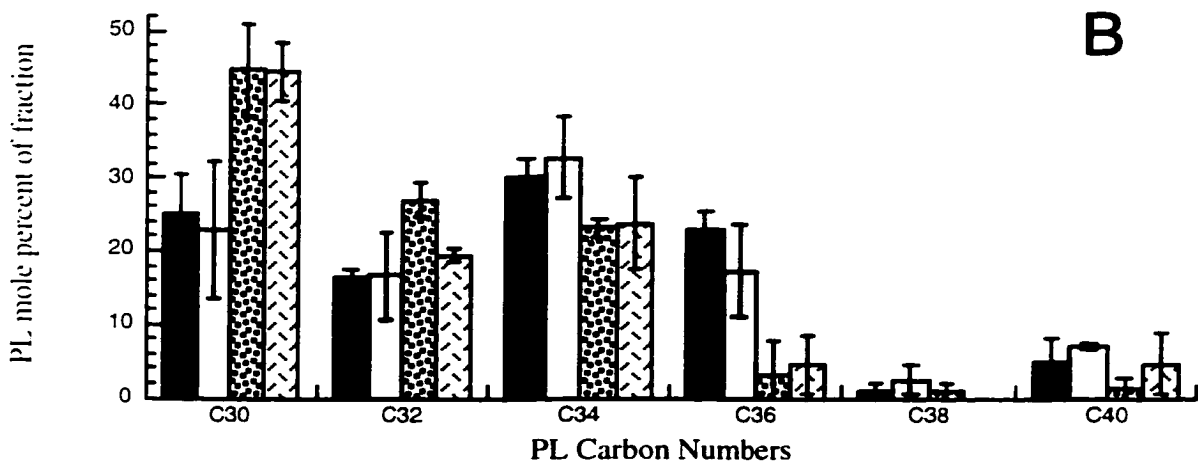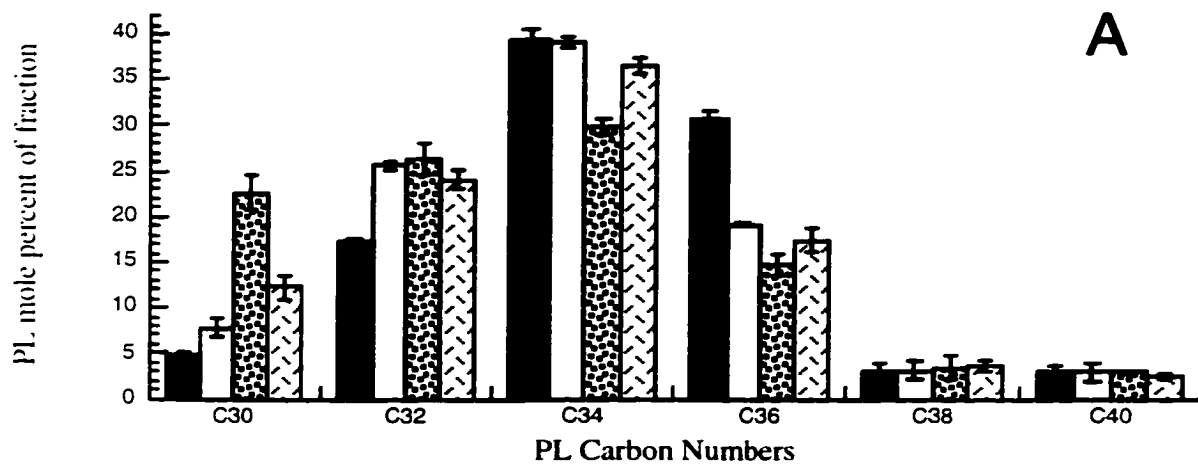
Figure 15

Figure 16: **Influence of a single exogenous fatty acid on the molecular distribution of** CE **secreted as distinct lipoproteins by Hep G2.** Hep G2 cells were incubated for 18 h with oleate– or myristate–BSA solutions. Controls for both incubations were incubated with BSA only on the same day. Conditioned medium was fractionated by heparin-Sepharose (A) and then HTP (B) chromatography, leaving a dual-unretained fraction (C). Total lipid profiles were determined by GLC. Results are percent of total moles of CE in the fraction, expressed as means with standard deviations from two incubations with duplicate analysis for each fraction. Incubation conditions: ■ =oleate; □ =BSA control; ▦ =myristate; and ▧ =BSA control. chol=cholesteryl; C18 CE=cholesterol esterified by C18 fatty acid.
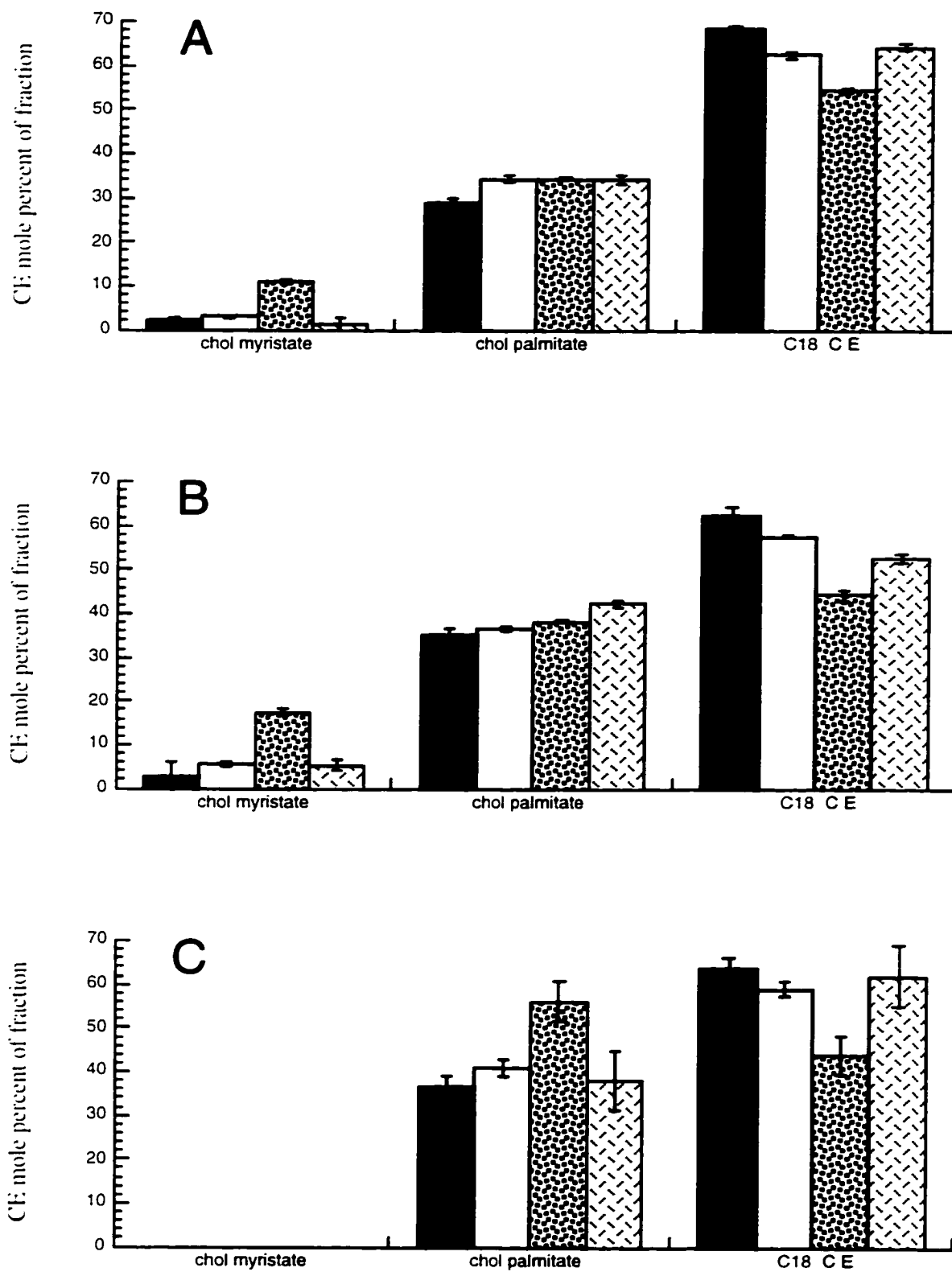
Figure 16

Figure 17: **Influence of a single exogenous fatty acid on the molecular distribution of TAG secreted as distinct lipoproteins by Hep G2.** Hep G2 cells were incubated for 18 h with oleate– or myristate–BSA solutions. Controls for both incubations were incubated with BSA only on the same day. Conditioned medium was fractionated by heparin-Sepharose (A) and then HTP (B) chromatography, leaving a dual-unretained fraction (C). Total lipid profiles were determined by GLC. Carbon numbers refer to the total number of carbon atoms in the fatty acid moieties of the TAG. Results are percent of total moles of TAG in the fraction, expressed as means with standard deviations from two incubations with duplicate analysis for each fraction. Incubation conditions: ■ = oleate; □ = BSA control; ▨ = myristate; and ☑ = BSA control.
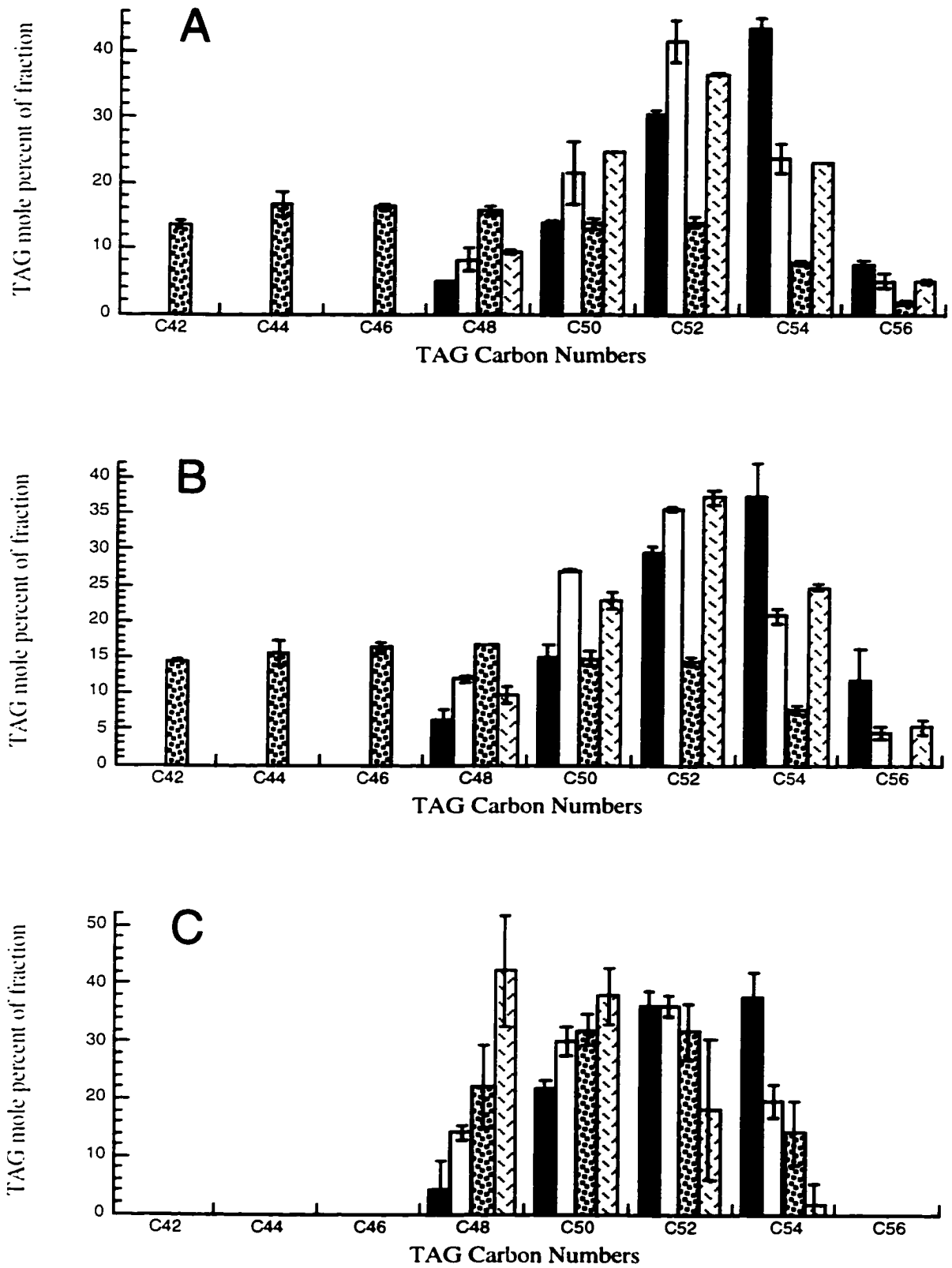
Figure 17

tion. Oleate skewed PL species towards longer-chain fatty acid species. Although C34 PL value was similar to controls, C36 PL (C18:C18) was elevated from 19.1±0.1 mol % in the control to 30.7±0.9 mol % with oleate treatment and was compensated by decreases in C32 and C30 PL. Similarly, the proportion of C30 PL (C14:C16) increased from 12.2±1.4 mol % in controls to 22.7±1.8 mol % with myristate incubation, whereas C34 and C36 PL decreased with myristic acid incubations. HTP-retained fractions demonstrated larger differences between oleate and myristate incubations than between individual fatty acid incubations and their controls. The proportions of PL molecular species in the dual-unretained fractions were also skewed towards PL species containing the exogenous fatty acid.

CE lipid species were consistent within all fractions. Cholesterol esterified by C18 fatty acids (C18 CE) was the dominant species (54−69 mol %) in the heparin-retained fraction, followed by cholesteryl palmitate (28−34 mol %), and cholesteryl myristate (1−11 mol %: Figure 16, panel A). Molecular species of CE were also skewed by addition of exogenous fatty acids. Incubations with oleate elevated C18 CE at the expense of cholesteryl palmitate. Incubations with myristate increased the proportion of cholesteryl myristate with a reciprocal decrease in C18 CE. Overall, the proportion of cholesteryl palmitate was insensitive to incubation conditions, in both the heparin-retained (28−34 mol %) and HTP-retained (35−42 mol %). Despite the presence of exogenous myristate, dual-unretained fractions contained no cholesteryl myristate.

Molecular species of TAG were extensively influenced by addition of exogenous fatty acid (Figure 17). In heparin- and HTP-retained fractions from control incubations, the major TAG species ranged from C48−C54, representing TAG combinations of C16 and C18 fatty acids. The dominant species in both retained fractions was C52 TAG (C16:C18:C18), which ranged from 35.7−41.6% of total TAG in control incubations. C50 (C16:C16:C18) and C54 TAG (typically triolein) were present in similar amounts, 21.4−27.0 mol % and 20.7−24.6 mol % respectively. C48 TAG (tripalmitin) was the least abundant of the major TAG species, ranging from 8.2−12.0 % of total TAG in the heparin- and HTP-retained fractions. Some C56 TAG were observed to be present, which must contain at least one C20 fatty acid moiety. With oleate supplementation, the TAG molecular species in heparin-retained fractions were skewed to longer species. C54 TAG (triolein) increased from 23.7 ±2.3 mol % in the control to 43.6±1.4 mol % with oleate treatment and became the prominent TAG species in heparin- and HTP-retained fractions. With myristate supplementation, new TAG species were observed as the species range was extended to C42−C56; however, a predominant TAG species was not observed. Molecular species of C42−C46 TAG, representing TAG molecular species containing 3, 2, and 1 molecules of myristate respectively, made up 46.6±2.0 mol % of the apo B-associated TAG. Molecular species of C48−C50 TAG

may also contain myristate acid in combination with C16 and C18 fatty acids. TAG molecular species larger than C42 contain some C16 and/or C18 fatty acids. Despite the large skewing of TAG species by myristate and oleate in the heparin-retained fraction, there was little variation in the lipid composition of the LpB (Figure 13).

The overall pattern of distribution of TAG species in heparin- and HTP-retained fractions was similar. However, the dual-unretained fraction was quite different. The dual-unretained fraction contained TAG which was not isolated with apo B or the majority of apo A-I. The dual-unretained fraction appears to be a distinct pool of lipid in the media which may originate from cellular debris or from albumin. However, even when incubated with myristate, C42−C46 TAG species were not detected in the dual-unretained fraction, which suggested that this lipid was a contamination introduced by BSA.

Determination of total lipid profiles for the analysis of lipid molecular species indicated exogenous fatty acids were readily incorporated into lipids which were secreted with apoproteins, especially apo B as seen in heparin-retained fractions. Contamination of HTP-retained and dual-unretained fractions with albumin made these fractions unsuitable for further study. The molecular species of lipid, especially TAG, were modulated by incubating with exogenous fatty acid and did not impact upon the lipid composition of LpB. The lipid found in HTP-retained and dual-unretained fractions reinforces the need to isolate LpB from whole media to focus upon the lipids associated with apo B.

vii. Heparin-Sepharose Recovery Estimates

To assess recovery from the heparin-Sepharose column, Hep G2 cells were incubated with ^{14}C-oleate to secrete LpB that contained radiolabelled lipids. Conditioned media were fractionated by heparin-Sepharose chromatography to isolate labelled LpB. The heparin-bound fraction was dialysed and re-applied to the heparin-Sepharose column. Comparing aliquots of the second isolation to aliquots of the first isolation, 61±5% of the radiolabel from the first heparin-bound fraction were re-isolated in the second heparin-bound fraction. However, aliquots from the first heparin-bound fraction were taken before dialysis. The total label recovered in both the second-bound and unretained fractions was only 65±5% of the label present in the first-bound fraction, which suggested approximately 35% of the label was lost during dialysis. The ratio of the second-bound radioactivity to the first-bound radioactivity was thought to under-estimate recovery.

The distribution of radiolabel between bound and unretained fractions could also be used to estimate recovery. The distribution of radioactivity between the second-bound and second-unretained fractions will be a better estimate than the distribution of label between the first-bound and unretained fractions since any oleate label not taken up by the Hep G2

cells will be in the first-unretained fraction. The distribution of label between second heparin-bound and -unretained fractions showed 93±3% of the radiolabel was in the bound fraction; thus, the reproducibility of the fractionation was very good. Mahley *et al.* (1979) reported a recovery of approximately 94% from a LDL sample that had been applied to heparin-Sepharose, which agreed with the distribution of label between the second-bound and second-unretained fractions. No corrections for lost mass were believed to be necessary.

B. Oleate-Load—Single Fatty Acid-Chase Incubations

i. Rationale

Based on the findings from incubations with a single fatty acid, pulse-chase experiments that employed mass of different fatty acids were designed to elucidate lipid recruitment to the site of LpB assembly. Hep G2 cells were loaded with oleate-containing lipid molecular species by incubations with oleate and the cells were then chased with myristate. Analysis of the lipid molecular species of secreted LpB and the molecular species of cellular lipid will provide evidence of the nature of lipid recruitment in LpB assembly.

Given sufficient time, the molecular species of cellular TAG will be influenced by both the supply of exogenous fatty acid and *de novo* synthesis of fatty acids. Before supplementation with exogenous fatty acid, the cellular TAG pool will be in its basal state. Approximately 40% of TAG from Hep G2 cells will be a C52 TAG molecular species (typically C16: C18:C18), as estimated from BSA control incubations (Figure 17). When Hep G2 cells are incubated with oleate, the lipid profile will shift towards TAG molecular species containing oleate and C54 TAG (typically triolein) will become the predominant TAG molecular species. By switching the incubation media to myristate, the molecular species profile of cellular TAG will shift towards molecular species containing myristate. Esterification of myristate to glycerol will introduce trimyristin, C44, and C46 TAG molecular species. Throughout the fatty acid incubations, *de novo* synthesis of fatty acids contributes palmitate to cellular lipids. After long incubations without exogenous fatty acid, the total lipid profiles will return to the pre-fatty acid incubation state as cell division and palmitate synthesis dilutes out the fatty acids taken up from the media.

The relationship between the molecular species of cellular and secreted TAG will depend upon the mechanism of LpB assembly. If *de novo* synthesis of TAG were the primary supplier of lipid to the site of LpB assembly, then the TAG secreted in association with apo B will reflect cellular TAG content of cells maintained only with MEM. Addition of exogenous fatty acid to the incubation media will skew the TAG molecular species towards lipids containing the exogenous fatty acid, as esterification of exogenous fatty acid contributes to *de novo* synthesis of TAG. Thus, lipid molecular species from LpB secreted by Hep G2

cells after oleate-load and myristate-chase incubations will resemble TAG molecular species from LpB isolated after incubations with only myristic acid, as the stored oleate-containing TAG would not impact strongly on the secreted lipid molecular species.

Stored TAG may be a major source of TAG in the assembly of LpB. The mechanism of TAG mobilization will determine the relationship between the cellular and secreted lipid. Specifically, if mobilization of stored TAG is a major source of TAG in LpB assembly, then the following possibilities for mobilization exist:

a) Stored TAG is mobilized *en bloc* or without modification. Thus, the secreted TAG molecular species will directly reflect the cellular TAG molecular species. Cells pre-incubated with oleate will contain cytosolic TAG of which approximately 40–45 mol % will be C54 TAG. Even with myristate chases, cells will secrete apo B associated with large quantities of C54 TAG until exogenous myristate can alter the cellular TAG profile (Figure 18, panel A).

b) Stored TAG is hydrolysed to DAG for mobilization. TAG will typically be lipolysed to a C18:C18 DAG due to the prominence of stored C54 TAG (C18:C18:C18). Since chase media supplies myristate, C14 fatty acids will be esterified to C18:C18 DAG producing C50 TAG (C18:C18:C14). Some C54 TAG will also be expected in secreted LpB as oleic acid released from the initial hydrolysis may be available to the site of TAG synthesis (Figure 18, panel B).

c) Stored TAG is hydrolysed to MAG for mobilization. Stored C54 TAG will be hydrolysed to C18 MAG which will be re-esterified with myristate at the ER to give a C46 TAG (C18:C14:C14). Since oleate could combine with the myristate. C50 and C54 TAG species will also be expected in secreted LpB (Figure 18, panel C).

d) Stored TAG is completely hydrolysed to fatty acids and glycerol for mobilization. Thus. TAG esterified for LpB assembly will represent combinations of stored oleate and exogenous myristate. If oleate and myristate are randomly esterified with G3P to form TAG. then the binomial distribution will calculate the proportions of C42 (trimyristin). C46 (C14:C14:C18), C50 (C14:C18:C18), and C54 TAG (triolein) synthesized (Table 4). For example, if oleate and myristate are available in similar molar quantities and are randomly esterified, then C42 (trimyristin). C46 (C14: C14:C18), C50 (C14:C18:C18), and C54 TAG (triolein) will be in molar ratios of 1:3:3:1, respectively. If oleate and myristate are not available in similar molar quantities. C46 and C50 TAG will represent substantial proportions of LpB TAG (Figure 18, panel D: Table 4).

Thus. C42. C46, C50, and C54 TAG will serve as marker species. Pronounced skewing

Cytosol   **ER**

A   ⌈ C18 ⌉   *en block*   ⌈ C18 ⌉
     ⊢ C18 ⊢   ───────────────────────►   ⊢ C18 ⊢
     ⌊ C18 ⌋   ⌊ C18 ⌋
        C54   C54

B   ⌈ C18 ⌉   partial   ⌈ C18 ⌉   C14   ⌈ C18 ⌉
     ⊢ C18 ⊢ hydrolysis   ⊢ C18 ⊢   ─────────► ⊢ C18 ⊢ + C54
     ⌊ C18 ⌋ ─────────►   ⌊   ⌋   ⌊ C14 ⌋
        C54   C36   C50

C   ⌈ C18 ⌉   partial   ⌈   ⌉   C14   ⌈ C14 ⌉   C50
     ⊢ C18 ⊢ hydrolysis   ⊢ C18 ⊢   ─────────► ⊢ C18 ⊢ + C54
     ⌊ C18 ⌋ ─────────►   ⌊   ⌋   ⌊ C14 ⌋
        C54   C18   C46

D   ⌈ C18 ⌉   complete   C14   ⌈ C18 ⌉ ⌈ C18 ⌉
     ⊢ C18 ⊢ hydrolysis   C18   ─────────► ⊢ C18 ⊢ ⊢ C18 ⊢
     ⌊ C18 ⌋ ─────────►   ⌊ C18 ⌋ ⌊ C14 ⌋
        C54   C18   C54   C50

                                                 ⌈ C18 ⌉ ⌈ C14 ⌉
                                                 ⊢ C14 ⊢ ⊢ C14 ⊢
                                                 ⌊ C14 ⌋ ⌊ C14 ⌋
                                                    C46   C42
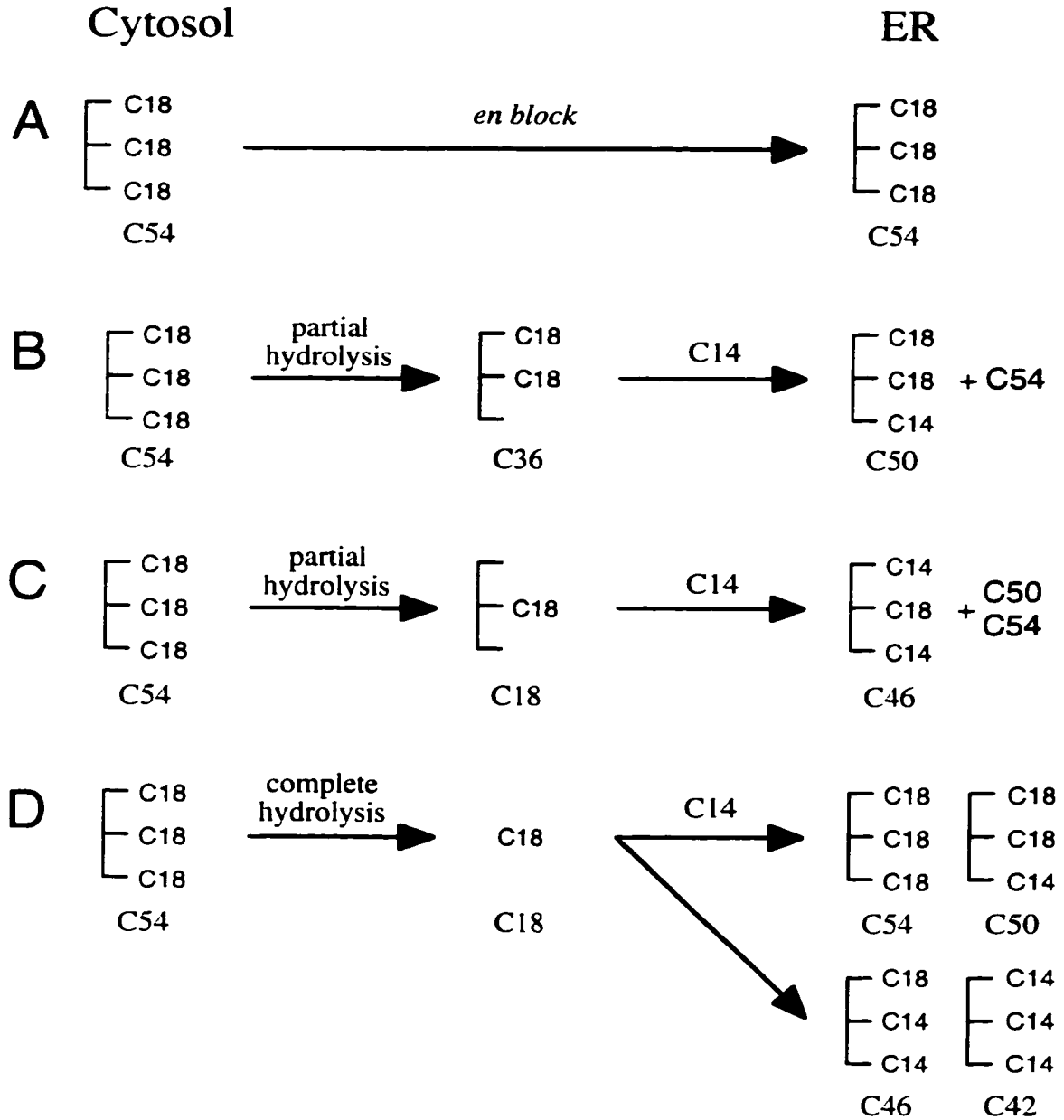
Figure 18: **Potential mechanisms for the mobilization of stored TAG for LpB assembly.** Movement of TAG from the storage pool to the site of LpB assembly is depicted as movement from left to right. C14 above an arrow represents addition of myristate during chase incubations. C14 and C18 to the right of glycerol (E) represents myristate and 18 carbon (typically oleate) fatty acid moieties, respectively. Labels under structures identifies the total number of carbon atoms in the fatty acid moieties of TAG, DAG, or MAG. In panel D, C18 represents a free fatty acid of 18 carbon length, typically oleate.

Availability of Fatty Acid		Proportions of TAG Molecular Species after Random Esterification				Sum
Myristate	Oleate	C42	C46	C50	C54	
100%	0%	100.0%	0.0%	0.0%	0.0%	1
90%	10%	72.9%	24.3%	2.7%	0.1%	1
80%	20%	51.2%	38.4%	9.6%	0.8%	1
70%	30%	34.3%	44.1%	18.9%	2.7%	1
60%	40%	21.6%	43.2%	28.8%	6.4%	1
50%	50%	12.5%	37.5%	37.5%	12.5%	1
40%	60%	6.4%	28.8%	43.2%	21.6%	1
30%	70%	2.7%	18.9%	44.1%	34.3%	1
20%	80%	0.8%	9.6%	38.4%	51.2%	1
10%	90%	0.1%	2.7%	24.3%	72.9%	1
0%	100%	0.0%	0.0%	0.0%	100.0%	1

Table 4: **Binomial distribution of** TAG **molecular species based on random esterification of myristate and oleate.** Assuming oleate and myristate are randomly esterified with glycerol, the binomial distribution of $p^3 + 3p^2q + 3pq^2 + q^3 = 1$ will calculate the proportions of TAG molecular species generated; where p equals the relative concentration of myristate. q equals the relative concentration of oleate, p^3 is the resulting proportion of C42 TAG. $3p^2q$ is the resulting proportion of C46 TAG, $3pq^2$ is the resulting proportion of C50 TAG. and q^3 is the resulting proportion of C54 TAG.

towards any of these marker species will provide evidence for the metabolic origin of TAG packaged in nascent VLDL in Hep G2 cells.

Similarly, stored PL and CE can be analyzed for their contributions of lipid versus exogenous fatty acid during assembly of LpB. Higher relative proportions of cholesteryl myristate in the secreted fraction compared to the cellular content suggests that cholesterol is actively esterified for secretion with apo B. Specific PL species may be selectively incorporated into the nascent VLDL. Also, PL may be hydrolysed to DAG and re-esterified to TAG for VLDL synthesis, providing an alternate source of DAG for TAG synthesis.

ii. Secreted Lipid Mass

The first pulse chase experiments with lipid mass had five separate harvests (Figure 9). Samples were harvested after the 18 h oleate treatment to establish oleate-load conditions (Figure 19, first bar of panels A & B). Hep G2 cells were incubated a second time with myristate for 3, 6, 9, or 12 h, which comprised the four remaining harvests. Controls were chased with oleate. The variation within Figure 19 was unusually large, especially in the oleate-load incubations, 6 h chases, and 12 h chases. Cells harvested on day 1 secreted more lipid mass than cells harvested on days 2 and 3 secreted (Table 2). Although a systemic error appeared to have occurred on day 1 of the experiment, those data were not rejected by Q tests and were kept. A continual increase of secreted lipid mass associated with apo B was observed over the 12 h time period (Figure 19). Despite the large variation observed in the secreted mass of lipid after the oleate-load–myristate-chase incubations, student t-tests supported the observed increase in secreted lipid mass with time. Cholesterol mass secreted after 9 h of oleate chase was significantly higher than the cholesterol mass secreted after 3 h of oleate chase (Figure 19, panel A). TAG mass secreted after 9 h of oleate chase was significantly higher than the TAG mass secreted after 3 h of oleate chase (Figure 19, panel A). Within each lipid class, the 9 h myristate chases secreted significantly more lipid than the 3 h myristate chases secreted and the 12 h myristate chases secreted significantly more lipid than the 6 h myristate chases secreted (Figure 19, panel B). After 9–12 h of myristate chase, secreted lipid mass began to approach the mass that accumulated in conditioned media during initial 18 h oleate-load incubations. The accumulation of secreted lipid was not even across the lipid classes. Secreted TAG displayed the largest increases in mass accumulation while CE made modest increases in mass accumulation over the 12 h of chase incubations. Myristate was more effective than oleate in stimulating TAG secretion, which was different from observations made during single fatty acid incubations. After 12 h of incubation, 0.82 ± 0.38 µg TAG/mg cell protein were secreted with myristate incubations which was significantly higher than cells that were chased with oleate (0.58 ± 0.35 µg

Figure 19: **Accumulation of lipid in secreted LpB from oleate-load–single myristate-chase incubations.** Cells were incubated for 18 h with oleate and were then re-incubated with myristate or oleate for 3, 6, 9, or 12 h. LpB were isolated by heparin-Sepharose chromatography and total lipid profiles were determined by GLC. Results are shown as means with standard deviations from 3 experiments. Incubation conditions, panel A: ■ = oleate load, ▨ = 3 h oleate, ▦ = 6 h oleate, ◪ = 9 h oleate, ▨ = 12 h oleate; and panel B: ■ = oleate load, ▨ = 3 h myristate, □ = 6 h myristate, ▨ = 9 h myristate, ◪ = 12 h myristate. chol = cholesterol. Secreted cholesterol mass was significantly higher after 9 h of oleate chase than after 3 h of oleate chase (a: p=0.035). Secreted TAG mass was significantly higher after 9 h of oleate chase than after 3 h of oleate chase (b: p=0.015). All secreted lipid classes were significantly higher after 9 h of myristate chase than after 3 h of myristate chase (c–f: p<0.014). All secreted lipid classes were significantly higher after 12 h of myristate chase than after 6 h of myristate chase (g–j: p<0.007). TAG mass was significantly higher after 12 h of myristate chase than after 12 h of oleate chase (k: p=0.039).

TAG/mg cell protein; Figure 19, panels A & B). However, the differences between the myr-istate chase and its oleate control for all other time points were not significant.

Accumulation of lipid was also observed in cellular samples (Figure 20). The total lipid mass of control incubations, which were chased with oleate, increased from 268 ± 55 μg lipid/mg cell protein after initial oleate-load incubations to 404 ± 92 μg lipid/mg cell protein after 12 h re-incubation with oleate. Myristate appeared not to stimulate as much accumulation of cellular lipid as oleate did: 350 ± 95 μg lipid/mg cell protein after a 12 h myristate chase. However, the difference between the cellular mass of lipid after 12 h of oleate and 12 h of myristate chase was not significant (Figure 20). The increase in cellular lipid mass was due to increased mass of TAG while cholesterol, PL, and CE cellular mass remained constant. Thus, exogenous fatty acid taken up by Hep G2 cells appeared to be esterified primarily to TAG.

Contrasting mass of lipid secreted in association with apo B to cellular lipid in Hep G2 cells demonstrated the minute level of secretion. Only 0.1–0.4% of the total cellular lipid was secreted in association with apo B.

iii. Lipid Percent Composition

When the mass of lipid classes were expressed as a percentage of the total lipid mass (Figure 21), variability was diminished as compared to the total mass values. As the incubation time of the chase lengthened, the relative amount of TAG in oleate-control chases and myristate chases increased from $38.4 \pm 7.2\%$ of lipid after oleate-load incubations to $43.2 \pm 5.9\%$ of lipid after oleate control chases and to $50.5 \pm 2.6\%$ of lipid after myristate chase incubations (Figure 21). Secreted TAG mass, as a percentage of total lipid mass, was significantly higher after 3, 9, or 12 h of myristate chase than after 3, 9, or 12 h of oleate chase, respectively (Figure 21, panels A & B). Thus, myristate appeared to be more effective in stimulating release of TAG. The myristate chases also tended to stimulate the secretion of TAG mass throughout the chase incubations. The percent content of TAG in the total lipid mass was each significantly higher after 6, 9, or 12 h of myristate chase than after the initial oleate-load incubation (Figure 21, panel B). After 9 or 12 h of myristate chase, the proportion of TAG in the total secreted lipid mass was significantly higher than after 3 h of myristate chase (Figure 21, panel B). However, the proportion of TAG in the total secreted lipid after 6, 9, and 12 h of myristate chase were not statistically distinct, which suggested that TAG secretion had reached a plateau.

Percentage of cholesterol and especially CE were constantly secreted during the incubation. CE represented 4.4–5.6% of lipid mass (Figure 21). CE:TAG mass ratios revealed differences between the oleate and myristate chases (Table 5). Cellular CE:TAG ratios were
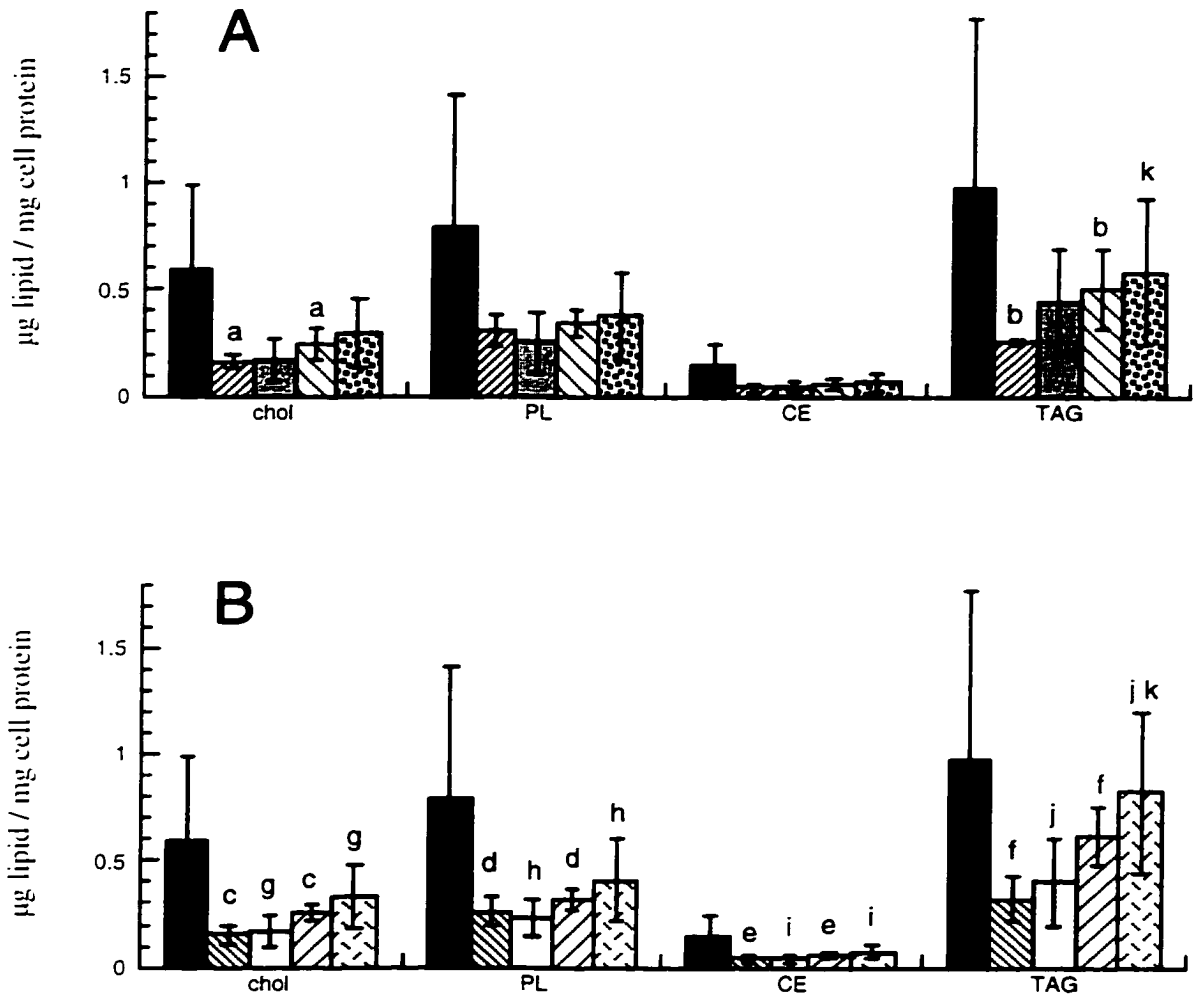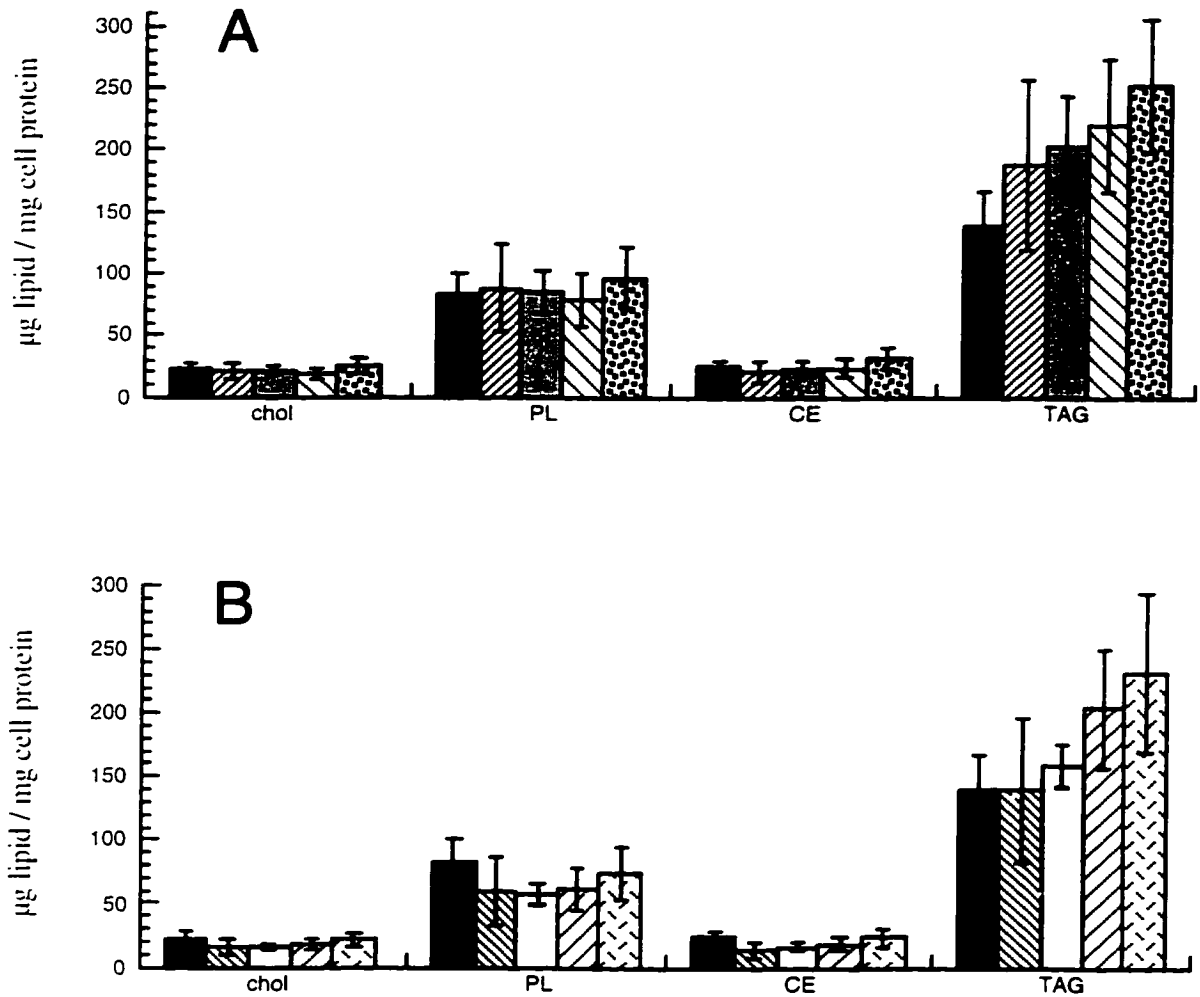
Figure 20: **Accumulation of lipid in Hep G2 cells from oleate-load–single myristate-chase incubations.** Cells were incubated for 18 h with oleate and then were chased with myristate or oleate for 3, 6, 9, or 12 h. Total lipid profiles were determined by GLC. Results are shown as means with standard deviations from 3 experiments. Incubation conditions, panel A: ■ =oleate load, ▨ =3 h oleate, ▦ =6 h oleate, ◩ =9 h oleate, ▨ =12 h oleate; and panel B: ■ =oleate load, ▨ =3 h myristate, □ =6 h myristate, ▨ =9 h myristate, ◪ =12 h myristate. chol=cholesterol.
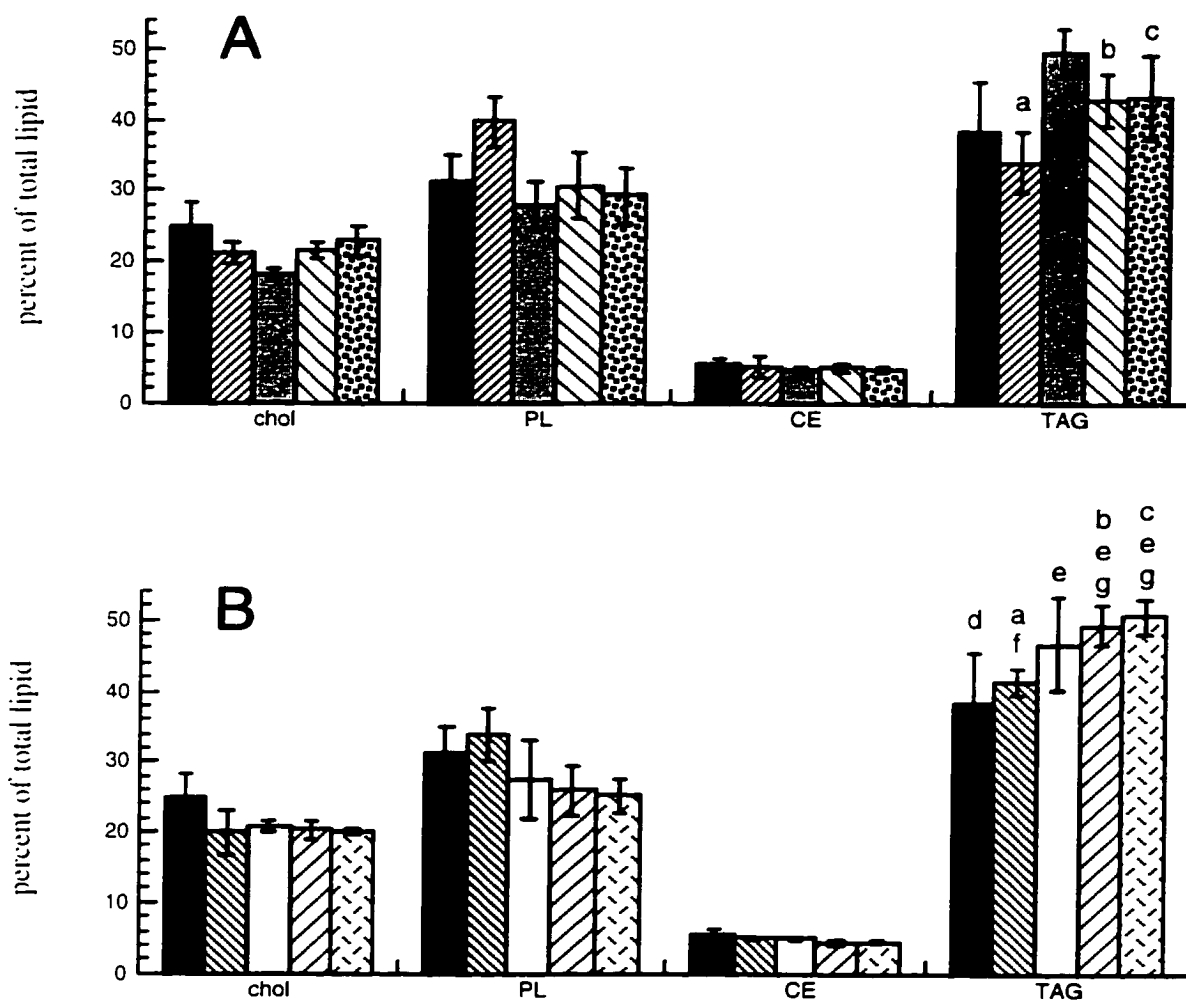
Figure 21: **Lipid class percent composition of LpB from oleate-load-single myristate-chase incubations.** Relative lipid classes are shown as a percentage of total lipid mass of isolated LpB secreted by Hep G2 cells. Results are shown as means with standard deviations from 3 experiments. Incubation conditions, panel A: ■ =oleate load, ▨ =3 h oleate, ▦ =6 h oleate, ◨ =9 h oleate, ◩ =12 h oleate; and panel B: ■ =oleate load, ◨ =3 h myristate, ☐ =6 h myristate, ▨ =9 h myristate, ◪ =12 h myristate. chol= cholesterol. The proportion of TAG in the secreted lipid mass was significantly higher after 3, 9, and 12 h of myristate chase than after 3, 9, and 12 h of oleate chase, respectively (a-c: $p < 0.005$). The proportion of TAG in the secreted lipid mass was significantly higher after 6, 9, or 12 h of myristate chase than the oleate-load incubation (d versus e: $p < 0.03$). The proportion of TAG in the secreted lipid mass was significantly higher after 9 or 12 h of myristate chase than after 3 h of myristate chase (f versus g: $p < 0.004$).

Incubation Time	Media CE:TAG Ratios		Cellular CE:TAG Ratios	
	Oleate Chase	Myristate Chase	Oleate Chase	Myristate Chase
oleate load	0.15±0.05		0.17±0.01	
3 h	0.16±0.07	0.119±0.005 a	0.11±0.01	0.10±0.02 a
6 h	0.09±0.01	0.11±0.02	0.11±0.01 e	0.10±0.01 e
9 h	0.115±0.008 c	0.090±0.006 c	0.10±0.01 f	0.09±0.01 f
12 h	0.11±0.02 d	0.088±0.007 b d	0.12±0.01 g	0.100±0.009 b g

Table 5: CE:TAG **mass ratios after oleate-load–myristate-chase incubations.** CE:TAG mass ratios are shown above for both isolated LpB and Hep G2 cells after oleate-load and myristate-chase incubations. Secreted CE:TAG ratios after 3 h of myristate chase were significantly higher than cellular CE:TAG ratios after 3 h of myristate chase (a: p= 0.0069) but secreted CE:TAG ratios after 12 h of myristate chase were significantly lower than cellular CE:TAG ratios after 12 h of myristate chase (b: p=0.019). After both 9 and 12 h of chase, secreted CE:TAG ratios after myristate chases were significantly lower than after oleate chases (c & d: p<0.02). After 6, 9, and 12 h of chase, cellular CE:TAG ratios after myristate chase was significantly lower than after oleate chase (e–g: p<0.006).

constant at 0.11 after oleate chases and 0.10 after myristate chases, which was significantly lower after 6, 9, and 12 h of chase (Table 5). Cells chased with oleate secreted LpB particles that had similar CE:TAG ratios as cellular ratios. However, secreted CE:TAG ratios after myristate chase were not constant, lowering from 0.12 after 3 h of myristate chase, which was significantly higher than cellular CE:TAG ratios after 3 h of myristate chase, to 0.088 after 12 h of myristate chase, which was significantly lower than cellular CE:TAG ratios after 12 h of myristate chase (Table 5). The declining CE:TAG ratios in secreted LpB particles after 9 and 12 h of myristate chase became significantly lower than secreted CE:TAG ratios after 9 and 12 h of oleate chase, respectively (Table 5). The steady drop in CE:TAG ratios in secreted LpB particles suggested the mass of TAG secreted with apo B was increasing while the mass of CE secreted in association with apo B was constant. Myristate appeared to be more effective than oleate in stimulating Hep G2 cells to secrete more TAG in its nascent VLDL. The constant levels of CE secreted in association with apo B may mean that a small amount of CE was used to lipidate apo B in the assembly of LpB in Hep G2 cells.

iv. Relative Lipid Molecular Species Distribution

a. Proportion of TAG Molecular Species in LpB and Cells

Although there was some variability in the lipid mass values, the molecular species distribution of TAG was very consistent. Figures 22 and 23 depict TAG species as a percent of total moles of TAG secreted or stored in the cell, respectively. Chasing cells with oleate encouraged further skewing of TAG towards oleate-containing species in isolated LpB. The proportion of C54 TAG (typically triolein) secreted with apo B increased from 40.8±2.7 mol % after the initial loading incubation to a maximum of 50.7±1.1 mol % after 9 h of re-incubation with oleate (Figure 22, panel A). Increases in the proportion of C54 TAG secreted with LpB were compensated by decreases in proportions of C48−C52 TAG. In myristate chases, trimyristin (C42) was observed in media associated with apo B after 3 h of chase, as well as C44 and C46, both of which must contain myristate. The rapid appearance of myristate-containing TAG molecular species suggested exogenous fatty acids were readily esterified to TAG and exogenous fatty acid-containing TAG was available for LpB assembly. The substantial proportions of C44 (C14:C14:C16) and C46 (C14:C16:C16 or C14:C14: C18) TAG molecular species present in the secreted LpB demonstrated exogenous myristate entered a common pool with endogenous palmitate and stored oleate. Mixing of fatty acids from various sources in the synthesis of TAG secreted with LpB suggests that Hep G2 cells did not segregate endogenous free fatty acid from exogenous free fatty acid.

The identification of predominant TAG molecular species observed after oleate-load and myristate-chase incubations was the basis for assaying the mechanism of mobilizing
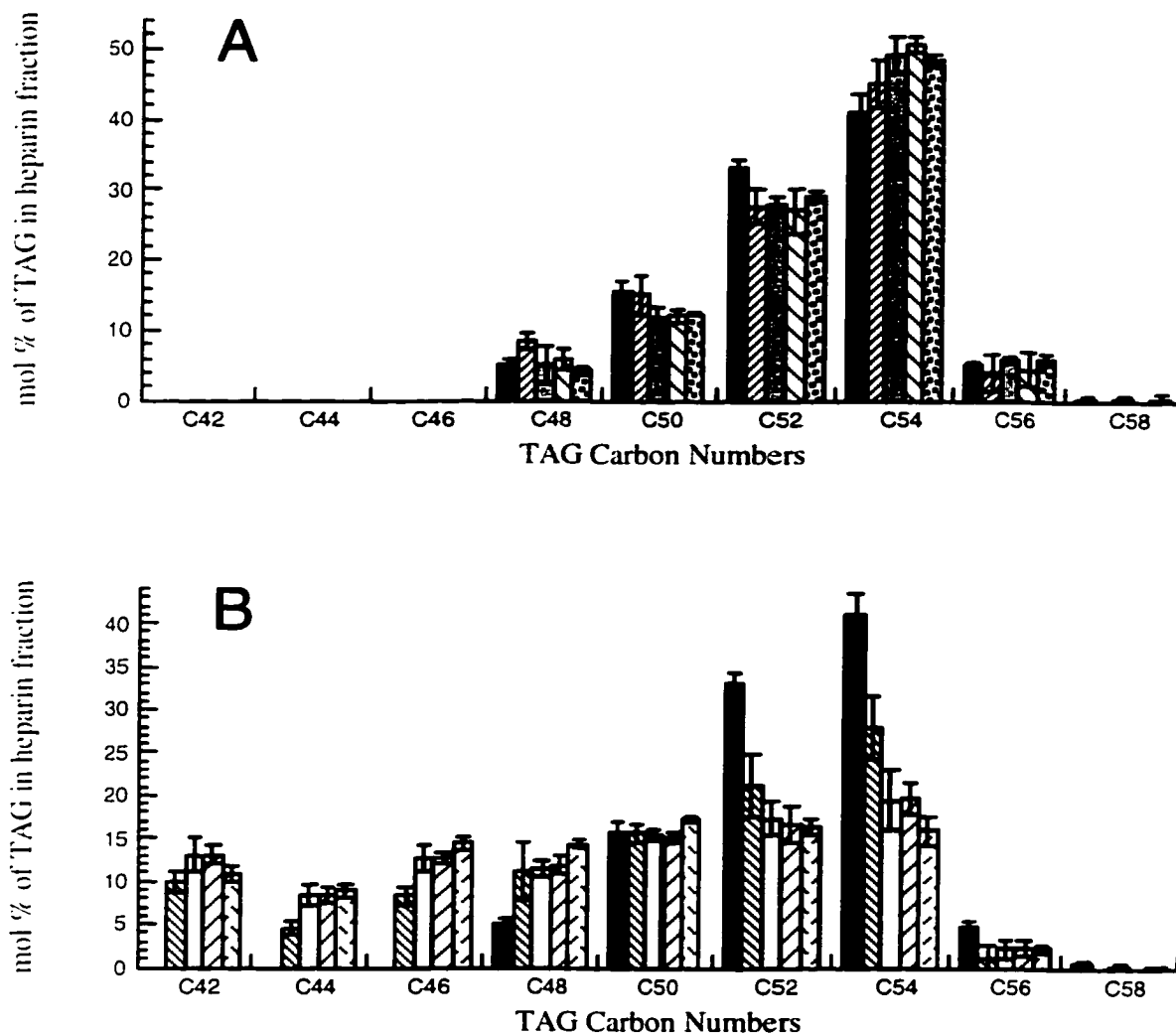
Figure 22: **Distribution of TAG molecular species in LpB from oleate-load–single myristate-chase incubations.** Relative TAG molecular species are shown as determined by GLC and are reported as a percent of total TAG moles. Carbon numbers refer to total carbons in the fatty acid moieties of TAG. Results are shown as means with standard deviations from 3 incubations. Fatty acid and incubation times, panel A: ■ =oleate load, ▨ =3 h oleate, ▣ =6 h oleate, ◩ =9 h oleate, ▨ =12 h oleate; and panel B: ■ =oleate load. ◩ =3 h myristate, □ =6 h myristate, ▨ =9 h myristate, ◪ =12 h myristate.
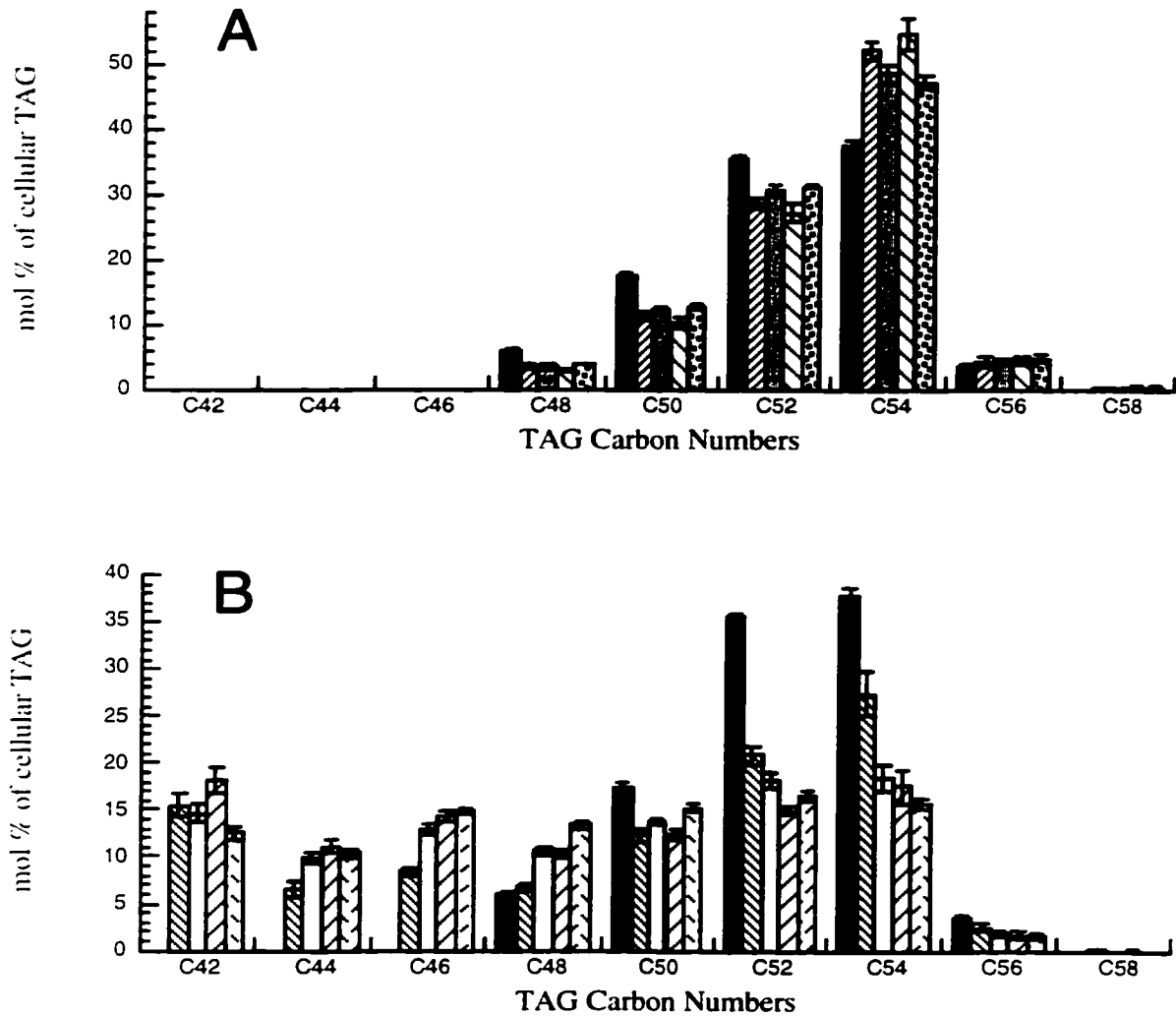
Figure 23: **Distribution of TAG molecular species in Hep G2 cellular samples from oleate-load—single myristate-chase incubations.** Relative TAG molecular species are shown as determined by GLC and are reported as a percent of total TAG moles. Carbon numbers refer to total carbons in the fatty acid moieties of TAG. Results are shown as means with standard deviations from 3 incubations. Fatty acid and incubation times. panel A: ■ =oleate load, ▨ =3 h oleate, ▨ =6 h oleate, ◨ =9 h oleate, ◨ =12 h oleate: and panel B: ■ =oleate load, ◨ =3 h myristate, □ =6 h myristate. ▨ =9 h myristate. ◨ =12 h myristate.

stored TAG for the assembly of LpB. The relative proportions of C42−C46 TAG increased over the myristate chase period while the relative proportions of C52−C54 TAG decreased, which reflected the switch of exogenous oleate to myristate (Figure 22, panel B). After 12 h of myristate incubation, all of the TAG species were in the range of 8.5−18 mol %. The TAG secreted in association with LpB had no predominant molecular species.

If Hep G2 cells mobilized stored TAG for LpB assembly via a mechanism that did not modify TAG but instead transported stored TAG en bloc, triolein was predicted to be a major species of secreted TAG after the oleate-load incubation even though myristate was available during the chase period (Figure 18, panel A). Although Hep G2 cells secreted triolein throughout the 12 h of myristate chase, C54 TAG was not a predominant TAG species. Over the myristate-chase period, the proportion of C54 TAG fell from 27.9±3.6 mol % after 3 h of myristate chase to 15.8±1.7 mol % after 12 h of myristate chase (Figure 22, panel B). The declining proportion of C54 TAG suggested mobilization of stored TAG without modification was not a major pathway in the assembly of LpB in Hep G2 cells.

If Hep G2 cells mobilized stored TAG for LpB assembly via a mechanism which hydrolysed stores TAG to DAG, C50 TAG was expected to be a major TAG molecular species secreted with LpB. The secreted C50 TAG originated from C54 TAG (C18:C18:C18) formed during the oleate-load incubation, which was hydrolysed to a C18:C18 DAG. During the myristate chase, C18:C18 DAG was esterified with myristate to form a C50 TAG (C18:C18: C14: Figure 18, panel B). C50 TAG secreted during the myristate chases ranged from 15.2−17.2 mol %, which was not significantly different from the initial oleate-chase secreted values (15.6±1.4 mol %; Figure 22, panel B). The constant proportion of C50 TAG secreted throughout the oleate-load and myristate-chase incubations, along with the lack of a dominant molecular species, suggested mobilization of stored TAG by hydrolysis to DAG was not a major source of TAG for assembly of VLDL in Hep G2 cells.

If Hep G2 cells mobilized stored TAG for LpB assembly via a mechanism that hydrolyses stored TAG to MAG, C46 TAG was expected to be a dominant TAG molecular species. By hydrolysing a C54 TAG (C18:C18:C18) to a C18 MAG and re-esterifying the MAG to TAG with myristate, a C46 TAG (C18:C14:C14) molecular species will be produced (Figure 18, panel C). C46 TAG first appeared after 3 h of myristate chase at 8.3±1.0 mol % and increased to 14.4±0.9 mol % after 12 h of myristate chase (Figure 22, panel B), which was similar in proportion to all other molecular species of TAG from C42−C54 after 12 h of myristate chase. Since C46 TAG was not a predominant molecular species of TAG, Hep G2 cells did not appear to hydrolyse stored TAG to MAG as a primary mechanism of mobilizing stored TAG for LpB assembly.

Finally, if stored TAG were mobilized by a mechanism of complete hydrolysis. then a range of molecular species of TAG was expected to be secreted with LpB. If oleate mobilized from the cellular pool mingled with exogenous myristate while being esterified to TAG, C42 (trimyristin), C46 (C18:C14:C14), C50 (C18:C18:C14), and C54 TAG (typically triolein) will be generated. If there were no selectivity in choosing a fatty acid during TAG synthesis, either based on structure or origin, then the ratios of C42, C46, C50, and C54 TAG will be determined by molar ratio of the precursor fatty acids. Assuming equal amounts of oleate and myristate, then C42, C46, C50, and C54 TAG will be in a ratio of 1:3:3:1. If one fatty acid were more abundant than the other, then the molar ratios of C42, C46, C50, and C54 will be skewed to either trimyristin or triolein (Table 4). However, G3P acyltransferase has higher activity with saturated fatty acyl-CoA esters and AGP acyltransferase has higher activity with unsaturated fatty acyl-CoA esters (Lehner & Kuksis, 1996). Thus, some skewing towards higher proportions of C46 and C50 TAG was expected under the conditions of the oleate-load–myristate-chase protocol due to the specificities of the enzymes within the TAG synthetic pathway. After 12 h of myristate chase, C42 TAG was 10.8±0.9 mol % of the total secreted TAG; C46, 14.4± 0.9 mol %; C50, 17.2±0.2 mol %; and C54, 15.8±1.7 mol % (Figure 22, panel B). The similar proportions of trimyristin and triolein suggested both fatty acids were available in similar proportions throughout the myristate chase and thus predicted a C42:C46:C50:C54 ratio similar to 1:3:3:1. The ratio was 1: 1.33:1.59:1.46, which does not fit into the pattern developed by Table 4. Considering the apparent equal availability of myristate and oleate along with the enzymatic preferences of both G3P and AGP acyltransferases, the proportions of C46 and C50 TAG were expected to be at least 2 fold higher. The oleate-load and myristate-chase incubations did not provide strong evidence to support a mechanism of complete hydrolysis followed by random esterification to mobilize TAG for LpB assembly.

De novo synthesis of fatty acid complicated the interpretation of the oleate-load and myristate-chase data. Control incubations from single fatty acid incubations demonstrated substantial lipogenesis: 0.4±0.1 µg TAG/mg cell protein (BSA control paired with myristate; Figure 12, panel A). With the addition of substantial TAG mass from de novo synthesis, palmitate may have played a role in levelling the proportions of TAG molecular species to similar values. For example, C44 TAG was a C14:C14:C16 TAG. After 3 h of myristate chase, C44 was 4.6±0.6 mol % of the total secreted TAG and the proportion of C44 increased to 9.0±0.7 mol % after 12 h of myristate chase (Figure 22, panel B). Thus, palmitate was supplied to the TAG pool that was used in assembling LpB. To determine the relative contribution of stored lipid and exogenous fatty acid in the assembly of LpB, de novo synthesis of fatty acid must be reduced.

The analysis of the proportions of the molecular species of TAG to determine the mechanism of lipid assembly into LpB assumed stored TAG was mobilized for the assembly of LpB in Hep G2 cells. During oleate-load—myristate-chase incubations, only 0.1–0.4% of the total cellular lipid was secreted in association with LpB. Hep G2 cells did not appear to mobilize cellular lipid and effective mechanisms for lipid mobilization may be absent from Hep G2 cells.

The rapid appearance of myristate-containing TAG species in isolated LpB suggested esterification of exogenous fatty acids was a major source of TAG in LpB assembly for Hep G2 cells. Some of the TAG molecular species associated with LpB after the myristate chase in the oleate-load—myristate-chase incubations (Figure 22) were observed to approach the LpB proportions from cells incubated only with myristate (Figure 17). The proportions of C42–C48 TAG molecular species after the single fatty acid incubation with myristate (Figure 17, panel B) were significantly higher than the respective proportions of C42–C48 TAG molecular species after 12 h of myristate chase (p<0.0045; Figure 22, panel B) whereas the proportions of C50–C54 TAG molecular species were significantly higher after 12 h of myristate chase (Figure 22, panel B) than the respective proportions of C50–C54 TAG molecular species from the single fatty acid incubations with myristate (p<0.004; Figure 17, panel B). The proportion of C54 TAG in LpB secreted after 12 h of myristate chase (Figure 22, panel B) was double the proportion of C54 TAG in LpB secreted after the single fatty acid incubation with myristate (Figure 17, panel B). Although the proportions of TAG molecular species secreted with LpB appeared to be approaching the proportions observed in LpB secreted from cells incubated only with myristate, the stored oleate from the load incubation seemed to be influencing the proportions of TAG molecular species well into the myristate chase. Exogenous fatty acid appeared to be a major source of TAG in the assembly of LpB in Hep G2 cells; however, Hep G2 cells still had some access to stored oleate-containing TAG.

A comparison of the proportions of cellular and secreted TAG molecular species may also provide evidence for the mechanism of LpB assembly. If Hep G2 cells only used TAG esterified from exogenous fatty acids to assemble LpB, then cellular and secreted proportions of TAG molecular species will be different. The proportions of molecular species of TAG secreted with apo B after myristate chases in oleate-load—myristate-chase incubations will approach the proportions of TAG molecular species secreted during the single fatty acid incubations with myristate; however, the proportions of TAG molecular species in the cells will be influenced by the oleate-containing, cellular lipids stored during the oleate-load incubation. Thus, secreted LpB will have higher proportions of trimyristin and lower proportions of oleate-containing TAG compared to the cellular TAG. If the proportions of molecular

species of cellular and LpB-associated TAG were similar, then Hep G2 cells had some access to cellular TAG throughout the myristate-chase incubation. The proportion of cellular C44–C48 TAG increased over the myristate-chase period while the proportion of cellular C52 and C54 TAG declined. After the myristate chases, the cellular proportions of C42 TAG ranged from 12.5–18.1 mol %; C46 TAG, 8.3–14.9 mol %; and C50 TAG, 12.2–15.2 mol % (Figure 23, panel B). After 12 h of myristate chase, the proportions of cellular C42 and C44 TAG were significantly higher than the respective proportions of C42 and C44 TAG in the secreted LpB (p<0.0008; Figures 22 & 23, panels B); the proportions of cellular C46, C52, and C54 TAG were not statistically different from the respective proportions of C46, C52, and C54 TAG secreted with LpB; and the proportions of cellular C48 and C50 were significantly lower than the respective proportions of LpB-associated C48 and C50 TAG (p<0.02; compare Figures 22 & 23, panels B). The lower proportion of trimyristin (C42 TAG) in LpB than in cellular samples suggested esterification of exogenous myristate had a larger impact upon cellular TAG than LpB TAG. The similar proportion of C54 TAG (typically triolein) in Hep G2 cells and in LpB secreted after 12 h of myristate chase suggested stored oleate-containing TAG species were contributing to the TAG pool used in the assembly of LpB. Thus, Hep G2 cells appeared to have some access to stored oleate-containing TAG during the 12 h of myristate chase. The lack of a predominant molecular species of TAG secreted with LpB obscured the mechanism by which TAG was mobilized for LpB assembly.

b. Proportion of PL Molecular Species in LpB and Cells

Myristate-chase incubations influenced the proportions of PL molecular species, which combined DAG and some ceramides, in Hep G2 cells. After oleate-load incubations, cellular C34 and C36 PL were the major molecular species. Cellular content of C36 PL increased with administration of oleate during chase incubations (Figure 24, panel A) and became a prominent peak. The relative molar amounts of cellular C32 and C34 PL declined significantly after the initial oleate-load incubation, as compared to each of the oleate-chase incubations, but accumulated consistently throughout the oleate-chase control incubations (Figure 24, panel A). The oleate chases also significantly increased the proportion of cellular C36 PL above the cellular proportion of C36 PL observed after the oleate-load incubation (Figure 24, panel A). Chasing the cells with myristate significantly increased the proportion of cellular C30 and C32 PL over the respective proportions after the oleate-load incubation (Figure 24, panel B), with the myristate chase quadrupling the proportion of cellular C30 PL compared to the oleate-load incubation. The proportion of cellular C34 and C36 PL declined with the myristate chase.

Figure 24: **Distribution of PL molecular species in Hep G2 cellular samples from oleate-load–single myristate-chase incubations.** Relative PL molecular species are shown as determined by GLC and are reported as a percent of total PL moles. Carbon numbers refer to total carbons in the fatty acid moieties of PL. Results are shown as means with standard deviations from 3 incubations. Fatty acid and incubation times, panel A: ▩ =oleate load, ▨ =3 h oleate, ▣ =6 h oleate, ◨ =9 h oleate, ▨ =12 h oleate; and panel B: ■ =oleate load, ▨ =3 h myristate, □ =6 h myristate, ▨ =9 h myristate, ▨ =12 h myristate. The cellular pool of PL contained significantly more C32 and C34 PL after the oleate-load incubation than after any oleate chase (a versus b: p<2 x 10⁻⁶; c versus d: p<0.0004, respectively). The cellular pool of PL contained significantly less C36 PL after the oleate-load incubation than after any oleate chase (e versus f: p<3 x 10⁻⁵). The cellular pool of PL contained significantly less C30 and C32 PL after the oleate-load incubation than after any myristate chase (g versus h: p<4 x 10⁻¹⁵; i versus j: p<0.0002, respectively).

Molecular species composition of PL in LpB isolated by heparin-Sepharose chroma-
tography were not identical to the composition of cellular PL. Oleate control chases only
stimulated a slight increase in the amount of secreted C36 PL relative to the load incubation,
which only became significant after 12 h of oleate chase (Figure 25, panel A). However, all
chases with myristate significantly increased the amount of C30 PL secreted relative to the
oleate-load incubations (Figure 25, panel B). Overall, exogenous fatty acid did skew the
molecular species of PL. In both oleate and myristate chases, a higher proportion of PL was
secreted as C30 (p<0.005) and C32 (p<0.03) PL, compared to cellular distributions. while
proportionately more C36 PL (p<0.04) was found in the cells than secreted with LpB (com-
pare Figures 24 & 25). Differences between cellular and secreted PL suggested Hep G2
cells had some preferential selection to assemble phospho- and/or sphingolipid molecular
species of lower mass in LpB than stored in the cells.

The hydrolysis of PL to DAG was proposed to provide an alternate source of DAG in
the synthesis of TAG for LpB assembly (Bar-On et al., 1971; Wiggins & Gibbons, 1996).
The two prominent molecular species of cellular PL after the oleate-load incubation were
C34 (typically C16:C18) and C36 (typically C18:C18) PL (Figure 25, oleate-load bar).
The removal of the PL head group and re-esterification with chased myristate will yield C48
(C16:C18:C14) and C50 (C18:C18:C14) TAG molecular species, respectively. However,
the oleate-load–myristate-chase incubations did not have a predominant molecular species
of TAG (Figure 22, panel B). Therefore, the hydrolysis of PL to provide TAG for LpB assem-
bly did not appear to be a major pathway in Hep G2 cells.

c. Proportion of CE Molecular Species in LpB and Cells

Distribution of CE species was influenced by chase incubations. By re-feeding cells
with oleate in control chases, secreted C18 CE increase from 70.0±0.6 mol % after oleate
load to 79.6±2.2 mol % after 12 h of oleate chase (Figure 26, panel A). Myristate chases
increased proportions of cholesteryl myristate from 2.0±1.8 mol % after the oleate load to
8.8±1.1 mol % after 12 h of myristate chase (Figure 26, panel B). Large variations in cho-
lesteryl myristate may have been due in part to the enhanced error in detecting the small se-
creted mass independent of PL molecular species (see appendix A). Introduction of signifi-
cant amount of cholesteryl myristate decreased relative proportions of cholesteryl palmitate
and C18 CE. However, C18 CE secreted during the myristate chase only became signifi-
cantly lower than the C18 secreted during the oleate control incubations after 12 h of chase
(Figure 26).

The cellular proportions of CE molecular species were similar to the proportions of
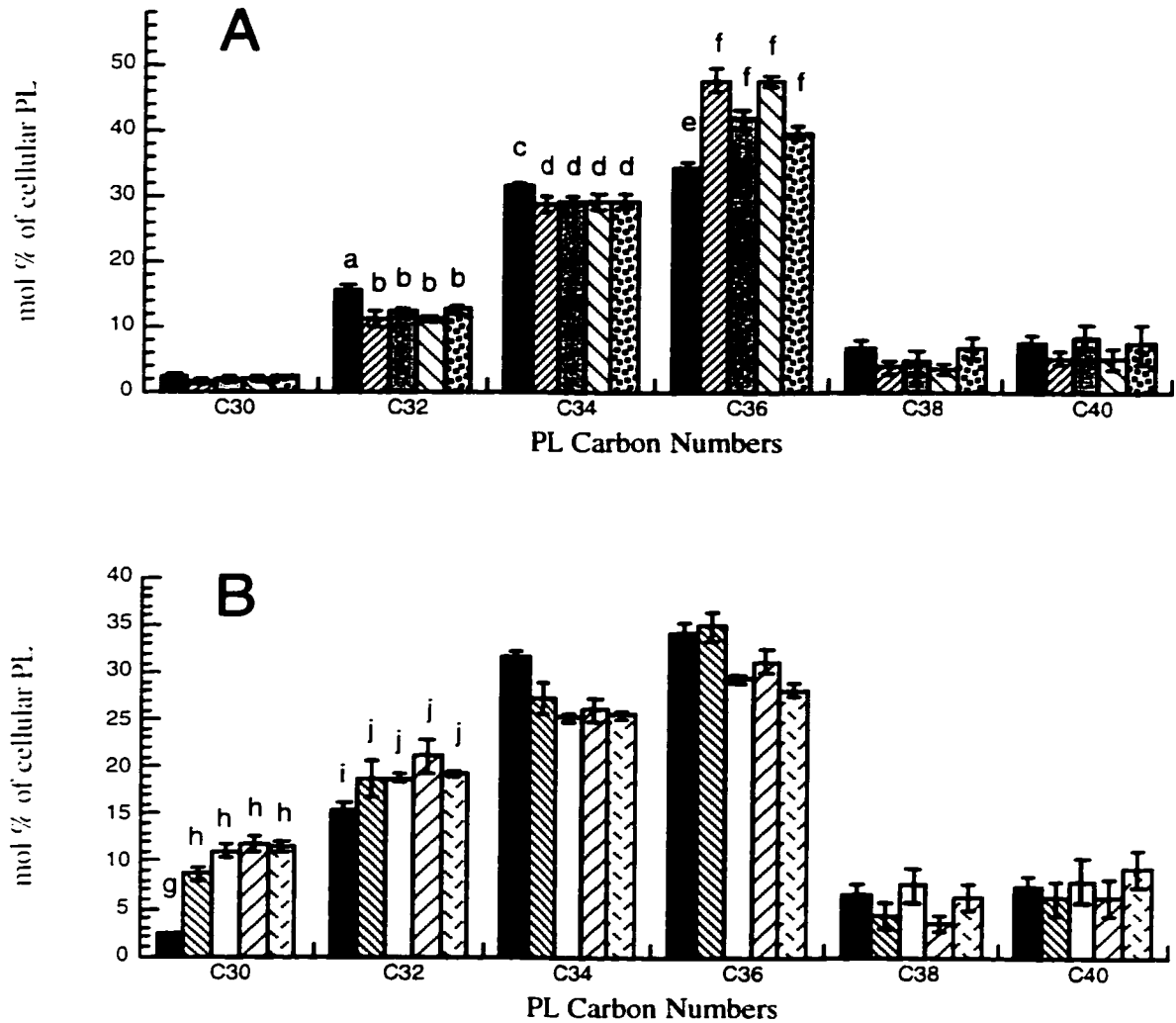CE molecular species from LpB (Figure 27). Hep G2 cells chased with oleate tended to
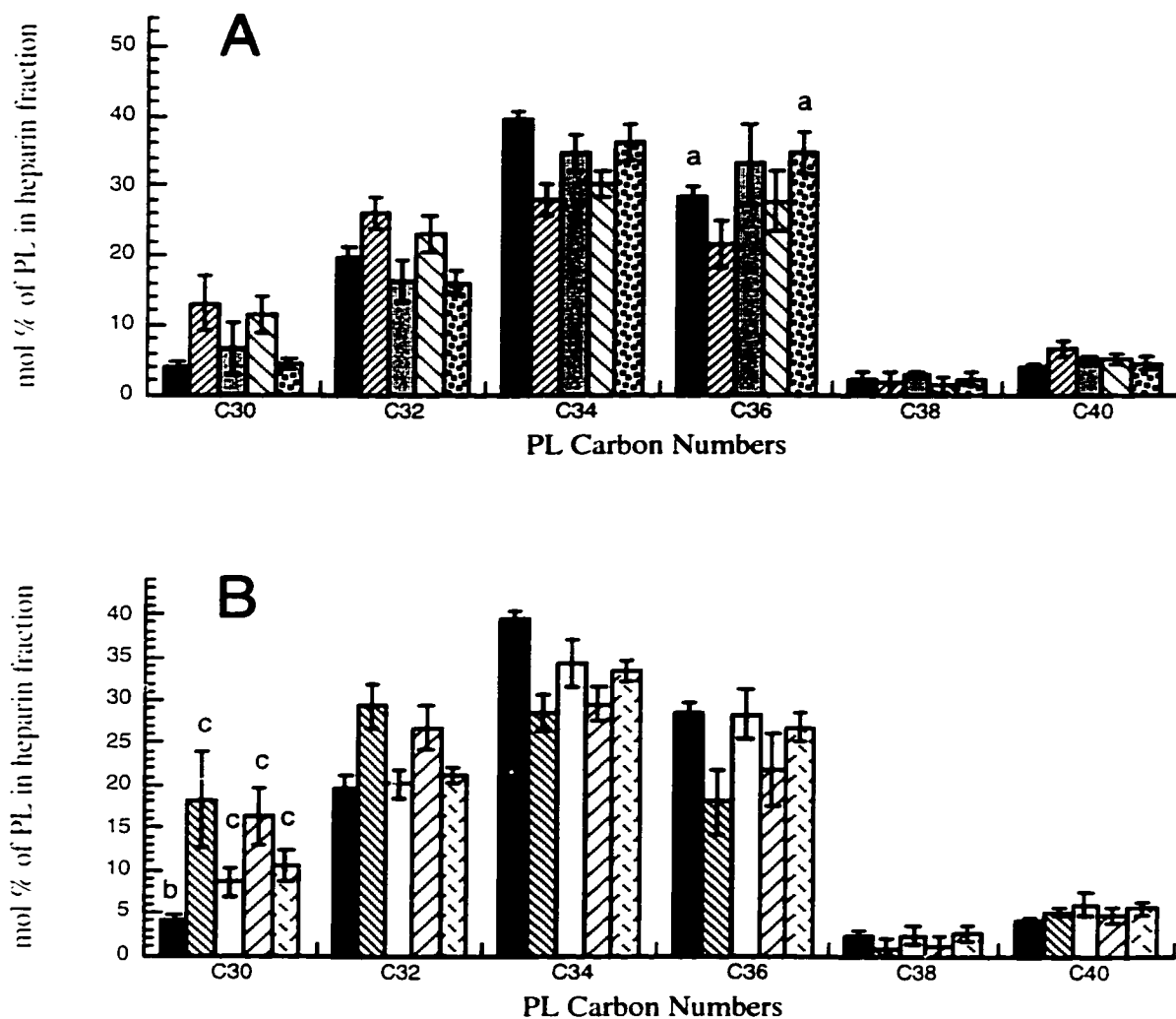
Figure 25: **Distribution of PL molecular species in LpB from oleate-load–single myristate-chase incubations.** Relative PL molecular species are shown as determined by GLC and are reported as a percent of total PL moles. Carbon numbers refer to total carbons in the fatty acid moieties of PL. Results are shown as means with standard deviations from 3 incubations. Fatty acid and incubation times, panel A: ■ =oleate load, ▨ =3 h oleate, ▦ =6 h oleate, ◪ =9 h oleate, ▩ =12 h oleate; and panel B: ■ =oleate load. ▩ =3 h myristate, ☐ =6 h myristate, ▨ =9 h myristate, ◨ =12 h myristate. C36 PL associated with LpB after 12 h of oleate chase was significantly higher than C36 PL secreted after the oleate-load incubation (a: p=0.0027). C30 PL secreted after any myristate chase was significantly higher than C30 PL secreted after the oleate-load incubation (b versus c: p<0.002).
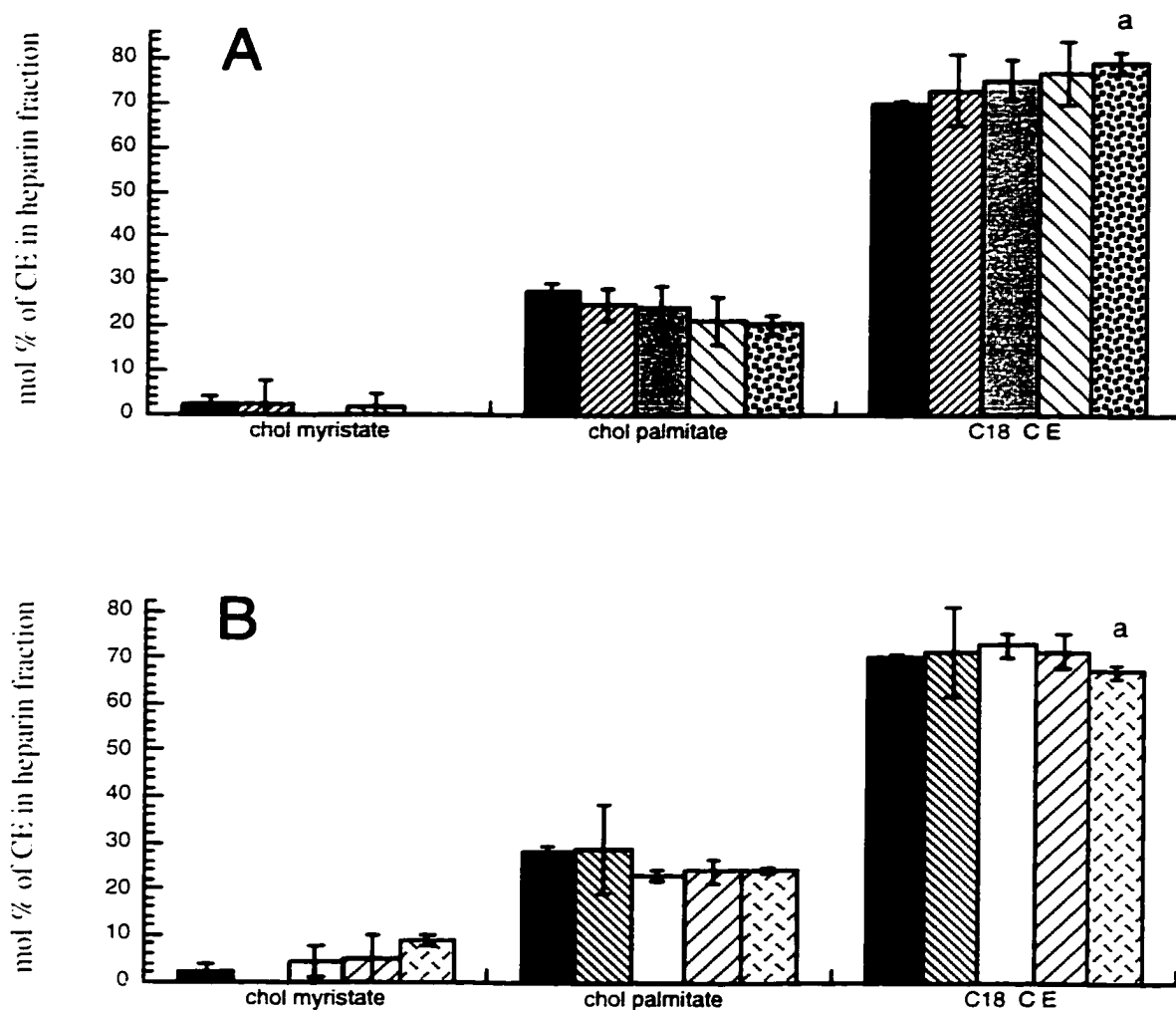
Figure 26: **Distribution of c e molecular species in LpB from oleate-load–single myristate-chase incubations.** Relative c E molecular species are shown as determined by GLC and are reported as a percent of total CE moles. Results are shown as means with standard deviations from 3 incubations. Fatty acid and incubation times, panel A: ■ =oleate load, ▨ =3 h oleate, ▦ =6 h oleate, ◪ =9 h oleate, ▨ =12 h oleate; and panel B: ■ =oleate load, ▨ =3 h myristate, □ =6 h myristate, ▨ =9 h myristate, ▨ =12 h myristate. chol=cholesteryl. C18 CE was significantly higher after 12 h of oleate chase than after 12 h of myristate chase (a: p=2 x 10^{-5}).
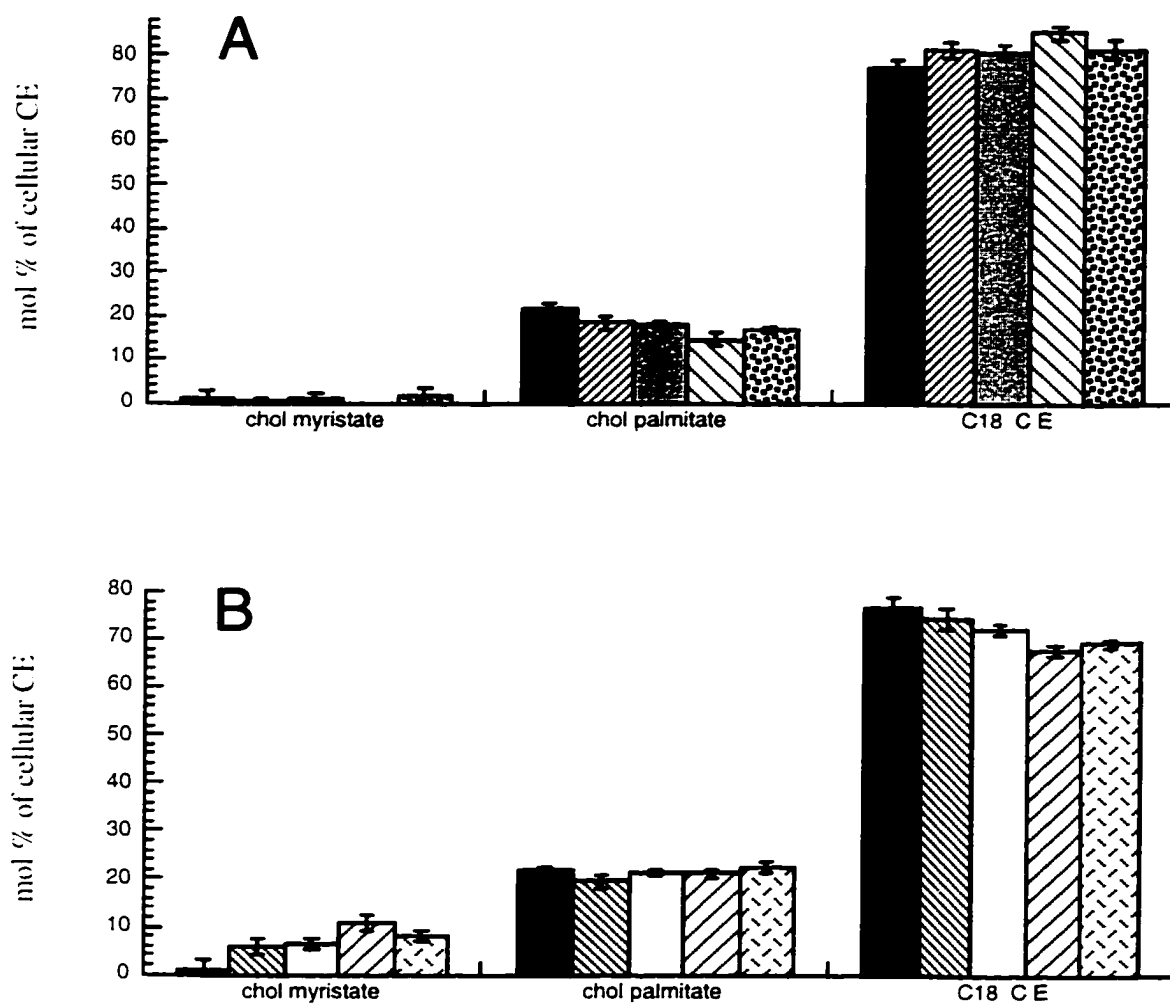
Figure 27: **Distribution of CE molecular species in Hep G2 cellular samples from oleate-load–single myristate-chase incubations.** Relative CE molecular species are shown as determined by GLC and are reported as a percent of total CE moles. Results are shown as means with standard deviations from 3 incubations. Fatty acid and incubation times, panel A: ■ =oleate load, ▨ =3 h oleate, ▨ =6 h oleate, ▨ =9 h oleate, ▨ =12 h oleate; and panel B: ■ =oleate load, ▨ =3 h myristate, □ =6 h myristate, ▨ =9 h myristate, ▨ =12 h myristate. chol=cholesteryl.

store more C18 CE than that secreted in association with LpB. The proportion of cholesteryl myristate was higher in cellular pools than that secreted in association with LpB, which was balanced by reciprocal decreases in C18 CE. The cellular cholesteryl palmitate proportions appeared to be constant. The slight differences between secreted and cellular CE species did not suggest a specific CE species was preferentially assembled into LpB; however, Hep G2 cells had a slight preference to secrete cholesterol that was esterified with the exogenous fatty acid.

V. TAG Secretion Rates

The decline in the proportion of oleate-containing molecular species of TAG associated with LpB over the myristate-chase incubation (Figure 21 & 22, panel B) suggested Hep G2 cells were switching from assembling LpB with oleate-containing molecular species of TAG during the oleate-load incubation to myristate-containing molecular species of TAG during the myristate chase. To improve the assessment of secretion of lipid mass, the molecular species of TAG were expressed as secretion rates. If a molecular species of TAG were secreted at a constant rate throughout the chase period, then that species of TAG was assembled and secreted with LpB. If the rate at which a molecular species of TAG were decreasing, then that molecular species of TAG was becoming less accessible for LpB assembly and may reflect diminishing mobilization and/or delivery of that TAG species for LpB assembly. Rates of secretion of C42, C44, and C46 TAG (Figure 28, panels A, B, & C) were constant throughout the myristate chase, as assessed at 3, 6, 9, and 12 h. Thus, C42–C46 TAG molecular species, which must contain myristate, appeared to be consistently available for LpB assembly throughout the myristate chase. Rates of secretion for C48 and C50 TAG molecular species tended to decline over the myristate-chase period (Figure 28, panels D & E). The secretion rates for C52 and C54 TAG dropped significantly between 3 and 6 h and then remained constant at a low value for the remainder of the 12 h myristate chase (Figure 28, panels F & G). The bulk of oleate-rich TAG species (C52 and C54) seemed to be secreted during the initial phase of the chase period; however, the availability of stored oleate-containing TAG was reduced during the later part of the 12 h myristate chase. Constant secretion of myristate-containing TAG species and decreased secretion of oleate-containing TAG species during myristate chases suggested that exogenous fatty acids had a primary influence and stored TAG was a diminishing influence on the molecular species of TAG secreted with LpB.

Figure 28: **Secretion rates of individual** TAG **species in LpB from oleate-load–single myristate-chase incubations.** Hep G2 cells were incubated with oleate–BSA for 18 h to load lipid storage pools with oleate-containing lipid species. Media were switched to myristate for 3, 6, 9, or 12 h and controls were re-incubated with oleate. Media were harvested and LpB were isolated with heparin-Sepharose chromatography. TAG molecular species were determined by GLC. Results are shown as means with standard deviations from 3 incubations. Fatty acid conditions: [___•___] oleate, [_ _■ _] myristate; TAG species: A=C42, B=C44, C=C46, D=C48, E=C50, F=C52, G=C54, H=C56, and I=total TAG. The secretion rate of C52 TAG fell significantly between 3 and 6 h of myristate chase (a: p=0.049; panel F). The secretion rate of C54 TAG fell significantly between 3 and 6 h of myristate chase (b: p=0.038; panel G).
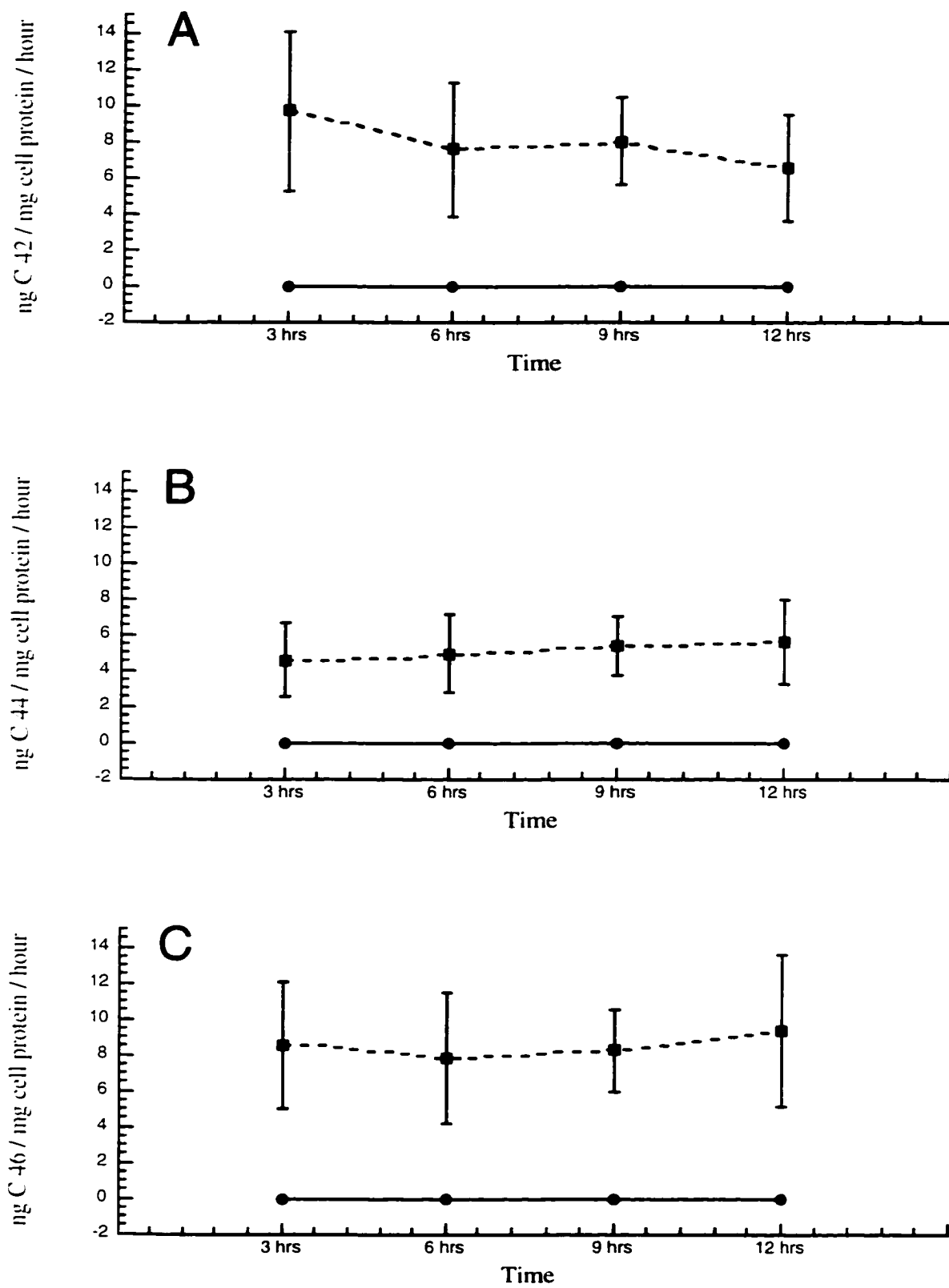
Figure 28
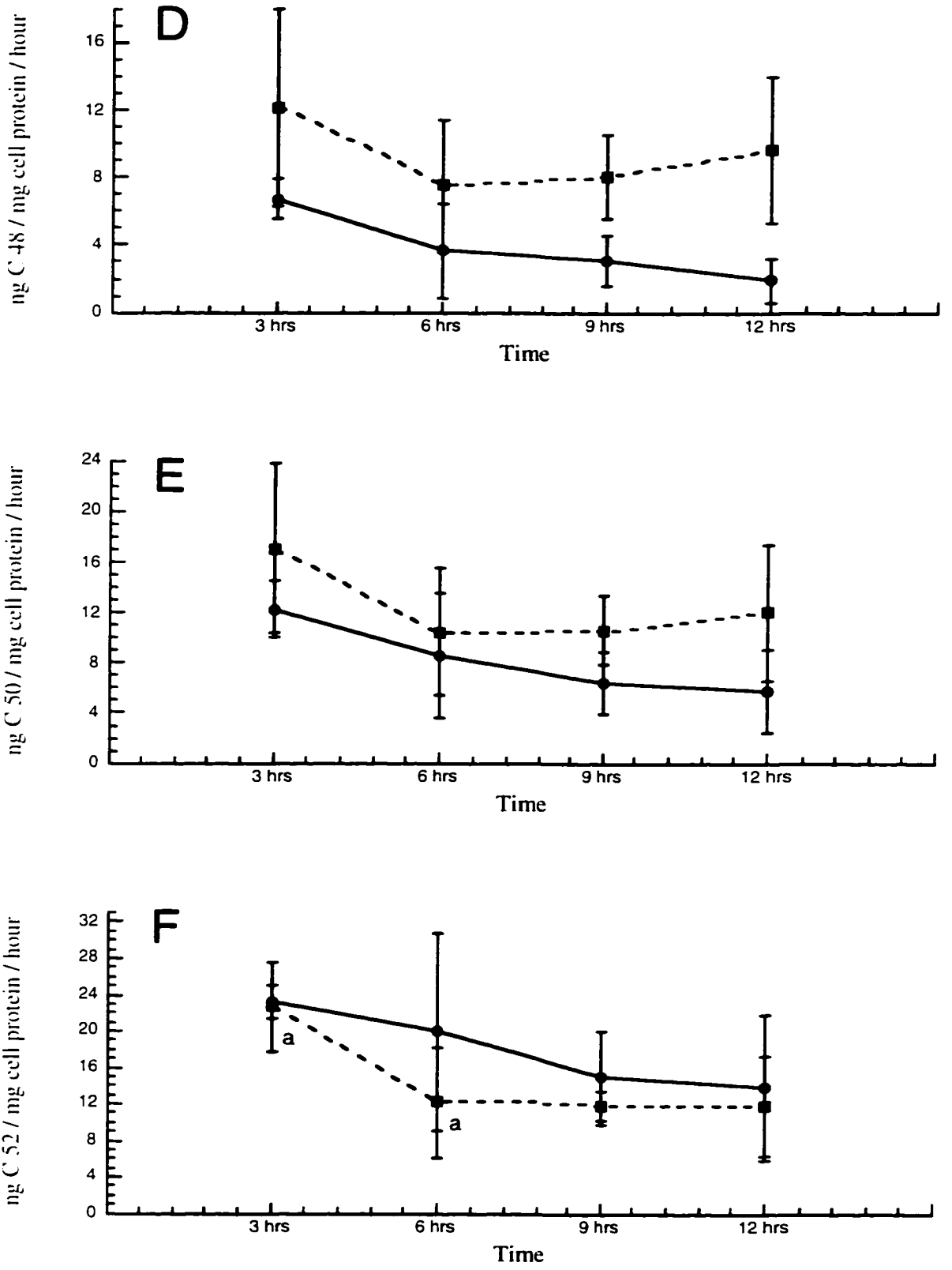
Figure 28
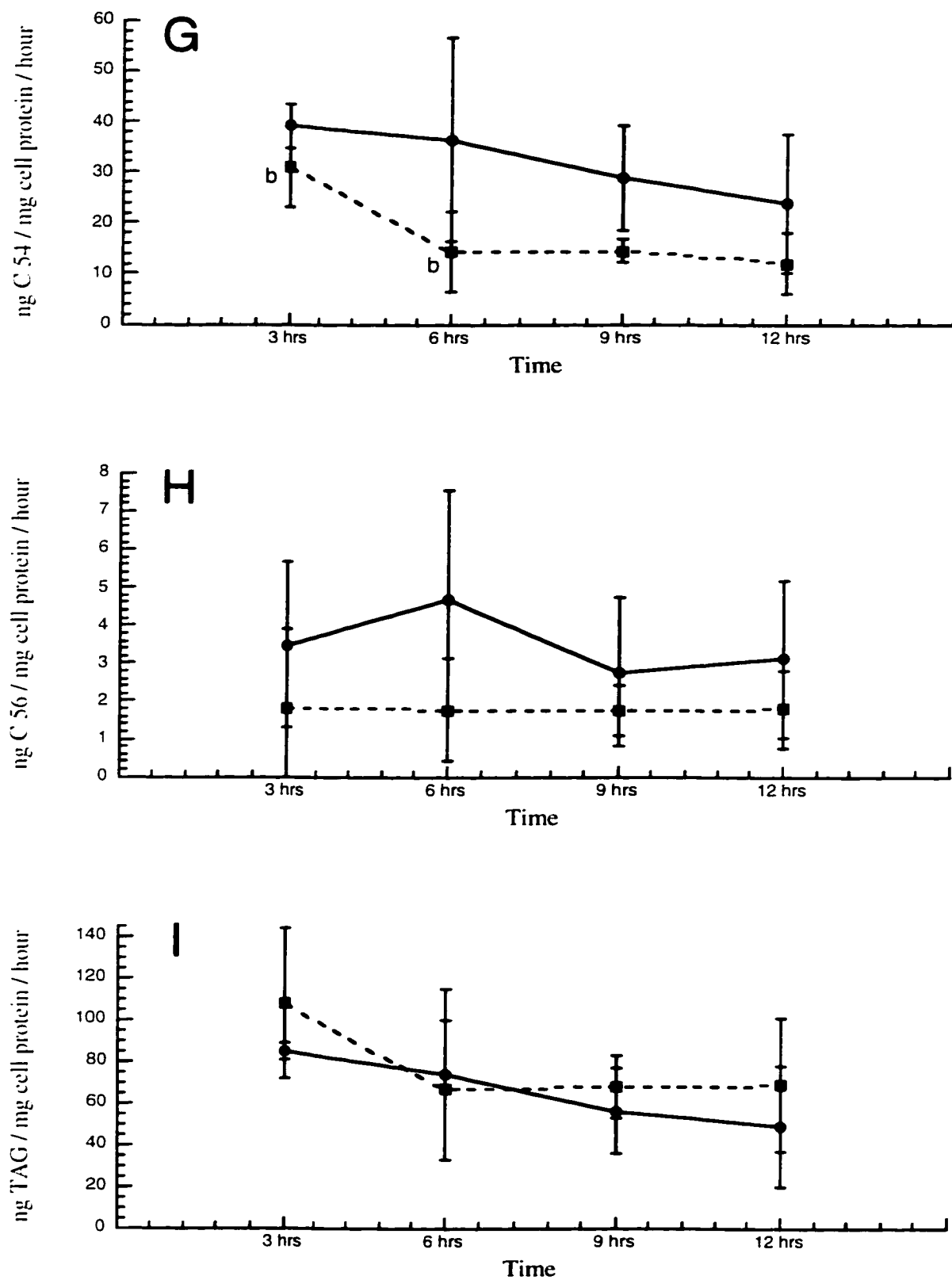
Figure 28

C. Oleate-Load–Double Myristate-Chase with Cerulenin

i. Rationale

TAG secretion rates from oleate-load and single myristate-chase incubations suggest-ed oleate-containing TAG species played a smaller role as myristate-chase time lengthened. Oleate-containing TAG species seemed to be eliminated from the LpB assembly pools, with exogenous myristate playing a more dominant role in supplying TAG for LpB assembly. In order to emphasize the changes in composition with time, Hep G2 cells were loaded with oleate and were followed by multiple chases of short duration with either myristate, oleate, or MEM. After each incubation period, cells were fed with fresh media (Figure 10). If Hep G2 cells rely primarily upon exogenous fatty acid to synthesize TAG for LpB assembly, chasing the cells twice with myristate will allow residual oleate-containing TAG species to move out of the assembly pathway and LpB secreted during the second sequential chase will tend to resemble LpB secreted during single fatty acid incubations with myristate. If Hep G2 cells retain access to stored TAG throughout the chase, then the first and second se-quential chases will be similar and LpB will be secreted with a substantial proportion of molecular species of oleate-containing TAG.

The palmitate-containing lipids observed during oleate-load and myristate-chase incubations were cause for concern. Palmitate may reduce the ability to observe clear rela-tionships between cellular and secreted lipids. To reduce confounding lipid molecular spe-cies from de novo synthesis of fatty acids, glucose concentrations were lowered and cells were incubated in the presence of cerulenin, an inhibitor of fatty acid synthase. Glucose concentrations were reduced from 27.7 mM to the basal MEM value of 5.5 mM, reducing the stimulation of fatty acid synthesis (Cianflone et al., 1992; Wang et al., 1988). Addition of cerulenin to the culture media throughout the load and chase incubations will also reduce synthesis of palmitic acid. Thus, fatty acids available for TAG synthesis and LpB assembly should be supplied by the culture media or mobilized from TAG stored during oleate-load incubations.

ii. Cerulenin Dose Response

Cerulenin dose-response incubations were done with Hep G2 cells to establish an optimal concentration of cerulenin. Cells were loaded with oleate during an 18 h incubation and were chased by two sequential incubations of myristate plus radiolabel for 6 h each ([1-^{14}C]acetate to test for fatty acid synthesis and [1-^{14}C]myristate to test for myristate elongation). Cerulenin was present in the media during the entire 30 h of incubation. Con-trols were incubated with an equivalent volume of the carrier solvent ethanol. Cytotoxicity of cerulenin was estimated by measuring lactate dehydrogenase (LDH) activity released into

the media (Figure 29). Cellular data on LDH activity was lost because of problems establishing proper dilutions of cellular extracts. Ethanol controls displayed uniform LDH activity in the media of all incubation times across the concentration range used. Thus, carrier solvent did not appear to have untoward effects on the cells. High variation and values for 2.5 µg/ml cerulenin incubations were observed, especially compared to the values for 5 µg/ml cerulenin. A systematic error appeared to have occurred during the determination of LDH activity for 2.5 µg/ml cerulenin. Thus, greater significance was placed on data from 5, 10, and 25 µg/ml cerulenin in estimating cytotoxicity. After the initial oleate load (Figure 29, panel A), control and cerulenin activity were identical at 5 µg/ml cerulenin. Media from 10 µg/ml cerulenin incubations were 40% elevated in absorbance and 25 µg/ml cerulenin incubations had double the absorbance of controls. After the first myristate-chase incubation (Figure 29, panel B), the activity of cerulenin and control was the same at 5 µg/ml cerulenin. Cerulenin-treated cells released 60% more activity into the media compared to controls at 10 µg/ml cerulenin. At concentrations of 25 µg/ml cerulenin, the cerulenin-treated cells released 3.5 fold more LDH activity than the control did. After the second sequential myristate-chase incubation (Figure 29, panel C), evidence of cellular toxicity increased for all concentrations. LDH activity at 5 µg/ml cerulenin was 1.4 fold higher compared to the control; at 10 µg/ml cerulenin, 2 fold; and at 25 µg/ml cerulenin, 3.8 fold. Therefore, a concentration of 25 µg/ml cerulenin displayed significant toxicity to the Hep G2 cells over the course of the oleate load and two sequential myristate incubations.

As an inhibitor of fatty acid synthase, cerulenin was expected to reduce incorporation of ^{14}C-acetate into cellular lipids. Cellular lipid extracts were separated on TLC using a solvent system to resolve neutral lipid and radioactivity isolated in TAG, PL, and cholesterol bands was reported (Figure 30, panels A, B, & C, respectively). TLC plates were scanned by a phosphoimager, which reported the radioactivity as counts over the thickness of the band. and the counts x mm were normalized with total cellular protein. Incubating Hep G2 cells with 5 µg/ml cerulenin resulted in a 30% decrease in the incorporation of ^{14}C-acetate into TAG compared to controls. At 10 µg/ml cerulenin, the incorporation of acetate label into cellular TAG was reduced to 25% of control levels and at 25 µg/ml cerulenin, the incorporation of acetate label into cellular TAG was reduced to 20% of control values (Figure 30, panel A). Cerulenin appeared to be an effective inhibitor of acetate incorporation into TAG. The incorporation of ^{14}C-acetate label into PL was also inhibited by cerulenin. At 10 and 25 µg/ml cerulenin, the amount of acetate incorporated into PL was 64 and 48% of controls, respectively (Figure 30, panel B). PL synthesis appeared to be less sensitive to cerulenin than TAG synthesis was, although the incorporation of acetate into PL was only 25% of that for TAG. Cerulenin was shown also to inhibit *de novo* synthesis of sterols (Omura, 1981).

Figure 29: **Cerulenin toxicity in Hep G2 cells as determined by lactate dehydrogenase release into the media.** Hep G2 cells were incubated with oleate–BSA solution plus cerulenin for 18 h. Media were harvested and cells were switched to myristate–BSA solution plus cerulenin for 6 h incubations. After the first myristate incubation, media were harvested and cells were incubated a second time with fresh myristate–BSA solution plus cerulenin. Controls were incubated with an equivalent volume of the cerulenin carrier solvent ethanol. Aliquots of conditioned media after initial oleate incubations (A), first myristate incubations (B), and second sequential myristate incubations (C) were analyzed for the presence of lactate dehydrogenase by an enzymatic kit from Promega. Results are shown as means with standard deviations from 3 experiments. Incubation conditions: ☐ =ethanol control and ⊠ =cerulenin.
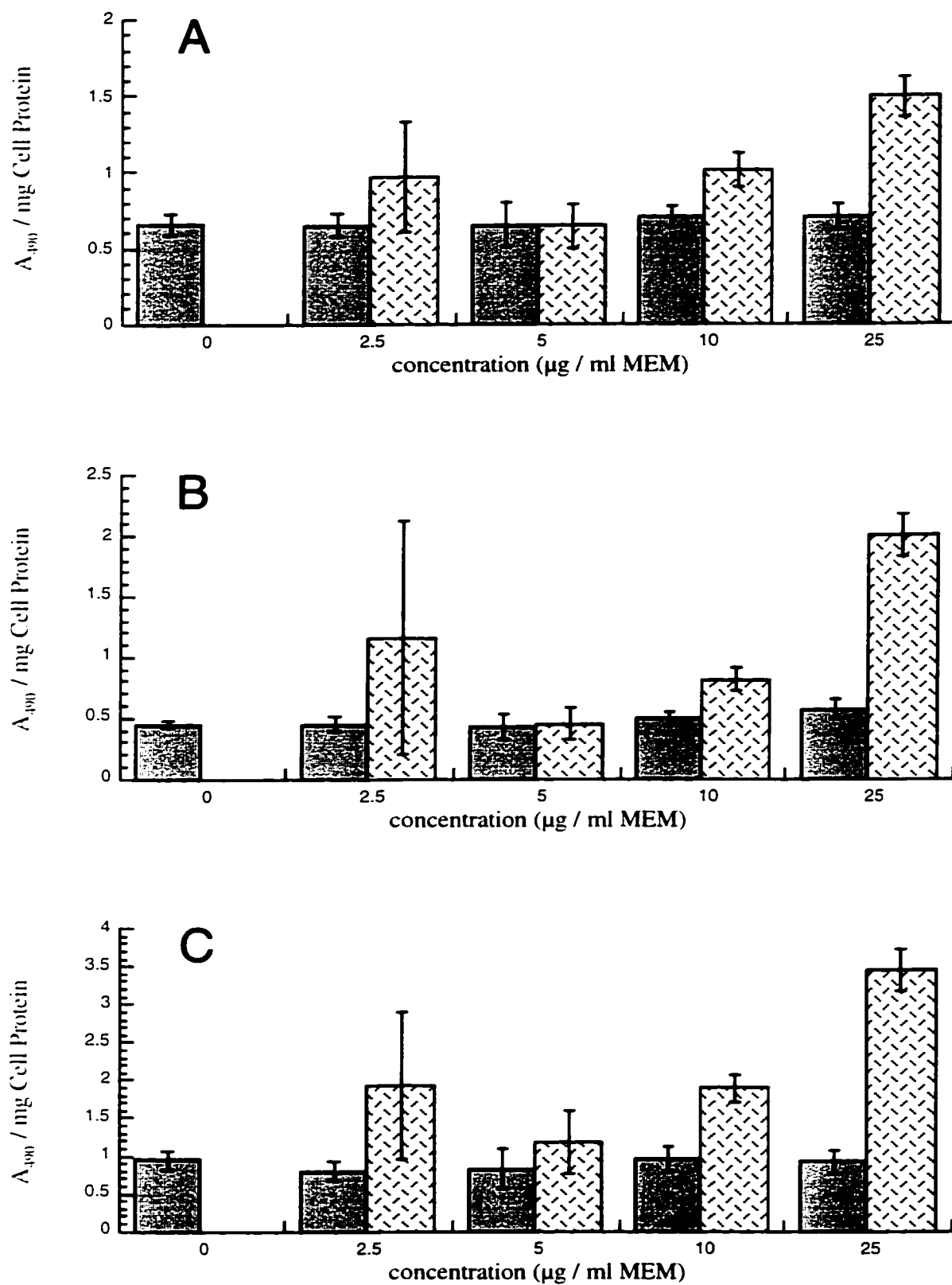
Figure 29

Figure 30: **Effect of cerulenin on acetate incorporation into cellular lipid of Hep G2 cells.** Hep G2 cells were incubated with oleate—BSA solution plus cerulenin for 18 h. Media were removed and cells were incubated with myristate—BSA solution containing cerulenin and 1 μCi/ml of [1-^{14}C]-acetate for 6 h. After first myristate incubations, cells were incubated a second time with fresh myristate—BSA solution plus cerulenin and acetate label. Controls were incubated with an equivalent volume of the cerulenin carrier solvent ethanol. Cellular aliquots were extracted with chloroform and lipids were separated on TLC. TAG bands (A), PL bands (B), and cholesterol bands (C) are shown. Results are means with standard deviations from 3 experiments. Incubation conditions: ▧ =ethanol control and ▧ =cerulenin.
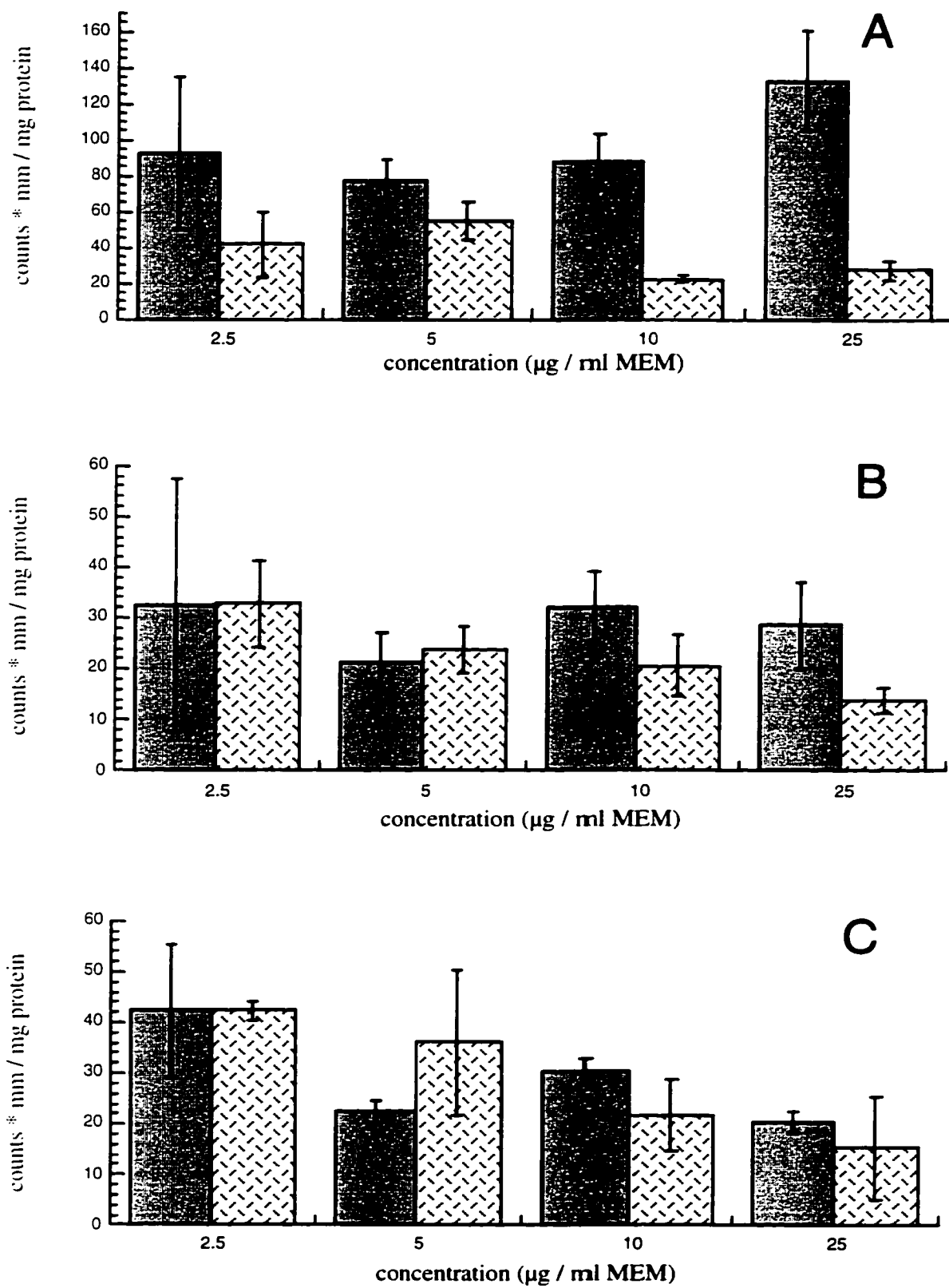
Figure 30

Cerulenin appeared to inhibit the incorporation of acetate into cholesterol to some degree. At 10 and 25 µg/ml cerulenin, acetate label incorporated into cholesterol was reduced to approximately 72% of the control values (Figure 30, panel C). Thus, cerulenin appeared to weakly inhibit cholesterol synthesis in Hep G2 cells. In summary, cerulenin inhibited the synthesis of fatty acids, which strongly impacted upon TAG synthesis, in Hep G2 cells.

Myristate may be elongated, which will provide palmitate to the cellular pool of lipid in addition to the palmitate from *de novo* synthesis of fatty acids. Cerulenin was reported also to inhibit the elongation of fatty acids (Omura, 1981). To test for the elongation of myristate, fatty acid methyl esters from the total saponifiable fraction of cellular aliquots were separated on reverse-phase TLC. Unlabelled standards demonstrated the following R_f values: myristic acid methyl ester=0.47, palmitic acid methyl ester=0.38, oleic acid methyl ester=0.39, and steric acid methyl ester=0.29. The appearance of radiolabel in palmitate-oleate or stearate bands from control incubations demonstrates elongation of ^{14}C-myristate whereas a reduction of radiolabel in the palmitate-oleate and stearate bands after cerulenin treatment indicates inhibition of myristate elongation. After incubating Hep G2 cells with ^{14}C-myristate, no label was observed with a R_f value equal to the stearate standard. Label was observed in the palmitate-oleate and myristate bands. The majority of label (85.8–89.3% of the counts) was in the myristate band while 10.7–14.2% of the label were present in palmitate-oleate band (Figure 31). At cerulenin concentrations equal to or less than 10 µg/ml cerulenin, the radioactivity in the palmitate-oleate band was similar to controls; however, the palmitate-oleate band was only 39% of controls at 25 µg/ml cerulenin (Figure 31, panel B). Similar trends were observed in the myristate band: the cerulenin counts equalled control counts except at 25 µg/ml cerulenin where cerulenin was also 39% of the control (Figure 31, panel A). If cerulenin inhibited elongation of myristate by 39% to palmitate-oleate, which was 5% of the total label, then the counts in the myristate band should have increased. However, total label declined with the addition of 25 µg/ml cerulenin, which may have resulted from impairment of fatty acid uptake due to cerulenin toxicity (Figure 29). Thus, elongation of myristate in Hep G2 cells appeared to be insensitive to cerulenin at concentrations up to 25 µg/ml.

The ability of cerulenin to inhibit the incorporation of acetate into fatty acid, and subsequently TAG, was most important in resolving the contribution of *de novo* synthesis of fatty acid to TAG synthesis for the assembly of LpB in Hep G2 cells. Cerulenin at concentrations of 10 and 25 µg/ml strongly inhibited the incorporation of acetate into TAG; however, concentrations of 25 µg/ml cerulenin indicated some cellular toxicity over the course of the 30 h incubation. Therefore, 10 µg/ml cerulenin was taken as the best concentration and was used in oleate-load and double myristate-chase incubations.
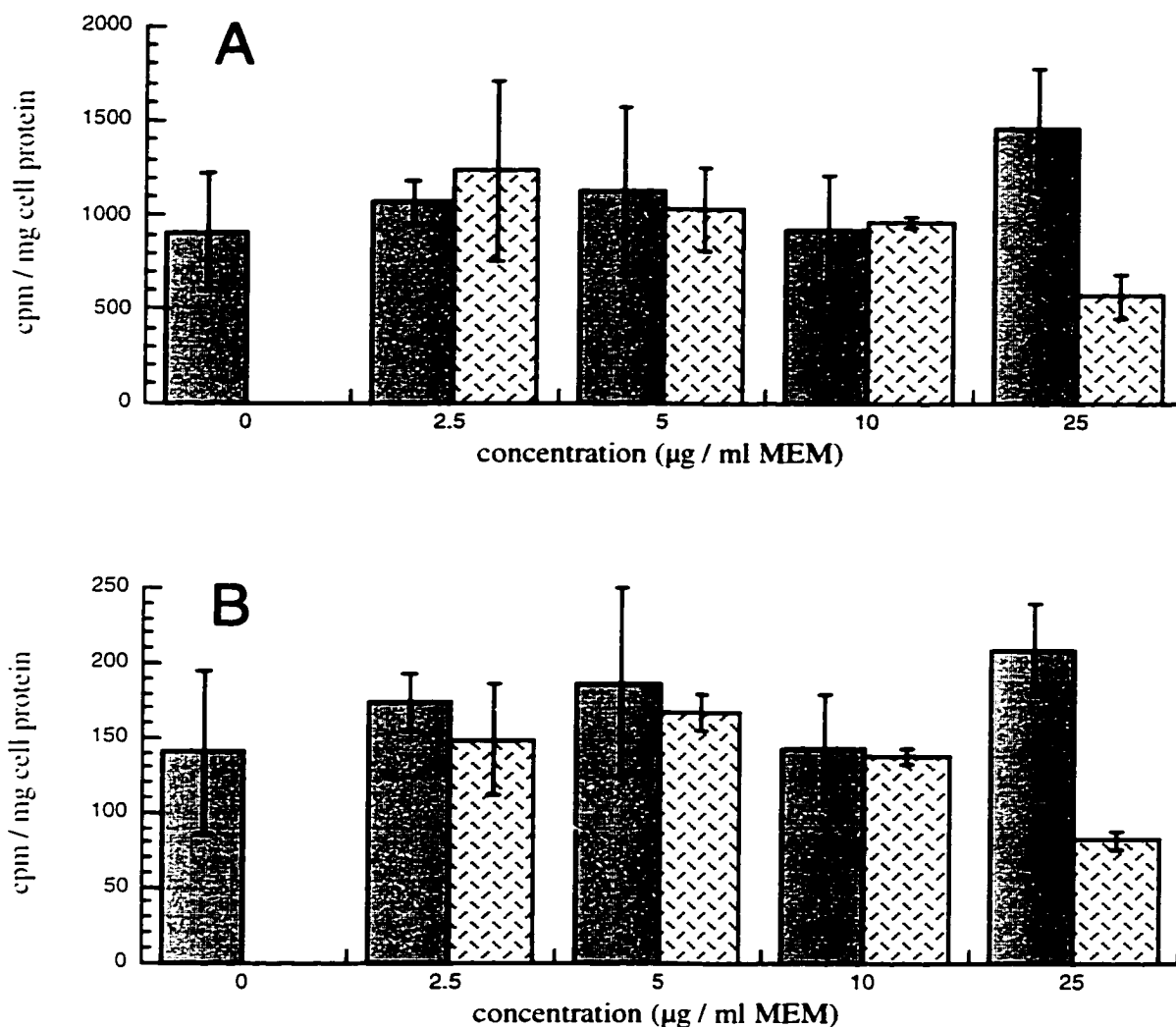
Figure 31: **Effect of cerulenin on myristate elongation in Hep G2 cells.** Hep G2 cells were incubated with oleate plus cerulenin for 18 h. Cells were then incubated with myristate plus cerulenin and 0.417 μCi/ml of ^{14}C-myristate for 6 h. After first myristate incubations, cells were incubated for another 6 h with fresh myristate plus cerulenin and myristate label. Controls were incubated with an equivalent volume of the cerulenin carrier solvent ethanol. Cellular extracts were saponified and fatty acid methyl esters were run on reverse-phase TLC. Myristate bands (A) and palmitate-oleate bands (B) are shown. Results are means with standard deviations from 3 experiments. Incubation conditions: ▇ =ethanol control and ▨ =cerulenin.

iii. Lipid Mass

Figure 32 shows accumulation of lipid mass, divided into lipid classes, for oleate-load–double myristate-chase incubations with cerulenin. Incubations that included cerulenin had unexpected results: when cells were chased with oleate or myristate, addition of 10 μg/ml cerulenin tended to result in significant stimulation of secreted LpB lipid compared to controls (Figure 32, panels A & B). By the end of the second sequential oleate chase, cells treated with cerulenin had secreted approximately 25% more PL and TAG than control cells did (Figure 32, panel B). After the second sequential myristate chase, the amount of PL and CE secreted after cerulenin treatments was 40% higher than in control incubations and TAG mass secreted after cerulenin treatments was 58% higher than in control incubations (Figure 32, panel B). All lipid classes secreted after the second myristate chase were significantly higher when treated with cerulenin, as compared to their respective controls. The mass of LpB TAG secreted by Hep G2 cells chased with oleate and myristate was similar, which contrasted with the oleate-load and single myristate-chase incubations that showed myristate stimulated the secretion of more LpB TAG mass than in oleate incubations (Figure 19). Hep G2 cells that were incubated with exogenous fatty acid appeared to secrete more lipid mass when fatty acid synthase was inhibited. De novo synthesis of fatty acids may stimulate lipid storage rather than LpB secretion in Hep G2 cells when combined with the uptake and esterification of exogenous fatty acid. When Hep G2 cells were chased with medium lacking exogenous fatty acid, total lipid mass secreted was approximately 60% of the secreted mass of lipid from cells incubated with oleate during chase incubations (Figure 32). Neutral lipids were most affected by the absence of fatty acid in the chase media, as CE and TAG mass secreted during chases with only MEM were half the mass secreted during oleate chases (Figure 32). When Hep G2 cells were deprived of exogenous fatty acid and treated with cerulenin during the two sequential chases, secreted lipid mass was significantly lowered compared to cells chased with media lacking fatty acid and not treated with cerulenin (Figure 32, panels A & B). Cells incubated without fatty acid and treated with cerulenin secreted half the CE and TAG mass compared to cells which were only deprived of exogenous fatty acid (Figure 32, panel A & B). Reduced secretion when fatty acid synthase was inhibited suggested de novo synthesis of fatty acids made a significant contribution of lipid to LpB assembly in the absence of exogenous lipid. However, an exogenous supply of fatty acid not only stimulated secretion of LpB lipid but stimulated sufficient TAG synthesis to protect against the lipid lost from de novo fatty acid synthesis.

Cellular lipid mass accumulated in Hep G2 cells showed no significant differences between incubations with cerulenin and controls for any class of lipid (Figure 32, panel C). Uptake and esterification of fatty acids appeared to play a dominant role in the accumulation

Figure 32: **Accumulation of lipid in secreted LpB and in Hep G2 cells from oleate-load—double myristate-chase incubations with cerulenin.** Cells were loaded with oleate-containing lipids by an 18 h incubation with oleate and cerulenin. After the loading incubation, the cells were chased with cerulenin and either myristate, oleate, or MEM for 6 h. At the end of the first 6 h chase, media were harvested, and the cells were chased for another 6 h with fresh media that were identical to the first chase (Figure 10). Controls were incubated without cerulenin. LpB were isolated from media by heparin-Sepharose chromatography for each chase period. Panel A shows LpB secreted during the first sequential incubation, panel B shows LpB secreted during the second sequential incubation, and panel C shows cellular lipid after all 30 h of incubation. Results are means with standard deviations from 3 incubations. Conditions for two sequential incubations after oleate load were: ■ = oleate; □ = oleate plus cerulenin; ◪ = myristate; ▨ = myristate plus cerulenin; ▥ = MEM; ▨ = MEM plus cerulenin. The mass of PL, CE, and TAG secreted with LpB after the first myristate chase was significantly lower than the respective PL, CE, and TAG secreted from cells that were also treated with cerulenin (a–c; p<0.02). All lipid classes secreted from cells chased with only MEM were significantly higher than the respective lipid classes from cells that were chased with both MEM and cerulenin (d–g; p<0.01). The mass of PL and TAG secreted with LpB after the second oleate chase was significantly lower than the respective PL and TAG secreted by cells that were chased with both oleate and cerulenin (h & i; p<0.03). All lipid classes secreted from cells chased with myristate were significantly lower than the respective lipid classes secreted from cells that were chased with both myristate and cerulenin (j–m; p<0.015). All lipid classes secreted from cells chased only with MEM were significantly higher than the respective lipid classes secreted from cells that were also treated with cerulenin (n–q; p<0.04). Cellular accumulation of PL in cells chased with myristate and cerulenin was significantly lower than the accumulated cellular mass of PL in cells chased with MEM and cerulenin (r; p=0.00017). The cellular pool of TAG after oleate chases was significantly higher than the cellular pool of TAG after myristate chases (s versus t; p<0.02). The cellular pool of TAG after myristate chases was significantly higher than the cellular pool of TAG after MEM chases (t versus u; p<0.04).
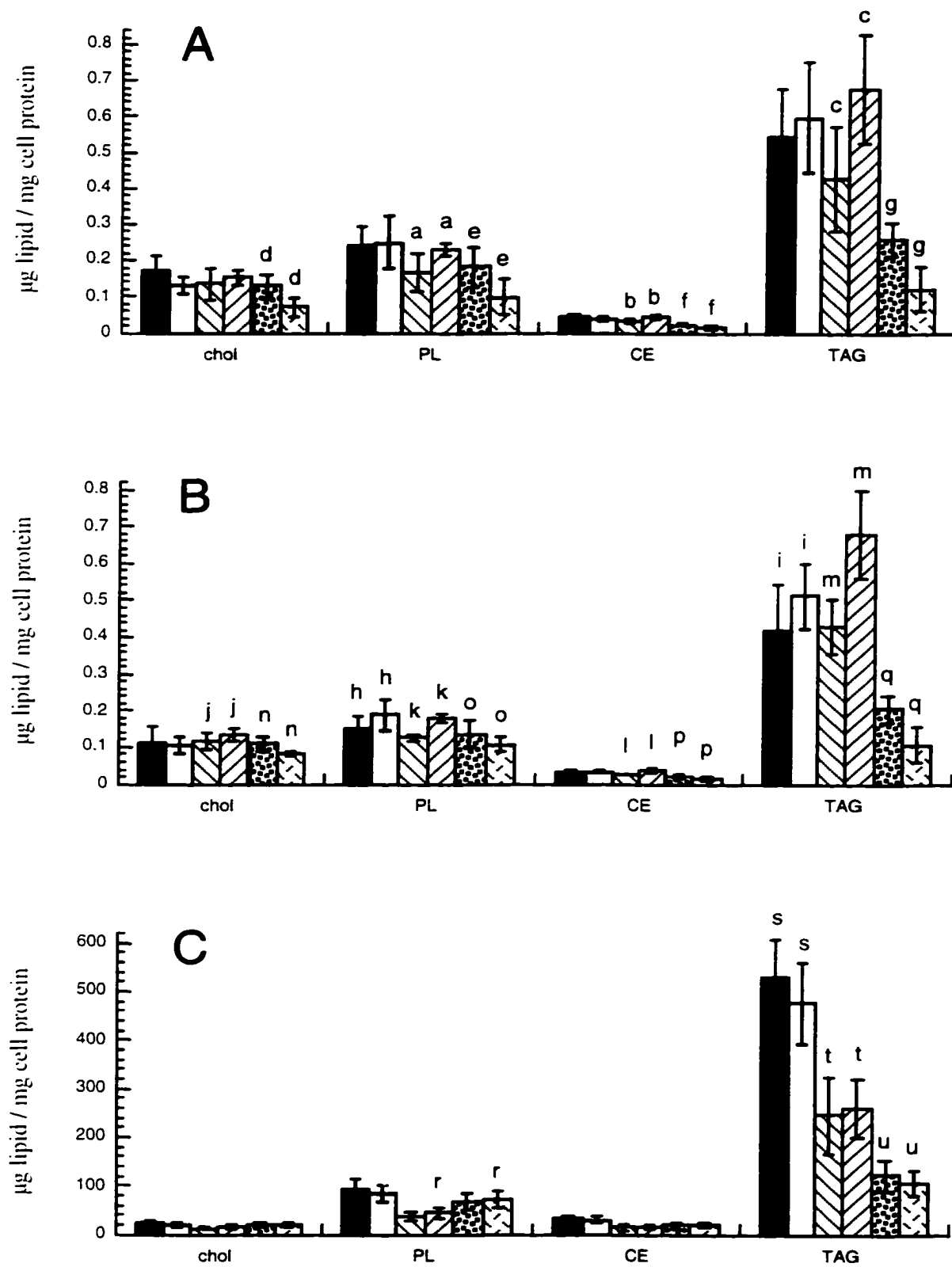
Figure 32

of cellular lipid since inhibition of *de novo* synthesis of fatty acids by cerulenin did not impact upon the accumulation of cellular lipid. Cells incubated with oleate had stored approximately twice as much lipid in every class compared to cells incubated with myristate (Figure 32. panel C). Thus, myristate did not appear to stimulate TAG storage to the same degree as oleate did. A similar trend was observed after the oleate-load–single myristate-chase incubation: however, the mass of lipid accumulated in the Hep G2 cells after a single oleate chase of 12 h was not significantly higher than the cellular lipid that accumulated after a single myristate chase of 12 h (Figure 20). Despite the chase time being equal with the two experiments that switch the media from oleate to myristate, the two sequential chases replenished the media after the first 6 h. The second sequential chase may have provided the extra fatty acid mass, which allowed the oleate-chased cells to accumulate significantly more cellular lipid than cells chased twice with myristate.

Hep G2 cells chased with MEM accumulated 4 fold less cellular TAG mass than cells chased with oleate and 2 fold less cellular TAG mass than cells chased with myristate (Figure 32. panel C). However, cells deprived of exogenous fatty acid during the chase incubations accumulated cholesterol and CE on par with oleate-chased cells. Thus, the uptake and esterification of exogenous fatty acid appeared to primarily affect accumulation of TAG mass. Cells that were deprived of exogenous fatty acid tended to accumulate more PL than in myristate-chased cells and the difference became significant when the cells were also treated with cerulenin (Figure 32, panel C). Although substantial quantities of myristate were esterified and contributed to TAG mass, myristate appeared to inhibit PL synthesis.

Hep G2 cells secreted only 0.10–0.33% of total lipid mass after oleate-load and double myristate-incubations, which agreed well with observations made during the oleate-load and single myristate-chase incubations. Hep G2 cells appeared to be unable to access lipid stored within the cells and may lack effective mechanisms to mobilize substantial lipid mass for LpB assembly.

iv. Lipid Percent Composition

When the lipid classes secreted with apo B were expressed as a percentage of the total lipid. the proportion of CE was very consistent. CE ranged from 3.7–4.7% across all conditions of the first and second chase incubations (Figure 33), thus the proportion of CE in the total lipid appeared to be independent of fatty acid or cerulenin treatment. A significant 7% increase was observed in the proportion of TAG secreted in association with apo B after both sequential chases from cells treated with cerulenin and either oleate or myristate compared to the proportion of TAG associated with LpB from cells treated only with fatty acid (Figure 33). This reflected the increased TAG mass secreted by Hep G2 cells that were

Figure 33: **Lipid class percent composition of LpB from oleate-load–double myristate-chase incubations with cerulenin.** Relative lipid classes are shown as a percentage of total lipid mass of secreted LpB. Panel A shows LpB from the first sequential chase incubation and panel B shows LpB from the second sequential chase incubation. Results are means with standard deviations from 3 incubations. Conditions for two sequential incubations after oleate load were: ■ =oleate; □ =oleate plus cerulenin; ◪ =myristate; ▨ =myristate plus cerulenin; ▦ =MEM; ◪ =MEM plus cerulenin. When cells were incubated with either oleate or myristate, significantly more cholesterol was secreted after both chases compared to respective incubations of oleate or myristate that were also treated with cerulenin (a–d; p<0.011). When cells were incubated with either oleate or myristate. significantly less TAG was secreted after both chases compared to respective incubations of oleate or myristate that were also treated with cerulenin (e–h; p<0.008). After the second chase, significantly less TAG was secreted when cells were deprived of fatty acid and incubated with cerulenin than the TAG secreted by cells that were only incubated without fatty acid (i; p=0.044). Significantly less PL was secreted by cells treated with myristate after the second chase as compared to the percentage of PL secreted after the first chase (j & k; p<0.005) and significantly more TAG was secreted by cells treated with myristate after the second chase as compared to the percentage of TAG secreted after the first chase (l & m; p<0.001). When cells were incubated with fatty acid, significantly more TAG was secreted after both chases compared to cells not incubated with exogenous fatty acid (n versus o & p versus q; p<0.003 and r versus s & t versus u; p<6 x 10^{-5}).
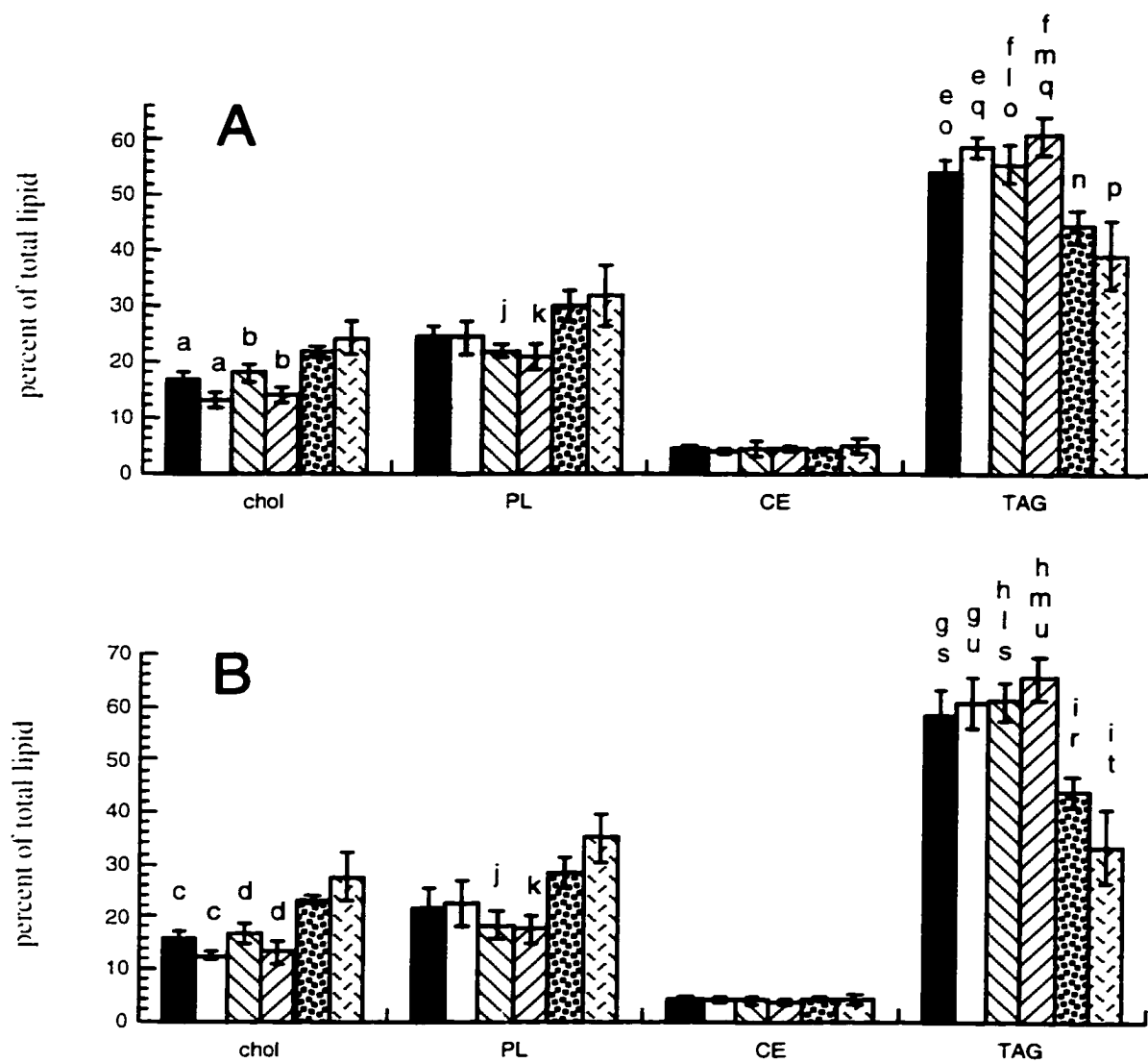
Figure 33

co-incubated with fatty acid and cerulenin (Figure 32, panels A & B). The increased proportion of TAG secreted with LpB after incubations with cerulenin and either oleate or myristate caused reciprocal, significant decreases in the proportion of cholesterol secreted with LpB after both chases by cells incubated with fatty acid and cerulenin compared to cells incubated only with myristate or oleate. Reflecting the reduced secretion of TAG by cells incubated without fatty acid, the proportion of TAG secreted with LpB from cells incubated with only MEM was approximately 30% lower than cells incubated with fatty acid (Figure 33). Cerulenin tended to reduce the secretion of TAG by approximately 20% from cells that were chased with MEM (Figure 33). This trend became significant after the second chase, as secreted TAG dropped from 44±3% of total lipid mass after incubation with MEM to 33±7% of total lipid when cells were also treated with cerulenin (Figure 33).

Cells chased with cerulenin and fatty acid secreted LpB particles that had lower CE: TAG ratios than from cells chased with fatty acid. Cells chased with MEM secreted LpB particles that had lower CE:TAG ratios than from cells chased with MEM and cerulenin (Table 6). CE content in secreted LpB was very consistent so changes in CE:TAG ratios reflected changes in the TAG content of LpB. CE:TAG ratios for LpB isolated from the media of cells incubated with myristate tended to be lower than LpB isolated from cells incubated with oleate. The CE:TAG trend of MEM>oleate>myristate became statistically significant during the second chase (Table 6). The low LpB CE:TAG ratio observed after myristate incubations suggested that myristate stimulated more secretion of TAG in association with apo B than oleate did. However, cellular CE:TAG ratios suggested oleate and myristate were equal in stimulating neutral lipid accumulation, since cellular CE:TAG ratios were similar with cerulenin treatment (Table 6). Oleate clearly stimulated accumulation of more lipid mass in the cells than myristate did (Figure 32, panel C); therefore, both oleate and myristate stimulated proportionately similar increases in cellular TAG and CE accumulation.

Cerulenin tended to increase the cellular CE:TAG ratios. The increase in cellular CE:TAG ratios were statistically significant after cells were chased with myristate or MEM (Table 6), despite the lack of significant differences between cellular CE or TAG mass from cells incubated with or without cerulenin. Cellular CE:TAG ratios from cells chased with MEM or MEM plus cerulenin were approximately 2.6 fold and 3.2 fold higher than the cellular CE:TAG ratios of cells chased with fatty acid or fatty acid plus cerulenin, respectively (Table 6). These significant increases in CE:TAG ratios reflected the increased accumulation of cellular TAG mass in cells chased with fatty acid. Cellular CE:TAG ratios of MEM-chased cells were also significantly higher than CE:TAG ratios of the LpB isolated from cells chased with MEM (Table 6), which suggested proportionately more TAG was secreted than stored and suggested apo B assembly retained some access to lipid of cellular origin throughout

Incubation Conditions		CE:TAG Ratios		
		Media from First Chase	Media from Second Chase	Cells
Oleate	Control	0.078±0.012 i	0.074±0.015 iop	0.060±0.004 ceh
	Cerulenin	0.069±0.010 t	0.067±0.010 q r	0.062±0.005 g
Myristate	Control	0.083±0.031 j	0.065±0.014 p	0.055±0.004 acej
	Cerulenin	0.071±0.012 t	0.057±0.008 r	0.062±0.007 a g
MEM	Control	0.090±0.008 l	0.098±0.002 l o	0.150±0.009 bdk
	Cerulenin	0.12±0.02 n s	0.12±0.02 n q	0.20±0.03 bfm

Table 6: CE:TAG **mass ratios after oleate-load–double myristate-chase incubations with cerulenin.** CE:TAG mass ratios are shown above for both isolated LpB and Hep G2 cells after oleate-load and two sequential myristate-chase incubations. Cerulenin treatments increased cellular CE:TAG ratios of cells incubated with myristate or MEM significantly (a–b; p<0.003). Cellular CE:TAG ratios were significantly higher in cells incubated with oleate than cells incubated with myristate (c; p=0.014). Cellular CE:TAG ratios were significantly higher in cells incubated with MEM than cells incubated with exogenous fatty acid. both with and without cerulenin (d versus e & f versus g; $p<2 \times 10^{-6}$). LpB isolated from cells incubated with oleate but not cerulenin after both chase incubations had significantly higher CE:TAG ratios than their respective cellular samples (h versus i; p<0.02). LpB isolated after the first chase with only myristate was significantly higher than the respective cellular samples (j; p=0.017). Conversely, cellular CE:TAG ratios were significantly higher than LpB ratios after both chases for cells incubated with MEM (k versus l & m versus n; $p<9 \times 10^{-5}$). After the second chase, CE:TAG ratios for isolated LpB were significantly higher in MEM incubated cells as compared to oleate incubate cells. Oleate incubated cells had a significantly higher LpB CE:TAG ratio than myristate chased cells (o–p; p<0.03 & q–r: p<0.002). After the first chase, LpB CE:TAG ratios were significantly higher in MEM plus cerulenin incubated cells than LpB CE:TAG ratios of cells incubated with cerulenin and either oleate or myristate (s versus t; p<0.02).

the two sequential MEM chases. However, when cells were incubated with fatty acid, CE:TAG ratios tended to be higher in the secreted LpB than the cells. This trend was significant when cells were not incubated with cerulenin (Table 6). The increased cellular CE:TAG ratios suggested that uptake and esterification of exogenous fatty acid had a larger influence on the accumulation of cellular TAG than stimulating secretion of LpB.

v. Relative Lipid Molecular Species Distribution

a. Proportions of TAG Molecular Species in LpB and Cells

The molecular species of TAG were readily skewed towards species that contained exogenous fatty acid and the addition of cerulenin to inhibit *de novo* synthesis of fatty acids tended to enhance the skewing of TAG molecular species towards species containing only exogenous fatty acid. When Hep G2 cells were chased with oleate, C54 (typically triolein) TAG became the predominant molecular species of TAG, significantly increasing from 61.4 ±0.8 mol % after the first oleate chase to 64.9±0.9 mol % after the second oleate chase (Figure 34, panels A & B). Co-incubating Hep G2 cells with oleate and cerulenin resulted in significant shifts in the proportions of the TAG molecular species secreted with apo B towards C54 TAG and reciprocal decreases of C48–C52 TAG molecular species. In the LpB isolated from media after oleate chases, C50–C52 TAG after the first chase and C48–C52 TAG after the second chase dropped 19% on average with cerulenin treatment, compared to control incubations, while C54 TAG increased approximately 5% with the addition of cerulenin throughout the incubation, compared to controls (Figure 34, panels A & B). Thus, inhibition of fatty acid synthase did skew the proportions of the TAG molecular species secreted with apo B away from species containing *de novo* synthesized fatty acid. However, substantial quantities of palmitate were present in the TAG molecular species even after the second sequential chase. The proportions of TAG molecular species from cells and LpB tended to be similar when the cells were treated with oleate. The differences were observed between the proportion of C54 TAG secreted in LpB and the proportion of cellular C54 TAG were not significant (Figure 34). Thus, incubating Hep G2 cells with oleate appeared to affect equally the proportions of TAG molecular species in LpB and cells.

When Hep G2 cells were incubated with oleate and then chased with myristate, the molecular species of TAG were skewed towards species containing myristate. Co-incubating Hep G2 cells with cerulenin and myristate tended to reduce the proportions of C44–C52 TAG molecular species and tended to increase the proportions of C42 and C54 TAG. But this effect was significant only for C42 TAG during the second chase with cerulenin—a 9% increase (Figure 34, panel B). The proportions of each of C42–C46 TAG molecular species, which included all TAG species that must contain myristate, secreted with LpB increased

Figure 34: **Molecular distribution of** TAG **from oleate-load–double myristate-chase incubations with cerulenin.** TAG molecular distribution was determined by GLC. TAG molecular species are reported as a percentage of total moles of TAG. Carbon numbers refer to total carbons in fatty acid moieties of TAG, ignoring glycerol. LpB from first sequential chases (panel A), LpB from second sequential chases (panel B), and cellular lipid after all 30 h of incubation (panel C) are shown. Results are means with standard deviations from 3 incubations. Conditions for two sequential incubations after oleate load were: ■ = oleate; □ = oleate plus cerulenin; ◩ = myristate; ◪ = myristate plus cerulenin; ▣ = MEM; ◨ = MEM plus cerulenin. After the first oleate chase, proportions of C50–C52 TAG in LpB were significantly higher in controls (a; $p < 0.004$) while the proportion of C54 TAG in LpB was significantly higher in cerulenin treatments (b; $p < 0.011$). After the second oleate chase, proportions of C48–C52 TAG in LpB were significantly higher in controls (c; $p < 0.011$) while the proportion of C54 TAG in LpB was significantly higher with cerulenin treatment (d; $p < 0.0002$). After the second myristate chase, the proportion of C42 TAG in LpB was significantly higher in cerulenin treatments than in controls (e; $p = 0.02$). After the second MEM chase, proportions of C48–C52 TAG in LpB were significantly higher in controls than in cerulenin treatments (f; $p < 0.001$) while the proportion of C54 TAG was significantly higher in cerulenin treatments than in controls (g; $p < 0.01$). Proportions of C48–C52 cellular TAG from cells chased with oleate were significantly higher in controls than in cerulenin treatments (h; $p < 0.00007$) while the proportion of C54 cellular TAG was significantly higher with cerulenin treatment than in controls (i; $p < 0.0003$). Proportions of C44, C48, and C52 cellular TAG from cells chased with myristate were significantly higher in controls than in cerulenin treatments (j; $p < 0.003$) while the proportion of C54 cellular TAG was significantly higher in cerulenin treatments than in controls (k; $p < 0.002$). Proportions of C48–C52 cellular TAG in cells chased with MEM were significantly higher in controls than in ceru lenin treatments(l; $p < 9 \times 10^{-8}$) while the proportion of C54 cellular TAG was significantly higher in cerulenin treatments than in controls (m; $p < 2 \times 10^{-7}$). The proportion of C54 TAG from LpB was significantly higher after the second oleate chase than after the first oleate chase, with or without cerulenin (n; $p < 0.003$). Proportions of C42–C48 TAG from LpB were significantly higher after the second myristate chase than after the first myristate chase (o; $p < 0.0005$) while proportions of C50–C54 TAG from LpB were significantly higher after the first myristate chase than after the second myristate chase (p; $p < 0.02$), with or without cerulenin. Proportions of C42–C48 TAG were significantly higher in cells chased with myristate than in the LpB from the first myristate chase (q; $p < 0.02$) while proportions of C50–C54 TAG were significantly higher in first myristate chase than cells chased with myristate (r; $p < 0.006$), irrespective of cerulenin treatment.
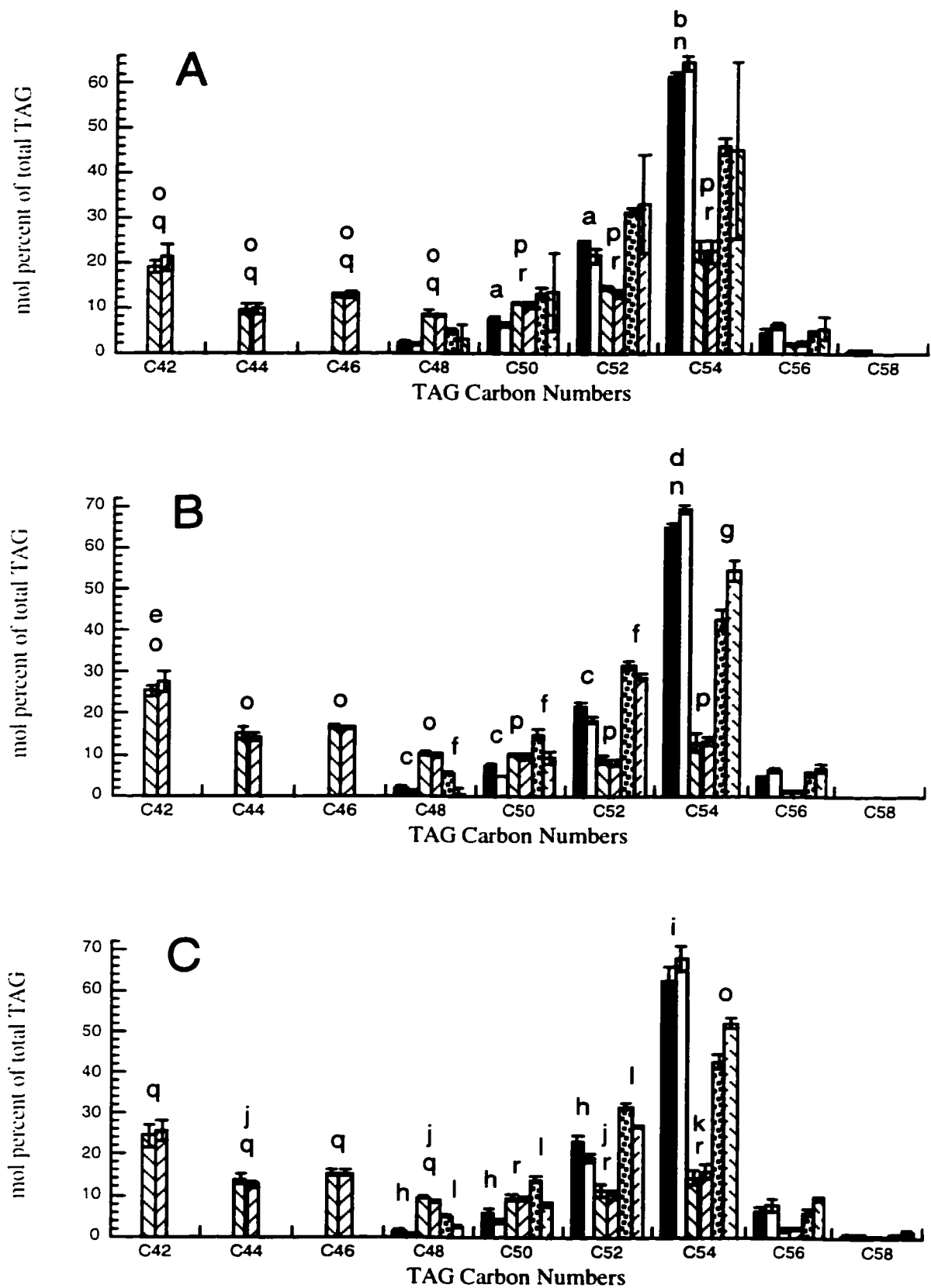
Figure 34

significantly by approximately a third from the first myristate chase to the second myristate chase while the proportion of C50–C54 TAG species dropped by approximately half from the first myristate chase to the second myristate chase. Cerulenin did not have a major effect on the distribution of TAG molecular species (Figure 34, panels A & B). Thus, re-incubating Hep G2 cells with myristate further skewed the proportions of TAG molecular species towards myristate-containing species.

Cerulenin treatment also had some influence upon the proportions of cellular TAG molecular species in cells chased twice with myristate. C42 and C54 TAG were approximately 7% higher proportion of the total TAG in cells chased with myristate and cerulenin (only C54 TAG was significantly higher) while C44–C52 TAG were approximately 6% lower proportion of the total TAG in cells chased with myristate and cerulenin (only C44, C48, and C52 TAG were significantly lower; Figure 34, panel C). C44, C48, and C52 TAG represent molecular species that contain palmitate and these species were predicted to be most affected by cerulenin. Their presence indicated that substantial quantities of palmitate was present in the cellular pool of TAG despite strong inhibition of incorporation of acetate into fatty acids. A pool of palmitate, which was accessible by LpB assembly, may have been formed prior to the exposure to cerulenin and persisted throughout both myristate chases. The proportions of C42–C48 TAG were significantly higher in cellular TAG than LpB TAG secreted during the first chase while the proportions of C50–C54 TAG were significantly higher in LpB secreted during the first chase than cellular TAG. However, the proportions of TAG molecular species in cellular TAG and LpB secreted during the second chase were not significantly different. Thus, the role of stored, oleate-containing TAG in the assembly of LpB in Hep G2 cells diminished between the first and second sequential chases. The first chase period may represent a transition phase between the use of oleate acquired from the culture media to the newly supplied myristate.

In agreement with observations made from the oleate-load and single myristate-chase incubations, analysis of the proportions of TAG molecular species secreted from the two sequential chases with myristate failed to provide strong evidence for mobilization of stored TAG as a major source of TAG in the assembly of LpB in Hep G2 cells. If stored TAG were mobilized without modification, then C54 TAG was anticipated to be major TAG molecular species in the secreted LpB (Figure 18, panel A). C54 TAG was not a predominant TAG species in LpB secreted during the two chases and the proportion of C54 TAG declined between the first and second chase, which suggested mobilization of stored TAG without modification for LpB assembly was not a major pathway in Hep G2 cells. If stored TAG were mobilized by a single hydrolytic event such that DAG was transported to the site of LpB assembly and then re-esterified to TAG, then C50 TAG was predicted to be a major TAG

molecular species (Figure 18, panel B). The proportion of C50 TAG in LpB dropped slightly, yet significantly, from 10.9±0.3% after the first chase with only myristate to 9.8± 0.3% after the second chase with only myristate. C50 TAG was not a major TAG molecular species in LpB isolated from both myristate chases and the proportions of C50 TAG in LpB from cells chased with myristate were marginally higher than the proportions of C50 TAG in LpB from cells chased with oleate. Thus, strong evidence for the mobilization of TAG by partial hydrolysis to DAG was not observed in the LpB secreted by Hep G2 cells. If stored TAG were mobilized via partial hydrolysis to MAG and re-esterified to TAG at the site of LpB assembly, then C46 TAG was anticipated to be a major TAG species (Figure 18, panel C). The proportions of C46 TAG increased significantly from 12.5±0.6% after the first chase with only myristate to 16.8±0.6% after the second chase with only myristate. Co-incubation with cerulenin did not significantly change these values. Despite this increase, C46 TAG was not a predominant TAG molecular species and constituted a smaller proportion of the total TAG than C42 TAG did. The increase of C46 TAG indicated that myristate was playing a stronger role in shaping the molecular species of TAG during the second chase as compared to the first chase; however, the proportion of C46 TAG did not provide strong evidence for the mobilization of stored TAG via partial hydrolysis to MAG in Hep G2 cells. Lastly, if stored TAG were mobilized by a mechanism of complete hydrolysis to fatty acids and then random re-esterification back to TAG, then the molar ratio of C42:C46:C50:C54 TAG was predicted by the binomial distribution (Table 4; Figure 18, panel D). After the second sequential chase with myristate, the molar ratio of C42:C46:C50:C54 TAG was 2.59:1.71: 1:1.32 for control chases and 2.89:1.72:1:1.39 for cerulenin treatments. These ratios did not match the pattern established by Table 4; therefore, if stored TAG were being mobilized by a mechanism of complete hydrolysis, the released and exogenous fatty acids were not randomly esteried to TAG. Hep G2 cells only secreted 0.078—0.26% of their total mass of cellular TAG. The minute secretion of TAG suggested cellular TAG was not effectively mobilized for LpB assembly.

The increasing proportions of myristate-containing TAG molecular species in LpB secreted from the first to the second chases suggested uptake and esterification of exogenous fatty acid was an important source of TAG for LpB assembly. If exogenous fatty acid were a major source of TAG for LpB assembly, then the proportions of molecular species of LpB TAG secreted during the myristate chase will resemble the proportions of molecular species of LpB TAG secreted from Hep G2 cells incubated only with myristate, despite the presence of substantial quantities of oleate-containing lipids stored in the cells during the oleate-load incubation. LpB-associated TAG isolated after the second chase with myristate will resemble LpB-associated TAG isolated after incubation with only myristate more so than

the LpB from the first sequential chase with myristate since the secretory pathway has the potential to chase out apo B that was synthesized when oleic acid was the exogenous fatty acid. Unlike the oleate-load and single myristate-chase experiment, both sequential chases with myristate secreted LpB with a significantly larger proportion of C42 TAG than that found in the LpB secreted from single fatty acid incubations with myristate (p<0.002). The proportion of C42 TAG secreted after the second sequential chase with myristate (Figure 34, panel B) was approximately double the proportion of C42 TAG secreted with LpB during incubations with only myristate (Figure 17, panel A). The proportions of C44 and C46 TAG. which must contain 2 and 1 myristate moieties respectively, increased from the first myristate chase to the second myristate chase and reached levels that were similar to C44 and C46 TAG secreted with LpB from incubations with only myristate (Figure 17 & 34). Thus. after replacing the chase media with fresh myristate–BSA solution, Hep G2 cells appeared to use exogenous fatty acid as a major source of lipid for LpB assembly and required up to 6 h to switch from oleate to myristate. However, significantly more C54 TAG was still being secreted with LpB during the two sequential chases as compared to cells incubated with only myristate (Figures 17 & 34). The proportion of C54 TAG was approximately three times higher after the first sequential myristate chase and approximately 50% higher after the second sequential myristate chase compared to the proportion of C54 TAG in LpB from single fatty acid incubations with myristate. Although uptake and esterification of exogenous myristate appeared to be the major source of TAG for LpB assembly in Hep G2 cells. LpB assembly appeared to retain some access to oleate-containing TAG from the initial oleate load.

Analysis of the proportions of molecular species of LpB and cellular TAG from cells chased with MEM demonstrated that *de novo* synthesis of fatty acids did not play a dominant role in determining TAG composition. If *de novo* synthesis of fatty acid played a major role in supplying TAG for LpB assembly, then palmitate-containing molecular species of TAG were expected to increase from the first MEM chase to the second MEM chase and the dominant TAG molecular species was predicted to shift from C54 TAG to C52 TAG. since C52 TAG was the dominant TAG molecular species in the controls from the single fatty acid incubations (Figure 17). LpB TAG secreted from Hep G2 cells chased with MEM were skewed towards C54 TAG, but not to the same degree as observed in cells that were chased with fresh oleate (Figure 34). For both the LpB TAG isolated from the second chase and the cellular TAG. the proportions of C48–C50 TAG were significantly lower when cells were chased with MEM and cerulenin than cells that were chased with MEM and the proportion of C54 TAG was significantly higher when the cells were chased with MEM and cerulenin than cells that were chased with MEM (Figure 34, panels B & C). The proportions of palmitate-

containing molecular species of TAG (C48–C52 TAG) did not significantly change between the first and second chases with MEM and without cerulenin. Thus, Hep G2 cells did not appear to utilize fatty acids from *de novo* synthesis as a major source of TAG for LpB assembly.

b. Proportions of PL Molecular Species in LpB and Cells

When PL molecular species were expressed as a percentage of total moles, exogenous fatty acids were seen to skew the molecular species of PL towards species containing exogenous fatty acid. When Hep G2 cells were loaded with oleate-containing lipid species and were chased with more oleate, PL molecular species were shifted towards C36 PL (Figure 35), as was observed in single chase incubations (Figure 23). When cells were chased with oleate, secreted C36 PL increased significantly from 39.9±2.4 mol % after the first oleate chase to 47.8±2.9 mol % after the second oleate chase (Figure 35, panels A & B). Incubating cells with cerulenin and oleate significantly enhanced skewing towards C36 PL, with C36 constituting 50.9±1.7 mol % of the PL after the second oleate chase. Cerulenin primarily caused a decline in the relative amount of C34 PL. When Hep G2 cells were chased with myristate, PL molecular species were shifted towards myristate-containing species. Secreted C30 PL increased significantly from 9.3±1.1 mol % after the first myristate chase to 15.3±1.6 mol % after the second myristate chase, compared to 3.0±0.5 mol % and 3.1±1.5 mol %, respectively, when cells were chased with oleate (Figure 35, panels A & B). Addition of cerulenin caused the proportion of C30 PL secreted in both myristate chases to decrease by approximately 16% compared to controls; however, these decreases were not significant. When chase media lacked fatty acid, C34 PL was the largest species of PL. Incubating cells with both MEM and cerulenin significantly shifted the distribution such that C36 PL was a larger component than C34 PL in LpB.

Cellular distribution of PL molecular species was similar to the PL profile of the media after both sequential chases. Cellular profiles were more strongly skewed towards exogenous fatty acid than media (Figure 35). In oleate-chase incubations, proportionately more C30–C34 PL molecular species were secreted in both oleate chases compared to cellular PL. When cells were chased with myristate, significantly more C30 and C32 PL was found in the cells. The addition of cerulenin tended to result in more cellular C36 PL for all chases treatments with reciprocal reductions of C30–C34 PL (Figure 35, panel C). The increase in C36 PL content reflected the inhibition of fatty acid synthase, which reduced palmitic acid content of lipids and shifted PL profiles towards oleate-containing PL species, even when the Hep G2 cells were chased with myristic acid.

Figure 35: **Molecular distribution of PL from oleate-load– double myristate-chase incubations with cerulenin.** PL molecular distribution was determined by GLC. Relative PL molecular species are reported as a percentage of total moles of PL. Carbon numbers refer to total carbons in the fatty acid moieties of PL, ignoring the glycerol backbone. Panel A shows LpB from the first sequential incubation, panel B shows LpB from the second sequential incubation, and panel C shows cellular lipid after all 30 h of incubation. Results are means with standard deviations from 3 incubations. Conditions for two sequential incubations after oleate load were: ■ =oleate; □ =oleate plus cerulenin; ⊠ =myristate; ▧ =myristate plus cerulenin; ▨ =MEM; ◨ =MEM plus cerulenin. The proportion of C36 PL was significantly greater than controls when treated with cerulenin for both oleate chases (a: p<0.05). Significantly more C36 PL was secreted during the second oleate chase than during the first oleate chase, with and without cerulenin (b; p<0.0002). Significantly more C30 PL was secreted during the second myristate chase than the first myristate chase, with and without cerulenin (c; p<0.002). The proportion of C34 PL was significantly less in MEM chases treated with cerulenin than treated without cerulenin (d; p<0.03) while a significantly larger proportion of C36 PL was secreted during MEM chases treated with cerulenin than treated without cerulenin (e; p<0.025). The proportions of C30–C34 PL were significantly larger in LpB than in cells when Hep G2 cells were incubated with oleate, except for C32 PL in the second chase (f versus g; p<0.05). After myristate chases, the proportions of C30–C32 PL were higher in cells than the proportions of C30–C32 PL secreted in LpB for both chases (h versus i; p<0.006). The proportion of cellular C36 PL was higher with cerulenin for all chase conditions (j; p<4 x 10⁻⁶) and the proportions of cellular C30–C34 PL were lower when treated with cerulenin for all chase conditions, except C32 PL with myristate (k; p<0.007).
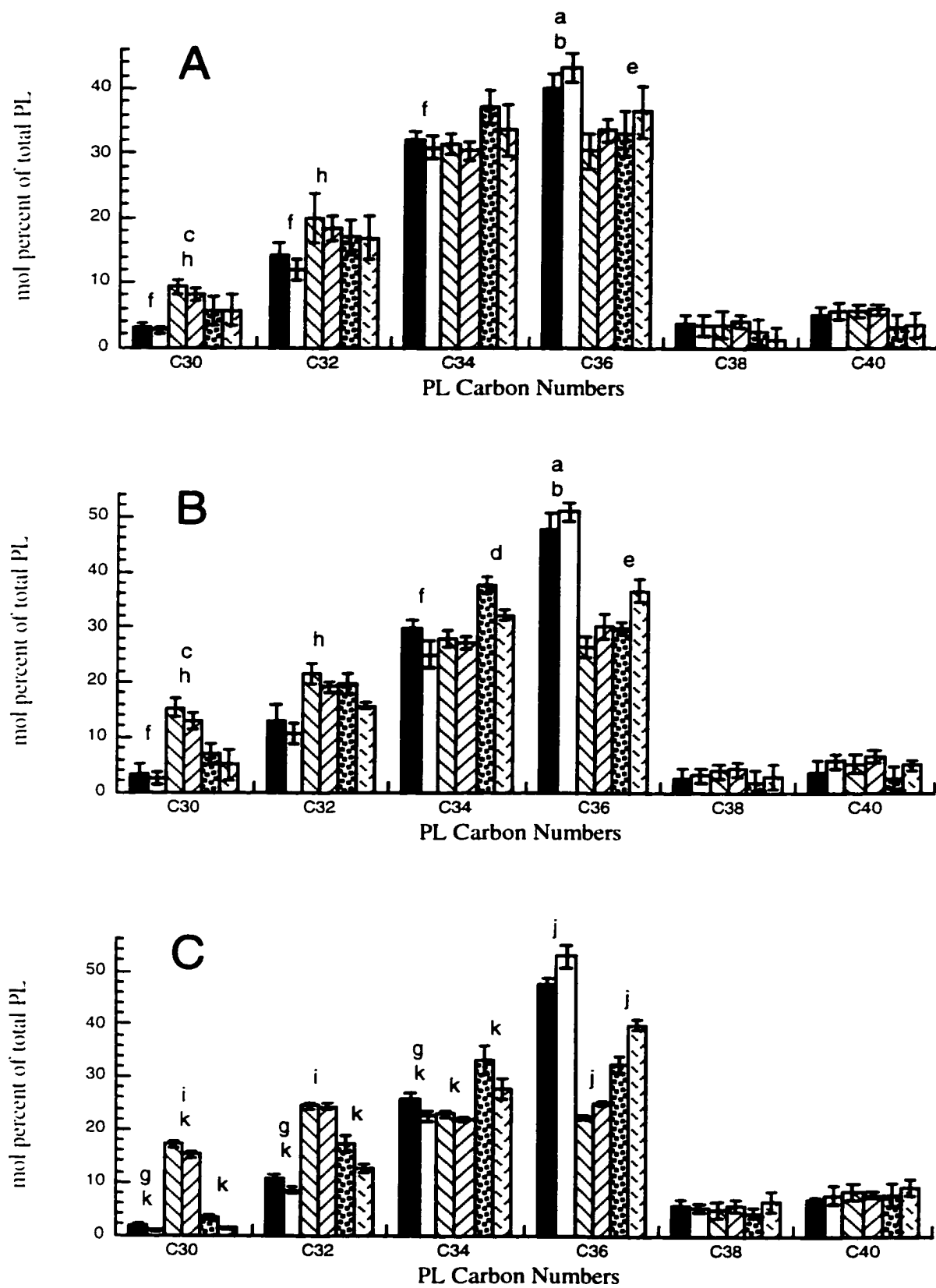
Figure 35

The proportions of PL and TAG molecular species were analyzed for evidence of PL being hydrolysed to DAG and then esterified to TAG for LpB assembly. Both C34 and C36 PL were prominent species in the first myristate chase. However, the proportions of C34 and C36 PL declined in the second myristate chase, which may reduce the ability to detect PL supplementing TAG mass in LpB assembly. C34 and C36 PL molecular species will produce C34 (typically C16:C18) and C36 (typically C18:C18) DAG which will become C48 (C14: C16:C18) and C50 (C14:C18:C18) TAG if esterified with myristate. If the hydrolysis of PL and subsequent esterification of DAG to TAG were a major source of TAG for LpB assembly in Hep G2, then C48 and C50 TAG was predicted to be prominent TAG species in the secreted LpB. Both C48 and C50 were minor species in the TAG molecular species profiles (Figure 34). Thus, Hep G2 cells did not appear to use PL to supplement TAG mass substantially during LpB assembly.

c. Proportions of CE Molecular Species in LpB and Cells

Incubations with fatty acids and cerulenin also affected the molecular species of CE (Figure 36). After the first chase, the proportions of CE molecular species were uniform. The proportion of cholesteryl palmitate was approximately one-fifth of the CE mass and C18 CE constituted four-fifths of the CE mass. Oleate significantly elevated C18 CE from 79.6 ± 4.8 mol % after the first chase to 89.0 ± 5.6 mol % after the second oleate chase. without cerulenin (Figure 36, panels A & B). Cerulenin treated cells displayed a similar increase in the proportions of C18 CE. Substantial quantities of cholesteryl myristate were only observed with incubations involving myristate chases. Cholesteryl myristate increased significantly from 3.9 ± 3.3 mol % after the first chase to 13.4 ± 2.1 mol % after the second myristate incubation, without cerulenin (Figure 36, panels A & B). The secreted mass of cholesteryl palmitate remained unchanged over the two chases in cells deprived of exogenous fatty acid (Figure 36, panels A & B). Based on increasing proportions of C18 CE during the two sequential chases with oleate and increasing proportions of cholesteryl myristate during the two sequential chases with myristate, Hep G2 cells appeared to be actively esterifying cholesterol with the exogenous fatty acid for LpB assembly.

When cells were incubated with cerulenin, the proportions of C18 CE tended to increase for all chase conditions (Figure 36, panel C). Differences between cerulenin and control in media samples from oleate chases were not significant, but differences between cerulenin and control for media samples of both myristate and fatty acid deprived cells chase were significant after the second chase (Figure 36, panel B). Cellular data were

Figure 36: **Molecular distribution of** CE **from oleate-load–double myristate-chase incubations with cerulenin.** CE molecular distribution was determined by GLC. Relative CE molecular species are reported as a percentage of total moles of CE. Panel A shows LpB from the first sequential incubation, panel B shows LpB from the second sequential incubation, and panel C shows cellular lipid after all 30 h of incubation. Results are means with standard deviations from 3 incubations. Conditions for two sequential incubations after oleate load were: ■ =oleate; □ =oleate plus cerulenin; ◪ =myristate; ◨ =myristate plus cerulenin; ▨ =MEM; ◪ =MEM plus cerulenin. The proportion of C18 CE was significantly higher in the second oleate chase then in the first oleate chase, with or without cerulenin (a; p<0.03). The proportion of cholesteryl myristate was significantly higher in the second myristate chase than in the first myristate chase, irrespective of cerulenin treatment (b; p<0.005). After the second chase, the proportion of C18 CE was significantly higher in cerulenin treated cells for both myristate and MEM chased cells (c; p< 0.05). The proportion of cellular C18 CE was significantly higher in cells treated with cerulenin for all chase conditions (d; p<0.002).
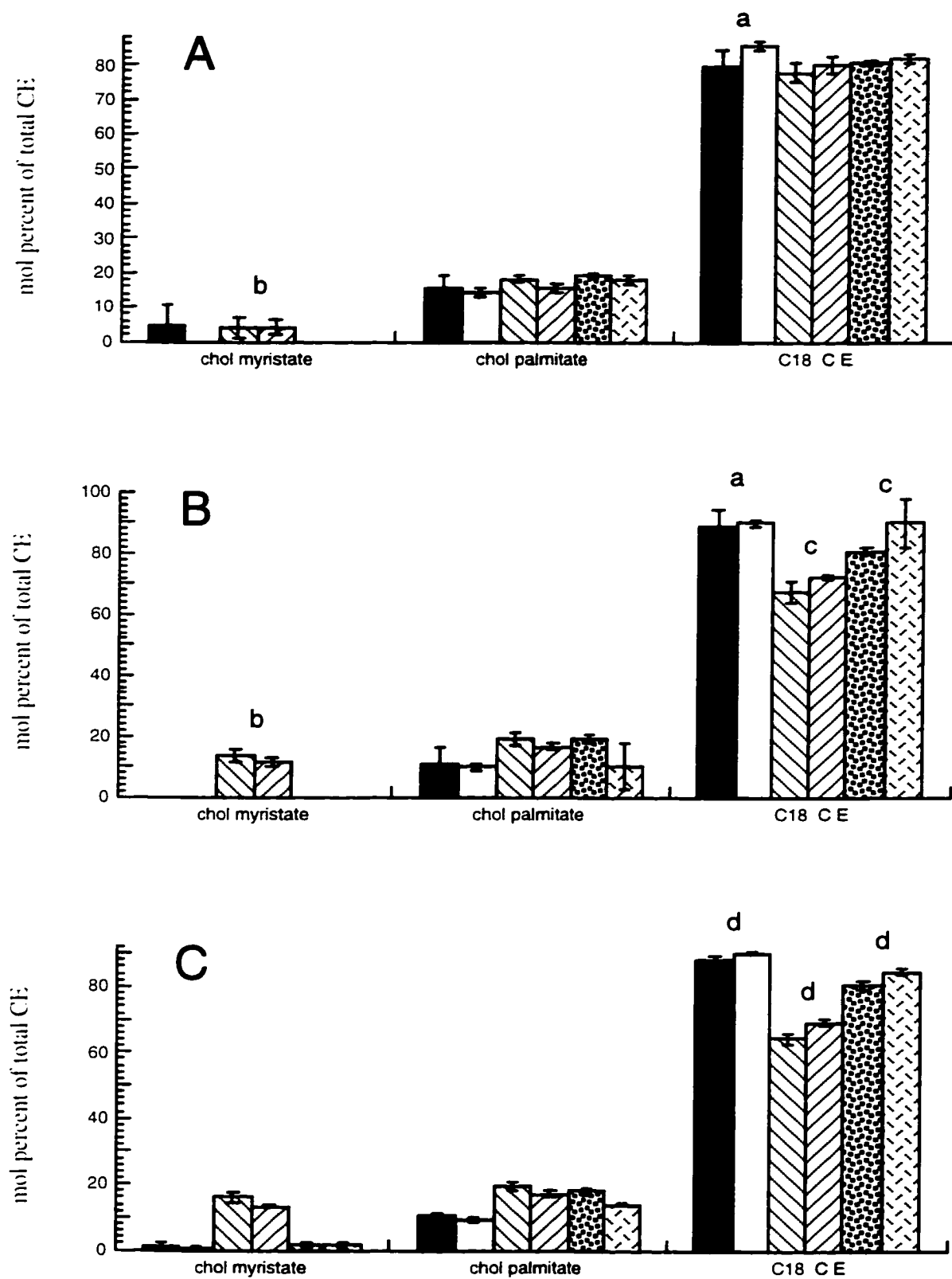
Figure 36

more consistent—the proportion of cellular C18 CE increased with cerulenin incubations, as compared to controls for all chase conditions (Figure 36, panel C). Thus, inhibiting fatty acid synthase increased the proportion of C18 CE content in Hep G2 cells.

IV. Discussion

The object of this project was to study the assembly of apo B and lipid, with emphasis upon TAG used in the synthesis of nascent VLDL, using the Hep G2 cell line as a model system. Apo B secreted by Hep G2 cells was isolated from apo A-I, apo E, and albumin by heparin-Sepharose chromatography. Although apo A-I and apo E were partially separated on HTP chromatography, they were not isolated from albumin by this procedure. Since the aim of the project was to study the assembly of LpB in Hep G2 cells, HTP chromatographic fractions were not pursued. The assembly of lipids with apo B was examined by a pulse-chase strategy that employed mass to label the lipid pools. Hep G2 cells were incubated with oleate to load the storage pool with oleate-containing lipid species. The incubation media was then switched to myristate. The lipid molecular species secreted in association with apo B after the oleate-load and myristate-chase incubations were analyzed. The proportions of the TAG molecular species suggested that Hep G2 cells were not mobilizing stored lipid but esterifying exogenous fatty acids as a major source of TAG in the assembly of nascent VLDL.

A. Isolation and Characterization of Lipoproteins Secreted by Hep G2 Cells

The total mass of secreted TAG for all chromatographic fractions observed after the single fatty acid incubation with oleate was approximately 2 µg TAG/mg cell protein/18 h, which was comparable to some reports in the literature (Gibbons et al., 1994; Pullinger et al., 1989) but lower than other reports (Dashti & Wolfbauer, 1987; Homan et al., 1991; Wang et al., 1988). Controls from single fatty acid incubations secreted similar amounts of TAG compared to cells incubated with fatty acid for 18 h. The lack of stimulation of TAG secretion by oleate in the single fatty acid incubations is contrary to previous reports that demonstrated 2-9 fold stimulation in TAG secreted with apo B by Hep G2 cells incubated with oleate (Cianflone et al., 1990; Dashti & Wolfbauer, 1987; Dixon et al., 1991; Homan et al., 1991; Pullinger et al., 1989; Wang et al., 1988); however, these studies incubated Hep G2 cells in MEM, which contains 5.5 mM glucose. In the current studies, single fatty acid incubations were done with elevated levels of glucose (27.7 mM) to stimulate the extremes of glucose concentration found in portal blood. Intraportal glucose concentrations of approximately 11.1 mM have been reported following oral glucose tolerance tests in non-diabetic, non-obese humans (Lund et al., 1975) and dogs (Barrett et al., 1985; Bergman et al., 1982). High glucose concentrations may have stimulated lipogenesis and reduced the impact of exogenous fatty acids on TAG synthesis. The literature contains contrasting reports of the effect of glucose on lipoprotein metabolism in Hep G2 cells. Increased concentra-

tions of glucose (20.5–50 mM) were reported to stimulate increased TAG secretion 2–4 fold in Hep G2 cells (Arrol *et al.*, 1991; Cianflone *et al.*, 1992; Kempen *et al.*, 1995; Wang *et al.*, 1988). Secretion of apo B by Hep G2 cells was found both to be stimulated (Arrol *et al.*, 1991; Kempen *et al.*, 1995) and not stimulated (Cianflone *et al.*, 1992) by elevated glucose concentrations. Recently, 30 mM glucose was reported to stimulate neither TAG synthesis nor apo B secretion in Hep G2 cells (Jiang *et al.*, 1998). These variable results in the literature may reflect different culture conditions. In the oleate-load and double myristate-chase experiments, the media contained 5.5 mM glucose. Cells that were chased with oleate secreted 2 fold more TAG mass than cells that were chased with MEM. Thus, Hep G2 cells incubated with 27.7 mM glucose in the single fatty acid experiments appeared to be stimulated to a point where exogenous fatty acids only had a minor impact on stimulation of lipid synthesis.

In order to analyze the nascent VLDL secreted by Hep G2 cells, LpB was isolated from conditioned media to remove other lipoproteins and lipid not associated with apo B. The low mass of lipid secreted by Hep G2 cells required either addition of carrier lipid or scaling up the number of flasks that are pooled to isolate lipoproteins by ultracentrifugation. A simple procedure was desired that preserved the integrity of the secreted lipoprotein. Thus, the primary goal of the chromatographic isolation was to isolate nascent VLDL from conditioned media of Hep G2 cells. As a secondary goal, the isolation of nascent HDL by HTP chromatography from the heparin-unretained fraction was also attempted.

Heparin-Sepharose chromatography isolated particles containing apo B but not apo A-I or apo E from conditioned media. The heparin-isolated particles appeared to represent nascent VLDL that contained only apo B. Earlier studies have reported on the composition of LpB particles secreted by Hep G2 cells. Thrift *et al.* (1986) used ultracentrifugation to isolate lipoproteins from large quantities of conditioned media and found that the $p<1.063$ g/ml fraction contained only apo B. Fazio *et al.* (1992) also observed Hep G2 cells to secrete apo E independently of apo B, which suggested apo E was not intracellularly associated with nascent VLDL. However, Dashti *et al.* (1987) isolated nascent VLDL secreted from Hep G2 cells by immunochromatography and concluded that 28% of the LpB also contained apo E (LpB:E). Previous reports identified subpopulations of human plasma VLDL that had low quantities of apo E. Huff and Telford (1984) fractionated a $p<1.006$ g/ml preparation from human plasma on a heparin-Sepharose column. The sample was loaded on the column after being dialysed to 50 mM NaCl. The bound fraction was eluted with 0.8 M NaCl, as was done in this work. The heparin-Sepharose retained and unretained fractions differed primarily by TAG content and apo E:apo C ratios. The heparin-bound fraction contained particles that were smaller, contained more apo E compared to apo C, and con-

tained more TAG than the unretained fraction. Huff and Telford suggested that heparin-retained particles were a catabolic product of the unretained fraction or that both fractions were synthesized independently. A similar study by Campos *et al.* (1996) separated normal human VLDL into two separate populations by anti-apo E chromatography, which produced a retained fraction rich in LpB:E. The anti-apo E-unretained fraction contained only apo B particles and was further separated into heparin-bound and unretained fractions. Heparin-bound, apo B particles were smaller than heparin-unretained apo B particles. Campos *et al.* (1996) concluded that the large apo B particles may represent VLDL which had not acquired apo E. Thus, the synthesis of VLDL in humans may include the secretion of a nascent VLDL population that does not contain apo E.

The LpB secreted by Hep G2 cells were of LDL size. EM revealed a diverse population of LpB with substantial amounts of particles of very small diameter. The majority of particles from the single fatty acid incubation was in the 100–250 Å range. The LDL-sized, LpB particles secreted by Hep G2 cells were rich in TAG and deficient in CE compared to human plasma LDL. The VLDL–LDL fraction isolated from Hep G2 cells by Thrift *et al.* (1986) was enriched in cholesterol and the mass of TAG was similar to the PL mass. They reported the VLDL ($p<1.006$ g/ml) was 240–920 Å in diameter and the LDL ($1.006<p<1.063$ g/ml) was more homogenous at 245±23 Å. The VLDL was only a minor component of the $p<1.063$ g/ml fraction. Dashti *et al.* (1987) observed that LpB:E and LpB particles isolated from Hep G2 cells by immunochromatography were rich in TAG and had near equal masses of cholesterol and CE. Their LpB particles were more homogenous in size (100–350 Å diameter) than the LpB:E particles (220–500 Å diameter). The LpB from the heparin-bound fraction were similar to the particles reported by Thrift *et al.* (1986) and Dashti *et al.* (1987), although LpB from the heparin-bound fraction tended to be smaller in diameter. The small size of the nascent VLDL secreted by Hep G2 cells may restrict its ability to acquire exchangeable apoproteins such as apo E.

The secretion-capture model of remnant clearance suggests that a pool of apo E bound to the extra-cellular matrix plays a significant role in the binding of remnant particles to receptors for clearance from the circulation (Cooper, 1997; Mahley *et al.*, 1994). Newly synthesized apo E was reported to be secreted into several different pools in Hep G2 cells, with up to 40% of the newly synthesized apo E being associated with the cell surface and extracellular matrix (Burgess *et al.*, 1999; Schmitt & Grand-Perret, 1999). Thus, secretion of apo E onto the hepatocyte cell surface may be part of the secretion-capture model of remnant clearance. Also, heparin treatments were shown to release apo E from Hep G2 cells during incubations of 15–30 minutes (Lilly-Stauderman *et al.*, 1993). Although the heparin treatments used a 10 fold lower concentration to remove HTGL in this thesis, the extracellular

pool of apo E may have been reduced thereby limiting the mass of apo E available to associate with the LpB. Thus, a combination of several factors including the small size of the secreted LpB and reductions in apo E mass may have lead to the absence of apo E in the nascent VLDL particles secreted by Hep G2 and isolated from the conditioned media by heparin-Sepharose chromatography.

The heparin-unretained fraction, which was further separated into HTP-bound and unretained fractions, contained apo A-I and E. Some success was achieved in using HTP chromatography to isolate apo A-I and E from the heparin-unretained fraction. The HTP-bound fraction was contaminated by albumin, which may have affected the retention of apo A-I and E by HTP. The HTP-bound fraction contained the majority of apo A-I and approximately 30% of the apo E mass, and was thought to represent nascent HDL secreted by Hep G2 cells. The HTP cartridge was able to bind all of the apo A-I whereas the BioGel HTP only bound 77% of the apo A-I. The HTP cartridge was estimated to retain the same proportion of apo E as in the BioGel HTP. This differential binding of apo A-I and E by the HTP cartridge suggested that a portion of the apo A-I and apo E were on separate particles. Schmitt and Grand-Perret (1999) reported that apo A-I was not bound to the surface of Hep G2 cells by heparan sulphate proteoglycans whereas the extracellular matrix did bind newly synthesized apo E. which suggested a pool of apo E was on particles distinct from apo A-I. The HTP-bound fraction also contained neutral lipid, 19.1−35.5% of the total secreted CE and 14.5−19.0% of the total secreted TAG, and had a high content of cholesterol. Because of contamination of the HTP-bound fraction with albumin, a substantial proportion of the cholesterol may not have been associated with apoproteins but may have been bound by albumin. A portion of the neutral lipid found in this fraction may not have been secreted with apo A-I and/or apo E. Hep G2 cells were reported to secreted LCAT (Chen et al., 1986), which may synthesize CE in the media due to the presence of apo A-I and cholesterol. Also, CETP was reported to be secreted by Hep G2 cells (Faust & Albers, 1987; Swenson et al., 1987), which may introduce TAG into nascent HDL via exchange of TAG from LpB for CE associated with apo A-I. Thus, some of the neutral lipid associated with apo A-I and/or apo E may have been added to the nascent HDL after secretion by metabolic activity in the media.

The dual-unretained fraction contained neither apo B nor the majority of apo A-I. The contamination of the dual-unretained fraction with albumin suggests that some of the cholesterol may be associated with the albumin and not apo A-I or E. PL in the dual-unretained fraction was 55.4−66.7% of the total lipid in the fraction and was 42.9−48.8% of the total PL secreted into the media. The dual-unretained fraction also contained 12.1−19.1 % of the total secreted CE and 7.2−10.5% of the total secreted TAG. The presence of neutral lipid in the dual-unretained fraction again demonstrates substantial lipid was not associated

with apo B, which makes it imperative to isolate lipoproteins based on apoprotein content from media, rather than analyzing whole media. Since oleate-load and myristate-chase experiments were designed to study the assembly of lipid with apo B, it was critical to isolate TAG that was associated only with apo B. Contamination of the LpB with TAG from cell lysis or TAG associated with nascent HDL may interfere with the interpretation of the molecular species of LpB TAG. The lipid molecular species isolated in the dual-unretained fraction from the single fatty acid incubation did not contain myristate-containing species when exogenous myristate was supplied in the media. If a cell were starting to necrose before the single fatty acid incubation, then its uptake of exogenous fatty acid and secretion of lipoproteins during the incubation may be impaired. When the cell does lyse, its diminished uptake of exogenous fatty acids may explain the lack of myristate-containing lipids observed in the dual-unretained fraction after myristate incubations. The high amount of PL may have originated from cellular debris as well. Comparing the minute mass of lipid secreted by Hep G2 cells to the lipid mass stored in the cells, the mass of lipid observed in the dual-unretained fraction may be achieved by the lysis of a very small percentage of cells.

To determine whether major changes in fatty acids supplied had significant effects on lipoproteins secreted, Hep G2 cells were incubated with different fatty acids with the aim of modifying the lipid content of the secreted lipoproteins. The modulation of lipid molecular species allowed for further experiments in which lipoproteins were labelled with lipid mass—not radioactivity—to investigate the role of stored cytosolic TAG in supplying lipid for LpB assembly. The addition of exogenous fatty acid skewed lipid molecular species towards lipid species containing the exogenous fatty acid. TAG and PL molecular species were most affected by the supply of exogenous fatty acid. When Hep G2 cells were incubated with oleate, the cells secreted nascent VLDL particles that were enriched in oleate-containing lipid species, particularly C54 TAG. Similarly, by incubating Hep G2 cells with myristate, lower molecular mass species of lipids were enriched and new species of TAG appeared in the total lipid profiles (C42–C46 TAG). Control incubations maintained molecular species of lipids containing C16 and C18 fatty acids, which demonstrated the robust lipogenesis found in Hep G2 cells (Gibbons et al., 1994). TAG molecular species were more easily skewed towards the exogenous fatty acid than PL were. To respond to a fatty acid challenge, Hep G2 cells appeared to esterify glycerol completely to TAG with fatty acid and the diversion of DAG from phosphatidic acid towards PL synthesis appeared to be either a minor or slow event. There may have been some selectivity in the use of molecular species of DAG for PL or TAG synthesis. In studies by others, Hep G2 cells incubated with oleate were shown not to alter the rate of glycerol incorporation into media and cellular PL whereas the rate of glycerol incorporation into media and cellular TAG increased 2.5 and 9

fold respectively (Wang *et al.*, 1988). Hep G2 cells appear to channel absorbed fatty acids into TAG synthesis rather than PL synthesis.

CE molecular species were not as readily affected by the exogenous fatty acid as TAG and PL were. ACAT was shown to prefer oleate as a substrate in human (Erickson & Cooper, 1980) and rat (Goodman *et al.*, 1964) liver. ACAT in Hep G2 cells appeared to prefer oleate as a substrate since the proportion of CE molecular species were fairly constant and C18 CE was the dominant CE molecular species regardless of incubation conditions. Some cholesteryl myristate was observed in the myristate incubations so myristate was a potential substrate for ACAT, although myristate may not have been a preferred substrate.

Remarkably, the exogenous fatty acids were able to skew the lipid molecular species of the secreted LpB with only minor effects on the proportion of lipid classes in the secreted LpB. The LpB secreted after myristate chases tended to contain a higher proportion of TAG than the LpB secreted after oleate chases (Figures 19 & 32). The general consistency of the percent composition of lipid in LpB suggested that the physico-chemical properties of myristate-containing versus oleate-containing lipid were sufficiently similar as not to alter lipid packing in the lipoprotein. If myristate-containing lipids had significantly different packing structures in LpB compared to oleate-containing lipids, then these differences were expected to be seen as large variations in the lipid composition of LpB. Hep G2 cells appeared to synthesize LpB with a very specific ratio of lipid classes and the addition of exogenous fatty acids impacted primarily on the molecular species content within the individual lipid classes. The lipid composition of the $p<1.063$ g/ml fraction reported by Thrift *et al.* (1986) was similar to the lipid composition in the heparin-retained fraction, although Thrift and colleagues reported a larger proportion of PL and a smaller proportion of TAG associated with apo B compared to this study.

The proportion of cholesterol in the secreted LpB was unusually high. EM observations indicated a large portion of LpB secreted by Hep G2 cells were small in diameter (<250 Å). The small size of these LpB required a higher proportion of surface lipids than the proportion normally observed in VLDL (Table 1). However, even compared to LDL, the secreted LpB from Hep G2 cells had a high proportion of cholesterol, with its cholesterol : PL ratio approaching unity. Miller and Small (1983) preformed a detailed analysis of chylomicrons and VLDL to determine the exact proportions of lipid classes in surface and core lipids. Based on VLDL measurements, they found 1−2% of the cholesterol mass was in the VLDL core. Calculations based on lipid phase diagrams suggested that up to 30% of cholesterol mass may be in the core of VLDL particles with diameters <750 Å (Miller & Small, 1983). The TAG-rich LpB secreted by Hep G2 cells may be carrying substantial quantities of cholesterol in the core. However, the average diameter of LpB as determined by EM

measurements agreed well with the calculated particle diameters. Since the calculation of LpB diameter from lipid percent composition assumed that all of the cholesterol was in the surface lipid, the effect of cholesterol mass in the particle core upon LpB diameter did not appear to be significant.

The proportion of CE in heparin-isolated LpB was very consistent: more so than any other lipid class. In both oleate-load and myristate-chase experiments, CE content ranged from 3.8−5.6% of the total LpB lipid, regardless of the chase conditions. The consistency of CE in the nascent VLDL of Hep G2 cells appears to support earlier observations that some initial lipidation of apo B with CE is important in VLDL assembly (Carr et al., 1996; Rudel et al., 1997; Teh et al., 1998). A specific stoichiometry of CE to apo B may be important in the assembly of nascent VLDL.

B. Assembly of VLDL in Hep G2 Cells

Several groups have suggested that mobilization of TAG stored in hepatocytes is required in the assembly of nascent VLDL (Bar-On et al., 1976; Francone et al., 1989; Lankester et al., 1998; Mooney & Lane, 1981; Wiggins & Gibbons, 1992; Yang et al., 1996, 1995). If mobilization of stored TAG were a major source of TAG for the assembly of nascent VLDL in Hep G2 cells, then molecular species of TAG secreted in LpB should contain species that originated from the TAG storage pool in preference to TAG molecular species containing only exogenous fatty acid. Analysis of molecular species of TAG secreted with LpB during both oleate-load−single myristate-chase and oleate-load−double myristate-chase incubations revealed that Hep G2 cells were not mobilizing stored TAG as a major source of TAG for LpB assembly. The proportions of TAG molecular species secreted after oleate-load and myristate-chase incubations did not contain a dominant TAG species (Figures 22, panel B & 34). The oleate-load incubation skewed stored lipids towards TAG molecular species containing oleate, i.e. C54 TAG. The hypothesis of mobilizing stored TAG for nascent VLDL assembly predicted that oleate-containing TAG species will be more prevalent than myristate-containing TAG species in the secreted LpB, until sufficient time had past for exogenous myristate to skew cellular TAG towards myristate-containing species. The total proportion of C52, C54, and C56 TAG (the TAG species that do not contain myristate) was assumed to be a minimum value for the percent of TAG mobilized en bloc for LpB assembly (Figure 18, panel A). The minimum amount of TAG mobilized en bloc declined with time from approximately 50% after 3 h of myristate chase to approximately 34% after 12 h of myristate chase in the oleate-load and myristate-chase incubations. By re-supplying fresh myristate media in oleate-load and double myristate-chase incubations, the minimum moles of TAG mobilized en bloc from the cytosol dramatically declined from approximately 39% of the TAG

after the first chase to approximately 22% after the second chase with myristate. With the refreshed supply of myristate in the second sequential chase, the potential importance of *en bloc* TAG mobilization diminished. Therefore, a minimum of only 22% of the TAG secreted with LpB may be attributed to *en bloc* mobilization of cellular TAG.

Partial hydrolysis of stored TAG to either DAG or MAG was proposed to be a mechanism of mobilizing stored TAG from the cytosol to the site of LpB assembly (Lankester *et al.*, 1998: Yang *et al.*, 1996, 1995). The proportion of C50 TAG in the LpB secreted by Hep G2 cells was assumed to be a minimum value for the percent of TAG mobilized via hydrolysis to DAG (Figure 18, panels B). The minimum amount of TAG mobilized via hydrolysis to DAG was constant at approximately 16% throughout the 12 h of myristate chase in the oleate-load–single myristate-chase incubations. However, this minimum was lower in the oleate-load and double myristate-chase incubations, at approximately 11% during the first myristate chase and lowering slightly to approximately 10% after the second myristate chase. Re-supplying myristate to the cells via a second sequential incubation appeared to reduce the potential importance of hydrolysing TAG to DAG for the mobilization of cellular TAG. Thus. a minimum of only 10% of the total TAG moles secreted with apo B may be attributed to mobilizing TAG via partial hydrolysis. Similarly, stored TAG may be partially hydrolysed to MAG for mobilization to the site of LpB assembly (Figure 18, panel C). The proportion of C46 TAG was assumed to be a minimum for the percent of TAG mobilized via hydrolysis to MAG. Thus, the minimum amount of TAG mobilized via partial hydrolysis to MAG increase from approximately 8% to 14% over the 12 h of chase in oleate-load–single myristate-chase incubations. In oleate-load–double myristate-chase incubations, the minimum percentage of TAG that may be mobilized from the cellular TAG by partial hydrolysis to MAG for LpB assembly increased from 13% after the first myristate chase to 17% after the second sequential chase with myristate. Therefore, a minimum of 17% of the TAG secreted with apo B may be attributed to the mobilization of cellular TAG via a mechanism of partial hydrolysis to MAG and re-esterification.

The complete hydrolysis of stored TAG followed by re-esterification was postulated to be a mechanism of mobilizing cellular TAG to the ER for LpB assembly (Wiggins & Gibbons. 1992). If there were no preference for either oleate released from cellular TAG or exogenous myristate in the esterification of G3P, then the proportions of C42. C46, C50, and C54 TAG can be determined by the binomial distribution (Table 4). Throughout the 3–12 h of chase in oleate-load and single myristate incubations, the proportion of C54 TAG was typically 66% larger than the proportion of C42 TAG (Figure 22). On Table 4, C54 TAG is 66% larger than the proportion of C42 TAG when oleate makes up between 50 and 60% of the fatty acid pool. However, this predicted the proportion of C50 to be double that of C54;

but. the proportion of C50 was never more than 1.1 fold larger than the proportion of C54. After the second sequential chase with myristate, the proportion of C42 TAG was approximately double the proportion of C54 TAG. On Table 4, the proportion of C42 TAG is double the proportion of C54 TAG when myristate makes up between 50 and 60% of the fatty acid pool. Table 4 predicted the proportion of C46 TAG to be double the proportion of C42 TAG; however, the proportion of C42 TAG was approximately 1.6 fold greater than the proportion of C46 TAG. The proportions of TAG molecular species, especially C46 and C50 TAG, do not support the hypothesis of mobilizing substantial amounts of cellular TAG by a complete hydrolysis and re-esterification cycle.

The presence of fatty acids other than oleate and myristate in total lipid profiles complicated the interpretation of TAG molecular species. Total lipid profiles demonstrated that some C20 fatty acid was present in TAG from all chase conditions of both oleate-load and myristate-chase experiments. For example, C56 TAG represented approximately 5% of the total TAG mass in secreted LpB from cells chased with oleate and contained a minimum of one C20 fatty acid (Figures 22 and 34). C20 fatty acids were probably added to the system from FBS used in the basic cell culture media prior to incubations with fatty acids. Palmitate-containing lipid species, i.e. C48 and C52 TAG, were secreted in LpB from all chases with myristate after loading the stored TAG pool with oleate, even in the presence of the fatty acid synthase inhibitor cerulenin (Figures 22, panel B & 34). The presence of C16 and C20 fatty acids in the TAG molecular species will dilute the proportions of C42. C46, C50, and C54 TAG species and obscure minor pathways in TAG mobilization. The persistence of C54 TAG throughout the myristate chases, both with increasing time in oleate-load–single myristate-chase incubations and over the two sequential myristate chases in oleate-load–double myristate-chase incubations, suggested that Hep G2 cells had some access to its stored TAG for up to 12 h after the oleate-load incubation. However, Hep G2 cells secreted <0.75% of their total cellular TAG mass, which was less than observations made by Gibbons et al. (1994) when they calculated Hep G2 cells secreted only 0.94% of their cellular TAG. Such minute secretion of TAG mass, as well as a lack of a predominant molecular species of TAG in secreted LpB, suggested that Hep G2 cells do not effectively draw upon stored TAG as a primary source of TAG in the assembly of nascent VLDL.

The best explanation of the proportions of TAG molecular species observed in the secreted LpB was the uptake and esterification of exogenous fatty acid. Proportions of molecular species of LpB TAG from oleate-load–single myristate-chase incubations tended to resemble more closely that of LpB from 18 h incubations with only myristate (Figure 17, panel A) as the chase time increased from 3–12 h (Figures 17, panel A & 22, panel B). Also. the proportions of molecular species of LpB TAG in the second sequential chase with

myristate resembled that of LpB secreted by cells incubated with only myristate for 18 h more so than first chase with myristate (Figures 17, panel A & 34). If Hep G2 cells esterify exogenous fatty acid as a primary source of TAG in the assembly of LpB, then the total proportion of C42 and C44 TAG (the TAG species that do not contain oleate) was assumed to be the minimum proportion of TAG assembled into LpB by esterifying exogenous myristate. In the oleate-load and single myristate-chase incubations, a minimum of 15% of the LpB TAG can be attributed to the esterification of exogenous myristate after 3 h of myristate chase and this minimum increased to 22% after 9 h of myristate chase. In oleate-load and double myristate-chase incubations, a minimum of 30% of the LpB TAG was attributed to the esterification of exogenous myristate after the first sequential myristate chase and this minimum increased to 41% after the second sequential myristate chase (Figure 34. panels A & B). Within 12 h of incubation, Hep G2 cells appeared to switch from using oleate supplied from the loading incubation to the myristate in the chase media in the assembly of LpB. Thus. the esterification of exogenous fatty acids appeared to supply a minimum of 41% of the TAG in the assembly of LpB in Hep G2 cells.

The addition of a specific exogenous fatty acid resulted in the rapid incorporation of that fatty acid into the lipid in the LpB assembly pool and cellular stores. After 3 h of myristate chase in oleate-load–single myristate-chase incubations, C42, C44, and C46 TAG species were isolated in association with secreted apo B and were found in large quantities in the cells. CM also appeared (Figure 26) and C30 PL was rapidly elevated (Figure 25) in LpB with myristate chases. In rat hepatocytes, however, exogenous fatty acid was suggested to be esterified to TAG and enter the storage pool before it was accessible by the LpB assembly pool (Gibbons et al., 1992). This lag period was said to be up to 12 h. Clearly, this was not the case in Hep G2 cells. Wu et al. (1996) concluded that Hep G2 cells divided newly synthesized TAG, both of endogenous and exogenous origin, between cytoplasmic storage and ER LpB assembly pools. The majority of lipid was diverted towards the storage pool and was not able to regulate apo B synthesis. The rapid incorporation of myristate-containing lipid species in VLDL synthesis supported the importance of newly synthesized lipid in VLDL assembly for Hep G2 cells. The poor mobilization of cellular lipid to the ER for VLDL assembly may be a defect in the lipoprotein metabolism of Hep G2 cells. A recently proposed hydrolase activity for the mobilization of TAG was reported to be absent from Hep G2 cells (Lehner et al., 1999; Lehner & Verger, 1997) and may be the reason for the lack of TAG mobilization during VLDL synthesis. The restoration of this activity to Hep G2 cells may help to isolate its flaw in VLDL assembly.

Apo B that is insufficiently lipidated is degraded. The degradation of apo B associated with microsomal membranes and on lipoproteins within the secretory pathway was

observed in Hep G2 cells (Adeli *et al.*, 1997b). The fate of the lipid associated with apo B is unknown when apo B is degraded in the secretory pathway. The lipid may remain in the ER and return to the VLDL assembly pool. Although there is little supporting data, apo B may act as a sacrificial protein, assisting in the mobilization and accumulation of lipid in the ER. If this were true, then lipid from degraded apo B may reflux back and be assembled into new VLDL. Lipid may cycle several times between recently degraded apo B and the newly translated/translocated apo B. The lag time between removing a source of lipid precursors from lipogenesis, *i.e.* exogenous myristate, and the actual clearance of synthesized lipid from the VLDL synthetic pool, *i.e.* myristate-containing TAG, may be very long. The persistence of oleate-containing lipid species, *i.e.* C54 TAG and C18 CE, for up to 12 h after the oleate-loading incubation in Hep G2 cells, as observed in oleate-load and single myristate-chase incubations, suggests the lag time of oleate-containing lipid being chased out of the ER pool may be several hours. The reduction in the secretion rate of oleate-containing TAG species observed over the 3 − 12 h of myristate chase in oleate-load−single myristate-chase incubations may reflect the gradual dilution of oleate TAG species in the ER pool by secretion of oleate-containing TAG from the pool and addition of new myristate-containing TAG to the pool. The persistence of significantly higher proportions of C54 TAG in the second sequential myristate chase in oleate-load−double myristate-chase incubations (Figure 34, panels A & B) compared to LpB secreted from cells incubated with only myristate (Figure 17, panel A), suggests that C54 TAG may be able to reflux back to the ER pool after 6 h in Hep G2 cells. Also, the persistence of palmitate-containing lipids, *i.e.* C48 & C52 TAG, in chases that included cerulenin (Figure 34, panels A & B) may be due to palmitate-containing lipids refluxing back from degraded apo B into the VLDL synthetic pool. The return of lipid from degraded apo B to the VLDL assembly pool may be a possible mechanism by which Hep G2 cells appear to retain access to stored lipid.

Many of the studies of VLDL assembly found in the literature have been done in rat hepatocytes or rat hepatoma cell lines like McA-RH7777. Comparing these studies to observations made in Hep G2 cells is complicated by the comparison of apo B_{100} synthesis in Hep G2 cells with apo B_{48} and B_{100} synthesis in rat liver cells. A growing body of knowledge suggests that apo B_{48} and apo B_{100} are handled differently by the VLDL assembly pathway, which may be linked to the relative importance of MTP in the assembly of apo B_{100} versus apo B_{48} into LpB. In a recent study by Wang *et al.* (1997), inhibition of MTP did not affect the addition of bulk lipid to HDL-sized LpB_{48} but inhibited the addition of bulk lipid to HDL-sized LpB_{100} in McA-RH7777 cells. Also, two contrasting reports have described MTP knockout mice. By conditionally knocking out MTP expression in the liver, Chang *et al.* (1999) found that both apo B_{48} and apo B_{100} secretion by mouse liver was eliminated. How-

ever. Raabe *et al.* (1999) found that only apo B_{100} secretion in the mouse liver was eliminated where as apo B_{48} secretion was only reduced by 20%. The livers of these mice also accumulated cytosolic lipid droplets which demonstrated that accumulated cellular lipid was not being mobilized to the ER. Raabe and co-workers suggested that the apo B_{48} was being secreted as an HDL-size particle, MTP was required for the process of mobilizing lipid to the ER. and MTP was only required for apo B_{100} secretion. These data agreed with conclusions made by Wang *et al.* (1997)—MTP activity was postulated to be critical only to apo B_{100} secretion. Therefore, the two forms of apo B may follow different paths in the assembly of VLDL. which may be a result of the increased hydrophobicity of the apo B_{100} in relation to apo B_{48}. The larger size of apo B_{100} may require it to be lipidated more rapidly than apo B_{48} to be secreted.

The experiments performed in this project were not designed to distinguish whether Hep G2 cells lipidated apo B via a one-step or two-step model. The impaired secretion of lipid by Hep G2 cells has led to the proposal that Hep G2 cells only preform the first step (lipidation during translocation) and its impaired mobilization of lipid prevents the second step (addition of bulk lipid; Gibbons *et al.*, 1994). Although there were a substantial number of small particles secreted by Hep G2 cells, the majority were of LDL size. The LpB secreted by Hep G2 cells were larger than the HDL-like particles found in the ER (Borén *et al.*, 1992: Boström *et al.*, 1988), which have been used to define the end of the first step of LpB assembly (Gordon *et al.*, 1996). Since the particles were larger than these HDL-sized LpB. Hep G2 cells appeared to begin the bulk loading of lipid in the assembly of LpB particles. Their inability to mobilize stored lipid effectively for LpB assembly appeared to restrict the addition of bulk lipid to the nascent VLDL, not eliminate it entirely.

C. Effects of Myristate and Oleate on Lipid Secretion and Storage

Myristate and oleate had different effects upon lipid metabolism in Hep G2 cells. Comparing the effects of both fatty acids upon the lipid stored in the cells, oleate stimulated more lipid storage than myristate. This trend was seen in all incubations but only became significant during oleate-load—double myristate-chase incubations (Figure 32, panel C). By incubating cells with three separate lots of fatty acid—BSA solution in the oleate-load and two sequential chase incubations, the increased supply of fatty acid caused the cells chased with oleate to store double the mass of lipid compared to cells that were chased with myristate (Figure 32, panel C). Also, oleate-load and double myristate-chase incubations were done at basal glucose concentrations. By eliminating a source of lipogenesis stimulation, only the exogenous fatty acids influenced accumulation of cellular lipid mass. However, myristate-chased cells showed a tendency to secrete more TAG mass than oleate-chased

cells. In oleate-load and single myristate-chase incubations, the TAG mass secreted in association with apo B after 12 h of myristate chase was significantly higher than the TAG mass secreted after 12 h of oleate chase (Figures 19). This tendency was also seen as a higher proportion of TAG in the lipid percent composition (Figures 21 & 33) and lower CE:TAG ratios (Tables 5 & 6) in LpB secreted from cells chased with myristate than oleate. A previous study compared the effects of diets enriched in fats containing myristate and oleate in humans and found that myristate caused a significant increase in the plasma concentration of LDL cholesterol over oleate (Temme et al., 1997). Oleate appears to be more effective than myristate in stimulating TAG accumulation, whereas myristate appears to be more effective than oleate in stimulating TAG secretion. Thus, stimulation of TAG storage and secretion appeared to be two different effects that may be independently regulated in Hep G2 cells.

D. Effects of Cerulenin upon Lipid Molecular Species

The stimulation of TAG secretion from cells co-incubated with exogenous fatty acid and cerulenin was not an anticipated result. Part of this stimulation may be due to altered enzymatic activities in Hep G2 cells. Hep G2 cells were reported to posses only 6% of the carnitine palmitoyltransferase specific activity and 31% of the s-3-hydroxylacyl-CoA dehydrogenase specific activity as compared to rat hepatocytes (Aguis, 1988). Further, Gibbons et al. (1994) were unable to detect ketone body synthesis in Hep G2 cells. Aguis (1988) also reported that the specific activity of pyruvate kinase in Hep G2 cells was an order of magnitude higher compared to normal rat hepatocytes. Thus, much of the energy requirements of Hep G2 cells appeared to be met by the complete oxidation of glucose—not by β-oxidation of fatty acids. Thus, the following scenario is postulated to occur in Hep G2 cells treated with cerulenin. By impairing the synthesis of fatty acid with cerulenin, acetyl-CoA will accumulate and may stimulate pyruvate carboxylase. This may result in some of the pyruvate taken up by the mitochondria returning to the cytosol as malate via the gluconeogenic route, causing an accumulation of glycolytic intermediates in the cytosol. Increased concentrations of DHAP and G3P may have provided increased substrate concentrations, relative to controls, with which to esterify exogenous fatty acid.

Cerulenin was expected to have a larger effect on the proportions of lipid molecular species. Since cerulenin inhibited the incorporation of acetate label into PL and TAG, palmitate-containing molecular species of PL, i.e. C32 & C34, and TAG, i.e. C44, C48, and C52, were expected to constitute a lower proportion of TAG than was observed. Although cerulenin inhibited the incorporation of acetate into TAG by 75% (Figure 30), palmitate-containing TAG species in the secreted LpB were not significantly different from control incubations (Figure 34). The possibility of lipid refluxing back from degraded apo B to newly

translocated apo B may reduce the perceived inhibition of fatty acid synthase. However, cerulenin was present in the media during the oleate load and both sequential myristate chases. Palmitate-containing lipids would have to persist in the VLDL synthetic pool for >24 h. Cerulenin was also reported to inhibit the elongation of fatty acids (Omura, 1981). However, cerulenin did not appear to have an effect upon the elongation of myristate. as up to 15% of the myristate was elongated regardless of cerulenin treatment (Figure 31). In combination with the remaining 25% of the fatty acid synthase activity, elongation of myristate may be an adequate source of palmitate for the resulting proportions of TAG molecular species.

Cerulenin did have a strong impact upon cells that were chased without fatty acid. The secreted mass of each lipid class from cells chased with cerulenin and without fatty acid was significantly reduced compared to cells that were only deprived of fatty acid in the chase media (Figure 32). In the case of secreted TAG, the cerulenin treatment halved the mass of TAG secreted with LpB in cells incubated with MEM. *De novo* synthesis of fatty acid appeared to be significant in the secretion of lipid mass in the absence of exogenous fatty acid. Despite the presence of newly synthesized lipids from the oleate-load incubation. Hep G2 cells appeared to require active lipogenesis for "effective" secretion of LpB.

E. Assembly of TAG and Apo B During VLDL Synthesis in Hep G2 Cells

The origin of TAG used by Hep G2 cells appeared to be primarily from the esterification of exogenous fatty acid (Figure 37). When fatty acids were taken up by Hep G2 cells and esterified to TAG, a major portion of this TAG appeared to enter the cellular lipid pool. Cellular TAG was not effectively mobilized from the cytosol to the VLDL synthetic pool and the mechanism of TAG mobilization in Hep G2 cells was not clear. Some of the TAG that was synthesized from exogenous fatty acid was able to enter the VLDL synthetic pool directly, which accounted for a minimum of 41% of the TAG assembled into nascent VLDL. A potential source of TAG for the VLDL synthetic pool was the refluxing of TAG from apo B that was degraded in the secretory pathway back to the VLDL synthetic pool. This may be a mechanism by which Hep G2 cells appear to retain access to cellular lipid.
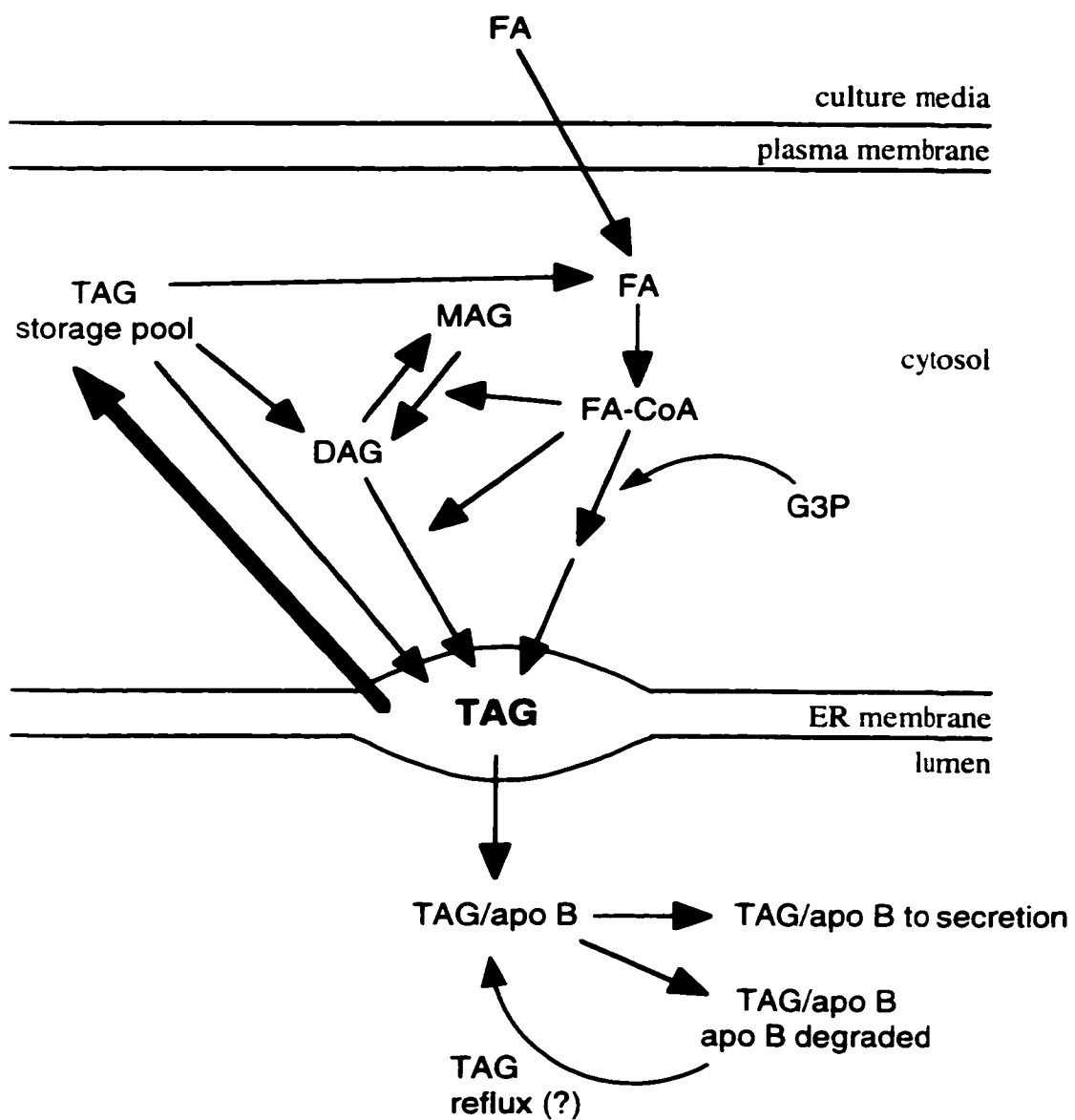
Figure 37: **Origin of TAG for VLDL synthesis in Hep G2 cells.** FA= fatty acid; FA-CoA=fatty acyl-coenzyme A.

Summary and Conclusions

The mechanisms involved in the assembly of TAG with apo B and their role in determining secreted LpB composition are not well defined. Relative use of exogenous fatty acids versus stored TAG after partial or complete hydrolysis in LpB assembly is controversial. The objective of this thesis was to use the human hepatoma cell line Hep G2 to investigate relative use of exogenous fatty acid versus stored cellular TAG as substrates for synthesis of TAG for secretion in LpB.

Initial experiments developed chromatographic methods to isolate secreted LpB. Hep G2 cells were incubated for 18 h with oleate, myristate, or BSA. Media were fractionated by heparin-Sepharose into retained and unretained fractions. Heparin-unretained fractions were further separated by HTP into retained and unretained fractions. Apoproteins were determined by electroimmunoassay and total lipid profiles were measured by GLC. LpB were isolated and concentrated in heparin-retained fractions while apo A-I and apo E were present in HTP-retained and -unretained fractions. Approximately 72% of secreted TAG were associated with apo B whereas approximately 28% of TAG were found in HTP-retained and -unretained fractions. Calculated particle diameters of heparin-retained fractions ranged from 173–232 Å, which agreed well with the EM average (215 Å). However, EM data revealed a diverse population of particles that was masked by the consistency of the lipid percent composition. HTP-retained and -unretained fractions were found to contain apo A-I, apo E. and neutral lipids. Analysis of molecular species of TAG indicated with extensive incorporation of exogenous fatty acids into cellular and secreted TAG. Heparin-Sepharose chromatography was effective in isolating LpB, which was essentially free of lipid associated with apo E. apo A-I, and cellular debris, for analysis of VLDL assembly.

The role of exogenous fatty acid and endogenous lipid in the assembly of LpB was studied in Hep G2 cells by sequential fatty acid incubations to label the molecular species of lipid. Hep G2 cells were incubated for 18 h with oleate to load lipid storage pools with oleate-containing TAG and the cells were chased for up to 12 h with myristate. Controls were chased with oleate. Total lipid profiles of heparin-retained LpB were determined by GLC. LpB lipid mass increased over the 12 h incubation, with oleate-loaded and myristate-chased cells secreting significantly more TAG mass than in cells chased with oleate after 12 h. This resulted in the proportion of TAG increasing from 34.1 to 50.5% of LpB lipid mass over time. with reciprocal decreases in PL mass. However, CE consistently contributed 4.4– 5.6% of the lipid in isolated LpB. Secretion rates of C42–C46 TAG molecular species were constant through myristate chases while the secretion rates C48–C54 TAG molecular species dropped during the first 6 h of myristate chase and then became constant. Thus, exogenous

myristate was rapidly added to lipid species secreted with LpB. The minimum amount of TAG that was consistent with mobilization *en bloc* from stored TAG for LpB assembly decreased from 50 to 34% over the 12 h of myristate chase. The minimum amount of TAG that was consistent with mobilization for LpB assembly by partial hydrolysis to DAG followed by re-esterification was constant across the 12 h of myristate chase at 17%. The minimum amount of TAG that was consistent with mobilization by partial hydrolysis to MAG followed by re-esterification increase from 8 to 14% over the 12 h of myristate chase. The distribution of TAG molecular species did not support the mobilization of stored TAG via a cycle of complete hydrolysis and re-esterification. However, the minimum proportion of LpB TAG that was consistent with originating from direct esterification of exogenous myristate increased from 15 to 22% over the 12 h of myristate chase.The importance of exogenous myristate to LpB assembly increased with time while the importance of stored oleate-containing TAG decreased with time.

To refine the origin of TAG used in LpB assembly, Hep G2 cells were incubated with oleate for 18 h and were chased with myristate for two sequential 6 h periods. The first chase should clear residual LpB formed during the oleate-load incubation out of the secretory pathway and the second chase should clarify the relative use of stored TAG versus exogenous fatty acid in LpB assembly. Controls were chased with oleate or MEM. To reduce *de novo* fatty acid synthesis, Hep G2 cells were incubated with 10 μg/ml cerulenin, which reduced acetate incorporation into TAG to 25% of controls. Cells treated with cerulenin and chased with fatty acid secreted up to 58% more LpB TAG compared to cells chased with fatty acids. However, when cells were chased with MEM instead of fatty acid, cerulenin reduced the mass of secreted LpB TAG to half that of control incubations after both the first and second sequential chases. Cells that were loaded with oleate and chased with myristate secreted more LpB TAG mass than cells that were chased with oleate: however, oleate stimulated 2 fold more cellular lipid accumulation than cells chased with myristate and 4 fold more than cells chased with MEM. The minimum proportion of TAG that was consistent with mobilization from cellular TAG *en bloc* for LpB assembly fell from 39% after the first chase to 22% after the second myristate chase. The minimum proportion of LpB TAG that was consistent with mobilization by a cycle of partial hydrolysis to DAG followed by re-esterification decreased slightly from 11% after the first myristate chase to 10% after the second myristate chase. The minimum proportion of LpB TAG that was consistent with mobilization by partial hydrolysis to MAG increased from 13% after the first myristate chase to 17% after the second myristate chase. As the cells were re-supplied with fresh myristate, the importance of stored oleate-containing TAG decreased significantly. However, the minimum proportion of LpB TAG that was consistent with originating from esterification of

exogenous myristate increased substantially from 30% after the first myristate chase to 41% after the second myristate chase, which was more than double the minimum contribution of TAG from any other potential source. Although Hep G2 cells were able to retain some access to stored TAG for LpB assembly throughout both chases, possibly by returning lipid from LpB degraded in the secretory pathway to the VLDL synthetic pool, the esterification of exogenous fatty acid was the primary source of TAG for the assembly of LpB, contributing a minimum of 41% of the total LpB TAG.

In conclusion, heparin-Sepharose chromatography effectively isolated LpB secreted from Hep G2 cells, which was free of apo A-I and apo E. After cells were incubated with oleate for 12 h, myristate chases of up to 12 h were more effective than oleate chases at stimulating the secretion of TAG with LpB, whereas oleate chases were more effective than myristate chases at stimulating the storage of cellular lipid. The primary source of TAG for LpB assembly in Hep G2 cells was the esterification of exogenous fatty acid, which accounted for a minimum of 41% of the LpB TAG.

Appendix A

The proceeding figures are total lipid profiles that represent typical data from a given incubation condition. Figures 38–40 are representative of LpB isolated by heparin-Sepharose from single fatty acid incubations, Figures 41–44 are representative data of both cellular and isolated LpB lipids from cells loaded with oleate and chased for 12 h with fatty acid, and Figures 45–47 are representative data of LpB isolated from cells treated with cerulenin during the oleate-load and double chase incubations. Profiles are digitally scanned images from reports generated from the HP ChemStation software. Figure 38–44 were produced by revision A.02.12 of the ChemStation software and Figures 45–47 were produced by revision A.04.02 of the ChemStation software using the enhanced integrator. Horizontal axes display counts from the flame-ionization detector and vertical axes show the retention times in minutes. The peak labelled int std was the internal standard tricaprin; chol, cholesterol; C30–C40, DAG and ceramide moieties from PL and sphingolipids in terms of carbon numbers of fatty acid moieties; CM, cholesteryl myristate; CP, cholesteryl palmitate; CO, C18 CE that was typically cholesteryl oleate; and C42–C58, TAG in terms of carbon numbers of fatty acid moieties. Temperature programming is shown in Figure 11. Figures 38–40 show data collected when a simple silica connector was used to join the analytical and guard columns. Figures 41–47 show data collected when the capillary Vu-Union connector sealed the analytical and guard columns.

C:\HPCHEM\1\DATA\NOV_04\DEC_14\061F0301.D
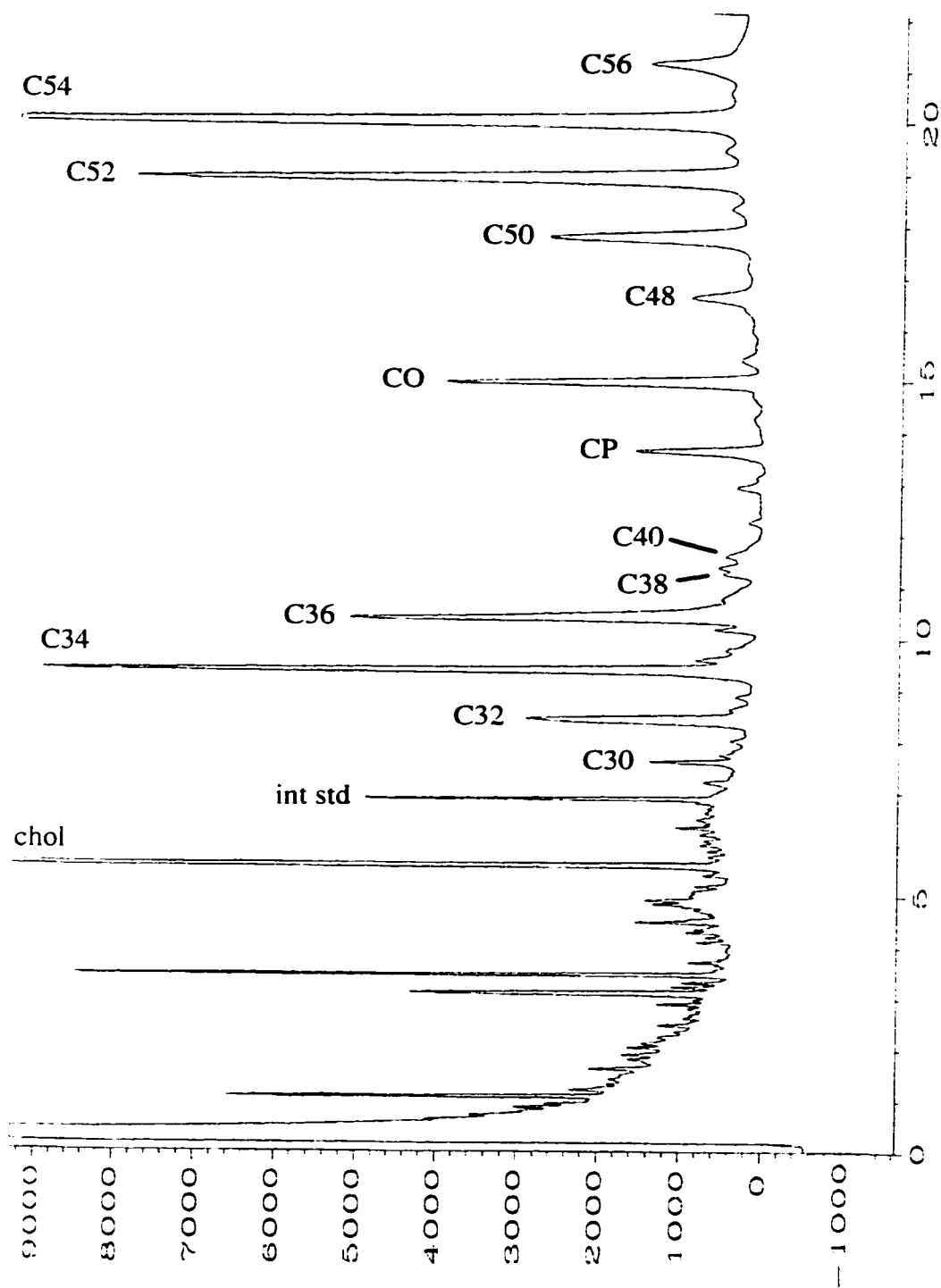
Figure 38: **Typical profile of LpB isolated by heparin-Sepharose after single oleate incubation.** Figure description on page 151.

C:\HPCHEM\...\MAR_20.95\064F0101.D

C56
C54
C52
C50
C48
C46
CO
C44
CP
C42
CM
C40
C38
C36
C34
C32
C30
int std
chol
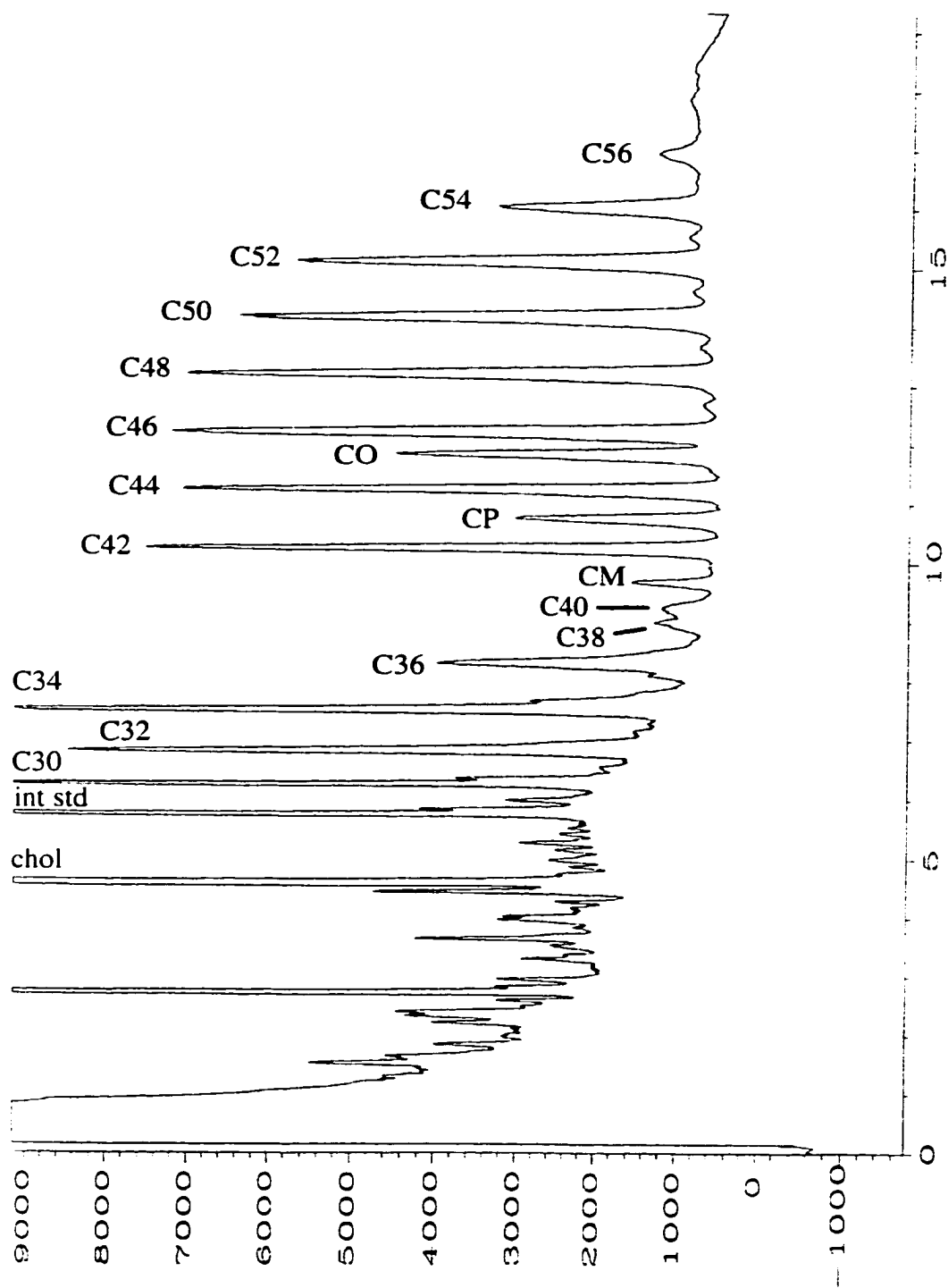
Figure 39: **Typical profile of LpB isolated by heparin-Sepharose after single myristate incubation.** Figure description on page 151.

C:\HPCHEM\...\MAR_20.95\068F0301.D
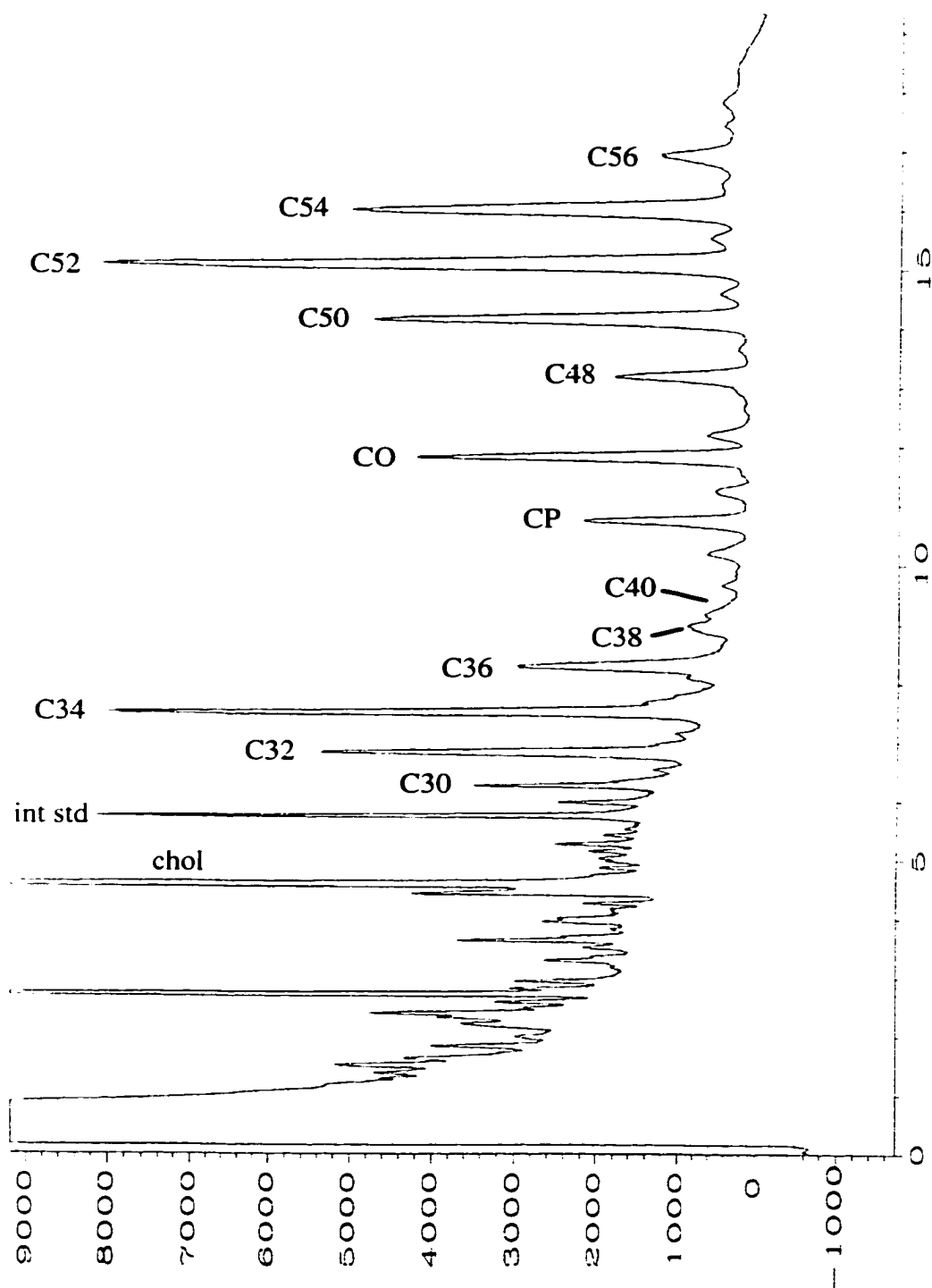
Figure 40: **Typical profile of LpB isolated by heparin-Sepharose after single control incubation with BSA.** Figure description on page 151.

A:\JULY_26.96\MEDIA\AUG_09.96\069F0101 D
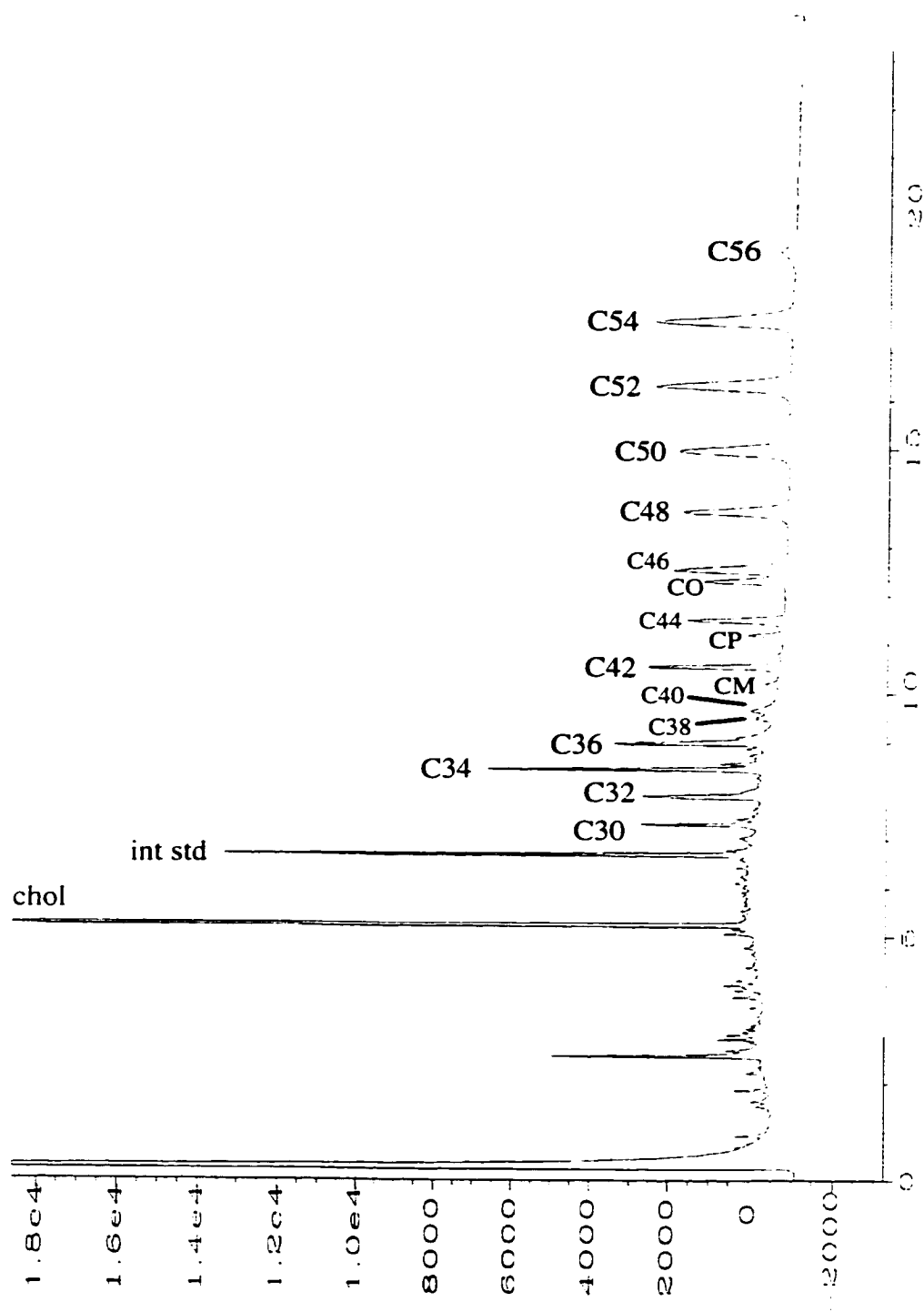
Figure 41: **Typical profile of LpB isolated after oleate-load and 12 h of myristate chase.** Figure description on page 151.

A:\JULY_26.96\CELLS\AUG_09.96\088F0301 D

C56

C54

C52

C50

C48

C46

CO

C44

C42

CP

C40 — CM

C38

C36

C34

C32

C30

int std

chol
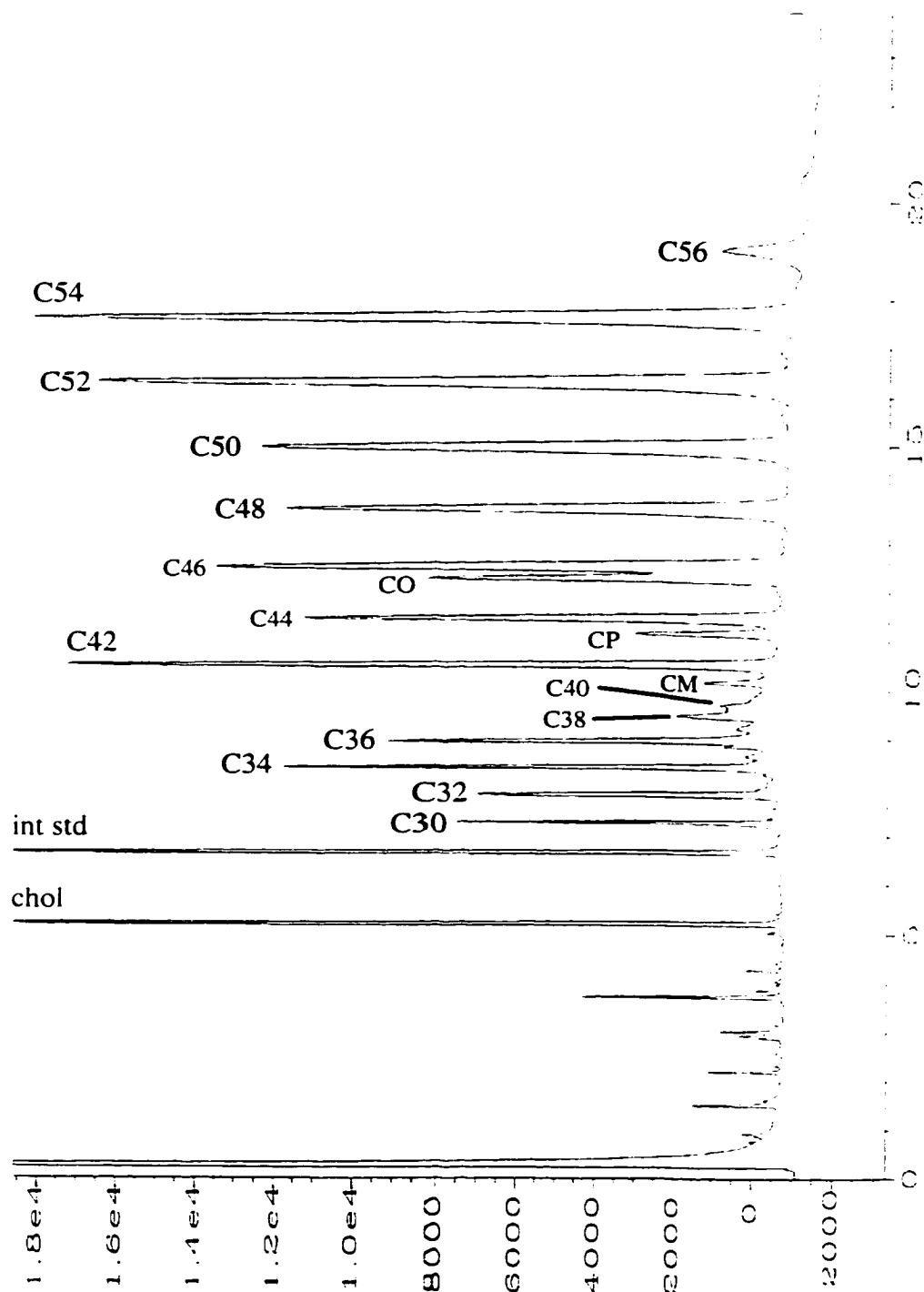
Figure 42: **Typical profile of cellular lipid after oleate-load and 12 h of myristate chase.** Figure description on page 151.
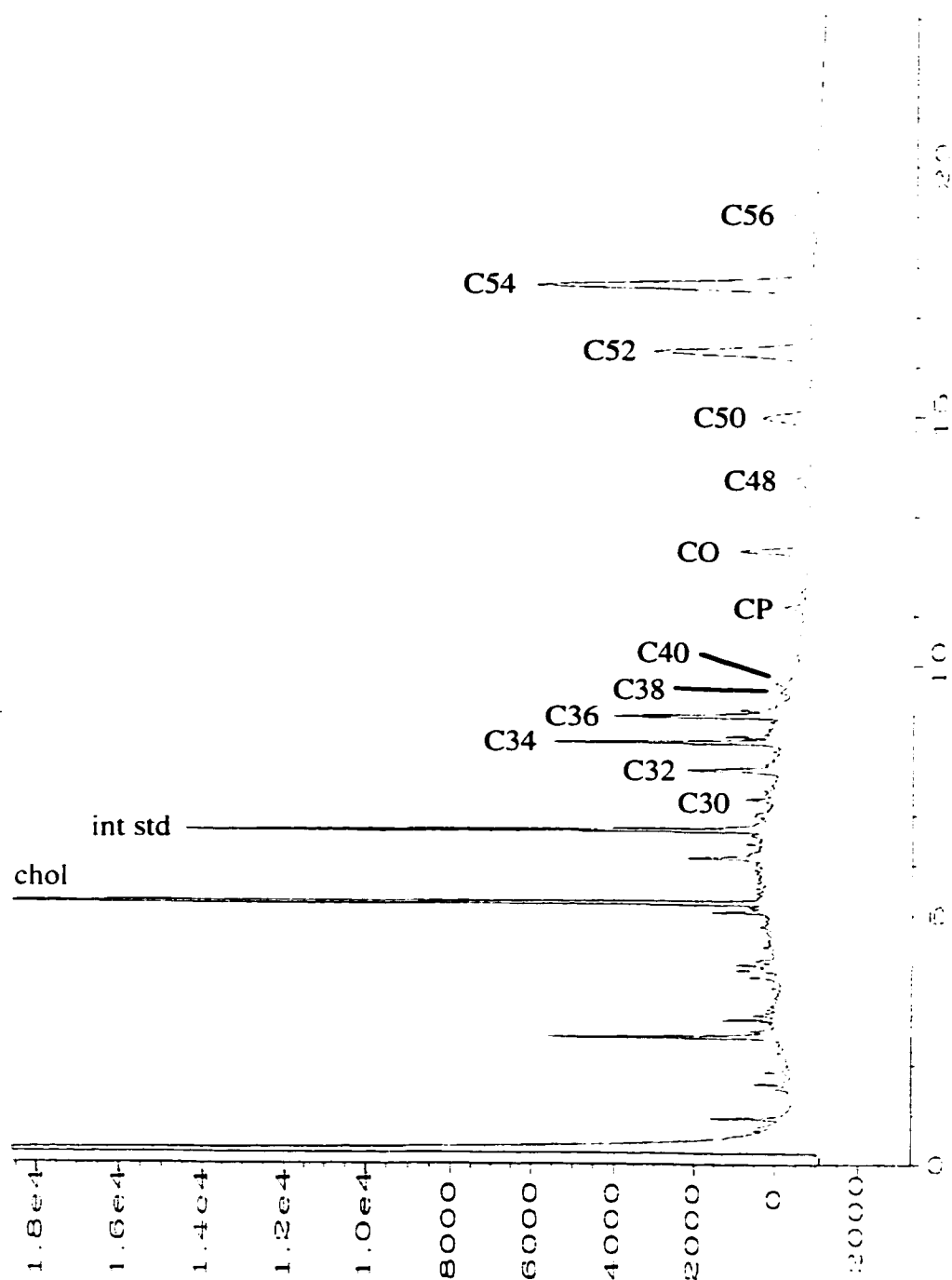
Figure 43: **Typical profile of LpB isolated after oleate-load and 12 h of oleate chase.** Figure description on page 151.

A:\JULY_26.96\CELLS\AUG_09.96\085FO301.D
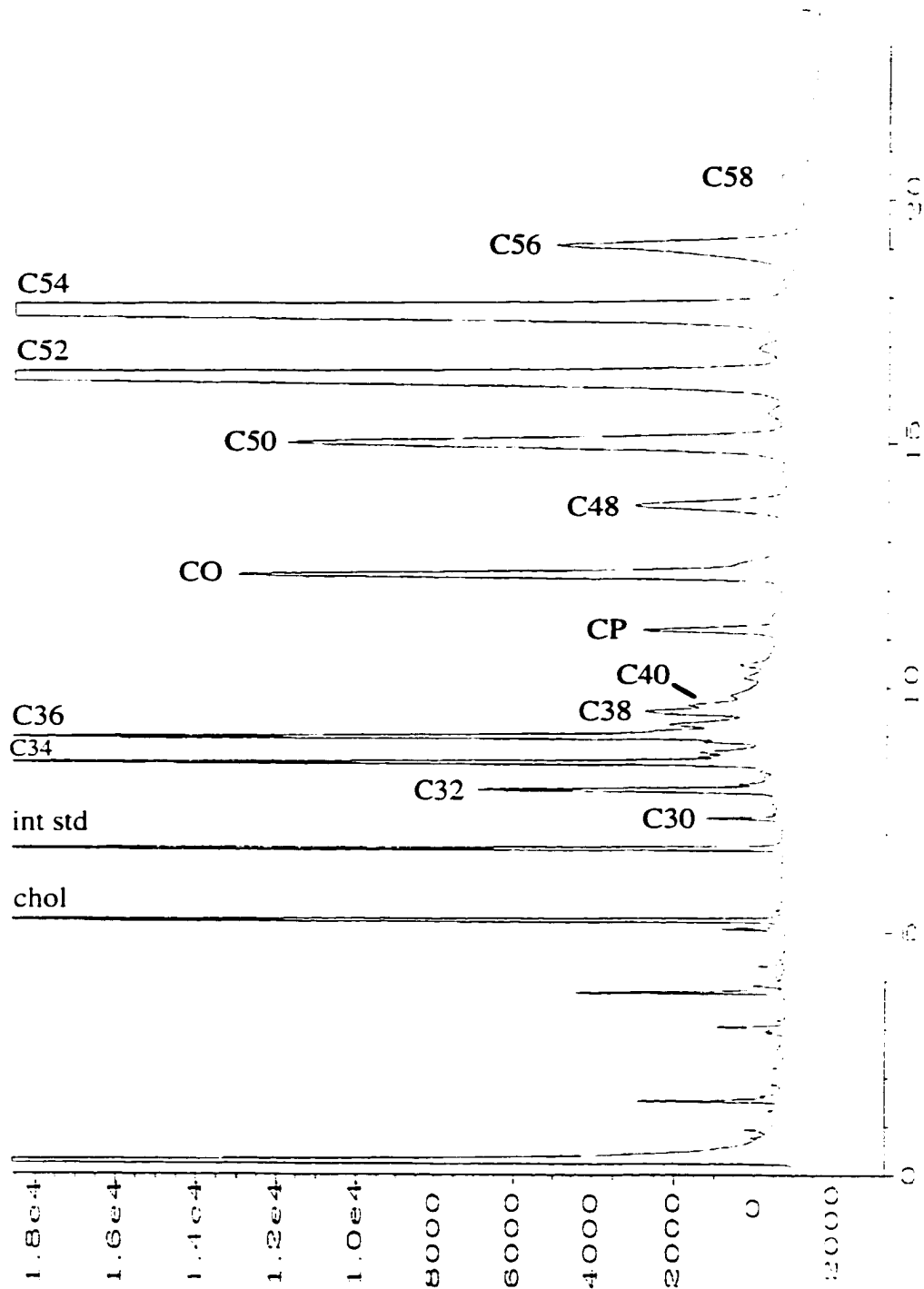
Figure 44: **Typical profile of cellular lipid after oleate-load and 12 h of oleate chase.** Figure description on page 151.
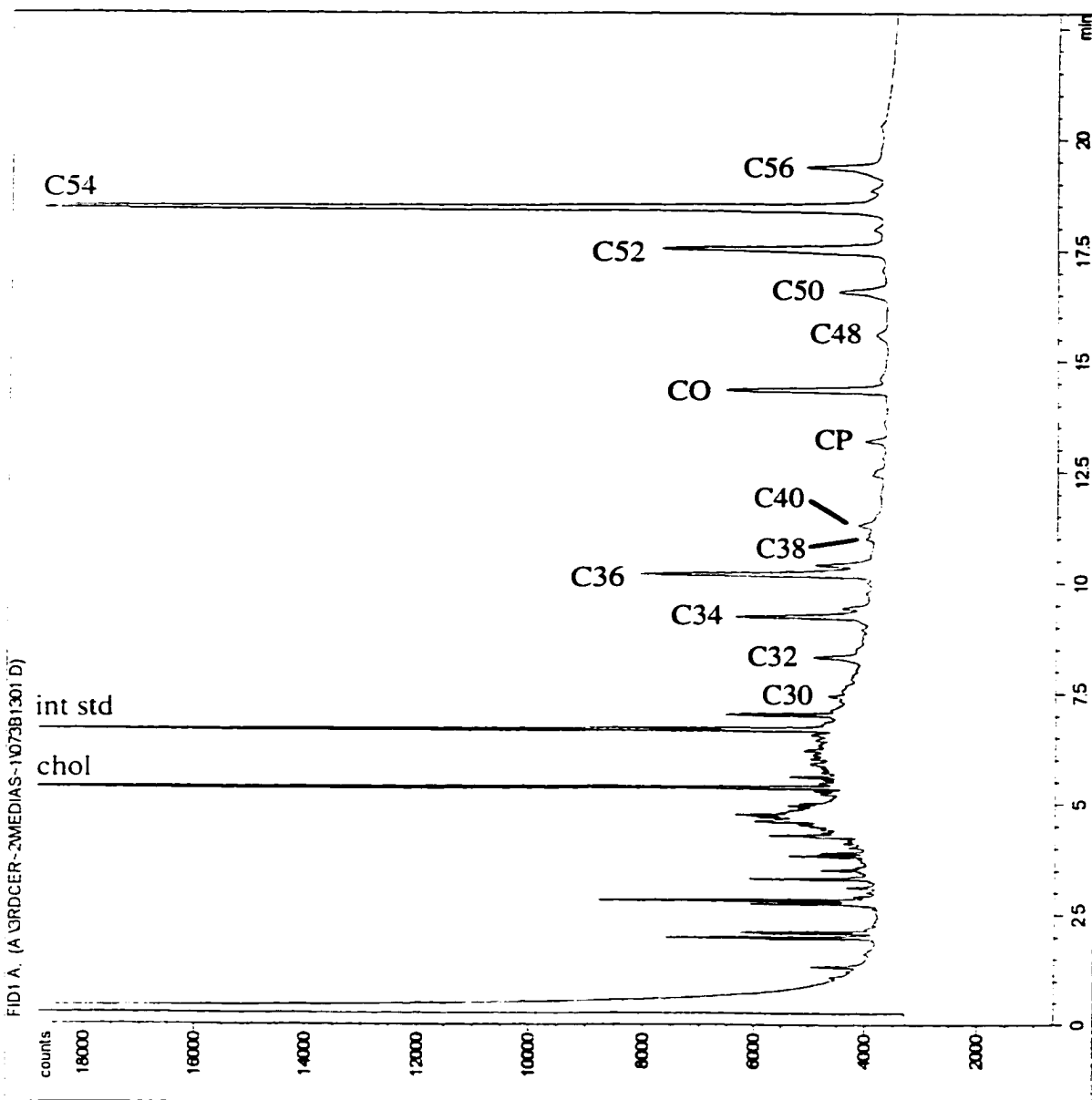
Figure 45: **Typical profile of LpB isolated after oleate-load and two sequential oleate chases with cerulenin.** Figure description on page 151.
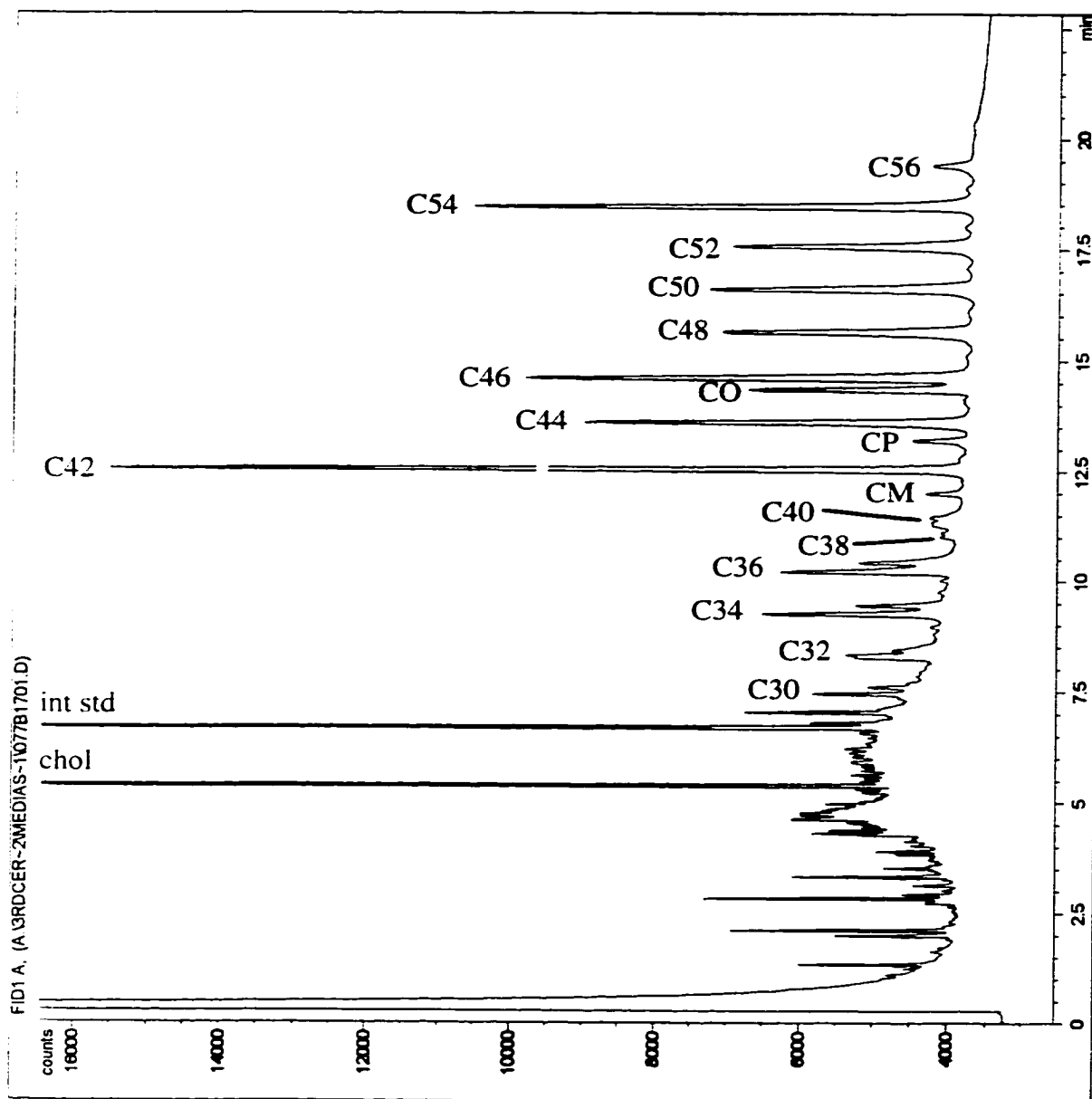
Figure 46: **Typical profile of LpB isolated after oleate-load and two sequential myristate chases with cerulenin.** Figure description on page 151.
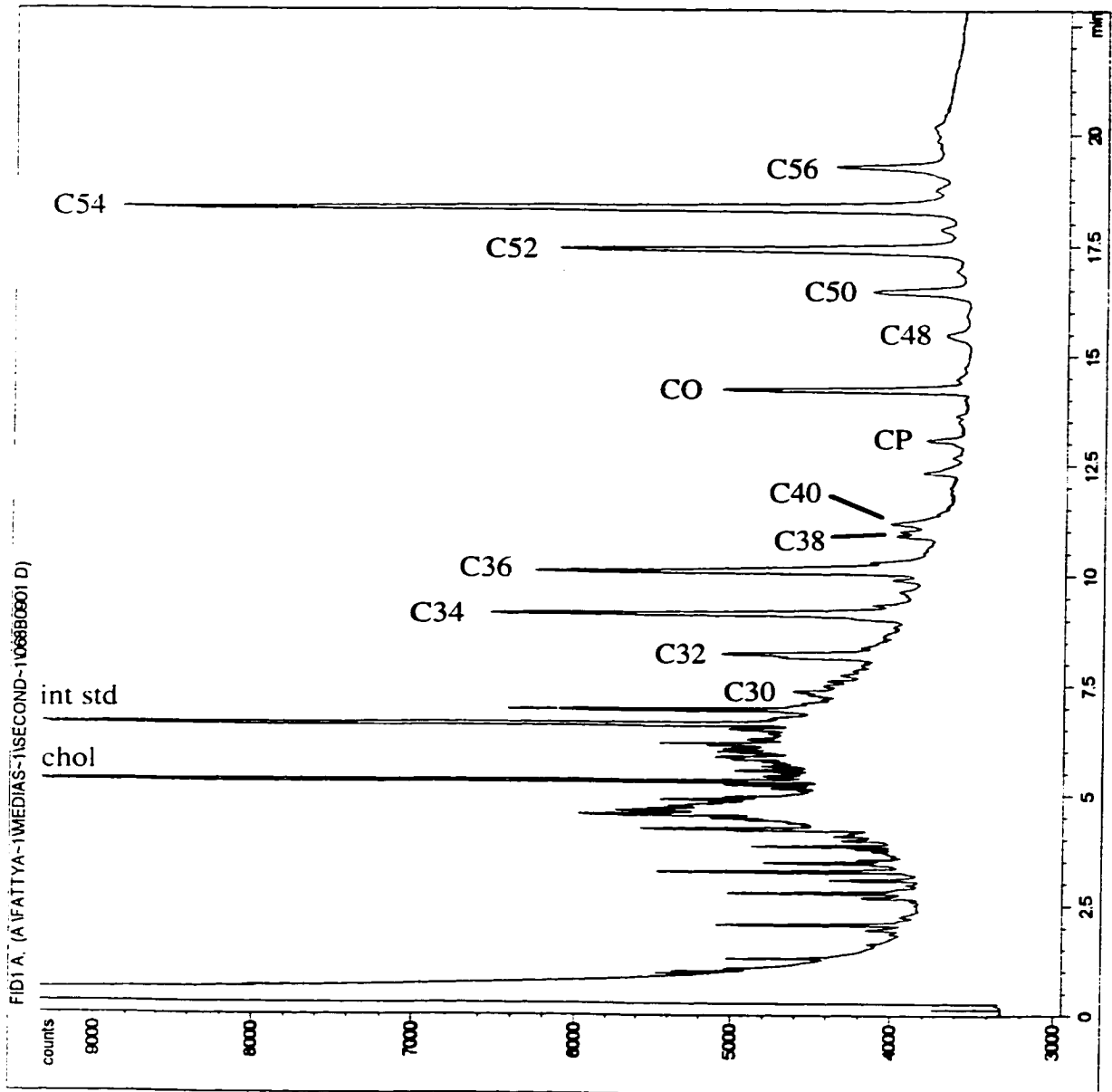
Figure 47: **Typical profile of LpB isolated after oleate-load and two sequential MEM chases with cerulenin.** Figure description on page 151.
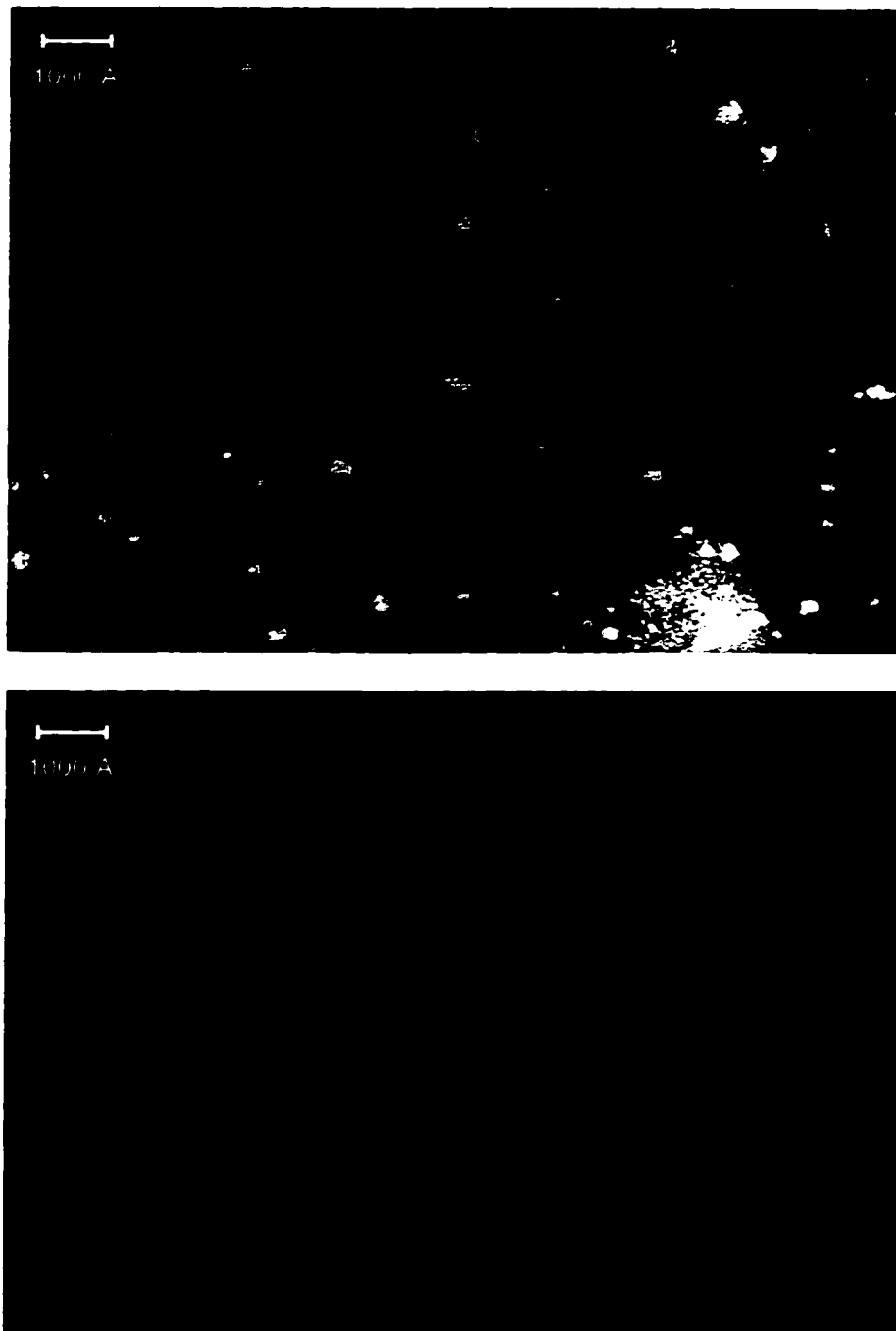
Figure 48: **Sample EM photographs of LpB particles.** LpB particles were an isolated by heparin-Sepharose chromatography after 18 h incubation with oleate. Magnification=87 300 X.

References

Acton. S.. Rigotti, A., Landschultz, K.T., Xu, S., Hobbs, H.H., and Krieger, M. (1996) Identification of scavenger receptor SR-BI as a high density lipoprotein receptor. *Science*. **271** (5248): 518–520.

Adeli. K.. Macri, J., Mohammadi, A., Kito, M., Urade, R., and Cavallo, D. (1997a) Apolipoprotein B is intracellularly associated with an ER-60 protease homologue in HepG2 cells. *J. Biol. Chem.* **272** (36): 22489–22494.

Adeli. K., Wettesten, M., Asp, L., Mohammadi, A., Macri, J., and Olofsson, S.-O. (1997b) Intracellular assembly and degradation of apolipoprotein B-100-containing lipoproteins in digitonin-permeabilized HEP G2 cells. *J. Biol. Chem.* **272** (8): 5031–5039.

Adeli. K. (1994) Regulated intracellular degradation of apolipoprotein B in semipermeable HepG2 cells. *J. Biol. Chem.* **269** (12): 9166–9175.

Aden. D. P.. Fogel, A., Plotkin, S., Damjanov, I., and Knowles, B.B. (1979) Controlled synthesis of HBsAg in a differentiated human liver carcinoma-derived cell line. *Nature*. **282** (5739): 615–616.

Aguis. L. (1988) Metabolic interactions of parenchymal hepatocytes and dividing epithelial cells in co-culture. *Biochem. J.* **252** (1): 23–28.

Alexander, C.A., Hamilton, R.L., and Havel, R.J. (1976) Subcellular localization of B apoprotein of plasma lipoproteins in rat liver. *J. Cell Biol.* **69** (2): 241–263.

Archer. T.K., Tam, S.-P., and Deeley, R.G. (1986) Kinetics of estrogen-dependent modulation of apolipoprotein A-I synthesis in human hepatoma cells. *J. Biol. Chem.* **261** (11): 5067–5074.

Archer. T.K.. Tam, S.-P., Deugau, K.V., and Deeley, R.G. (1985) Apolipoprotein C-II mRNA levels in primate liver. *J. Biol. Chem.* **260** (3): 1676–1681.

Arrol. S.. Mackness, M.I., Laing, I., and Durrington, P.N. (1991) Lipoprotein secretion by the human hepatoma cell line Hep G2: Differential rates of accumulation of apolipoprotein B and lipoprotein lipids in tissue culture media in response to albumin. glucose and oleate. *Biochim. Biophys. Acta.* **1086** (1): 72–80.

Attie, A.D., Weinstein, D.B., Freeze, H.H., Pittman, R.C., and Steinberg, D. (1979) Unaltered catabolism of desialylated low-density lipoprotein in the pig and in cultured rat hepatocytes. *Biochem. J.* **180** (3): 647–654.

Atzel. A. and Wetterau, J.R. (1993) Mechanism of microsomal triglyceride transfer protein catalyzed lipid transport. *Biochemistry.* **32** (39): 10444–10450.

Backus. J.W. and Smith, H.C. (1992) Three distinct RNA sequence elements are required for efficient apolipoprotein B (apoB) RNA editing *in vitro*. *Nucleic Acids Res.* **20** (22): 6007–6014.

Backus. J.W. and Smith, H.C. (1991) Apolipoprotein B mRNA sequences 3′ of the editing site are necessary and sufficient for editing and editosome assembly. *Nucleic Acids Res.* **19** (24): 6781–6786.

Bakillah, A., Jamil, H., and Hussain, M.M. (1998) Lysine and arginine residues in the N-terminal 18% of apolipoprotein B are critical for its binding to microsomal triglyceride transfer protein. *Biochemistry.* **37** (11): 3727–3734.

Bamberger, M.J. and Lane, M.D. (1988) Assembly of very low density lipoprotein in the hepatocyte: Differential transport of apoproteins through the secretory pathway. *J. Biol. Chem.* **263** (24): 11868–11878.

Bar-On, H., Roheim, P.S., Stein, O., and Stein, Y. (1971) Contribution of floating fat triglyceride and of lecithin towards formation of secretory triglyceride in perfused rat liver. *Biochim. Biophys. Acta.* **248** (1): 1–11.

Barrett, E.J., Ferrannini, E., Gusberg, R., Bevilacqua, S., and DeFronzo, R.A. (1985) Hepatic and extrahepatic splanchnic glucose metabolism in the postabsorptive and glucose fed dog. *Metabolism.* **34** (5): 410–420.

Beisiegel, U. (1998) Lipoprotein metabolism. *Eur. Heart. J.* **19** (suppl. A): A20–A23.

Beisiegel, U. (1995) Receptors for triglyceride-rich lipoproteins and their role in lipoprotein metabolism. *Curr. Opin. Lipidol.* **6** (3): 117–122.

Beisiegel, U., Weber, W., and Bengtsson-Olivecrona, G. (1991) Lipoprotein lipase enhances the binding of chylomicrons to low density lipoprotein receptor-related protein. *Proc. Natl. Acad. Sci. USA.* **88** (19): 8342–8346.

Benoist, F. and Grand-Perret, T. (1997) Co-translational degradation of apolipoprotein B100 by the proteasome is prevented by microsomal triglyceride transfer protein: Synchronized translation studies on HepG2 cells treated with an inhibitor of microsomal triglyceride transfer protein. *J. Biol. Chem.* **272** (33): 20435–20442.

Berg, K. (1963) A new serum type system in man—the Lp system. *Acta Pathol. Microbol. Scand.* **59** (3): 369–382.

Bergman, R.N., Beir, J.R., and Hourigan, P.M. (1982) Intraportal glucose infusion matched to oral glucose absorption: Lack of evidence for "gut factor" involvement in hepatic glucose storage. *Diabetes.* **31** (1): 27–35.

Bernfeld, P., Donahue, V.M., and Berkowitz, M.E. (1957) Interaction of human serum β-lipoglobulin with polyanions. *J. Biol. Chem.* **226** (1): 51–64.

Berthois, Y., Katzenellenbogen, J.A., and Katzenellenbogen, B.S. (1986) Phenol red in tissue culture media is a weak estrogen: Implications concerning the study of estrogen-responsive cells in culture. *Proc. Natl. Acad. Sci. USA.* **83** (8): 2496–2500.

Blackhart, B.D., Ludwig, E.M., Pierotti, V.R., Caiati, L., Onasch, M.A., Wallis, S.C., Powell, L., Pease, R., Knott, T.J., Chu, M.-L., Mahley, R.W., Scott, J., McCarthy, B.J., and Levy-Wilson, B. (1986) Structure of the human apolipoprotein B gene. *J. Biol. Chem.* **261** (33): 15364–15367.

Bligh, E.G. and Dyer, W.J. (1959) A rapid method of total lipid extraction and purification. *Can. J. Biochem. Physiol.* **37** (8): 911–917.

Bonnardel, J.A. and Davis, R.A. (1995) In HepG2 cells, translocation, not degradation, determines the fate of the *de novo* synthesized apolipoprotein B. *J. Biol. Chem.* **270** (48): 28892–28896.

Borchardt, R.A., and Davis, R.A. (1987) Intrahepatic assembly of very low density lipoproteins: Rate of transport out of the endoplasmic reticulum determines rate of secretion. *J. Biol. Chem.* **262** (34): 16394–16402.

Borén, J., Lee, I., Zhu, W., Arnold, K., Taylor, S., and Innerarity, T.L. (1998a) Identification of the low density lipoprotein receptor-binding site in the apolipoprotein B100 and the modulation of its binding activity by the carboxyl terminus in familial defective apo-B100. *J. Clin. Invest.* **101** (5): 1084–1093.

Borén, J., Véniant, M.M., and Young, S.G. (1998b) Apo B100-containing lipoproteins are secreted by the heart. *J. Clin. Invest.* **101** (6): 1197–1202.

Borén, J., Rustæus, S., and Olofsson, S.-O. (1994) Studies on the assembly of apolipoprotein B-100- and B-48-containing very low density lipoproteins in McA-RH7777 cells. *J. Biol. Chem.* **269** (41): 25879–25888.

Borén, J., Graham, L., Wettesten, M., Scott, J., White, A., and Olofsson, S.-O. (1992) The assembly and secretion of apoB 100-containing lipoproteins in Hep G2 cells: ApoB 100 is cotranslationally integrated into lipoproteins. *J. Biol. Chem.* **267** (14): 9858–9867.

Borén, J., Wettesten, M., Sjöberg, A., Thorlin, T., Bondjers, G., Wiklund, O., and Olofsson, S.-O. (1990) The assembly and secretion of apoB 100 containing lipoproteins in Hep G2 cells: Evidence for different sites for protein synthesis and lipoprotein assembly. *J. Biol. Chem.* **265** (18): 10556–10564.

Boström, K., Borén, J., Wettesten, M., Sjöberg, A., Bondjers, G., Wiklund, O., Carlsson, P., and Olofsson, S.-O. (1988) Studies on the assembly of apo B-100-containing lipoproteins in HepG2 cells. *J. Biol. Chem.* **263** (9): 4434–4442.

Boström, K., Wettesten, M., Borén, J., Bondjers, G., Wiklund, O., and Olofsson, S.-O. (1986) Pulse-chase studies on the synthesis and intracellular transport of apolipoprotein B-100 in HepG2 cells. *J. Biol. Chem.* **261** (29): 13800–13806.

Breckenridge, W.C. and Kuksis, A. (1968) Specific distribution of short-chain fatty acids in molecular distillates of bovine milk fat. *J. Lipid Res.* **9** (3): 388–393.

Broadway, N.M. and Saggerson, E.D. (1995a) Microsomal carnitine acyltransferases. *Biochem. Soc. Trans.* **23** (3): 490–494.

Broadway, N.M. and Saggerson, E.D. (1995b) Solubilization and separation of two distinct carnitine acyltransferases from hepatic microsomes: Characterization of the malonyl-CoA-sensitive enzyme. *Biochem. J.* **310** (3): 989–995.

Brown, J.R. (1975) Structure of bovine serum albumin. *Fed. Proc.* **34** (3): 591.

Brown, M.S. and Goldstein, J.L. (1986) A receptor-mediated pathway for cholesterol homeostasis. *Science.* **232** (4746): 34–47.

Bulleid, N. J. and Freedman, R.B. (1988) Defective co-translational formation of disulphide bonds in protein disulphide-isomerase-deficient microsomes. *Nature*. **335** (6191): 649–651.

Burgess, J.W., Liang, P., Vaidyanath, C., and Marcel, Y.L. (1999) ApoE of the HepG2 cell surface includes a major pool associated with chondroitin sulfate proteoglycans. *Biochemistry*. **38** (2): 524–531.

Burnett, J.R., Wilcox, L.J., Telford, D.E., Kleinstiver, S.J., Barrett, P.H.R., and Huff, M.W. (1998) Inhibition of cholesterol esterification by DuP 128 decreases hepatic apolipoprotein B secretion in vivo: Effect of dietary fat and cholesterol. *Biochim. Biophys. Acta*. **1393** (1): 63–79.

Busch, S.J., Krstenansky, J.L., Owen, T.J., and Jackson, R.L. (1989a) Human hepatoma (HepG2) cells secret a single 65 k dalton triglyceride lipase immunologically identical to postheparin plasma hepatic lipase. *Life Sci*. **45** (7): 615–622.

Callow, M.J. and Rubin, E.M. (1995) Site-specific mutagenesis demonstrates that cysteine 4326 of apolipoprotein B is required for covalent linkage with apolipoprotein(a) in vivo. *J. Biol. Chem*. **270** (41): 23914–23917.

Campos, E., Jäckle, S., Chen, G.C., and Havel, R.J. (1996) Isolation and characterization of two distinct species of human very low density lipoproteins lacking apolipoprotein E. *J. Lipid Res*. **37** (9): 1897–1906.

Cardin, A.D., Randall, C.J., Hirose, N., and Jackson, R.L. (1987) Physical-chemical interactions of heparin and human plasma low-density lipoproteins. *Biochemistry*. **26** (17): 5513–5518.

Cardin, A.D., Witt, K.R., Barnhart, C.L., and Jackson, R.L. (1982) Sulfhydryl chemistry and solubility properties of human plasma apolipoprotein B. *Biochemistry*. **21** (18): 4503–4511.

Carlson, T.L. and Kottke, B.A. (1989) Effect of 25-hydroxylcholesterol and bile acids on the regulation of cholesterol metabolism in Hep G2 cells. *Biochem. J*. **264** (1): 241–247.

Carlsson, P., Darnfors, C., Olofsson, S.-O., and Bjursell, G. (1986) Analysis of the human apolipoprotein B gene; complete structure of the B-74 region. *Gene*. **49** (1): 29–51.

Carr, T.P., Hamilton, R.L., Jr., and Rudel, L.L. (1995) ACAT inhibitors decrease secretion of cholesteryl esters and apolipoprotein B by perfused livers of African green monkeys. *J. Lipid Res*. **36** (1): 25–36.

Cartwright, I.J. and Higgins, J.A. (1996) Intracellular degradation in the regulation of secretion of apolipoprotein B-100 by rabbit hepatocytes. *Biochem. J*. **314** (3): 977–984.

Cartwright, I.J. and Higgins, J.A. (1995) Intracellular events in the assembly of very-low-density-lipoprotein lipid with apolipoprotein B in isolated rabbit hepatocytes. *Biochem. J*. **310** (3): 897–907.

Cartwright, I.J. and Higgins, J.A. (1992) Quantification of apolipoprotein B-48 and B-100 in rat liver endoplasmic reticulum and Golgi fractions. *Biochem. J*. **285** (1): 153–159.

Chang. B. H.-J., Liao, W., Li, L., Nakamuta, M., Mack, D., and Chan, L. (1999) Liver-specific inactivation of the abetalipoproteinemia gene completely abrogates very low density lipoprotein/low density lipoprotein production in a viable conditional knockout mouse. *J. Biol. Chem.* **274** (10): 6051–6055.

Chao. F.-F., Stiers, D.L., and Ontko, J.A. (1986) Hepatocellular triglyceride synthesis and transfer to lipid droplets and nascent very low density lipoproteins. *J. Lipid Res.* **27** (11): 1174–1181.

Chapman. M.J., Guérin, M., and Bruckert, E. (1998) Atherogenic, dense low-density lipoproteins. *Eur. Heart. J.* **19** (suppl. A): A24–A30.

Chapman, M.J. (1980) Animal lipoproteins: Chemistry, structure, and comparative aspects. *J. Lipid Res.* **21** (7): 789–853.

Chatterton, J.E., Phillips, M.L., Curtiss, L.K., Milne, R., Fruchart, J.-C., and Schumaker. V.N. (1995) Immunoelectron microscopy of low density lipoproteins yields a ribbon and bow model for the conformation of apolipoprotein B on the lipoprotein surface. *J. Lipid Res.* **36** (9): 2027–2037.

Chatterton, J.E., Phillips, M.L., Curtiss, L.K., Milne, R.W., Marcel, Y.M., and Schumaker. V.N. (1991) Mapping apolipoprotein B on the low density lipoprotein surface by immunoelectron microscopy. *J. Biol. Chem.* **266** (9): 5955–5962.

Chen. C.-H., Forte, T.H., Cahoon, B.E., Thrift, R.N., and Albers. J.J. (1986) Synthesis and secretion of lecithin–cholesterol acyltransferase by human hepatoma cell line HepG2. *Biochim. Biophys. Acta.* **877** (3): 433–439.

Chen. S.-H., Habib, G., Yang, C.-Y., Gu, Z.-W., Lee, B.R., Weng, S.-A., Silberman. S.R., Cai. S.-J., Deslypere, J.P., Rosseneu, M., Gotto, A.M., Jr., Li, W.-H., and Chan, L. (1987) Apolipoprotein B-48 is the product of a messenger RNA with an organ-specific in-frame stop codon. *Science.* **238** (4825): 363–366.

Chen. S.-H., Yang, C.-Y., Chen, P.-F., Setzer, D., Tanimura, M., Li, W.-H., Gotto, A.M., Jr., and Chan, L. (1986) The complete cDNA and amino acid sequence of human apolipoprotein B-100. *J. Biol. Chem.* **261** (28): 12918–12921.

Christie. W.W., Hunter, M.L., and Clegg, R.A. (1981) The effects of cerulenin on lipid metabolism in vitro cellular preparations from the rat. *Biochim. Biophys. Acta.* **666** (2): 284–290.

Chuck. S.L. and Lingappa, V.R. (1993) Analysis of a pause transfer sequence from apolipoprotein B. *J. Biol. Chem.* **268** (30): 22794–22801.

Chuck. S.L. and Lingappa, V.R. (1992) Pause Transfer: A topogenic sequence in apolipoprotein B mediates stopping and restarting of translocation. *Cell.* **68** (1): 9–21.

Chuck. S.L., Yao, Z., Blackhart, B.D., McCarthy, B.J., and Lingappa, V.R. (1990) New variation on the translocation of proteins during early biogenesis of apolipoprotein B. *Nature.* **346** (6282): 382–385.

Cianflone, K., Dahan, S., Monge, J.C., and Sniderman, A.D. (1992) Pathogenesis of carbohydrate-induced hypertriglyceridemia using HepG2 cells as a model system. *Arterioscler. Thromb.* **12** (3): 271–277.

Cianflone, K.M., Yasruel, Z., Rodriguez, M.A., Vas, D., and Sniderman, A.D. (1990) Regulation of apoB secretion from HepG2 cells: Evidence for a critical role for cholesteryl ester synthesis in the response to a fatty acid challenge. *J. Lipid Res.* **31** (11): 2045–2055.

Cladaras, C., Hadzopoulou-Cladaras, M., Nolte, R.T., Atkinson, D., and Zannis, V.I. (1986) The complete sequence and structural analysis of human apolipoprotein B-100: Relationship between apoB-100 and apoB-48. *EMBO J.* **5** (13): 3495–3507.

Coleman, R.A. and Haynes, E.B. (1984) Hepatic monoacylglycerol acyltransferase: Characterization of an activity associated with the suckling period in rats. *J. Biol. Chem.* **259** (14): 8934–8938.

Cooper, A.D. (1997) Hepatic uptake of chylomicron remnants. *J. Lipid Res.* **38** (11): 2173–2192.

Coux, O., Tanaka, K., and Goldberg, A.L. (1996) Structure and functions of the 20S and 26S proteasomes. *Annu. Rev. Biochem.* **65**: 801–847.

Curtiss, L.K. and Edgington, T.S. (1982) Immunochemical heterogeneity of human plasma apolipoprotein B: Apolipoprotein B binding of mouse hybridoma antibodies. *J. Biol. Chem.* **257** (24): 15213–15221.

Dashti, N. (1992) The effect of low density lipoproteins, cholesterol, and 25-hydroxylcholesterol on apolipoprotein B gene expression in HepG2 cells. *J. Biol. Chem.* **267** (10): 7160–7169.

Dashti, N., Alaupovic, P., Knight-Gibson, C., and Koren, E. (1987) Identification and partial characterization of discrete apolipoprotein B containing lipoprotein particles produced by human hepatoma cell line HepG2. *Biochemistry.* **26** (15): 4837–4846.

Dashti, N. and Wolfbauer, G. (1987) Secretion of lipids, apolipoproteins, and lipoproteins by human hepatoma cell line, HepG2: Effects of oleic acid and insulin. *J. Lipid Res.* **28** (4): 423–436.

Dashti, N., Wolfbauer, G., Koren, E., Knowles, B., and Alaupovic, P. (1984) Catabolism of human low density lipoproteins by human hepatoma cell line HepG2. *Biochim. Biophys. Acta.* **794** (3): 373–384.

Davis, R.A., Thrift, R.N., Wu, C.C., and Howell, K.E. (1990) Apolipoprotein B is both integrated into and translocated across the endoplasmic reticulum membrane: Evidence for two functionally distinct pools. *J. Biol. Chem.* **265** (17): 10005–10011.

Davis, R.A., Prewett, A.B., Chan, D.C.F., Thompson, J.J., Borchardt, R.A., and Gallaher, W.R. (1989) Intrahepatic assembly of very low density lipoproteins: Immunologic characterization of apolipoprotein B in lipoproteins and hepatic membrane fractions and its intracellular distribution. *J. Lipid Res.* **30** (8): 1185–1196.

Davis. R.A., Clinton, G.M., Borchardt, R.A., Malone-McNeal, M., Tan, T., and Lattier, G.R. (1984) Intrahepatic assembly of very low density lipoproteins. *J. Biol. Chem.* **259** (6): 3383–3386.

Deeb. S.S., Disteche, C., Motulsky, A.G., Lebo, R.V., and Kan, Y.W. (1986) Chromosomal localization of the human apolipoprotein B gene and detection of homologous RNA in monkey intestine. *Proc. Natl. Acad. Sci. USA.* **83** (2): 419–422.

De Loof. H., Rosseneu, M., Yang, C.-Y., Li, W.-H., Gotto, A.M., Jr., and Chen, L. (1987) Human apolipoprotein B: Analysis of internal repeats and homology with other apolipoproteins. *J. Lipid. Res.* **28** (12): 1455–1465.

Demmer. L.A., Levin, M.S., Elovson, J., Reuben, M.A., Lusis, A.J., and Gordon, J.I. (1986) Tissue-specific expression and developmental regulation of the rat apolipoprotein B gene. *Proc. Natl. Acad. Sci. USA.* **83** (21): 8102–8106.

Dixon. J.L. and Ginsberg, H.N. (1993) Regulation of hepatic secretion of apolipoprotein B-containing lipoproteins: Information obtained from cultured liver cells. *J. Lipid Res.* **34** (2): 167–179.

Dixon. J.L.. Furukawa, S., and Ginsberg, H.N. (1991) Oleate stimulates secretion of apolipoprotein B-containing lipoproteins from Hep G2 cells by inhibiting early intracellular degradation of apolipoprotein B. *J. Biol. Chem.* **266** (8): 5080–5086.

Dolphin. P.J., Wong, L., and Rubinstein, D. (1978) A comparison of some immunological characteristics of very low density lipoproteins of normal and hypercholesterolemic rat sera. *Can. J. Biochem.* **56** (6): 673–683.

Donaldson. J.G., Cassel, D., Kahn, R.A., and Klausner, R.D. (1992) ADP-ribosylation factor. a small GTP-binding protein, is required for binding of the coatomer protein β-COP to Golgi membranes. *Proc. Natl. Acad. Sci. USA.* **89** (14): 6408–6412.

Driscoll, D.M. and Zhang, Q. (1994) Expression and characterization of p27, the catalytic subunit of the apolipoprotein B mRNA editing enzyme. *J. Biol. Chem.* **269** (31): 19843–19847.

Driscoll, D.M., Lakhe-Reddy, S., Oleksa, L.M., and Martinez, D. (1993) Induction of RNA editing at heterologous sites by sequences in apolipoprotein B mRNA. *Mol. Cell. Biol.* **13** (12): 7288–7294.

Du. E.Z.. Kurth, J., Wang, S.-L., Humiston, P., and Davis, R.A. (1994) Proteolysis-coupled secretion the N terminus of apolipoprotein B: Characterization of a transient, translocation arrested intermediate. *J. Biol. Chem.* **269** (39): 24169–24176.

Du. X.. Stoops, J.D., Mertz, J.R., Stanley, C.M., and Dixon, J.L. (1998) Identification of two regions in apolipoprotein B100 that are exposed on the cytosolic side of the endoplasmic reticulum membrane. *J. Cell. Biol.* **141** (3): 585–599.

Duerden, J.M. and Gibbons, G.F. (1990) Storage, mobilization and secretion of cytosolic triacylglycerol in hepatocyte cultures: The role of insulin. *Biochem. J.* **272** (3): 583–587.

Ellsworth, J.L., Erickson, S.K., and Cooper, A.D. (1986) Very low and low density lipoprotein synthesis and secretion by the human hepatoma cell line Hep-G2: Effects of free fatty acid. *J. Lipid Res.* **27** (8): 858–874.

Elovson, J., Huang, Y.O., Baker, N., and Kannan, R. (1981) Apolipoprotein B is structurally and metabolically heterogeneous in the rat. *Proc. Natl. Acad. Sci. USA.* **78** (1): 157–161.

Erickson, S.K. and Cooper, A.D. (1980) Acyl-coenzyme A:cholesterol acyltransferase in human liver: In vitro detection and some characteristics of the enzyme. *Metabolism.* **29** (10): 991–996.

Falk, P.M., Sabater, R.T., and Carballo, D.D., Jr. (1995) Response of the human hepatic tissue cultures HEP-G2 and WRL-68 to cocaine. *J. Pharmacol. Toxicol. Methods.* **33** (2): 113–120.

Fast, D.G. and Vance, D.E. (1995) Nascent VLDL phospholipid composition is altered when phosphatidylcholine biosynthesis is inhibited: Evidence for a novel mechanism that regulates VLDL secretion. *Biochim. Biophys. Acta.* **1258** (2): 159–168.

Faust, R.A. and Albers, J.J. (1987) Synthesis and secretion of plasma cholesteryl ester transfer protein by human hepatocarcinoma cell line, HepG2. *Arteriosclerosis.* **7** (3): 267–275.

Fazio, S., Yao, Z., McCarthy, B.J., and Rall, S.C., Jr. (1992) Synthesis and secretion of apolipoprotein E occur independently of synthesis and secretion of apolipoprotein B-containing lipoproteins in Hep G2 cells. *J. Biol. Chem.* **267** (10): 6941–6945.

Fesmire, J.D., McConathy, W.J., and Alaupovic, P. (1984) Use and significance of reference serum as a secondary standard for electroimmunoassay of apolipoprotein A-I. *Clin. Chem.* **30** (5): 712–716.

Fisher, E.A., Zhou, M., Mitchell, D.M., Wu, X., Omura, S., Wang, H., Goldberg, A.L., and Ginsberg, H.N. (1997) The degradation of apolipoprotein B100 is mediated by the ubiquitin-proteasome pathway and involves heat shock protein 70. *J. Biol. Chem.* **272** (33): 20427–20434.

Folch, J., Lees, M., and Stanley, G.H.S. (1957) A simple method for the isolation and purification of total lipides from animal tissue. *J. Biol. Chem.* **226** (1): 497–509.

Forte, T.M. and Nordhausen, R.W. (1986) Electron microscopy of negatively stained lipoproteins. *Methods Enzymol.* **128**: 442–456.

Francone, O.L., Kalopissis, A.-D., and Griffaton, G. (1989) Contribution of cytoplasmic storage triacylglycerol to VLDL-triacylglycerol in isolate rat hepatocytes. *Biochim. Biophys. Acta.* **1002** (1): 28–36.

Froom, D. (1992) *Studies of Hep G2 cells as a model system for the production of very low density lipoproteins of defined acyl composition*, a Masters of Science thesis, pp. 46–64, 68–76. Dalhousie University, Halifax.

Fujino, T., Navaratnam, N., and Scott, J. (1998) Human apolipoprotein B RNA editing deaminase gene (APOBEC1). *Genomics.* **47** (2): 266–275.

Fujioka, Y., Taniguchi, T., Ishikawa, Y., Shiomi, M., and Yokoyama, M. (1994) Relation of ℕ-glycosylation of apolipoprotein B-100 to cellular metabolism of low density lipoprotein. *Atherosclerosis.* **108** (1): 91–102.

Fujiwara, T., Oda, K., Yokota, S., Takatsuki, A., and Ikehara, Y. (1988) Brefeldin A causes disassembly of the Golgi complex and accumulation of secretory proteins in the endoplasmic reticulum. *J. Biol. Chem.* **263** (34): 18545–18552.

Furukawa, S. and Hirano, T. (1993) Rapid stimulation of apolipoprotein B secretion by oleate is not associated with cholesteryl ester biosynthesis in HepG2 cells. *Biochim. Biophys. Acta.* **1170** (1): 32–37.

Furukawa, S., Sakata, N., Ginsberg, H.N., and Dixon, J.L. (1992) Studies of the sites of intracellular degradation of apolipoprotein B in Hep G2 cells. *J. Biol. Chem.* **267** (31): 22630–22638.

Gaffney, D., Reid, J.M., Cameron, I.M., Vass, K., Caslake, M.J., Shepherd, J., and Packard, C.J. (1995) Independent mutations at codon 3500 of the apolipoprotein B gene are associated with hyperlipidaemia. *Arterioscler. Thromb. Vasc. Biol.* **15** (8): 1025–1029.

Gibbons, G.F. and Wiggins, D. (1995a) Intracellular triacylglycerol lipase: Its role in the assembly of hepatic very-low-density lipoprotein (VLDL). *Adv. Enzyme Regul.* **35**: 179–198.

Gibbons, G.F. and Wiggins, D. (1995b) The enzymology of hepatic very-low-density lipoprotein assembly. *Biochem. Soc. Trans.* **23** (3): 495–500.

Gibbons, G.F., Khurana, R., Odwell, A., and Seelænder, M.C.L. (1994) Lipid balance in HepG2 cells: Active synthesis and impaired mobilization. *J. Lipid Res.* **35** (10): 1801–1808.

Gibbons, G.F., Bartlett, S.M., Sparks, C.E., and Sparks, J.D. (1992) Extracellular fatty acids are not utilized directly for the synthesis of very-low-density lipoprotein in primary cultures of rat hepatocytes. *Biochem. J.* **287** (3): 749–753.

Gibbons, G.F. and Burnham, F.J. (1991) Effect of nutritional state on the utilization of fatty acids for hepatic triacylglycerol synthesis and secretion as very-low-density lipoprotein. *Biochem. J.* **275** (1): 87–92.

Glaumann, H., Bergstrand, A., and Ericsson, J.L.E. (1975) Studies on the synthesis and intracellular transport of lipoprotein particles in rat liver. *J. Cell Biol.* **64** (2): 356–377.

Glickman, R.M., Rogers, M., and Glickman, J.N. (1986) Apolipoprotein B synthesis by human liver and intestine *in vitro*. *Proc. Natl. Acad. Sci. USA.* **83** (14): 5296–5300.

Goodman, D.S., Deykin, D., and Shiratori, T. (1964) The formation of cholesterol esters with rat liver enzymes. *J. Biol. Chem.* **239** (5): 1335–1345.

Gordon, D.A. (1997) Recent advances in elucidating the role of the microsomal triglyceride transfer protein in apolipoprotein B lipoprotein assembly. *Curr. Opin. Lipidol.* **8** (3): 131–137.

Gordon. D.A.. Jamil, H., Gregg, R.E., Olofsson, S.-O., and Borén, J. (1996) Inhibition of the microsomal triglyceride transfer protein blocks the first step of apolipoprotein B lipoprotein assembly but not the addition of bulk core lipid in the second step. *J. Biol. Chem.* **271** (51): 33047–33053.

Graham. A.. Wood, J.L., and Russell, L.J. (1996) Cholesterol esterification is not essential for secretion of lipoprotein components by HepG2 cells. *Biochim. Biophys. Acta.* **3102** (1): 46–54.

Greeve. J., Navaratnam, N., and Scott, J. (1991) Characterization of the apolipoprotein B mRNA editing enzyme: No similarity to the proposed mechanism of RNA editing in kinetoplastid protozoa. *Nucleic Acids Res.* **19** (13): 3569–3576.

Gretch. D.G.. Sturley, S.L., Wang, L., Lipton, B.A., Dunning, A., Grunwald, K.A.A., Wetterau. J.R., Yao, Z., Talmud, P., and Attie, A.D. (1996) The amino terminus of apolipoprotein B is necessary but not sufficient for microsomal triglyceride transfer protein responsiveness. *J. Biol. Chem.* **271** (15): 8682–8691.

Hamilton. R.L., Wong, J.S., Cham, C.M., Nielsen, L.B.. and Young, S.G. (1998) Chylomicron-sized lipid particles are formed in the setting of apolipoprotein B deficiency. *J. Lipid Res.* **39** (8): 1543–1557.

Harris. S.G., Sabio, I., Mayer, E., Steinberg, M.F., Backus, J.W., Sparks, J.D., Sparks, C.E.. and Smith, H.C. (1993) Extract-specific heterogeneity in high-order complexes containing apolipoprotein B mRNA editing activity and RNA-binding proteins. *J. Biol. Chem.* **268** (10): 7382–7392.

Hashimoto, S. and Fogelman, A.M. (1980) Smooth microsomes: A trap for cholesteryl ester formed in hepatic microsomes. *J. Biol. Chem.* **255** (18): 8678–8684.

Havekes. L., Van Hinsbergh, V., Kempen, H.J., and Emeis, J. (1983) The metabolism *in vitro* of human low-density lipoprotein by the human hepatoma cell line Hep G2. *Biochem. J.* **214** (3): 951–958.

Havel. R.J. and Kane, J.P. (1995a) Introduction: Structure and metabolism of plasma lipoproteins, In *The metabolic and molecular bases of inherited disease, 7th edn, vol II.* (Scriver, C.R., Beaudet, A.L., Sly, W.S., Valle, D., Stanbury, J.B., Wyngaarden, J.B., and Fredrickson, D.S., eds.), **pp 1841–1851**. McGraw-Hill, Toronto.

Havel. R.J. and Kane, J.P. (1995b) Disorders of the biogenesis and secretion of lipoproteins containing the B apolipoproteins, In *The metabolic and molecular bases of inherited disease, 7th edn, vol II.* (Scriver, C.R., Beaudet, A.L., Sly, W.S., Valle, D.. Stanbury, J.B.. Wyngaarden, J.B., and Fredrickson, D.S., eds.), **pp 1841–1851**. McGraw-Hill, Toronto.

Hebbachi, A.-M., Seelænder, M.C., Baker, B.W., and Gibbons, G.F. (1997) Decreased secretion of very-low-density lipoprotein triacylglycerol and apolipoprotein B is associated with decreased intracellular triacylglycerol lipolysis in hepatocytes derived from rats fed orotic acid or *n*–3 fatty acids. *Biochem. J.* **325** (3): 711–719.

Hegde. R.S. and Lingappa, V.R. (1996) Sequence-specific alteration of the ribosome-membrane junction exposes nascent secretory proteins to the cytosol. *Cell.* **85** (2): 217–228.

Helms, J.B., Palmer, D.J., and Rothman, J.E. (1993) Two distinct populations of ARF bound to Golgi membranes. *J. Cell. Biol.* **121** (4): 751–760.

Herscovitz, H., Hadzopoulou-Cladaras, M., Walsh, M.T., Cladaras, C., Zannis, V.I., and Small, D.M. (1991) Expression, secretion, and lipid-binding characterization of the N-terminal 17% of apolipoprotein B. *Proc. Natl. Acad. Sci. USA.* **88** (16): 7313–7317.

Higgins, J.A. (1988) Evidence that during very low density lipoprotein assembly in rat hepatocytes most of the triacylglycerol and phospholipid are packaged with apolipoprotein B in the Golgi complex. *FEBS Lett.* **232** (2): 405–408.

Higuchi, K., Monge, J.C., Lee, N., Law, S.W., Brewer, H.B., Jr., Sakaguchi, A.Y., and Naylor, S.L. (1987) ApoB-100 is encoded by a single copy gene in the human genome. *Biochem. Biophys. Res. Commun.* **144** (3): 1332–1339.

Hirose, N., Blankenship, D.T., Krivanek, M.A., Jackson, R.L., and Cardin, A.D. (1987) Isolation and characterization of four heparin-binding cyanogen bromide peptides of human plasma apolipoprotein B. *Biochemistry.* **26** (17): 5505–5512.

Hodges, P.E., Navaratnam, N., Greeve, J.C., and Scott, J. (1991) Site-specific creation of uridine from cytidine in apolipoprotein B mRNA editing. *Nucleic Acids Res.* **19** (6): 1197–1201.

Hoeg, J.M., Meng, M.S., Ronan, R., Demosky, S.J., Jr., Fairwell, T., and Brewer, H.B., Jr. (1988) Apolipoprotein B synthesized by Hep G2 cells undergoes fatty acid acylation. *J. Lipid Res.* **29** (9): 1215–1220.

Homan, R., Grossman, J.E., and Pownall, H.J. (1991) Differential effects of eicosapentaenoic acid and oleic acid on lipid synthesis and secretion by HepG2 cells. *J. Lipid Res.* **32** (2): 231–241.

Huang, G., Lee, D.M., and Singh, S. (1988) Identification of the thiol ester linked lipid in apolipoprotein B. *Biochemistry.* **27** (5): 1395–1400.

Huang, X.F. and Shelness, G.S. (1997) Identification of cysteine pairs within the amino-terminal 5% of apolipoprotein B essential for hepatic lipoprotein assembly and secretion. *J. Biol. Chem.* **272** (50): 31872–31876.

Huby, T., Chapman, J., and Thillet, J. (1997) Pathophysiological implication of the structural domains of lipoprotein(a). *Atherosclerosis.* **133** (1): 1–6.

Huff, M.W. and Telford, D.E. (1984) Characterization and metabolic fate of two very-low-density lipoprotein subfractions separated by heparin-Sepharose chromatography. *Biochim. Biophys. Acta.* **796** (3): 251–261.

Hui, D.Y., Innerarity, T.L., Milne, R.W., Marcel, Y.L., and Mahley, R.W. (1984) Binding of chylomicron remnants and β-very low density lipoproteins to hepatic and extrahepatic lipoprotein receptors: A process independent of apolipoprotein B48. *J. Biol. Chem.* **259** (24): 15060–15068.

Hussain, M.M., Bakillah, A., Nayak, N., and Shelness, G.S. (1998) Amino acids 430–570 in apolipoprotein B are critical for its binding to microsomal triglyceride transfer protein. *J. Biol. Chem.* **273** (40): 25612–25615.

Hussain. M.M., Bakillah, A., and Jamil, H. (1997) Apolipoprotein B binding to microsomal triglyceride transfer protein decreases with increases in length and lipidation: Implications in lipoprotein biosynthesis. *Biochemistry.* **36** (42): 13060–13067.

Ingram, M.F. and Shelness, G.S. (1997) Folding of the amino-terminal domain of apolipoprotein B initiates microsomal triglyceride transfer protein-dependent lipid transfer to nascent very low density lipoproteins. *J. Biol. Chem.* **272** (15): 10279–10286.

Ingram. M.F. and Shelness, G.S. (1996) Apolipoprotein B-100 destined for lipoprotein assembly and intracellular degradation undergoes efficient translocation across the endoplasmic reticulum membrane. *J. Lipid Res.* **37** (10): 2202–2214.

Iverius. P.-H. (1972) The interaction between human plasma lipoproteins and connective tissue glycosaminoglycans. *J. Biol. Chem.* **247** (8): 2607–2613.

Jackson. T.K., Salhanick, A.I., Elovson, J., Deichman, M.L., and Amatruda, J.M. (1990) Insulin regulates apolipoprotein B turnover and phosphorylation in rat hepatocytes. *J. Clin. Invest.* **86** (5): 1746–1751.

Jamil. H., Gordon, D.A., Eustice, D.C., Brooks, C.M., Dickson, J.K., Jr., Chen, Y., Ricci. B., Chu, C.-H., Harrity, T.W., Ciosek, C.P., Jr., Biller, S.A., Gregg, R.E., and Wetterau. J.R. (1996) An inhibitor of the microsomal triglyceride transfer protein inhibits apoB secretion from HepG2 cells. *Proc. Natl. Acad. Sci. USA.* **93** (21): 11991–11995.

Jamil. H., Dickson, J.K., Jr., Chu, C.-H., Lago, M.W., Rinehart, J.K., Biller, S.A., Gregg. R.E., and Wetterau, J.R. (1995) Microsomal triglyceride transfer protein: Specificity of lipid binding and transport. *J. Biol. Chem.* **270** (12): 6549–6554.

Janero. D.R., Siuta-Mangano, P., Miller, K.W., and Lane, M.D. (1984) Synthesis, processing, and secretion of hepatic very low density lipoprotein. *J. Cell. Biochem.* **24** (2): 131–152.

Janero. D.R. and Lane, M.D. (1983) Sequential assembly of very low density lipoprotein apolipoproteins, triacylglycerol, and phosphoglycerides by the intact liver cell. *J. Biol. Chem.* **258** (23): 14496–14504.

Javitt. N.B. (1990) Hep G2 cells as a resource for metabolic studies: Lipoprotein, cholesterol, and bile acids. *FASEB J.* **4** (2): 161–168.

Jiang. H., Ginsberg, H.N., and Wu, X. (1998) Glucose does not stimulate apoprotein B secretion from HepG2 cells because of insufficient stimulation of triglyceride synthesis. *J. Lipid Res.* **39** (11): 2277–2285.

Johnson. D.F., Poksay, K.S., and Innerarity, T.L. (1993) The mechanism for apo-B mRNA editing is deamination. *Biochem. Biophys. Res. Commun.* **195** (3): 1204–1210.

Kalopissis, A.-D., Griglio, S., Malewiak, M.-I., Rozen, R., and Le Liepvre, X. (1981) Very-low-density-lipoprotein secretion by isolated hepatocytes of fat-fed rats. *Biochem. J.* **198** (2): 373–377.

Kane. J.P., Hardman, D.A., and Paulus, H.E. (1980) Heterogeneity of apolipoprotein B: Isolation of a new species from human chylomicrons. *Proc. Natl. Acad. Sci. USA.* **77** (5): 2465–2469.

Kaptein. A., Roodenburg, L., and Princen, H.M.G. (1992) Butyrate stimulates the secretion of apolipoprotein A-I and apolipoprotein B-100 in Hep G2 cells by different mechanisms. *Clin. Biochem.* **25** (5): 317–319.

Kaptein. A., Roodenburg, L., and Princen, H.M.G. (1991) Butyrate stimulates the secretion of apolipoprotein (apo) A-I and apo B100 by the human hepatoma cell line Hep G2: Induction of apo A-I mRNA with no change of apo B100 mRNA. *Biochem. J.* **278** (2): 557–564.

Kempen. H.J., Imbach, A.P., Giller, T., Neumann, W.J., Hennes, U., and Nakada. N. (1995) Secretion of apolipoproteins A-I and B by HepG2 cells: Regulation by substrates and metabolic inhibitors. *J. Lipid Res.* **36** (8): 1796–1806.

Kivlen. M.H., Dorsey, C.A., Lingappa, V.R., and Hegde, R.S. (1997) Asymmetric distribution of pause transfer sequences in apolipoprotein B-100. *J. Lipid Res.* **38** (6): 1149–1162.

Knott. T.J., Pease, R.J., Powell, L.M., Wallis, S.C., Rall, S.C., Jr., Innerarity, T.L., Blackhart. B., Taylor, W.H., Marcel, Y., Milne, R., Johnson, D., Fuller. M., Lusis. A.J., McCarthy, B.J., Mahley, R.W., Levy-Wilson, B., and Scott, J. (1986a) Complete protein sequence and identification of structural domains of human apolipoprotein B. *Nature.* **323** (6090): 734–738.

Knott. T.J., Wallis. S.C., Powell, L.M., Pease. R.J., Lusis, A.J., Blackhart, B., McCarthy. B.J., Mahley, R.W., Levy-Wilson, B., and Scott, J. (1986b) Complete cDNA and derived protein sequence of human apolipoprotein B-100. *Nucleic Acids Res.* **14** (18): 7501–7503.

Knott. T.J., Rall, S.C., Jr., Innerarity, T.L., Jacobson, S.F., Urdea, M.S., Levy-Wilson, B., Powell, L.M., Pease, R.J., Eddy, R., Nakai, H., Byers, M., Priestly. L.M., Robertson. E., Rall, L.B., Betsholtz, C., Shows, T.B., Mahley, R.W., and Scott. J. (1985) Human apolipoprotein B: Structure of carboxyl-terminal domains, sites of gene expression, and chromosomal localization. *Science.* **230** (4721): 37–43.

Knowles, B.B., Howe, C.C., and Aden. D.P. (1980) Human hepatocellular carcinoma cell lines secrete the major plasma proteins and hepatitis B surface antigen. *Science.* **209** (4455): 497–499.

Kohen Avramoglu, R., Cianflone, K., and Sniderman, A.D. (1995) Role of the neutral lipid accessible pool in the regulation of secretion of apoB-100 lipoprotein particles by HepG2 cells. *J. Lipid Res.* **36** (12): 2513–2528.

Koschinsky, M.L., Côté, G.P., Gabel, B., and van der Hoek, Y.Y. (1993) Identification of the cysteine residue in apolipoprotein(a) that mediates extracellular coupling with apolipoprotein B-100. *J. Biol. Chem.* **268** (26): 19819–19825.

Kostner. G.M. and Holasek, A. (1977) The separation of human high density lipoproteins by hydroxyapatite column chromatography: Evidence for the presence of discrete subfractions. *Biochim. Biophys. Acta.* **488** (3): 417–431.

Kostner. G.M., Petek, W., and Holasek, A. (1974) Immunochemical measurement of lipoprotein-X. *Clin. Chem.* **20** (6): 676–681.

Krebs. K.G., Heusser, D., and Wimmer, H. (1969) Spray reagents, In Thin-layer chromatography: a laboratory handbook, 2nd edn. (Stahl, E., ed.; Ashworth, M.R.F., trans.), pp 863. Springer-Verlag, New York.

Kuksis. A., Myher, J.J., Marai, L., Little, J.A., McArthur, R.G., and Roncari, D.A.K. (1986) Usefulness of gas chromatographic profiles of plasma total lipids in diagnosis of phytosterolemia. J. Chromatogr. Biomed. Appl. 381 (1): 1-12.

Kuksis. A., Breckenridge, W.C., Myher, J.J., and Kakis, G. (1978a) Replacement of endogenous phospholipids in rat plasma lipoproteins during intravenous infusion of an artificial emulsion. Can. J. Biochem. 56 (6): 630-639.

Kuksis. A., Myher, J.J., Geher, K., Hoffman, A.G.D., Breckenridge, W.C., Jones., G.J.L.. and Little, J.A. (1978b) Comparative determination of plasma cholesterol and triacylglycerol levels by automated gas-liquid chromatographic and autoanalyzer methods. J. Chromatogr. Biomed. Appl. 146 (3): 393-412.

Lankester. D.L., Brown, A.M., and Zammit, V.A. (1998) Use of cytosolic triacylglycerol hydrolysis products and of exogenous fatty acid for the synthesis of triacylglycerol secreted by cultured rat hepatocytes. J. Lipid Res. 39 (9): 1889-1895.

Lau. P.P., Zhu, H.-J., Nakamuta, M., and Chan, L. (1997) Cloning of an apobec-1-binding protein that also interacts with apolipoprotein B mRNA and evidence for its involvement in RNA editing. J. Biol. Chem. 272 (3): 1452-1455.

Lau. P.P., Zhu, H.-J., Baldini, A., Charnsangavej, C., and Chan, L. (1994) Dimeric structure of a human apolipoprotein B mRNA editing protein and cloning and chromosomal localization of its gene. Proc. Natl. Acad. Sci. USA. 91 (18): 8522-8526.

Laurell. C.-B. (1972) Electroimmuno assay. Scand. J. Clin. Lab. Invest. 29 (suppl. 124): 21-37.

Law. S.W., Grant, S.M., Higuchi, K., Hospattankar, A., Lackner, K., Lee, N., and Brewer, H.B., Jr. (1986) Human liver apolipoprotein B-100 cDNA: Complete nucleic acid and derived amino acid sequence. Proc. Natl. Acad. Sci. USA. 83 (21): 8142-8146.

Law. S.W., Lackner, K.J., Hospattankar, A.V., Anchors, J.M., Sakaguchi. A.Y., Naylor, S.L.. and Brewer, H.B., Jr. (1985) Human apolipoprotein B-100: Cloning, analysis of liver mRNA, and assignment of the gene to chromosome 2. Proc. Natl. Acad. Sci. USA. 82 (24): 8340-8344.

Lee. D.M. (1991) Inter- and intramolecular thiolester linkages in apolipoprotein B. Prog. Lipid Res. 30 (2-3): 245-252.

Lee. P. and Breckenridge, W.C. (1976) Isolation and carbohydrate composition of glycopeptides of human apo low-density lipoprotein from normal and type II hyper-lipoproteinemic subjects. Can. J. Biochem. 54 (9): 829-833.

Lehner. R., Cui, Z., and Vance, D.E. (1999) Subcellullar localization, developmental expression and characterization of a liver triacylglycerol hydrolase. Biochem. J. 338 (3): 761-768.

Lehner. R. and Verger, R. (1997) Purification and characterization of a porcine liver microsomal triacylglycerol hydrolase. *Biochemistry.* **36** (7): 1861–1868.

Lehner. R. and Kuksis, A. (1996) Biosynthesis of triacylglycerols. *Prog. Lipid Res.* **35** (2): 169–210.

Leiper. J.M., Harrison, G.B., Bayliss, J.D., Scott, J., and Pease, R.J. (1996) Systematic expression of the complete coding sequence of apoB-100 does not reveal transmembrane determinants. *J. Lipid Res.* **37** (10): 2215–2231.

Leiper. J.M., Bayliss, J.D., Pease, R.J., Brett, D.J., Scott, J., and Shoulders. C.C. (1994) Microsomal triglyceride transfer protein, the abetalipoproteinemia gene product, mediates the secretion of apolipoprotein B-containing lipoproteins from heterologous cells. *J. Biol. Chem.* **269** (35): 21951–21954.

Liao. W., Yeung, S.-C.J., and Chan, L. (1998) Proteasome-mediated degradation of apolipoprotein B targets both nascent peptides cotranslationally before translocation and full-length apolipoprotein B after translocation into the endoplasmic reticulum. *J. Biol. Chem.* **273** (42): 27225–27230.

Lilly. K., Bugaisky, G.E., Umeda, P.K., and Bieber, L.L. (1990) The medium-chain carnitine acyltransferase activity associated with rat liver microsomes is malonyl-CoA sensitive. *Arch. Biochem. Biophys.* **280** (1): 167–174.

Lilly-Stauderman, M., Brown, T.L., Balasubramaniam, A., and Harmony, J.A.K. (1993) Heparin releases newly synthesized cell surface-associated apolipoprotein E from HepG2 cells. *J. Lipid Res.* **34** (2): 190–200.

Linnik. K.M. and Herscovitz, H. (1998) Multiple molecular chaperones interact with apolipoprotein B during its maturation: The network of endoplasmic reticulum-resident chaperones (ERp72, GRP94, calreticulin, and BiP) interacts with apolipoprotein B regardless of its lipidation state. *J. Biol. Chem.* **273** (33): 21368–21373.

Lowry. O.H., Rosebrough, N.J., Farr, A.L., and Randall, R.J. (1951) Protein measurement with the Folin phenol reagent. *J. Biol. Chem.* **193** (1): 265–275.

Lund. B., Schmidt, A., and Deckert, T. (1975) Portal and cubital serum insulin during oral, portal and cubital glucose tolerance tests. *Acta Med. Scand.* **197** (4): 275–281.

Mahley. R.W., Ji, Z.-S., Brecht, W.J., Miranda, R.D., and He, D. (1994) Role of heparan sulfate proteoglycans and the LDL receptor-related protein in remnant lipoprotein metabolism. *Ann. NY Acad. Sci.* **737**: 39–52.

Mahley. R.W., Weisgraber. K.H., and Innerarity, T.L. (1979) Interaction of plasma lipoproteins containing apolipoprotein B and E with heparin and cell surface receptors. *Biochim. Biophys. Acta.* **575** (1): 81–91.

Malmendier. C.L., Delcroix, C., and Fontaine, M. (1980) Effect of sialic acid removal on human low density lipoprotein catabolism in vivo. *Atherosclerosis.* **37** (2): 277–284.

Marcel. Y.L., Hogue, M., Théolis, R., Jr., and Milne, R.W. (1982) Mapping of antigenic determinants of human apolipoprotein B using monoclonal antibodies against low density lipoproteins. *J. Biol. Chem.* **257** (22): 13165–13168.

Marcovina, S.M., Zhang, Z.-H., Gaur, V.P., and Albers, J.J. (1993) Identification of 34 apolipoprotein(a) isoforms: Differential expression of apolipoprotein(a) alleles between American Blacks and Whites. *Biochem. Biophys. Res. Commun.* **191** (3): 1192–1196.

Markwell, M.A.K., Haas, S.M., Bieber, L.L., and Tolbert, N.E. (1978) A modification of the Lowry procedure to simplify protein determination in membrane and lipoprotein samples. *Anal. Biochem.* **87** (1): 206–210.

Markwell, M.A.K., McGroarty, E.J., Bieber, L.L., and Tolbert, N.E. (1973) The subcellular distribution of carnitine acyltransferases in mammalian liver and kidney: A new peroxisomal enzyme. *J. Biol. Chem.* **248** (10): 3426–3432.

Marques-Vidal, P., Jauhiainen, M., Metso, J., and Ehnholm, C. (1997) Transformation of high density lipoprotein 2 particles by hepatic lipase and phospholipid transfer protein. *Atherosclerosis.* **133** (1): 87–95.

Mathur, S.N., Born, E., Bishop, W.P., and Field, F.J. (1993) Effect of okadaic acid on apo B and apo A-I secretion by CaCo-2 cells. *Biochim. Biophys. Acta.* **1168** (2): 130–143.

Mayes, P.A. (1976) Control of hepatic triacylglycerol metabolism. *Biochem. Soc. Trans.* **4** (4): 575–580.

McLean, J.W., Tomlinson, J.E., Kuang, W.-J., Eaton, D.L., Chen, E.Y., Fless, G.M., Scanu, A.M., and Lawn, R.M. (1987) cDNA sequence of human apolipoprotein(a) is homologous to plasminogen. *Nature.* **330** (6144): 132–137.

McNamara, J.R., Small, D.M., Li, Z., and Schaefer, E.J. (1996) Differences in LDL subspecies involve alterations in lipid composition and conformational changes in apolipoprotein B. *J. Lipid Res.* **37** (9): 1924–1935.

Merrill, A.H., Jr., Lingrell, S., Wang, E., Nikolova-Karakashian, M., Vales, T.R., and Vance, D.E. (1995) Sphingolipid biosynthesis *de novo* by rat hepatocytes in culture: Ceramide and sphingomyelin are associated with, but not required for, very low density lipoprotein secretion. *J. Biol. Chem.* **270** (23): 13834–13841.

Miller, K.W. and Small, D.M. (1983) Surface-to-core and interparticle equilibrium distributions of triglyceride-rich lipoprotein lipids. *J. Biol. Chem.* **258** (22): 13772–13784.

Milne, R., Théolis, R., Jr., Maurice, R., Pease, R.J., Weech, P.K., Rassart, E., Fruchart, J.-C., Scott, J., and Marcel, Y.L. (1989) The use of monoclonal antibodies to localize the low density lipoprotein receptor-binding domain of apolipoprotein B. *J. Biol. Chem.* **264** (33): 19754–19760.

Milne, R.W. and Marcel, Y.L. (1985) The use of monoclonal antibodies to probe human apolipoprotein B structure and function. *Can. J. Biochem. Cell Biol.* **63** (8): 906–912.

Milne, R.W., Théolis, R., Jr., Verdery, R.B., and Marcel, Y.L. (1983) Characterization of monoclonal antibodies against human low density lipoprotein. *Arteriosclerosis.* **3** (1): 23–30.

Moberly, J.B., Cole, T.G., Alpers, D.H., and Schonfeld, G. (1990) Oleic acid stimulation of apolipoprotein B secretion from HepG2 and Caco-2 cells occurs post-transcriptionally. *Biochim. Biophys. Acta.* **1042** (1): 70–80.

Mollenhauer, H.H., Morré, D.J., and Rowe, L.D. (1990) Alteration of intracellular traffic by monensin: mechanism, specificity and relationship to toxicity. *Biochim. Biophys. Acta.* **1031** (2): 225−246.

Mooney, R.A. and Lane, M.D. (1981) Formation and turnover of triglyceride-rich vesicles in the chick lever cell: Effects of cAMP and carnitine on triglyceride mobilization and conversion to ketones. *J. Biol. Chem.* **256** (22): 11724−11733.

Murthy, M.S.R. and Pande, S.V. (1994) Malonyl-CoA-sensitive and -insensitive carnitine palmitoyltransferase activities of microsomes are due to different proteins. *J. Biol. Chem.* **269** (28): 18283−18286.

Murthy, M.S.R. and Pande, S.V. (1993) Carnitine medium/long acyltransferase of microsomes seems to be the previously cloned ~54 kDa protein of unknown function. *Mol. Cell. Biochem.* **122** (2): 133−138.

Navaratnam, N., Morrison, J.R., Bhattacharya, S., Patel, D., Funahashi, T., Giannoni, F., Teng, B.-B., Davidson, N.O., and Scott, J. (1993a) The p27 catalytic subunit of the apolipoprotein B mRNA editing enzyme is a cytidine deaminase. *J. Biol. Chem.* **268** (28): 20709−20712.

Navaratnam, N., Shah, R., Patel, D., Fay, V., and Scott, J. (1993b) Apolipoprotein B mRNA editing is associated with UV crosslinking of proteins to the editing site. *Proc. Natl. Acad. Sci. USA.* **90** (1): 222−226.

Nielsen, L.B., Véniant, M., Borén, J., Raabe, M., Wong, J.S., Tam, C., Flynn, L., Vanni-Reyes, T., Gunn, M.D., Goldberg, I.J., Hamilton, R.L., and Young, S.G. (1998) Genes for apolipoprotein B and microsomal triglyceride transfer protein are expressed in the heart: Evidence that the heart has the capacity to synthesize and secrete lipoproteins. *Circulation.* **98** (1): 13−16.

Oka, K., Kobayashi, K., Sullivan, M., Martinez, J., Teng, B.-B., Ishimura-Oka, K., and Chan, L. (1997) Tissue-specific inhibition of apolipoprotein B mRNA editing in the liver by adenovirus-mediated transfer of a dominant negative mutant APOBEC-1 leads to increased low density lipoprotein in mice. *J. Biol. Chem.* **272** (3): 1456−1460.

Olofsson, S.-O., Bjursell, G., Boström, K., Carlsson, P., Elovson, J., Protter, A.A., Reuben, M.A., and Bondjers, G. (1987) Apolipoprotein B: Structure, biosynthesis and role in the lipoprotein assembly process. *Atherosclerosis.* **68** (1-2): 1−17.

Omura, S. (1981) Cerulenin. *Methods Enzymol.* **72**: 520−532.

Owen, M.R., Corstorphine, C.C., and Zammit, V.A. (1997) Overt and latent activities of diacylglycerol acyltransferase in rat liver microsomes: Possible roles in very-low-density lipoprotein triacylglycerol secretion. *Biochem. J.* **323** (1): 17−21.

Packard, C.J. and Shepherd, J. (1997) Lipoprotein heterogeneity and apolipoprotein B metabolism. *Arterioscler. Thromb. Vasc. Biol.* **17** (12): 3542−3556.

Parthasarathy, S. and Barnett, J. (1990) Phospholipase A_2 activity of low density lipoprotein: Evidence for an intrinsic phospholipase A_2 activity of apolipoprotein B-100. *Proc. Natl. Acad. Sci. USA.* **87** (24): 9741−9745.

Patel. S.B. and Grundy, S.M. (1996) Interactions between microsomal triglyceride transfer protein and apolipoprotein B within the endoplasmic reticulum in a heterologous expression system. *J. Biol. Chem.* **271** (31): 18686–18694.

Pease. R.J., Leiper, J.M., Harrison, G.B., and Scott, J. (1995) Studies on the translocation of the amino terminus of apolipoprotein B into the endoplasmic reticulum. *J. Biol. Chem.* **270** (13): 7261–7271.

Pease. R.J., Harrison, G.B., and Scott, J. (1991) Cotranslational insertion of apolipoprotein B into the inner leaflet of the endoplasmic reticulum. *Nature.* **353** (6343): 448–450.

Pease. R.J., Milne, R.W., Jessup, W.K., Law, A., Provost, P., Fruchart. J.-C., Dean, R.T., Marcel, Y.L., and Scott, J. (1990) Use of bacterial expression cloning to localize the epitopes for a series of monoclonal antibodies against apolipoprotein B100. *J. Biol. Chem.* **265** (1): 553–568.

Phillips. M.L. and Schumaker, V.N. (1989) Conformation of apolipoprotein B after lipid extraction of low density lipoproteins attached to an electron microscope grid. *J. Lipid Res.* **30** (3): 415–422.

Planas-Bohne, F. and Duffield, J. (1988) Factors influencing the uptake of iron and plutonium into cells. *Int. J. Radiat. Biol.* **53** (3): 489–500.

Powell. L.M., Wallis, S.C., Pease, R.J., Edwards, Y.H., Knott, T.J., and Scott, J. (1987) A novel form of tissue-specific RNA processing produces apolipoprotein-B48 in intestine. *Cell.* **50** (6): 831–840.

Protter. A.A., Hardman, D.A., Schilling, J.W., Miller, J., Appleby, V., Chen, G.C., Kirsher. S.W., McEnroe, G., and Kane, J.P. (1986) Isolation of a cDNA clone encoding the amino-terminal region of human apolipoprotein B. *Proc. Natl. Acad. Sci. USA.* **83** (5): 1467–471.

Pullinger. C.R., North, J.D., Teng, B.-B., Rifici, V.A., Ronhild de Brito. A.E., and Scott, J. (1989) The apolipoprotein B gene is constitutively expressed in HepG2 cells: Regulation of secretion by oleic acid, albumin, and insulin, and measurement of the mRNA half-life. *J. Lipid Res.* **30** (7): 1065–1077.

Raabe. M., Véniant, M.M., Sullivan, M., Zlot. C.H., Björkegren, J., Nielson, L.B., Wong. J.S., Hamilton, R.L., and Young, S.G. (1999) Analysis of the role of microsomal triglyceride transfer protein in the liver of tissue-specific knockout mice. *J. Clin. Invest.* **103** (9): 1287–1298.

Randazzo. P.A., Yang, Y.C., Rulka, C., and Kahn, R.A. (1993) Activation of ADP-ribosylation factor by Golgi membranes: Evidence for a brefeldin A- and protease-sensitive activating factor on Golgi membranes. *J. Biol. Chem.* **268** (13): 9555–9563.

Rash. J.M., Rothblat, G.H., and Sparks, C.E. (1981) Lipoprotein apolipoprotein synthesis by human hepatoma cells in culture. *Biochim. Biophys. Acta.* **666** (2): 294–298.

Reisfeld. N., Lichtenberg, D., Dagan, A., and Yedgar, S. (1993) Apolipoprotein B exhibits phospholipase A_1 and phospholipase A_2 activities. *FEBS Lett.* **315** (3): 267–270.

Rosseneu, M., Vercæmst, R., Steinberg, K.K., and Cooper, G.R. (1983) Some considerations of methodology and standardization of apolipoprotein B immunoassays. *Clin. Chem.* **29** (3): 427–433.

Rudel. L.L., Haines, J., Sawyer, J.K., Shah, R., Wilson, M.S., and Carr, T.P. (1997) Hepatic origin of cholesteryl oleate in coronary artery atherosclerosis in African green monkeys: Enrichment by dietary monosaturated fat. *J. Clin. Invest.* **100** (1): 74–83.

Rusiñol, A.E., Hegde, R.S., Chuck, S.L., Lingappa, V.R., and Vance, J.E. (1998) Translocational pausing of apolipoprotein B can be regulated by membrane lipid composition. *J. Lipid. Res.* **39** (6): 1287–1294.

Rusiñol, A.E., Jamil, H., and Vance, J.E. (1997) *In vitro* reconstitution of assembly of apolipoprotein B48-containing lipoproteins. *J. Biol. Chem.* **272** (12): 8019–8025.

Rusiñol, A.E., Lysak, P.S., Sigurdson, G.T., and Vance, J.E. (1996) Monomethylethanolamine reduces plasma triacylglycerols and apolipoprotein B and increases apolipoprotein A-I in rats without induction of fatty liver. *J. Lipid. Res.* **37** (11): 2296–2304.

Rusiñol. A.E. and Vance, J.E. (1995) Inhibition of secretion of truncated apolipoprotein B by monomethylethanolamine is independent of the length of the apolipoprotein. *J. Biol. Chem.* **270** (22): 13318–13325.

Rusiñol, A.E., Chan, E.Y.W., and Vance, J.E. (1993a) Movement of apolipoprotein B into the lumen of microsomes from hepatocytes is disrupted in membranes enriched in phosphatidylmonomethylethanolamine. *J. Biol. Chem.* **268** (33): 25168–25175.

Rusiñol. A., Verkade, H., and Vance, J.E. (1993b) Assembly of rat hepatic very low density lipoproteins in the endoplasmic reticulum. *J. Biol. Chem.* **268** (5): 3555–3562.

Rustæus, S., Stillemark, P., Lindberg, K., Gordon, D., and Olofsson, S.-O. (1998) The microsomal triglyceride transfer protein catalyzes the post-translational assembly of apolipoprotein B-100 very low density lipoprotein in McA-RH7777 cells. *J. Biol. Chem.* **273** (9): 5196–5203.

Rustæus. S., Lindberg, K., Borén, J., and Olofsson, S.-O. (1995) Brefeldin A reversibly inhibits the assembly of apoB containing lipoproteins in McA-RH777 cells. *J. Biol. Chem.* **270** (48): 28879–28886.

Sakata. N., Wu., X., Dixon, J.L., and Ginsberg, H.N. (1993) Proteolysis and lipid-facilitated translocation are distinct but competitive processes that regulate secretion of apolipoprotein B in Hep G2 cells. *J. Biol. Chem.* **268** (31): 22967–22970.

Salter. A.M., Wiggins, D., Sessions, V.A., and Gibbons, G.F. (1998) The intracellular triacylglycerol/fatty acid cycle: A comparison of its activity in hepatocytes which secrete exclusively apolipoprotein (apo) B_{100} very-low-density lipoprotein (VLDL) and in those which secrete predominately apoB$_{48}$ VLDL. *Biochem. J.* **332** (3): 667–672.

Sato. R., Imanaka, T., Takatsuki, A., and Takano, T. (1990) Degradation of newly synthesized apolipoprotein B-100 in a pre-Golgi compartment. *J. Biol. Chem.* **265** (20): 11880–11884.

Scanu, A.M. and Edelstein, C. (1995) Kringle-dependent structural and functional polymorphism of lipoprotein(a). *Biochim. Biophys. Acta.* **1265** (1): 1–12.

Schmitt, M. and Grand-Perret, T. (1999) Regulated turnover of a cell surface-associated pool of newly synthesized apolipoprotein E in HepG2 cells. *J. Lipid Res.* **40** (1): 39–49.

Segrest, J.P., Jones, M.K., Mishra, V.K., Anatharamaiah, G.M., and Garber, D.W. (1994) ApoB-100 has a pentapartite structure composed of three amphipathic α-helical domains alternating with two amphipathic β-strand domains. Detection by the computer program LOCATE. *Arterioscler. Thromb.* **14** (10): 1674–1685.

Semenkovich, C.F. and Ostlund, R.E., Jr. (1987) Estrogens induce low-density lipoprotein receptor activity and decrease intracellular cholesterol in human hepatoma cell line Hep G2. *Biochemistry.* **26** (16): 4987–4992.

Shah, R.R., Knott, T.J., Legros, J.E., Navaratnam, N., Greeve, J.C., and Scott, J. (1991) Sequence requirements for the editing of apolipoprotein B mRNA. *J. Biol. Chem.* **266** (25): 16301–16304.

Sharp, D., Blinderman, L., Combs, K.A., Kienzle, B., Ricci, B., Wager-Smith, K., Gil, C.M., Turck, C.W., Bouma, M.-E., Rader, D.J., Aggerbeck, L.P., Gregg, R.E., Gordon, D.A., and Wetterau, J.R. (1993) Cloning and gene defects in microsomal triglyceride transfer protein associated with abetalipoproteinemia. *Nature.* **365** (6441): 65–69.

Shelness, G.S. and Thornburg, J.T. (1996) Role of intermolecular disulfide bond formation in the assembly and secretion of apolipoprotein B-100-containing lipoproteins. *J. Lipid Res.* **37** (2): 408–419.

Shelness, G.S., Morris-Rogers, K.C., and Ingram, M.F. (1994) Apolipoprotein B48-membrane interactions: Absence of transmembrane localization in nonhepatic cells. *J. Biol. Chem.* **269** (12): 9310–9318.

Shen, B.W., Scanu, A.M., and Kézdy, F.J. (1977) Structure of human serum lipoproteins inferred from compositional analysis. *Proc. Natl. Acad. Sci. USA.* **74** (3): 837–841.

Shireman, R.B. and Fisher, W.R. (1979) The absence of a role of the carbohydrate moiety in the binding of apolipoprotein B to the low density lipoprotein receptor. *Biochim. Biophys. Acta.* **572** (3): 537–540.

Shore, V.G. and Shore, B. (1972) The apolipoproteins: Their structure and functional roles in human-serum lipoproteins, *In Blood lipids and lipoproteins: Quantitation, composition, and metabolism.* (Nelson, G.J., ed.), **pp 508, 514.** Wiley-Interscience, Toronto.

Simon, D., Aden, D.P., and Knowles, B.B. (1982) Chromosomes of human hepatoma cell lines. *Int. J. Cancer.* **30** (1): 27–33.

Siuta-Mangano, P., Janero, D.R., and Lane, M.D. (1982) Association and assembly of triglyceride and phospholipid with glycosylated and unglycosylated apoproteins of very low density lipoprotein in the intact liver cell. *J. Biol. Chem.* **257** (19): 11463–11467.

Smith, H.C., Kuo, S.-R., Backus, J.W., Harris, S.G., Sparks, C.E., and Sparks, J.D. (1991) *In vitro* apolipoprotein B mRNA editing: Identification of a 27S editing complex. *Proc. Natl. Acad. Sci. USA.* **88** (4): 1489–1493.

Soria. L.F., Ludwig, E.H., Clarke, H.R.G., Vega, G.L., Grundy, S.M., and McCarthy, B.J. (1989) Association between a specific apolipoprotein B mutation and familial defective apolipoprotein B-100. *Proc. Natl. Acad. Sci. USA.* **86** (2): 587–591.

Sparks, J.D. and Sparks, C.E. (1990) Insulin modulation of hepatic synthesis and secretion of apolipoprotein B by rat hepatocytes. *J. Biol. Chem.* **265** (15): 8854–8862.

Sparks, J.D., Sparks, C.E., Roncone, A.M., and Amatruda, J.M. (1988) Secretion of high and low molecular weight phosphorylated apolipoprotein B by hepatocytes from control and diabetic rats: Phosphorylation of apo B_H and apo B_L. *J. Biol. Chem.* **263** (11): 5001–5004.

Spin, J.M. and Atkinson, D. (1995) Cyroelectron microscopy of low density lipoprotein in vitreous ice. *Biophys. J.* **68** (5): 2115–2123.

Struck, D.K., Siuta, P.B., Lane, M.D., and Lennarz, W.J. (1978) Effect of tunicamycin on the secretion of serum proteins by primary cultures of rat and chick hepatocytes: Studies of transferrin, very low density lipoprotein, and serum albumin. *J. Biol. Chem.* **253** (15): 5332–5337.

Swaminathan, N. and Aladjem, F. (1976) The monosaccharide composition and sequence of the carbohydrate moiety of human serum low density lipoproteins. *Biochemistry.* **15** (7): 1516–1522.

Swenson, T.L., Simmons, J.S., Hesler, C.B., Bisgaier, C., and Tall, A.R. (1987) Cholesteryl ester transfer protein is secreted by Hep G2 cells and contains asparagine-linked carbohydrate and sialic acid. *J. Biol. Chem.* **262** (34): 16271–16274.

Swift, L.L. (1996) Role of the Golgi apparatus in the phosphorylation of apolipoprotein B. *J. Biol. Chem.* **271** (49): 31491–31495.

Swift, L.L. (1995) Assembly of very low density lipoproteins in rat liver: A study of nascent particles recovered from the rough endoplasmic reticulum. *J. Lipid Res.* **36** (3): 395–406.

Tai, D.-Y., Pan, J.-P., and Lee-Chen, G.-J. (1998) Identification and haplotype analysis of apolipoprotein B-100 $Arg_{3500} \rightarrow Trp$ mutation in hyperlipidemic Chinese. *Clin. Chem.* **44** (8): 1659–1665.

Tall, A.R. (1998) An overview of reverse cholesterol transport. *Eur. Heart. J.* **19** (suppl. A): A31–A35.

Tall, A. (1995) Plasma lipid transfer proteins. *Annu. Rev. Biochem.* **64**: 235–257.

Tam, S.-P. and Breckenridge, W.C. (1987) The interaction of lipolysis products of very low density lipoprotein with plasma high density lipoprotein (HDL): Perfusate HDL with plasma HDL subfractions. *Biochem. Cell. Biol.* **65** (3): 252–260.

Tam, S.-P., Archer, T.K., and Deeley, R.G. (1986) Biphasic effects of estrogen on apolipoprotein synthesis in human hepatoma cells: Mechanism of antagonism by testosterone. *Proc. Natl. Acad. Sci. USA.* **83** (10): 3111–3115.

Tam. S.-P., Archer, T.K., and Deeley, R.G. (1985) Effects of estrogen on apolipoprotein secretion by the human hepatocarcinoma cell line, HepG2. *J. Biol. Chem.* **260** (3): 1670–1675.

Tam. S.-P. and Breckenridge, W.C. (1983) Apolipoprotein and lipid distribution between vesicles and HDL-like particles formed during lipolysis of human very low density lipoproteins by perfused rat heart. *J. Lipid Res.* **24** (10): 1343–1357.

Tam. S.-P., Dory, L., and Rubinstein, D. (1981) Fate of apolipoproteins C-II, C-III, and E during lipolysis of human very low density lipoproteins *in vitro*. *J. Lipid Res.* **22** (4): 641–651.

Tanaka. M.. Jingami, H., Otani, H., Cho, M., Ueda, Y., Arai, H., Nagano. Y., Doi. T., Yokode. M.. and Kita. T. (1993) Regulation of apolipoprotein B production and secretion in response to the change of intracellular cholesteryl ester content in rabbit hepatocytes. *J. Biol. Chem.* **268** (17): 12713–12718.

Taniguchi, T., Ishikawa, Y., Tsunemitsu, M., and Fukuzaki, H. (1989) The structures of the asparagine-linked sugar chains of human apolipoprotein B-100. *Arch. Biochem. Biophys.* **273** (1): 197–205.

Teh. E.M.. Dolphin, P.J., Breckenridge, W.C.. and Tan. M.-H. (1998) Human plasma CETP deficiency: Identification of a novel mutation in exon 9 of the CETP gene in a Caucasian subject from North America. *J. Lipid Res.* **39** (2): 442–456.

Temme, E.H.M.. Mensink, R.P., and Hornstra, G. (1997) Effects of medium chain fatty acids (MCFA), myristic acid, and oleic aicd on serum lipoproteins in healthy subjects. *J. Lipid Res.* **38** (9): 1746–1754.

Teng. B.-B., Burant, C.F., and Davidson, N.O. (1993) Molecular cloning of an apolipoprotein B messenger RNA editing protein. *Science.* **260** (5115): 1816–1819.

Teng. B.-B.. Sniderman, A., Krauss, R.M., Kwiterovitch, P.O., Jr., Milne. R.W., and Marcel. Y.L. (1985) Modulation of apolipoprotein B antigenic determinants in human low density lipoprotein subclasses. *J. Biol. Chem.* **260** (8): 5067–5072.

Thrift. R.N.. Forte, T.M.. Cahoon, B.E.. and Shore, V.G. (1986) Characterization of lipoproteins produced by the human liver cell line, Hep G2, under defined conditions. *J. Lipid Res.* **27** (3): 236–250.

Thuren. T., Wilcox, R.W., Sisson, P., and Waite, M. (1991) Hepatic lipase hydrolysis of lipid monolayers: Regulation by apolipoprotein. *J. Biol. Chem.* **266** (8): 4853–4861.

Tikkanen, M.J.. Dargar, R., Pfleger, B., Gonen, B., Davie, J.M., and Schonfeld, G. (1982) Antigenic mapping of human low density lipoprotein with monoclonal antibodies. *J. Lipid Res.* **23** (7): 1032–1038.

Tran. K.. Borén, J., Macri, J., Wang, Y., McLeod, R., Kohen Avramoglu, R.. Adeli, K., and Yao, Z. (1998) Functional analysis of disulfide linkages clustered within the amino terminus of human apolipoprotein B. *J. Biol. Chem.* **273** (13): 7244–7251.

Tsunemitsu, M., Ishikawa, Y., Taniguchi, T., Fukuzaki, H., and Yokoyama, M. (1992) Association of N-glycosylation of apolipoprotein B-100 with plasma cholesterol levels in Watanabe heritable hyperlipidemic rabbits. *Atherosclerosis.* **93** (3): 229–235.

Vance. D.E. (1996) Glycerolipid biosynthesis in eukaryotes, In *Biochemistry of lipids, lipoproteins and membranes, 3rd edn.* (Vance, D.E. & Vance, J.E., eds.). **pp 153–155, 169.** Elsevier, New York.

Vance. J.E. (1991) Secretion of VLDL, but not HDL, by rat hepatocytes is inhibited by the ethanolamine analogue N-monomethylethanolamine. *J. Lipid Res.* **32** (12): 1971–1982.

Vance. J.E. (1989) The use of newly synthesized phospholipids for assembly into secreted hepatic lipoproteins. *Biochim. Biophys. Acta.* **1006** (1): 59–69.

Van Harken. D.R., Dixon, C.W., and Heimberg, M. (1969) Hepatic lipid metabolism in experimental diabetes. V. Effect of concentration of oleate on metabolism of triglycerides and on ketogenesis. *J. Biol. Chem.* **244** (9): 2278–2285.

Vauhkonen. M.. Viitala, J., Parkkinen, J., and Rauvala, H. (1985) High-mannose structure of apolipoprotein-B from low-density lipoproteins of human plasma. *Eur. J. Biochem.* **152** (1): 43–50.

Verkade. H.J., Fast, D.G., Rusiñol, A.E., Scraba, D.G., and Vance, D.E. (1993) Impaired biosynthesis of phosphatidylcholine causes a decrease in the number of very low density lipoprotein particles in the Golgi but not in the endoplasmic reticulum of rat liver. *J. Biol. Chem.* **268** (33): 24990–24996.

Vermeulen. P.S., Lingrell, S., Yao, Z., and Vance, D.E. (1997) Phosphatidylcholine biosynthesis is required for secretion of truncated apolipoprotein Bs from McArdle RH7777 cells only when a neutral lipid core is formed. *J. Lipid Res.* **38** (3): 447–458.

Wagener. R., Pfitzner, R., and Stoffel, W. (1987) Studies on the organization of the human apolipoprotein B100 gene. *Biol. Chem. Hoppe-Seyler.* **368** (4): 419–425.

Wang, C.-N., Hobman, T.C., and Brindley, D.N. (1995) Degradation of apolipoprotein B in cultured rat hepatocytes occurs in a post-endoplasmic reticulum compartment. *J. Biol. Chem.* **270** (42): 24924–24931.

Wang. S.R.. Pessah, M., Infante, J., Catala, D., Salvat, C., and Infante, R. (1988) Lipid and lipoprotein metabolism in Hep G2 cells. *Biochim. Biophys. Acta.* **961** (3): 351–363.

Wang, Y.. McLeod, R.S., and Yao, Z. (1997) Normal activity of microsomal triglyceride transfer protein is required for the oleate-induced secretion of very low density lipoproteins containing apolipoprotein B from McA-RH7777 cells. *J. Biol. Chem.* **272** (19): 12272–12278.

Weisgraber, K.H. and Rall, S.C., Jr. (1987) Human apolipoprotein B-100 heparin-binding sites. *J. Biol. Chem.* **262** (23): 11097–11103.

Weisgraber. K.H., Innerarity, T.L., and Mahley, R.W. (1978) Role of the lysine residues of plasma lipoproteins in high affinity binding to cell surface receptors on human fibroblasts. *J. Biol. Chem.* **253** (24): 9053–9062.

Werner. E.D., Brodsky, J.L., and McCracken, A.A. (1996) Proteasome-dependent endoplasmic reticulum-associated protein degradation: An unconventional route to a familiar fate. *Proc. Natl. Acad. Sci. USA.* **93** (24): 13797–13801.

Wetterau. J.R., Gregg, R.E., Harrity, T.W., Arbeeny, C., Cap, M., Connolly, F., Chu, C.-H., George, R.J., Gordon, D.A., Jamil, H., Jolibois, K.G., Kunselman. L.K., Lan, S.-J., Maccagnan, T.J., Ricci, B., Yan, M., Young, D., Chen, Y., Fryszman, O.M., Logan, J.V.H., Musial, C.L., Poss, M.A., Robl, J.A., Simpkins, L.M., Slusarchyk, W.A., Sulsky. R., Taunk, P., Magnin, D.R., Tino, J.A., Lawrence, R.M., Dickson, J.K., Jr., and Biller. S.A. (1998) An MTP inhibitor that normalizes atherogenic lipoprotein levels in WHHL rabbits. *Science.* **282** (5389): 751–754.

Wetterau. J.R., Lin, M.C.M., and Jamil, H. (1997) Microsomal triglyceride transfer protein. *Biochim. Biophys. Acta.* **1345** (2): 136–150.

Wetterau. J.R., Aggerbeck, L.P., Bouma, M.-E., Eisenberg, C., Munck, A., Hermier, M., Schmitz. J., Gay, G., Rader, D.J., and Gregg, R.E. (1992) Absence of microsomal triglyceride transfer protein in individuals with abetalipoproteinemia. *Science.* **258** (5084): 999–1001.

Wetterau. J.R., Aggerbeck, L.P., Laplaud, P.M., and McLean, L.R. (1991a) Structural properties of the microsomal triglyceride-transfer protein complex. *Biochemistry.* **30** (18): 4406–4412.

Wetterau, J.R., Combs, K.A., McLean, L.R., Spinner, S.N., and Aggerbeck, L.P. (1991b) Protein disulfide isomerase appears necessary to maintain the catalytically active structure of the microsomal triglyceride transfer protein. *Biochemistry.* **30** (40): 9728–9735.

Wetterau. J.R. and Zilversmit. D.B. (1986) Localization of intracellular triacylglycerol and cholesteryl ester transfer activity in rat tissues. *Biochim. Biophys. Acta.* **875** (3): 610–617.

Wetterau, J.R. and Zilversmit, D.B. (1985) Purification and characterization of microsomal triglyceride and cholesteryl ester transfer protein from bovine liver microsomes. *Chem. Phys. Lipids.* **38** (1, 2): 205–222.

Wetterau. J.R. and Zilversmit, D.B. (1984) A triglyceride and cholesteryl ester transfer protein associated with liver microsomes. *J. Biol. Chem.* **259** (17): 10863–10866.

White. A.L. and Lanford, R.E. (1995) Biosynthesis and metabolism of lipoprotein(a). *Curr. Opin. Lipidol.* **6** (2): 75–80.

White. A.L., Graham, D.L., LeGros, J., Pease, R.J., and Scott, J. (1992) Oleate-mediated stimulation of apolipoprotein B secretion from rat hepatoma cells: A function of the ability of apolipoprotein B to direct lipoprotein assembly and escape presecretory degradation. *J. Biol. Chem.* **267** (22): 15657–15664.

Wiertz. E.J.H.J., Tortorella, D., Bogyo, M., Yu, J., Mothes, W., Jones, T.R., Rapoport, T.A., and Ploegh, H.L. (1996) Sec61-mediated transfer of a membrane protein from the endoplasmic reticulum to the proteasome for destruction. *Nature.* **384** (6608): 432–438.

Wiggins. D. and Gibbons, G.F. (1996) Origin of hepatic very-low-density lipoprotein tri-acylglycerol: The contribution of cellular phospholipid. *Biochem. J.* **320** (2): 673–679.

Wiggins. D. and Gibbons, G.F. (1992) The lipolysis/esterification cycle of hepatic triacyl-glycerol: Its role in the secretion of very-low-density lipoprotein and its response to hormones and sulphonylureas. *Biochem. J.* **284** (2): 457–462.

Wong. L. and Torbati, A. (1994) Differentiation of intrahepatic membrane-bound and secretory apolipoprotein B by monoclonal antibodies: Membrane-bound apolipoprotein B is more glycosylated. *Biochemistry.* **33** (7): 1923–1929.

Wu. X.. Shang, A., Jiang, H., and Ginsberg, H.N. (1996) Low rates of apoB secretion from HepG2 cells result from reduced delivery of newly synthesized triglyceride to a "secretion-coupled" pool. *J. Lipid Res.* **37** (6): 1198–1206.

Wu. X.. Sakata, N., Lui, E., and Ginsberg, H.N. (1994) Evidence for a lack of regulation of the assembly and secretion of apolipoprotein B-containing lipoprotein from HepG2 cells by cholesteryl ester. *J. Biol. Chem.* **269** (16): 12375–12382.

Yamanaka. S.. Poksay, K.S., Balestra, M.E., Zeng, G.-Q., and Innerarity, T.L. (1994) Cloning and mutagenesis of the rabbit apoB mRNA editing protein: A zinc motif is essential for catalytic activity, and noncatalytic auxiliary factor(s) of the editing complex are widely distributed. *J. Biol. Chem.* **269** (34): 21725–21734.

Yang. C.-Y.. Gu. Z.-W., Yang, M., and Gotto, A.M., Jr. (1994) Primary structure of apoB-100. *Chem. Phys. Lipids.* **67/68**: 99–104.

Yang. C.-Y.. Kim, T.W., Weng, S.-A., Lee, B., Yang, M., and Gotto, A.M.. Jr. (1990) Isolation and characterization of sulfhydryl and disulfide peptides of human apolipoprotein B-100. *Proc. Natl. Acad. Sci. USA.* **87** (14): 5523–5527.

Yang. C.-Y.. Gu. Z.-W., Weng, S.-A., Kim, T.W., Chen, S.-H., Pownall. H.J., Sharp. P.M.. Liu. S.-W., Li, W.-H., Gotto, A.M.. Jr., and Chan, L. (1989) Structure of apo-lipoprotein B-100 of human low density lipoproteins. *Arteriosclerosis.* **9** (1): 96–108.

Yang. C.-Y.. Chen, S.-H., Gianturco, S.H., Bradley, W.A.. Sparrow, J.T.. Tanimura. M., Li. W.-H.. Sparrow, D.A., DeLoof, H., Rosseneu, M., Lee, F.-S., Gu, Z.-W. Gotto. A.M.. Jr.. and Chan. L. (1986) Sequence, structure, receptor-binding domains and internal repeats of human apolipoprotein B-100. *Nature.* **323** (6090): 738–742.

Yang. L.-Y.. Kuksis, A., Myher, J.J., and Steiner, G. (1996) Contribution of de novo fatty acid synthesis to very low density lipoprotein triacylglycerols: Evidence from mass isotopomer distribution analysis of fatty acids synthesized from [$2H_6$]ethanol. *J. Lipid Res.* **37** (2): 262–274.

Yang. L.-Y.. Kuksis, A., Myher, J.J., and Steiner, G. (1995) Origin of triacylglycerol moiety of plasma very low density lipoproteins in the rat: Structural studies. *J. Lipid Res.* **36** (1): 125–136.

Yang. Y.. Yang, Y., Kovalski, K., and Smith. H.C. (1997) Partial characterization of the auxiliary factors involved in apolipoprotein B mRNA editing through APOBEC-1 affinity chromatography. *J. Biol. Chem.* **272** (44): 27700–27706.

Yao. Z.. Tran, K., and McLeod, R.S. (1997) Intracellular degradation of newly synthesized apolipoprotein B. *J. Lipid Res*. **38** (10): 1937–1953.

Yao. Z. and Vance, D.E. (1988) The active synthesis of phosphatidylcholine is required for very low density lipoprotein secretion from rat hepatocytes. *J. Biol. Chem*. **263** (6): 2998–3004.

Yeung, S.J., Chen, S.H., and Chan, L. (1996) Ubiquitin-proteasome pathway mediates intracellular degradation of apolipoprotein B. *Biochemistry*. **35** (43): 13843–13848.

Young, S.G., Bertics, S.J., Scott, T.M., Dubois, B.W., Curtiss, L.K., and Witztum. J.L. (1986) Parallel expression of the MB19 genetic polymorphism in apoprotein B-100 and apoprotein B-48: Evidence that both apoproteins are products of the same gene. *J. Biol. Chem*. **261** (7): 2995–2998.

Zammit. V.A. (1996) Role of insulin in hepatic fatty acid partitioning: Emerging concepts. *Biochem. J.* **314** (1): 1–14.

Zannis. V.I., Breslow, J.L., SanGiacomo, T.R., Aden, D.P., and Knowles. B.B. (1981) Characterization of the major apolipoproteins secreted by two human hepatoma cell lines. *Biochemistry*. **20** (25): 7089–7096.

Zhao. Y. and Marcel, Y.L. (1996) Serum albumin is a significant intermediate in cholesterol transfer between cells and lipoproteins. *Biochemistry*. **35** (22): 7174–7180.

Zhou. M., Fisher, E.A., and Ginsberg, H.N. (1998) Regulated co-translational ubiquitination of apolipoprotein B100: A new paradigm for proteasomal degradation of a secretory protein. *J. Biol. Chem*. **273** (38): 24649–24653.

Zhou. M., Wu, X., Huang, L.-S., and Ginsberg, H.N. (1995) Apoprotein B100, an inefficiently translated secretory protein, is bound to the cytosolic chaperone, heat shock protein 70. *J. Biol. Chem*. **270** (42): 25220–25224.